Word Embeddings-based Sentence-Level Sentiment Analysis considering Word Importance

Toshitaka Hayashi, Hamido Fujita

Iwate Prefectural University, 152-52 Sugo, Takizawa, 020-0693, Japan

E-mail: g236r002@s.iwate-pu.ac.jp, HFujita-799@acm.org

Abstract: Word2vec has been proven to facilitate various Natural Language Processing (NLP) tasks. We suppose that it could separate the vector space of word2vec into positive and negative. Hence, word2vec can be applied to Sentiment Analysis tasks. In our previous research, we proposed the word embeddings (WEMB) based Sentence-level Sentiment Analysis method. Word's vectors from WEMB are utilized to calculate the sentence vector. Training of the classification model is done using sentence vector and the polarity. After training, the model predicts the polarity of the unlabeled sentence. However, the sentence vector was insufficient because the method treats all words with the same weight for calculating a sentence vector. In this paper, we propose a method to solve this problem. We consider word weight according to their importance for calculating sentence vector. The proposed method is compared with the method without word importance, and the accuracy is improved. However, there is still a grim difference with state of the art. We discuss the next improvement and present future work.

Keywords: Sentiment Analysis; Polarity Classification; Word Embeddings; Word Importance

1 Introduction

A human can detect emotion or sentiment in written language. However, social media and other tools have increased the number of sources and volumes of information; it is too voluminous and complex for humans. Sentiment Analysis [3, 4, 10] [18, 22] (SA: also known as Opinion Mining) is the challenge. SA is one of the most active research areas in Natural Language Processing (NLP) and machine learning [10], with a particular interest in the classification of text into positive, negative, neutral. Such a task is known as the Polarity Classification problem. The goal is classifying the polarity of a given text at the document, sentence, or feature/aspect level.

There are two main types of methods for SA, lexicon-based approach or machine learning based approach. Lexicon-based approach processes the text data by keyword matching using sentiment lexicon. Lexicon has sentiment information of words. For an example of the lexicon, SentiWordNet [1, 2] is proposed by Esuli et al., and SenticNet [7, 8, 9] [11, 12] is proposed by Cambria et al... Lexicon alone does not give much accuracy [38], but combining it with a language rule called Semantic Rule [23, 31, 40] produces good results [11, 24, 25]. Semantic Rule is utilized to handle the exception of the language like negation. It has a good impact on polarity classification. However, the method requires the definition of Semantic Rule, which has to done manually.

Machine learning based approach [28] aims at building predictive models for the sentiment, which use supervised learning. In this approach, a model is created to predict unlabeled vectors by training feature vectors and labels. There is an issue, the feature vector of the text is required to apply supervised learning to SA. The main problem is how to extract a feature vector from the text data.

As one of the conversions from text into the vector, word2vec [35] is introduced, which trains text corpus and outputs Word Embeddings (WEMB) that are the set of word vectors. The idea of word2vec (WEMB) originated from the concept of distributed representation of words. Word2vec has been proven to facilitate various NLP tasks [5, 14, 20]. It can be expected to prove polarity classification too.

In light of such trends, we use a machine learning based approach because it can do automatically. Also, we use word2vec because it has proven various NLP tasks. Our goal is to extract a feature vector of a sentence. WEMB is utilized to obtain word vectors, and the word vectors are combined to make a sentence vector. The main problem is how to combine word vectors to make sentence vector.

In our previous research [34], we propose the method for Sentence-level Sentiment Analysis using a supervised approach with WEMB-based feature extraction. Our process extracts each word vector in a sentence from WEMB. Also, sentence vector is calculated using simple calculation such as the average, the variance, and the geometric mean of the word vectors. However, there is a problem that the method treats important words for polarity and not important words for polarity with the same weight.

In this paper, we consider word importance to solve this problem. In our proposed method, a word that has a bias in the rate of occurrence due to polarity is considered important. Hence, word importance is calculated from training data. Also, sentence vector is calculated by a weighted average using word vector and word importance. It makes a better result than our previous research [34]. The rest of the paper is structured as follows. Section 2 summarizes the previous work regarding machine learning based Sentiment Analysis, word2vec and WEMB, and WEMB based method. In Section 3, our proposed method about how to calculate word importance and how to calculate sentence vector are written. In Section 4, experiment results for public datasets are given. In our experiment, Twitter datasets and movie review datasets are utilized. In Section 5, the discussion about our method is done. In Section 6, conclusion and future work are written.

2 Related Work

2.1 Machine Learning-based Sentiment Analysis

In this paper, a machine learning based approach is presented. Machine learning based sentiment analysis aims at building predictive models for sentiment by training labeled datasets. This approach builds a feature vector of each text entry from certain aspects or word frequencies. Standard machine learning tools train the feature vectors and the labels to establish the corresponding model is validated against labeled texts [15].

The main problem of machine learning based sentiment analysis is how to extract feature vector from the text. For an example of the feature vector, five features are described in the review of Pang and Lee [4], which are Term presence/frequency, Term based features beyond unigrams [17], Part of Speech, Syntax, and Negation. Also, Socher et al. propose Sentiment Treebank [28], a model in which semantic composition is considered hierarchically. It makes good results for polarity classification.

2.2 Word2vec and Word Embeddings

Mikolov et al. introduced word2vec [35] that can obtain word vectors called word embeddings by training text corpus. The idea of word2vec is originated from the concept of distributed representation of words. Word2vec algorithms such as Skip-gram, CBOW [35, 36] and GloVe [16] have been proven to facilitate various NLP tasks, such as word analogy [35], parsing [20], POS tagging [5], aspect extraction [28], topic extraction [37], translation [14], WordNet [14, 26] and so on. These approaches have shown the ability to improve classification accuracy. However, these have limited challenge to polarity classification. In this paper, the polarity classification is improved using our approach based on word2vec.

2.3 Word Embeddings-based Sentiment Analysis

In previous work, we have presented a WEMB-based sentiment analysis [34], which is a supervised method using WEMB. As shown in Figure 1, it is divided into two steps: Training and Classification. In the training part, sentence vector is extracted using WEMB. In the process, the vectors of each word in the sentence are extracted from WEMB. Then, sentence vector is calculated by average, variance, and the geometric mean of the word vectors. After that, the Classifier is trained using sentence vectors and polarities. In the classification part, sentence vector is calculated in the same way as training. Prediction is made using Classifier that is trained in the training part. In the sentence vector calculation, all words are treated with the same weight; this causes the inappropriate assignment to accuracy. Hence, considering word importance; it becomes important to evaluate and enhance the accuracy of the system. In the following section, we are presenting the proposal.

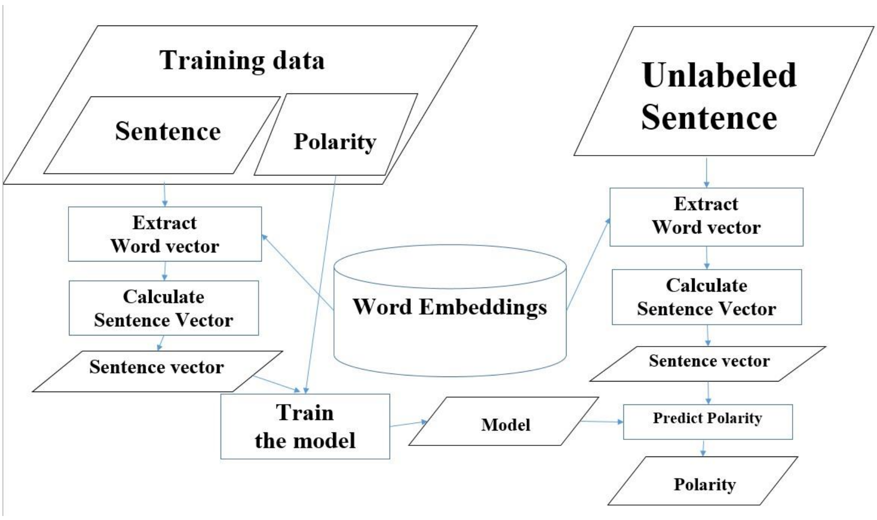

Figure 1
Word Embeddings-based Sentiment Analysis

3 The Proposed Method

The proposed method is described in this section. Section 3.1 shows the general framework of our proposed system which consists of three procedures: (1) Calculate word importance, (2) Extract sentence vector, (3) Training and Classification. Section 3.2, 3.3, 3.4 shows each procedure.

3.1 General Framework

Our approach is shown in Figure 2. The proposed method is tackling the problem of sentence vector calculation. In this paper, we could improve the classification accuracy using word importance, compared with previous studies reported in [34]. Word importance could provide better classification accuracy in comparison to previous research.

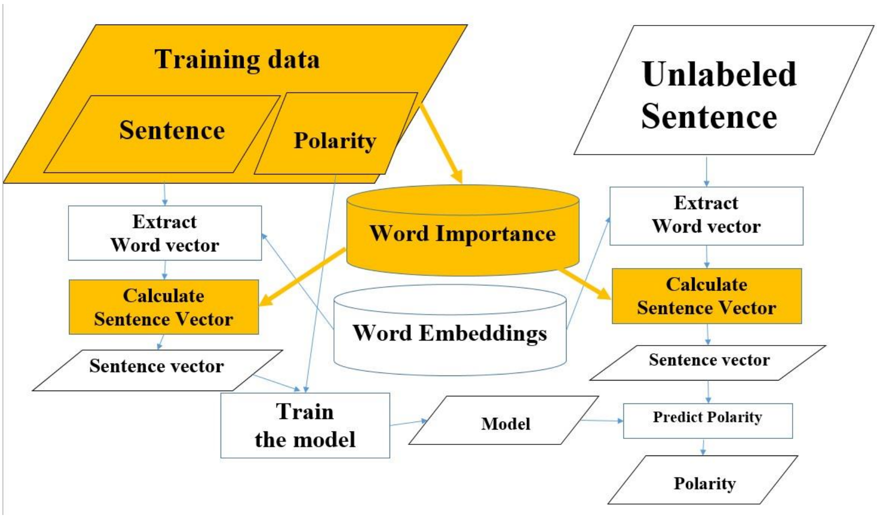

Figure 2
Word Embeddings-based Sentiment Analysis with Word Importance

Our proposal requires three elements, (1) Training data which consists of sentences and polarities, (2) WEMB, (3) classification algorithm. Also, it consists of three steps, (1) Build word importance, (2) Training, (3) Classification. Each step is described as follows:

(1) The list of word importance is built by training data as written in Section 3.2.

(2) The input of the training step is the training data which is consist of training sentences and polarities. The output of the training step is a classification model. Training step is carried out as in the following process:

1. Extract sentence vectors from training sentences as written in Section 3.3.
2. Train sentence vector and polarity using a classification algorithm as Section 3.4.

(3) The input of the classification step is an unlabeled sentence. The output of the classification step is polarity prediction of the unlabeled sentence. Classification step is done as the following process:

1. Extract sentence vector from unlabeled sentence as explained in Section 3.3.
2. Predict the polarity from sentence vector using the trained classification model as Section 3.4.

3.2 How to Calculate Word Importance

The goal of this process is to calculate word importance of all words in the training data. Hence, the output is list of word importance. Word importance is calculated from training data. Training data consists of sentences and polarities.

In this work; a word of high word importance has a bias of occurrence rate due to polarity. Therefore, we propose the notion of word importance calculation as represented in Algorithm 1.

Algorithm 1 : Word Importance Calculation

Input (Training Data)

Output(List of Word Importance)

1. Decide which polarity is major and which polarity is minor by comparing to the number of appearance in positive sentences and negative sentences.

IF $|Word_i \ in \ Positive \ Sentences| > |Word_i \ in \ Negative \ Sentences|$:

$$major\ Polaity(Word_i) = Positive$$

$$minor\ Polaity(Word_i) = Negative$$

ELSE:

$$major\ Polaity(Word_i) = Negative$$

$$minor\ Polaity(Word_i) = Positive$$

2. Calculate word importance as given in formula (1)

$$WI(Word_i) = 1 - \frac{|Word_i \ in \ Sentences \ of \ minor \ Polarity|}{|Word_i \ in \ Sentences \ of \ major \ Polarity|} \tag{1}$$

3.3 How to Process Sentence to Sentence Vector

In order to apply a classification algorithm, sentence vector should be extracted from sentence. The sentence vector is calculated using word vectors and word importance. We propose how to extract sentence vector from sentence as follows:

1. Let Sentence as "$Word_1 Word_2 \ldots Word_i \ldots Word_n$"
2. Extract word vectors of all words of a sentence from WEMB. If a word does not exist in WEMB, ignore the word. Each word vector is as shown in formula (2), where *m* is the dimension of the word vector.
$$\overrightarrow{Word_i} = (num_{i1}, num_{i2}, \ldots, num_{id}, \ldots, num_{im}) \quad (2)$$
3. Extract I_i, which is word importance of $Word_i$ from word importance list
$$I_i = WI(Word_i)$$
4. Calculate I_{total} which is the SUM of word importance in the sentence as given in formula (3).
$$I_{total} = \sum_{i=1}^{n} I_i \quad (3)$$
5. Calculate the weight of a word W_i as given in formula (4).
$$W_i = \frac{I_i}{I_{total}} \quad (4)$$
6. Calculate Sentence Vector as given in formula (5).
$$\overrightarrow{Sentence} = (value_1, value_2, \ldots, value_d, \ldots, value_m)$$
$$value_d = \sum_{i=1}^{n} (W_i \, num_{id}) \quad (5)$$

3.4 Training and Classification

The classification model is trained using training sentence vectors and the labels (Polarities). Also, the classification model is utilized to predict polarity for unlabeled sentence vector. In this paper, we apply XBboost classification algorithm to this procedure. XGBoost [33] is utilized in our training and classification process. It is a package of gradient boosting, which produce a prediction model from an ensemble of weak decision trees [33]. XGBoost works well for high dimension features. We utilize the scikit-learn of Python because it is easy for training. The parameters of XGBoost that is utilized in our experiment are shown in Table 1. Each parameter is explained in the documentation of XGBoost that is available at:

http://xgboost.readthedocs.io/en/latest/python/python_intro.html#setting-parameters.

Table 1
Parameters for XGBoost

Parameter	value
test_size	0.2
Objective	"binary: logistics"
eval_metric	"error"
eta	0.1
max_depth	10
number of iteration	500

4 Experiment

The proposed approach has been validated against the data listed in Section 4.1.

In our experiment, pre-trained WEMB are utilized. The embeddings are listed in Section 4.2. Our measurement of evaluation is listed in Section 4.3. Experiment results are shown in Section 4.4

4.1 The Data

Public datasets for Sentence-level SA are utilized for evaluating our method. In this paper, three Twitter datasets (TSATC, Vader, STS-Gold) and two movie review datasets (PL05, IMDB) are utilized. The balance of each dataset is shown in Table 2.

Table 2
The balances of the datasets

Dataset	Domain	Positive	Negative	Total
TSATC	Twitter	790178	788436	1578614
Vader	Twitter	2901	1299	4200
STS-Gold	Twitter	632	1402	2304
PL05	Movie	5331	5331	10662
IMDB	Movie	25000	25000	50000

The datasets are shown as follows:

4.1.1 Twitter Datasets

Twitter Sentiment Analysis Training Corpus (TSATC) contains approximately a million and a half classified tweets, and each row is marked as 1 for positive sentiment and 0 for negative sentiment. The dataset is based on data from two sources: the University of Michigan Sentiment Analysis competition on Kaggle and the Twitter Sentiment Corpus by Niek Sanders. It is available at:

http://thinknook.com/twitter-sentiment-analysis-training-corpus-dataset-2012-09-22/.

Vader contains 2901 positive and 1299 negative tweet-like messages. It is available at:

https://github.com/cjhutto/vaderSentiment/blob/master/additional_resources/hutto_ICWSM_2014.tar.gz.

STS-Gold has been generated for SA evaluation in the Twitter domain. The dataset contains 632 positive and 1402 negative sentences. It is available at https://github.com/pollockj/world_mood/blob/master/sts_gold_v03/sts_gold_tweet.csv.

4.1.2 Movie Review Datasets

PL05 consists of 5331 positive and 5331 negative processed sentences of movie reviews. The dataset is introduced by Pang/Lee ACL 2005. It is available at:

http://www.cs.cornell.edu/people/pabo/movie-review-data/.

IMDB contains 25000 positive and 25000 reviews from the review site. The target of the review is movies in the online platform. It is available at:

https://www.kaggle.com/iarunava/imdb-movie-reviews-dataset.

4.2 Pre-trained Word Embeddings

In our experiment, two different pre-trained WEMB(Google News Embeddings and Glove Twitter Embeddings) are utilized, which WEMB is as follows:

Google-news-vectors-negative-300.bin is published by Google. The Embeddings is trained on the part of Google News dataset (about 100 billion words). It is available at: https://code.google.com/archive/p/word2vec/.

Glove.twitter.27B is trained on 2 billion tweets (about 27 billion tokens). It is available at: https://nlp.stanford.edu/projects/glove/.

Also, the number of vocabulary and dimensions for each pre-trained WEMB are shown in Table 3.

Table 3
Number of vocabulary and dimensions for pre-trained word Embeddings

Pre-trained Word Embeddings	Number of Vocabulary	Dimensions
GoogleNewsNegative300.bin	3,000,000	300
Glove Twitter.27B	1,200,000	200

4.3 Measurements of the Evaluation

In this paper, four measurements of evaluation are utilized, Which, is shown in given formulas (6)-(9). Also, the confusion matrix is shown in Table 3.

$$Accuracy = \frac{TP + TN}{TP + FP + TN + FN} \tag{6}$$

$$precision = \frac{TP}{TP + FP} \tag{7}$$

$$recall = \frac{TP}{TP + FN} \tag{8}$$

$$f1 - score = \frac{2 \times precision \times recall}{precision + recall} \tag{9}$$

Table 4
Confusion Matrix

	Actual Positive	Actual Negative
Predict Positive	TP	FP
Predict Negative	FN	TN

4.4 Experiment Result

The experiment for TSATC is done using 4-fold cross-validation. The data have been separated into several folds identified by an ID, as shown in Table 4. Each fold has 400,000 sentences. However, the last fold has only 378,614 sentences. The number of positive/negative sentence in each fold are shown in Table 4.

Table 5
Data balance for TSATC

ID	Positive	Negative	Total
0000000-0399999	233453	166547	400000
0400000-0799999	212330	187670	400000
0800000-1199999	177064	222936	400000
1200000-1578613	167331	211283	378614
Total	790178	788436	1578614

The classification result for TSATC is shown in Table 5. Two different pre-trained WEMB (Google News Embeddings and Glove Twitter Embeddings) are utilized for feature extraction. The dimension in Table 5 is the number of dimensions of the feature vector. The accuracy is 77.7% using Google News Embeddings. Also, precision, recall, and F-score are shown in Table 5.

Table 6
4-fold cross-validation result for TSATC (%)

Word Embeddings	Dimension	Accuracy	Precision	Recall	F1
GoogleNews300d	300	**77.7**	**77.6**	**77.4**	**77.5**
GloveTwitter200d	200	76.9	76.7	77.4	77.0

Further experiments for other datasets are also, carried out. However, the dataset is small for cross-validation. Hence, TSATC model is utilized to do prediction on other data set. The results are shown in Table 6. Overall, Google News Embeddings has prodcued better results than Glove Twitter Embeddings. It has 88.5% accuracy for STS-Gold dataset and 84.8% F1-score for Vader dataset.

Table 7
Experiment results for datasets using TSATC model (%)

Dataset	Embeddings	Accuracy	Precision	Recall	F1-score
STS-Gold	Google	**88.5**	**77.5**	88.6	**82.7**
	Glove	86.0	72.1	**89.7**	79.9
Vader	Google	**79.5**	**86.4**	83.4	**84.8**
	Glove	77.1	83.4	83.4	83.4
PL05	Google	64.4	60.9	80.5	69.3
	Glove	61.8	58.2	83.5	68.6
IMDB	Google	71.5	76.3	62.5	68.7
	Glove	70.7	71.9	68.0	69.9

5 Discussion

In this section, we discuss the comparison result with other papers and highlighted issues in our experiment. We could prove better performance using the proposed method in relation to other previous method [34] using the evaluation on the effect of word importance. Also, we compare the proposed method with state of the art reported in [26] to better evaluation finding more improvement of WEMB based SA. The experiment carried out in this paper provide more better outcome in terms of prediction accuracy in relation to [26] [34].

A comparison of result for TSATC is shown in Table 7 in which, we have compared on accuracy and processing speed relative to our methods. We do not include training time as processing time. Our training time for 1.2 million 900-dimensional data is almost 10 hours (on our environment, CPU: Intel Core i5-6600L 3.5 GHz Quad-Core, RAM: 32 GB DDR4-2400, SSD: Samsung 850 EVO-Series 500GB).

Table 8

Comparison of accuracy of 4-fold cross-validation result for TSATC against previous research

Author	WEMB	Dimension	Accuracy (%)	Speed(Sentence/s)
Our previous method[34]	GoogleNews	900	76.3	452
	GloveTwitter	600	76.4	948
		300	75.6	**1719**
		75	71.2	**2479**
Our method	GoogleNews	300	**77.7**	712
	GloveTwitter	200	**76.9**	1129

However, processing speed is slower than the previous one. Hence, considering word importance requires processing time. Also, the number of dimensions of the feature vector decreased to one third. We think the processing time can be reduced using GPU as will be shown in our future paper.

Also, our method is compared against state of the art. The research of Araque et al. [26] is utilized for comparison. Their method is based on similarity-based approach. The similarities are calculated against certain words which becomes a feature vector. The comparison results of STS-Gold, Vader, IMDB, and PL05 are shown in Table 8. In the paper of Araque et al. [26], many experimental results are shown. In Table 9 Our method has achieved a better outcome comparing with the work reported in [26].

Table 9
Comparison of F1-score against [26]

Method		Vader	STS-Gold	IMDB	PL05
[26]	LIU_WPath+Liu_Embeddings+W2V	90.28	82.95	**89.06**	78.19
	SWN_WPath+SWN_Embeddings+W2V	89.85	82.01	88.80	78.08
	ANEW_WPath+ANEW_Embeddings+W2V	86.91	79.91	88.85	78.03
	AFINN_WPath+ANEW_Embeddings+W2V	**90.41**	**83.39**	89.00	**78.29**
Our Method		84.88	82.71	68.72	69.30

Our method has a fair result for Twitter data (Vader, STS-Gold). However, our method is insufficient for movie review data (IMDB, PL05). There are differences between our method and Araque et al. [26]. In our method, only word embeddings are utilized for feature vector. On the other hand, in their method, word embeddings and lexical resources are combined to get semantic similarity. Also, the usage of WEMB is different. In our method, WEMB is utilized for doing the weighted average calculation for making a sentence vector. In their method, WEMB is utilized for getting similarity, and the similarity becomes a feature vector. The difference of similarity based method and our method is shown in Table 9. In Table 9, each method is using only word embeddings.

Table 10
Comparison of F1-score against Similarity-based Method only use WEMB

Approach	Vader	STS-Gold	IMDB	PL05
Similarity based Method[26]	**88.19**	**83.75**	**88.55**	**76.25**
Our Method	84.88	82.71	68.72	69.30

Overall, the similarity-based method has better accuracy than our direct calculation. In Future work, we are modifying our results especially result for movie review based on graph embedding.

Further issues are highlighted in from our experiment as follows.

5.1 Unknown Words Challenge

The sentence vector is calculated by word vectors that are gotten from word embeddings. However, some word is not included in word embeddings. Hence the word's vector is not sufficient. In the worst case scenario, words in the sentence could be unknown words. We have investigated the influence of unknown words. We define *KnownRatio(KR)* in as in formula (13).

$$KnownRatio = \frac{|Word \in Sentence \,\&\, Word \in WordEmbeddings|}{|Word \in Sentence|} \tag{13}$$

We investigate *KR* for each word embeddings and dataset pairs. The average of KR for each pair and Accuracy of our previous method (without weight) and this research (with weight) is as shown in Table 10.

Table 11
Known Ratio for Dataset and Word Embeddings pairs

Dataset	WEMB	Average of KR	Accuracy (with weight)	Accuracy (without weight) [34]
TSATC	GoogleNews300	**0.84**	**77.7**	76.1
	GloveTwitter200	0.76	76.9	76.4
PL05	GoogleNews300	0.72	64.4	67.6
	GloveTwitter200	**0.94**	61.8	59.6

As a result of considering Table 8, when word importance is considered, if the average of KR is high the accuracy is high. On the other hand, when word importance is not considered, if the average of KR is high the accuracy is low. This result shows that all word's vectors are not necessarily needed; but instead important word's vectors become important for such computation. We think all words should be known for concluding which ones are important or else. In most cases, the unknown word is caused by mistyping or orthographical variants. In order to solve this problem, the preprocessing algorithm for mistyping or orthographical variants can provide better solution. Also, creating WEMB which has robust vocabulary will be also, other good solution.

5.2 Sentence Vector Calculation

In our previous research, all words are utilized with the same weight for making a sentence vector. In this research, the weight of words are changed according to their importance, and it makes better accuracy than the method without word importance [34]. Hence, word importance is considered as effective approach for improving accuracy. Moreover, in this research, the dimension of each word vector is a black box; hence, the dimension of the sentence vector is also a black box. We think Similarity-based method does not have this problem.

5.3 Difference between Twitter and Movie Review

In our experiment, the result for Twitter data is sufficient. However, the result for movie review data is insufficient because there is a difference between Twitter and Movie review. In our opinion, movie review data include words titles of the movies. In our proposed word importance calculation, some words of the movie's title are considered as important. Also, if the movie’s title is transformed into a vector, it has polarity. Hence, a named entity should be considered to solve this problem.

Conclusions

In this paper, we proposed word embeddings based Sentence-level Sentiment Analysis method using word weight according to their importance. The word importance is calculated by training data, and it is utilized for sentence vector calculation. In our experiment, we confirm that word importance makes a better effect on accuracy. However, there is still an accuracy difference between our method and state of the art [26]. Our method has a fair result for Twitter data, but it has a problem with movie review data. The weighted average of word vectors is insufficient for sentence vector.

There is much future work for improving accuracy and doing an extension.

We consider future work for improving accuracy as follows:

- A preprocessing algorithm for fixing mistyping or orthographical variants is required to solve an unknown word problem.
- Create WEMB that have much vocabulary to solve an unknown word problem.
- We need many experiments for finding the best calculation for sentence vector.

  Our thought is as follows:
  - The meaning of the word should be considered using a named entity. Also, using the relational graph structure of the language [21, 27] will be suitable for meanings.
  - The similarity-based method outperforms our method. Hence, the usage of WEMB should be reconsidered.

We consider the following extension as future work:

- In this paper, only binary classification for positive and negative is considered. However, neutral polarity and polarity intensity should be considered too.
- This method should be applied to other SA problems such as irony, sarcasm detection [13] or emotion detection [6, 29].
- Our method is a supervised approach. Hence, it requires many training data. However, labeling data is a difficult/hard task. The classification algorithm that works well with small training data is required. We think Semi-supervised learning [19, 30] will solve this problem.

References

[1] A Esuli, F Sebastiani, "Determining the semantic orientation of terms through gloss classification," Proceedings of the 14th ACM International Conference on Information and Knowledge Management, pp. 617-624, October 2005

[2] A Esuli, F. Sebastiani, "SentiWordNet – A Publicly Available Lexical Resource for Opinion Mining." In Proceedings of the 5th Conference on Language Resources and Evaluation, pp. 417-422, May 2006

[3] B Liu, "Sentiment Analysis and Opinion Mining." Morgan and Claypool Publishers: Synthesis Lectures on Human Language Technologies, 1st edition, USA, May 2012

[4] B Pang, L Lee, "Opinion mining and sentiment analysis," Foundation and Trends in Information Retrieval, Volume 2, pp. 1-135, January 2008

[5] C Lin, W Ammar, C Dyer, L Levin. "Unsupervised POS Induction with word embeddings." In: NAACL HLT 2015, The 2015 Conference of the North American Chapter of the Association for Computational Linguistics: Human Language Technologies, pp. 1311-1316, May 2015

[6] E Cambria, A Livingstone, A Hussain, "The Hourglass of Emotions," Cognitive behavioural systems, pp. 144-157, January 2012

[7] E Cambria, C Havasi, A Hussain, "SenticNet 2: A Semantic and Affective Resource for Opinion Mining and Sentiment Analysis", Proceedings of FLAIRS, pp. 202-207, May 2012

[8] E Cambria, D Olsher, D Rajagopal, "SenticNet 3: A Common and Common-Sense Knowledge Base for Cognition-Driven Sentiment Analysis", Proceedings of AAAI, pp. 1515-1521, July 2014

[9] E Cambria, R Speer, C Havasi, A Hussain, "SenticNet: A Publicly Available Semantic Resource for Opinion Mining," Proceedings of Commonsense Knowledge Symposium, pp. 14-18, November 2010

[10] E Cambria, S Poria, A Gelbukh, M Thelwall. "Sentiment analysis is a big suitcase." IEEE Intelligent Systems 32, pp. 74-80, November 2017

[11] E Cambria, S Poria, D Hazarika, K Kwok. "SenticNet 5: Discovering conceptual primitives for sentiment analysis by means of context embeddings". In: AAAI, pp. 1795-1802, February 2018

[12] E Cambria, S Poria, R Bajpai, B Schuller, "SenticNet 4: A Semantic Resource for Sentiment Analysis Based on Conceptual Primitives", Proceedings of COLING, pp. 2666-2677, December 2016

[13] E Sulis, DIH Farías, P Rosso, V Patti, G Ruffo, "Figurative messages and affect in Twitter," Knowledge-Based Systems, Volume .108, pp. 132-143, September 2016

[14] J Goikoetxea, A Soroa, E Agirre, "Bilingual embeddings with random walks over multilingual wordnets," Knowledge-Based Systems, Volume 150, pp. 218-230, June 2018

[15] J Lin, W Mao, D D. Zeng, "Personality-based refinement for sentiment classification in microblog," Knowledge-Based Systems, Volume 132, pp. 204-214, September 2017

[16] J Pennington, R Socher, C Manning. “Glove: Global vectors for word representation.” In: Proceedings of the 2014 Conference on Empirical Methods in Natural Language Processing (EMNLP) October 2014

[17] JPP Duran, G Sidorov, HG Adorno, I Batyrshin, EM Melendez, GP Duran, LC Hernandez, Algorithm for Extraction of Subtrees of a Sentence Dependency Parse Tre, Acta Polytechnica Hungarica, Volume 14(3), pp. 79-98, March 2017

[18] K Ravi, V Ravi, "A survey on opinion mining and sentiment analysis: Tasks, approaches and applications," Knowledge-Based Systems, Volume 89, pp. 14-46, November 2015

[19] L Oneto, F Bisio, E Cambria, D Anguita. “Semi-supervised learning for affective common-sense reasoning.” Cognitive Computation, Volume 9, pp. 1842, February 2017

[20] M Bansal, K Gimpel, K Livescu. “Tailoring continuous word representations for dependency parsing.” In: ACL (2), pp. 809-815, June 2014

[21] M J Cobo. “A Relational Database Model for Science Mapping Analysis,” Acta Polytechnica Hungarica, Volume 12, pp. 43-62, June 2015

[22] M Soleymani, D Garcia, B Jou, B Schuller, SF Chang, M Pantic, “A survey of multimodal sentiment analysis,” Image and Vision Computing 65, pp. 3-14, September 2017

[23] O Appel, F Chiclana, J Carter, H Fujita “Successes and challenges in developing a hybrid approach to sentiment analysis,” Applied Intelligence Volume 48, pp. 1176-1188, July 2018

[24] O Appel, F Chiclana, J Carter, H Fujita,” A Hybrid Approach to the Sentiment Analysis Problem at the Sentence Level,” Knowledge-Based Systems, Volume 108, pp. 110-124, September 2016

[25] O Appel, F Chiclana, J Carter, “Main Concepts, State of the Art and Future Research Questions in Sentiment Analysis,” Acta Polytechnica Hungarica, Volume 12(3), pp. 87-108, March 2015

[26] O Araque, G Zhu, Carlos A. Iglesias, “A semantic similarity-based perspective of affect lexicons for sentiment analysis,” Knowledge-Based Systems, Volume 165, pp. 346-359, February 2019

[27] P Goyal, E Ferrara, “Graph embedding techniques, applications, and performance: A survey,” Knowledge-Based Systems, Volume 151, pp. 78-94, July 2018

[28] R Socher, A Perelygin, J Wu, J Chuang, C Manning, A Ng, C Potts. “Recursive deep models for semantic compositionality over a sentiment treebank.” In: Proceedings of the conference on empirical methods in natural language processing (EMNLP), pp. 1631-1642, October 2013

[29] S Poria, A Gelbukh, E Cambria, A Hussain, GB Huang, EmoSenticSpace: "A Novel Framework for Affective Common-Sense Reasoning," Knowledge-Based Systems, Volume 69, pp. 108-123, October 2014

[30] S Poria, E Cambria, A Gelbukh, "Aspect extraction for opinion mining with a deep convolutional neural network." Knowledge-Based Systems 108: pp. 42-49, September 2016

[31] S Poria, E Cambria, G Winterstein, GB Huang, "Sentic patterns: Dependency-based rules for concept-level sentiment analysis." Knowledge-Based Systems, Volume 69, pp. 45-63, October 2014

[32] SL Lo, E Cambria, R Chiong, D Cornforth. "A multilingual semi-supervised approach in deriving Singlish sentic patterns for polarity detection." Knowledge-Based Systems 105, pp. 236-247, August 2016

[33] T Chen, C. Guestrin. (2016) "XGBoost: A Scalable Tree Boosting System." In Proceedings of the 22nd ACM SIGKDD International Conference on Knowledge Discovery and Data Mining (KDD '16) ACM, New York, NY, USA, pp. 785-794, August 2016

[34] T Hayashi, H Fujita, "Sentence-level Sentiment Analysis using feature vectors from word embeddings," In Proceedings of THE 17th International Conference on Intelligent Software Methodologies, Tools and Techniques (SOMET 18) pp. 749-758, September 2018

[35] T Mikolov, I Sutskever, K Chen, GS Corrado, J Dean, "Distributed representations of words and phrases and their compositionality, "Advances in neural information processing systems, Volume 26, pp. 3111-3119, December 2013

[36] T Mikolov., K Chen, G Corrado, J Dean, "Efficient estimation of word representations in vector space." CoRR, arXiv:1301.3781; January 2013

[37] X Fu, X Sun, H Wu, L Cui, J Z Huang, "Weakly supervised topic sentiment joint model with word embeddings," Knowledge-Based Systems, Volume 147, pp. 43-54, May 2018

[38] X Zou, J Yang, J Zhang, H Han, Microblog sentiment analysis with weak dependency connections, Knowledge-Based Systems, Volume 142, pp. 170-180, February 2018

[39] Y Li, Q Pan, T Yang, SH Wang, JL Tang, E Cambria. Learning word representations for sentiment analysis. Cognitive Computation, Volume 9, pp. 843-851, June 2017

[40] Y Xie, Z Chen, K Zhang, Y Cheng, D K Honbo, A Agrawal, AN Choudhary. MuSES: a multilingual sentiment elicitation system for Social Media Data. IEEE Intelligent Systems, Volume 29, pp. 34-42, January 2014

Bus Transport Process Network Synthesis

Albert Nagy[1], Zsolt Ercsey[2], József Tick[3], Zoltán Kovács[4]

[1] Applied Informatics, Óbuda University, Bécsi út 96/b, 1034 Budapest, Hungary, e-mail: albert.nagy@me.com

[2] Department of System and Software Technology, Faculty of Engineering and Information Technology, University of Pécs, Boszorkány u. 2, 7624 Pécs, Hungary, e-mail: ercsey@mik.pte.hu

[3] Department of Applied Informatics, John von Neumann Faculty of Informatics, Óbuda University, Bécsi út 96/b, 1034 Budapest, Hungary, e-mail: tick@uni-obuda.hu

[4] Optin Ltd. Oroszlán u. 4. 6720 Szeged, Hungary, e-mail: zoltan.kovacs@optin.hu

Abstract: The current paper is about bus transport process network synthesis. Unlike previously discussed urban traffic modelling and solution methods, here, it is presented as a novel application of the p-graph methodology, while exploiting the peculiarities of the problem. The focus is on the synthesis step, where the set of potentially feasible solutions is determined, in other words, the maximal bus transport process structure is generated. The classical process network instances together with their properties are adapted to this new application field, i.e. to meet the special requirements of the bus transport. First, the meaning of the material type nodes and the operating unit type nodes are described in details. A new axiom is given to complete the set of p-graph's axioms. In addition, the utilization of the conventional maximal structure and solution structure generation algorithms, they are extended to gain advantage of the new axiom and to generate the potential solution structure in a more effective manner. Based on the solution structures a mathematical programming model is generated containing the constraints and the objective function of the bus transport problem. Thus, the generation of the bus launching list is prepared. The solution method presented for bus transport problems meets the high level expectations of decision-makers, i.e. the resulting system is complete, flexible and robust.

Keywords: bus transport; mathematical programming model; process network; p-graph; synthesis

1 Introduction

The importance of public transportation is indisputable. It contributes to the flourishing of cities, as well as, to a higher quality everyday life for citizens. A well-organized urban public transport system may offer more opportunities, including faster access to jobs, easier approach to recreational activities etc. Even though public transport now goes beyond buses, metros, boats, trams and trains, these traditional modes serve as a backbone in cities. This vitally important sector is constantly evolving as the hosting cities evolve, the number of passengers increases, and technology develops. Deployment of general digitalization, as well as, problem specific software solutions has become a norm. The arising novel information system development technologies, adapted sensor networks as well as info communication systems and devices renders it possible to implement more complex systems, like urban bus transport networks, as part of smart cities projects. Obviously, each bus transport system has its own peculiarities.

As companies started to focus on and invest in innovative solutions to optimize their services, striving for operational excellence is a general feature of public transportation companies. However, keeping this in a sustainable manner casts an immense burden on the sector players. Cost effectiveness remains one of the most fundamental goals. The major part of the costs of a public transport company arise from their vehicles, including the vehicle fleet, fuel, maintenance costs and drivers' salaries, in other words, a significant fraction of the costs corresponds to the operation of the vehicles, therefore, finding the optimal scheduling of the vehicles is a critical task to be performed. Nevertheless, this optimization problem is an immensely complex issue, including the scheduling of the vehicles and the drivers, while considering all sorts of labor standards etc. These subtasks may already lead to NP hard problems to be solved by themselves. Besides it complexity, it is of importance to note that the surrounding environment can change suddenly, immediately requiring intervention, which may only be realized should an algorithmic solution be available, as background support.

2 Materials and Methods

2.1 Vehicle Scheduling Problems

To overcome the difficulties this discipline has been extensively researched in the past decades, mainly focusing on the mathematical programming models and the corresponding solution of the mathematical models. The single depot vehicle scheduling problem equation was presented in Bodin and Golden [1] and later Bodin [2] presented the problem with minimum two depots, known as a multiple depot vehicle scheduling problem; while Bertossi [3] showed its NP-hardness.

There are applications available for the general cases [4], nevertheless, in practice there are always additional constraints that also have to be taken into consideration, which always bring the solution process to a more cumbersome situation. For example, Kliewer [5] considered the multiple depot vehicle scheduling problem, and assigned buses to cover a given set of timetabled trips with some practical requirements related to vehicle types, depot capacities etc. Later Li and Head [6] considered the bus-scheduling problem and evaluates new types of buses that use alternative energy sources to reduce emissions, including toxic air pollutants and carbon dioxide. Steinzen [7] discussed timetables in ex-urban bus traffic that consist of many trips serviced every day together with some exceptions that do not repeat daily. Dias [8] gave a genetic algorithm to the bus driver scheduling problem, allowing the simultaneous consideration of several complex criteria. Desaulniers and Hickman [9] reviewed state-of-the-art operations research models and approaches for solving public transit problems from the network design point of view. There are several other applicable models and solution methods available, for a detailed overview see [10].

2.2 P-Graph Methodology

The original idea of the P-graph methodology was published by Friedler [11]. This rigorously developed mathematical programming approach was first used to describe chemical engineering problems. The synthesis problem is defined by the (P, R, O) triplet, where P represents the set of products, R represents the set of raw materials and O represents the set of operating units of the problem. First, a directed bipartite graph is used to represent the process system, i.e. operating units serve as one type of the vertices of the graph, while the connecting materials, both raw materials, products and intermediate materials serve as the other type of vertices of the graph. Should a material be consumed or produced by an operating unit, there is a directed connection between the material and the operating unit, i.e. an arc of the graph. Each subgraph of the bipartite directed graph constructed before is a feasible process structure, p-graph in short, if and only if it satisfies the following axioms, representing necessary and sufficient combinatorial properties. Please note that the largest p-graph is called to be the maximal structure, while all other p-graphs are called to be solution structures. The axioms are as follows: (S1) Every final product is represented in the subgraph. (S2) A material type node in the subgraph has no input if and only if it represents a raw material. (S3) Every operating unit type node in the subgraph represents an operating unit defined in the synthesis problem. (S4) Every operating unit type node has at least one path leading to a product in the subgraph. (S5) If a material type node belongs to the subgraph it has to be an input to or an output from at least one operating unit type node in the subgraph. One of the main advantage of this methodology is that the maximal structure, as well as, all feasible solution structures can be algorithmically generated, i.e. MSG generates the maximal structure and SSG generates the solution structures, see [12]. The recursive algorithm exploits the advantages of a decision mapping, i.e. for a given material it is decided which operating units take part in the production of this given material and which operating units are excluded. Throughout the decision process, consistency has to be guaranteed, specifically, should an operating unit be excluded from the solution based on the decision at a given material, this operating unit cannot be chosen to be included in the solution later on based on the decision at another material. Moreover, should an operating unit be part of the solution structure, all of its input and output materials have to be included in the structure. With these algorithms all structures can be generated for the defined synthesis problem, that can be potentially optimal according to the objective.

The p-graph methodology is now used in various fields. For example, separation network synthesis problems with multiple feed streams and sharp separators were considered by Kovacs [13] and [14]. Bertok [15] investigated optimal design of supply chains. Barany [16] solved vehicle assignment problems to minimize cost and environmental impact of transportation. Garcia-Ojeda [17] solved the routing and scheduling of evacuees, facing a life-threatening situation. Lam [18] presented an extended implementation of the p-graph for an open structure biomass network synthesis. Tick [19], and [20] investigated workflow problems which were extended in the direction of business process modelling, called to be the robust Process Network Synthesis (PNS) problem by Almási [21]. An organization-based multi-agent system is modelled according to the framework of Organization Model for Adaptive Complex Systems and this design model is transformed into a process-network model by Garcia-Ojeda [22]. Heckl [23] considered multi-period operations, while Atkins [24] used the p-graph methodology to investigate economically feasibility of utilizing various wood processing residues in bio refineries. Vincze [25] transformed CPM problems to p-graphs to handle alternatives within one step. Ercsey [26] solved a clothing manufacturer's problem with p-graphs. Benjamin [27] proposed a methodology for criticality analysis of component units or plants in an integrated bioenergy system to increase the robustness against disruptions. Aviso [28] considered multi-period optimization of sustainable energy system to contribute reduction in greenhouse gas emissions.

2.3 Problem Definition

The organization and control of urban transport that system planners and transit operators have to cope with is immensely complex. Obviously, each country and city has its own peculiarities, and the resulting protocols may vary widely. The present paper considers bus transport problems from a novel point of view, namely the solution is based on the p-graph methodology, considering the below problem definition.

Timetables of buses highly depend on the specialties of the considered city, namely geographic locations, roadmaps, workplace distributions, residential densities of various districts, performance and disposition of other types of transport systems, passenger habits, as well as, social considerations have to also be taken into account. In this particular case, let us consider the timetable of buses as preliminary given, and the goal is its realization. Obviously, this primary goal has to be completed with optimality in a sense of economy, pollution, sustainability, rules and regulations etc.

Let us consider the situation, where the departure station and the terminal station are given together with the driving time of the bus within a turn. Other type of times should also be given beside the driving time of the turn, for example, time for technical tasks, changeover time, etc. Obviously, these types of times are important from the operation point of view, therefore exact values have to be precisely known, however, these are constant values, therefore their separate management is less important from the synthesis point of view, as it is discussed in details later.

Should the timetable be given, various parts of the day can be clearly identified when the launching density of the buses is the same, these will be considered as periods of the problem. Moreover, based on the timetable, the number of turns to be performed can also be calculated. Obviously, the size of the bus fleet, i.e. the number of buses is also known and it is assumed that there is a driver available for each bus. Moreover, it is assumed that changeover may occur once a day, in other words, the given driver may optionally leave the bus and hand it over to another driver. Labor standards and rules should also be considered. One of the simplest rules from the standards point of view is the minimal and maximal limit for the daily working hours. Rest period should be considered once a day in a way that the continuous driving time must not exceed a given number of working hours. Rest and changeover may only take place at the departure station. Time constants for the technical tasks are also assumed to be given, i.e. exact times for the stance, when the bus leaves the garage, entering the garage, changeover and discharge are given.

In summary:

- Periods, $P_1, P_2, \ldots, P_s$
- Number of turns to be performed during the periods, $r_1, r_2, \ldots, r_s$
- Launching density within a period, in minutes, $t_1, t_2, \ldots, t_s$
- Driving time within a route, in minutes, T
- Number of buses, B
- Number of drivers, D
- Time for the rest period, in minutes, RT
- Time for changeover, in minutes, HT
- Time for discharge, in minutes, LT
- Time for stance, in minutes, ST
- Time for entering the garage, in minutes, GT

- Minimum working hours, in minutes, NWH
- Maximum working hours, in minutes, XWH
- Minimum working hours to rest, in minutes, RWH

Beside the mandatory goal, namely, that the timetable should be fulfilled, some other type of goals may also be solved, for example, the mandatory goal should be solved with a minimal number of buses or a minimal number of drivers etc. This extension will be explained in detail in the the mathematical model of this paper.

3 Results

3.1 Solution Framework

The bus transport optimization and resource allocation problem specified in the previous section is proposed to be solved by an algorithmic method with three main phases as follows. Details of the phases are given in the following chapters of the paper with the focus on the synthesis part.

First phase: the structural model of the problem is generated. here a p-graph, namely the maximal structure of the problem is generated and the parameters of the arcs and nodes are set.

Second phase: the feasible solution structures are generated. here exploiting the peculiarities of the current problem, ssg algorithm is modified to enumerate all potentially feasible solution structures. for each solution structure, the corresponding mathematical programming model is generated, which contains linear constraints and it is mixed integer linear programming (milp) in case the considered cost function is linear and nonlinear programming (nlp) in case the considered cost function is nonlinear.

Third phase: the launching table of the buses including a scheduling is generated for the original problem. based on the solutions of the mathematical programming models generated in the second phase a scheduling algorithm generates the launching table of the buses.

3.2 Bus Transport Process Network, Concepts and Definitions

The p-graph framework aims to solve optimization problems from the synthesis point of view, originating in the chemical engineering industry. The terminology used related to the nodes and arcs also reflects these origins, i.e. the nodes of the bipartite, directed p-graphs are called to be of material types and of operating units; moreover, their operating rules also correspond to this interpretation. As graphs can be understood better and faster than mathematical equation, complex problems can be surveyed more easily when graphs illustrating them. In addition to the easier understanding, graphs serve as essential background for the algorithmic generation of mathematical models. In this paper, the p-graph methodology is applied to model, manage and optimize urban bus transport with respect to specific circumstances. Here, material type nodes are interpreted as some given states, or occurrence of some events (the bus is in the station), or a resource (time, driver, bus), or a physical object (garage). The operating unit type nodes are interpreted as some given activities (stance) or some transition between two states; moreover, this type of node may identify an activity which triggers an event or on the other hand, prevents another event from occurring. The operating unit type nodes for the current interpretation are as follows see Figure 1, represented horizontal bar.

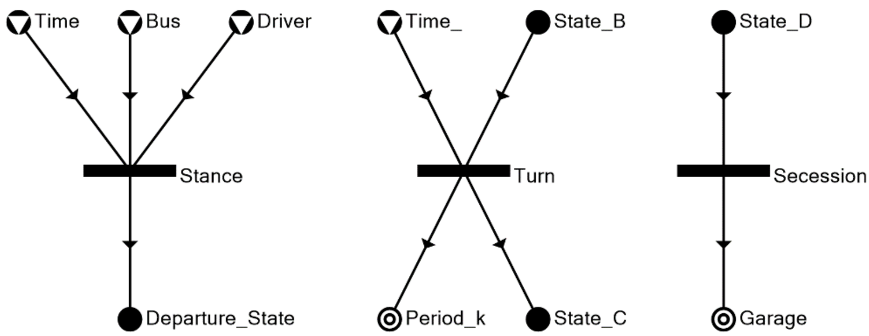

Figure 1

Operating units Stance, Turn and Secession of bus transport process networks

Stance: This operating unit type node represent the activity when a driver takes the bus from the garage to the departure station in *ST* minutes, i.e. from the driver's working hours point of view *ST* minutes is spent, i.e. the very event occurs that the z^{th} bus is driven by the k^{th} driver and they both get to the departure station, Departure_State event occurred.

Turn: This operating unit type node represents that a given bus and the corresponding driver left the departure station, went all the way to the terminal station and then returned from there back to the departure station, while obviously routed all intermediate stations in both directions. In other words, the state of the system has changed, i.e. the system transited from *State_B* to *State_C*, while *T* minutes passed from the available working hours of the driver; moreover, a turn is also performed in the k^{th} period. The period is again a material type node, moreover it is a product, since the timetable is prescribed by the problem definition, and as a result it is calculated how many turns have to be performed within a period.

Secession: Entering the garage, i.e. opposite to stance. This operating unit type node represents bus and the corresponding driver that returns to the garage, the

Garage event occurs and the overall process ends. Garage event is a material type node, moreover it is a product, since it serves as the desired aim to be achieved by the buses. Obviously, this activity may only happen should the given bus together with its driver(s) performed its daily tasks as well as the corresponding labor standards including the rest criteria were also satisfied.

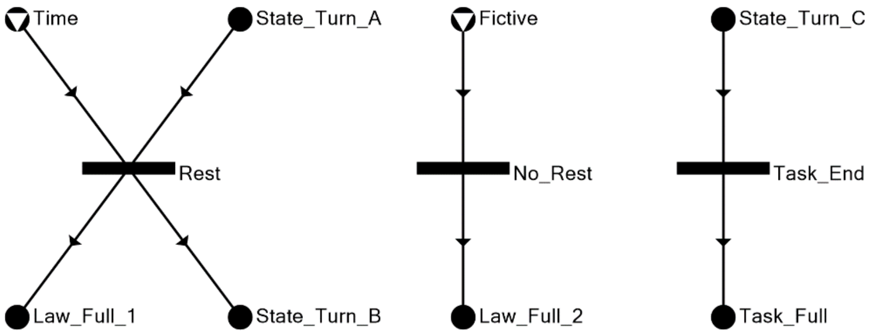

Figure 2

Operating units Rest, No_Rest and Task_End of bus transport process networks

Rest: This operating unit type node represents that a bus and the corresponding driver are at the departure station and the driver rests: after a performed number of turns (*State_Turn_A*) the driver pulls over and rests. This happens according to the labor standards and time regulations. The driver has to work minimum time to receive the right for rest, i.e. *RWH* has to be satisfied. The resting time, *RT* minutes, counts into the overall working hours of the driver. Should a driver rest, the corresponding labor standard is satisfied *Law_Full_1*. When the rest is over, the driver returns to the departure station (*State_Turn_B* occurs) and performs further turns. The operating unit Rest in the current interpretation is depicted in Figure 2, represented by a horizontal bar.

No_Rest: This operating unit type node represents the situation when the length of the working hours does not reach the limit, *RWH*, when rest time should be given to the driver. In other words, the given bus and the corresponding driver will return to the garage and finish work without a rest. Obviously, labor standards are met in this particular case also *Law_Full_2*. To meet the requirements of the axiom system, a raw material, Fictive, must be added to the p-graph. The operating unit No_Rest in the current interpretation is depicted in Figure 2, represented by a horizontal bar.

Task_End: This operating unit type node represents that a given bus and the corresponding driver are at the departure station and prepares to drive back to the garage to discharge and finish work. The operating unit Task_End in the current interpretation is depicted in Figure 2, represented by a horizontal bar.

Changeover: This operating unit type node represents that a given bus and the corresponding driver are at the departure station and the driver finishes work and hands the bus over to a new driver, who starts his work as if this was a stance within the garage. Please note that each driver has his/her own time frame therefore separate input material *Time* is part of the graph. The operating unit Changeover in the current interpretation is depicted in Figure 3, represented by a horizontal bar.

The material type nodes, namely raw materials for the current interpretation are as follows.

Time: This material type node represents the available working hours, the assigned parameter is the length of the working hours in minutes. Its minimal value is *NWH*, while its maximal value is *XWH*.

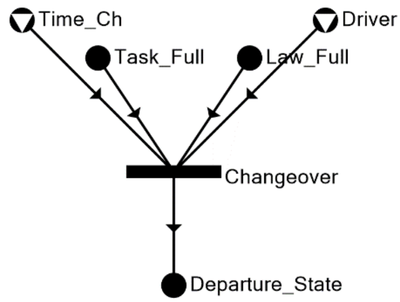

Figure 3

Operating unit Changeover of bus transport process networks

Bus: This material type node represents the available bus fleet, the assigned parameter is the number of buses, i.e. B.

Driver: This material type node represents the available drivers, the assigned parameter is the number of staff, i.e. D.

The material type nodes, namely products for the current interpretation are as follows.

Garage: This material type node represents the garages. This garage node has to be represented in the p-graph as many times as many garages are within the network of the buses. It is a product, since the process ends here and obviously, all buses have to return to one of the garages.

Period: This material type node represents the various periods identified within the timetable, each period is a product node. The assigned parameter is the number of turns to be performed within the period. Obviously, this has to be achieved.

Further nodes of the material type, which are neither raw materials, nor products for the current interpretation are as follows.

Departure_state: This material type node represents the state when a given bus and the corresponding driver are at the departure station and ready to perform turns.

State_Turn: This material type node represents the state when a given bus and the corresponding driver during the working hours are at the departure station and ready to i) perform further turns, ii) finish work, iii) go to rest or iv) perform a changeover.

Task_Full: This material type node represents the state when a given driver fulfilled his duties received for the day. After this state the driver either drives the bus to the garage for secession, or hands over the bus to another driver, for changeover. Please note that each driver corresponds to one and only one *Task_Full* node.

Law_Full: This material type node represents the labor standards corresponding to the working hours. Please note that each driver corresponds to one and only one *Law_Full* node.

Now following the p-graph methodology, the maximal structure is to be generated and then all different and feasible solution structures are to be derived. Essentially, during the generation of the p-graphs a relaxation of the original problem is performed, since only the main conditions are considered. For example, it is considered whether the rest is given or not, i.e. satisfying the labor standards, but the details of the rest are not yet considered, i.e. its exact rest duration, starting conditions etc. are not yet verified. These additional conditions will be handled in the second phase. Therefore, it may happen that a subgraph will be accepted as a feasible solution, but further on, for example in the second phase when further constraints are also added to the mathematical programming model, it turns out that this p-graph is infeasible from the original problem point of view. Conversely, it has to be clear that in this phase no structures are excluded which may result the correct solution of the original problem.

The result of the first phase is the generated maximal structure for the bus transport process network problem. The maximal structure of the following bus transport process network synthesis problems are given: a one period and one bus without changeover problem in Figure 4, a one period and one bus with changeover problem in Figure 5, and a two period and one bus without changeover problem in Figure 6.

When the aforementioned maximal structure is available for the problem, all feasible solution structures can be generated in the second phase. An early process, i.e. the *SSG* algorithm has been developed by Friedler [11] to generate these structures. To exploit all peculiarities of the current problem, it is advisable to extend the axiom system of the general p-graphs, therefore axiom (S6) is constructed and added to the set of axioms:

(S6) The IN degree, as well as the OUT degree is only one for all material type nodes, representing neither a raw material, nor a product.

Based on the set of axioms extended with axiom (S6) algorithm *SSG* is modified to exploit this special feature. A feasible solution of one bus and one period problem generated by the algorithm is given in Figure 7.

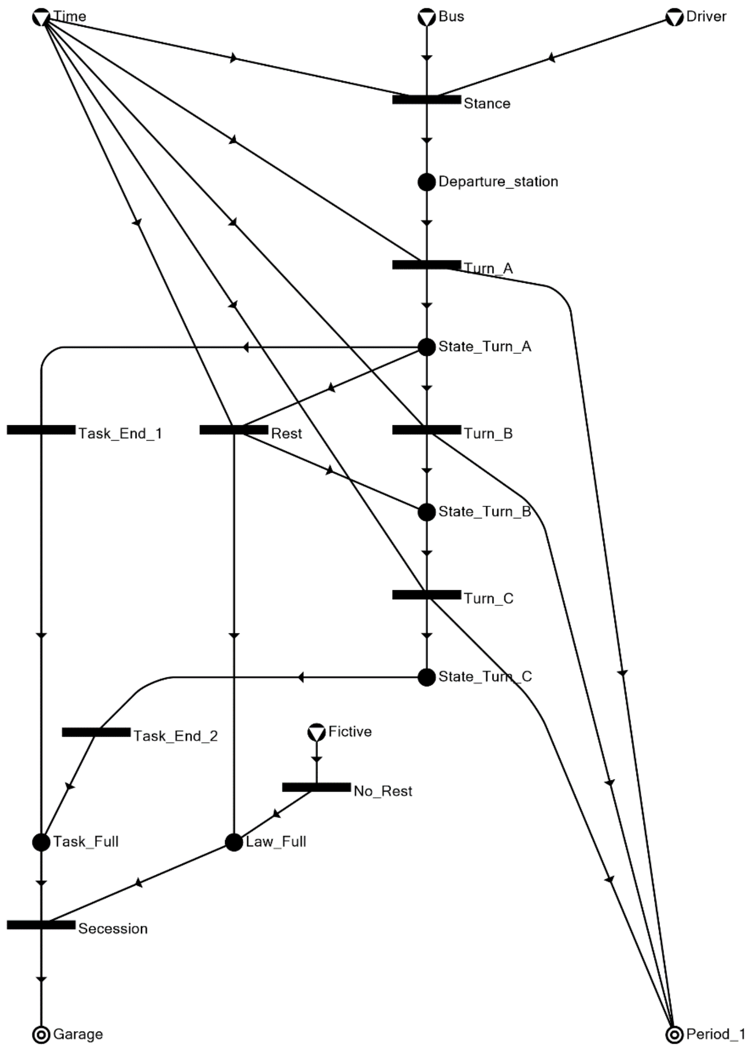

Figure 4

Bus transport process network synthesis

Maximal structure for a one period and one bus without changeover problem

The axiom reflects the following consideration. In reality, i.e. in a feasible solution structure any state should have only one predecessor, and similarly any state should have only one successor. See for example *State_Turn_*A in Figure 4, where the driver has various options: continue the turns: *Turn_B*, go to rest: Rest, or finish work: *Task_1_End*, but from all these options, obviously only Rest will be realized, see Figure 7.

3.3 Mathematical Programming Model

In the previous chapters it is illustrated, how the potentially feasible solution structures of a bus transport process network synthesis problem are developed. As mentioned before, these solution structures serve as relaxed solutions of the original problem, since some specific prescriptions are not yet considered.

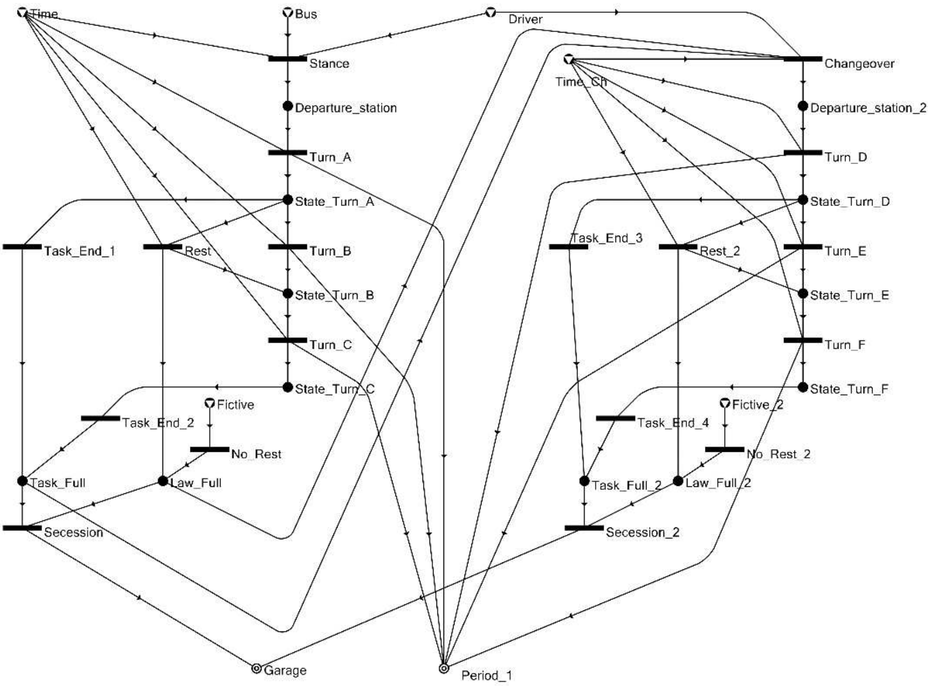

Figure 5

Bus transport process network synthesis.

Maximal structure for a one period and one bus with changeover problem

For example, the length of the rest period, when the rest may be taken and when it should be taken, the lengths of the working hours etc. are not considered with exact values when these solution structures are generated. The corresponding constraints will be satisfied through the MILP or NLP mathematical programming models assigned to the solution structures. Obviously, at this point, it may also turn out that there is no solution, i.e. the given solution structure together with the assigned mathematical programming model has to be discarded, and the next solution structure has to be considered.

Let *G* bipartite, directed graph be a solution structure generated by the modified SSG algorithm consider for example the network in Figure 7. Let an index set be generated, i.e. a non-negative integer is assigned to each node of the maximal structure.

One type of the constraints corresponds to maximal number of turns performed by every driver in every period at the nodes type *Turn_A*, *Turn_B*, *Turn_C*. The x_{ijA}, x_{ijB}, x_{ijC} non negative integer variables are assigned to these nodes, where *ijA* index corresponds to the variable representing the i^{th} driver, in the j^{th} period's *Turn_A*.

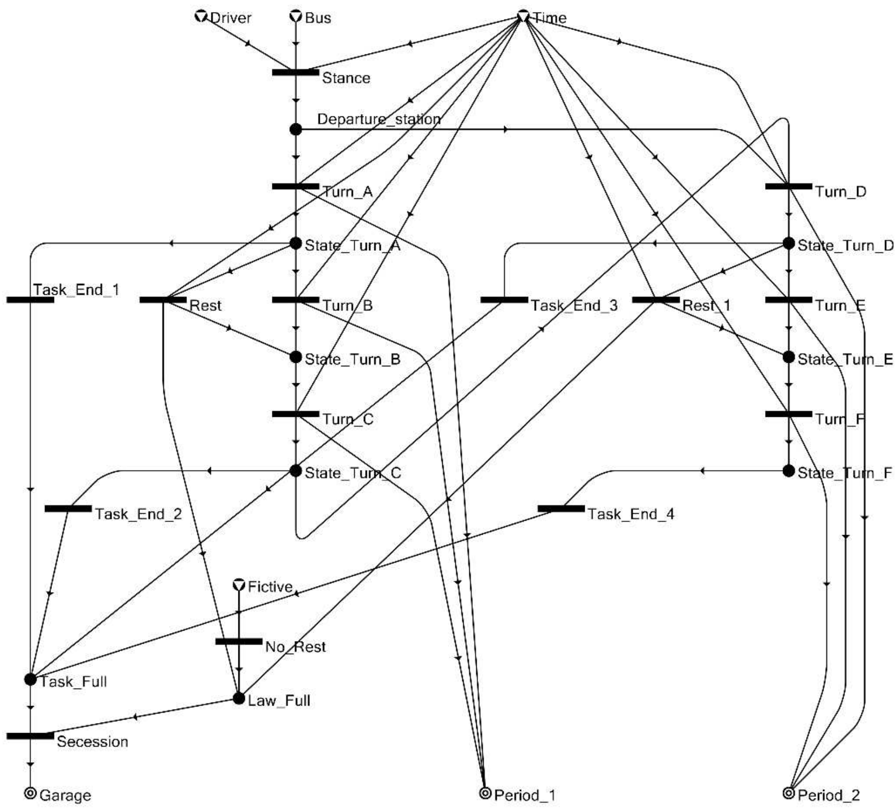

Figure 6

Bus transport process network synthesis

Maximal structure for a two period and one bus without changeover problem

Should the I^{th} driver rest in the j^{th} period, then p_{ij} binary variable is one, otherwise it is zero, which can be seen from the solution structure.

$$p_{ij} \cdot RT + T \cdot (x_{ijA} + x_{ijB} + x_{ijC}) \leq (r_j - 1) \cdot t_j + T \tag{1}$$

equation (1) describes the obvious expectation that the length of the period cannot be shorter than the number of turns performed by the driver multiplied by the driving time of the bus within a turn, plus the time for the potential rest period. This inequality has to be given for each *ij* pairs which are included in the solution structure.

The minimal and maximal length of the working hours are also specified by the original problem. Should the solution structure under consideration contain no changeover, then the corresponding inequalities are specified in the following way, see equation (2) and (3). These inequalities have to be given for each driver without changeover.

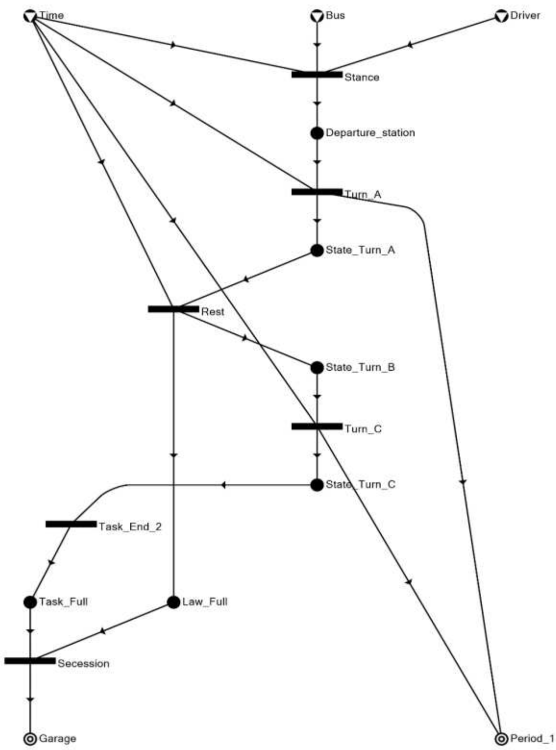

Figure 7
Bus transport process network.
A feasible solution of one bus and one period problem

$$ST + GT + RT \cdot \sum_{j=1}^{s} p_{ij} + T \cdot \sum_{j=1}^{s} (x_{ijA} + x_{ijB} + x_{ijC}) \leq XWH \tag{2}$$

$$ST + GT + RT \cdot \sum_{j=1}^{s} p_{ij} + T \cdot \sum_{j=1}^{s} (x_{ijA} + x_{ijB} + x_{ijC}) \geq NWH \qquad (3)$$

Should the solution structure contain a changeover, and it is considered exactly at the i th driver in the k th period after the state *State_Turn_B*, then the following inequalities have to be given for the driver who started from the garage, equation (4) and (5). Obviously, these inequalities have to be given for each driver where changeover takes place.

$$ST + RT \cdot \sum_{j=1}^{k-1} p_{ij} + T \cdot \sum_{j=1}^{k-1} (x_{ijA} + x_{ijB} + x_{ijC}) + x_{ijA} + x_{ijB} \leq XWH \qquad (4)$$

$$ST + RT \cdot \sum_{j=1}^{k-1} p_{ij} + T \cdot \sum_{j=1}^{k-1} (x_{ijA} + x_{ijB} + x_{ijC}) + x_{ijA} + x_{ijB} \geq NWH \qquad (5)$$

On the other hand, the other part of the changeover situation, i.e. the case of the new driver, has the following inequalities, equation (6) and (7).

$$HT + RT \cdot \sum_{j=k+1}^{s} p_{ij} + x_{ikC} + T \cdot \sum_{j=k+1}^{s} (x_{ijA} + x_{ijB} + x_{ijC}) \leq XWH \qquad (6)$$

$$HT + RT \cdot \sum_{j=1}^{k-1} p_{ij} + x_{ikC} + T \cdot \sum_{j=1}^{s} (x_{ijA} + x_{ijB} + x_{ijC}) \geq NWH \qquad (7)$$

With the help of the above equation minimal and maximal length of the driving times for both drivers are specified. This inequality has to be given for each driver.

Let the non-negative, real variable w_{ij} for every driver and every period be given to illustrate the waiting time of the given driver in the given period, see equation (8).

$$w_{ij} = (r_j - 1) \cdot t_j - (x_{ijA} + x_{ijB} + x_{ijC}) \cdot T - p_{ij} \cdot RT \qquad (8)$$

Now, the cost function of the mathematical programming model can be given, which in this particular case corresponds to the effectiveness of the human workforce, i.e. minimizing the overall waiting time of the drivers, see equation (9).

$$\sum_{i} \sum_{j} w_{ij} \quad \rightarrow \quad min \qquad (9)$$

Obviously, the above given cost function may be extended or changed according to the desired goal. In some cases, the target to be optimized can even be specified directly from the solution structure; for example, in cases where the number of buses or the number of drivers are to be minimized. If so, the inequality system is to be solved in order to guarantee whether the solution is feasible or not, moreover, to determine the values of all the variables.

4 Discussion

As a result of the previously described method, namely when a solution of the assigned mathematical programming model is generated, the only remaining step is the generation of the actual bus launching list, i.e. creation of the bus schedule. As an advantage of the structural representation, this is a tightly constrained problem. It is tightly constrained, in the sense that each period is to be sharply separated, the turns are given for the buses separately, and the corresponding times are given separately.

Conclusion

Determination of the optimal solution of a complex system is a cumbersome task. In general, methods focus on the automatic generation of the mathematical programming model, with an immense number of variables. The classical process network synthesis originating in the chemical industry proved that should the focus be on the synthesis step, i.e. should the first step of the solution method be the exact generation of the potentially feasible process structures, then the resultant mathematical programming model together with its solution can be generated with relative ease. In this paper the urban bus transport process network synthesis problem is presented as a novel application of the classical p-graph methodology. First, the urban public transport is briefly reviewed, then the vehicle scheduling problems and the methodology are discussed. The model is focusing on the synthesis step of the problem solution. Both the concept, notations, definitions, axioms and algorithms are applied to exploit the peculiarities of the problem, i.e. the bus transport process network is defined. The meaning of the material type nodes and the operating unit type nodes are described in details. A new axiom is given to complete the set of classical p-graph’s axioms. The mathematical programming model of the bus transport process network is detailed resulting in the schedules. This mathematical programming model can algorithmically be produced from the generated solution structures. The presented solution method prepares the generation of the bus launching list, i.e. the solution of the bus scheduling problem can be achieved with relative ease due to the resultant tight conditions. This novel approach can be used to solve real-world problems with the existing constraints. Research on advanced process network synthesis for transport management systems proves to be a relevant area of further examinations. The expected results hold the promise to improve the operational planning activities of public transport systems.

References

[1] Bodin, Lawerence and Golden, Bruce. Classification in vehicle routing and scheduling. Networks, 11(1) pp. 97-108, 1981

[2] Bodin, Lawerence, Golden, Bruce, Assad, Arjang, and Ball, Mark. Routing and scheduling of vehicles and crews: The state of the art. Computers and Operations Research, 10(1) pp. 63-212, 1983

[3] Bertossi, Alan A, Carraresi, Paolo, and Gallo, Giorgio. On some matching problems arising in vehicle scheduling models. Networks, 17(1) pp. 271-281, 1987

[4] Meilton, M.: Selecting and implementing a computer aided scheduling system for a large bus company, Algorithms: Combinatorial Analysis. In Computer-Aided Scheduling of Public Transport, (eds. S. Voss and J. R. Daduna), 203-214, Springer-Verlag, Berlin, 2001

[5] Kliewer N., T. Mellouli, and L. Suhl. A time-space network based exact optimization model for multi-depot bus scheduling, European Journal of Operational Research, 175, pp. 1616-1627, 2006

[6] Li, J-Q and K. L. Head: Sustainability provisions in the bus-scheduling problem, Transportation Research, Part D, 49, 50-60, 2009

[7] Steinzen I., L. Suhl, N. Kliewer: Branching Strategies to Improve Regularity of Crew Schedules in Ex-Urban Public Transit. OR Spectrum (2009) 31: 727. DOI 10.1007/s00291-008-0136-5

[8] Dias, T. G., JP de Sousa, and JF Cunha. Genetic algorithms for the bus driver scheduling problem: a case study. Journal of the Operational Research Society, 53 (3), pp. 324-335, 2002

[9] Desaulniers, G. and M. D. Hickman: Public Transit, In Handbook in OR & MS, (eds. C. Barnhart and G. Laporte), Vol. 14, Chapter 2, Elsevier B.V., 2007

[10] Bunte, Stefan and Kliewer, Natalia. An overview on vehicle scheduling models. Journal of Public Transport, 1(4) pp. 299-317, 2009

[11] Friedler, F., K. Tarjan, Y. W. Huang, and L. T. Fan. Combinatorial Algorithms for Process Synthesis, Computers Chem. Engng, (1992b) 16, S313-320

[12] Friedler, F., K. Tarjan, Y. W. Huang, and L. T. Fan. Graph-Theoretic Approach to Process Synthesis: Axioms and Theorems, Chem. Engng Sci., (1992a) 47, 1973-1988

[13] Kovacs Z, Z Ercsey, F Friedler and L. T. Fan, Exact super-structure for the synthesis of separation-networks with multiple feed-streams and sharp separators; (1999) Computers and Chemical Engineering 23:(Supplement 1) pp. S1007-S1010

[14] Kovacs Z, Z. Ercsey, F. Friedler, L. T. Fan. Separation-network synthesis: global optimum through rigorous super-structure. (2000) Computers and Chemical Engineering 24:(8) pp. 1881-1900

[15] Bertok, B., R. Adonyi, F. Friedler. Optimal Design of Supply Chains by the P-Graph Framework. Computer-Aided Chemical Engineering, 25: pp. 1445-1450 (2009)

[16] Barany, M., B. Bertok • Z. Kovacs, F. Friedler • L. T. Fan. Solving vehicle assignment problems by process-network synthesis to minimize cost and environmental impact of transportation. Clean Techn Environ Policy. (2011) DOI 10.1007/s10098-011-0348-2

[17] Garcia-Ojeda, JC., B. Bertok, F. Friedler, Planning evacuation routes with the P-graph framework, Chemical Engineering Transactions, (2012) 29, 1531-1536

[18] Lam H. L., J. J. Klemeš, P. S. Varbanov, Z. Kravanja. P-graph synthesis of open-structure biomass networks. Ind. Eng. Chem. Res. (2012) 52, 172-180

[19] Tick, József, Csanád Imreh, Zoltán Kovács, Business Process Modeling and the Robust PNS Problem, Acta Polytechnica, Volume 10, Issue Number 6, (2013) 193-204. DOI: 10.12700/APH.10.06.2013.6.11

[20] Tick, J, P-Graph-based Workflow Modelling, Acta Polytechnica Hungarica, 4:1 pp. 75-88., 14 p. (2007)

[21] Almási, D; Cs, Imreh; T, Kovács; Tick, J, Heuristic Algorithms for the Robust PNS Problem, Acta Polytechnica Hungarica, 11: 4 pp. 169-181, 13 p. (2014)

[22] Garcia-Ojeda, JC; B. Bertok, F. Friedler; A. Argoti, L. T. Fan. A preliminary study of the application of the P- graph methodology for organization-based multiagent system designs: Assessment (2015) Acta polytechnica hungarica 12:2 pp. 103-122

[23] Heckl, I, L. Halász, A. Szlama, H. Cabezas, F. Friedler. Process synthesis involving multi-period operations by the P-graph framework. (2015) Computers and Chemical Engineering 83 pp. DOI 157-164. 10.1016/j.compchemeng.2015.04.037

[24] Atkins, M. J., Walmsley, T. G., Ong, B. H. Y., Walmsley, M. R. W., & Neale, J. R. (2016) Application of P-graph techniques for efficient use of wood processing residues in bio refineries. Chemical Engineering Transactions, 52, 499-504, https://doi.org/10.3303/CET1652084

[25] Vincze, N., Z. Ercsey, T. Kovács, J. Tick, Z. Kovács. Process network solution of extended CPM problems with alternatives, Acta Polytechnica 13:3 pp. 101-117 (2016)

[26] Ercsey, Z. Process network solution of a clothing manufacturer’s problem. Pollack Periodica 12:(1) pp. 59-67 (2017) DOI 10.1556/606.2017.12.1.5

[27] Benjamin, M. F. D., C.D. Cayamanda, R. R. Tan, L. F. Razon. P-graph approach to criticality analysis in integrated bioenergy systems. Clean Techn Environ Policy (2017) 19: 1841-1854. https://doi.org/10.1007/s10098-017-1368-3

[28] Aviso, K. B., J-Y. Lee, J. C. Dulatre, V. R. Madria, J. Okusa, R. R. Tan. A P-graph model for multi-period optimization of sustainable energy systems. (2017) Journal of Cleaner Production. Volume 161, 10 September 2017, pp. 1338-1351, DOI 10.1016/j.jclepro.2017.06.044

A Metaheuristic Approach to the Waste Collection Vehicle Routing Problem with Stochastic Demands and Travel Times

Danijel Marković[1], Goran Petrović[1], Žarko Ćojbašić[1], Dragan Marinković[2]

[1]Faculty of Mechanical Engineering, University of Niš, Department of Transport Engineering and Logistics, Aleksandra Medvedeva 14, 18000 Niš, Serbia, E-mail: danijel.markovic@masfak.ni.ac.rs, goran.petrovic@masfak.ni.ac.rs, zarko.cojbasic@masfak.ni.ac.rs

[2]Technical University of Berlin, Institute of Mechanics, Strasse des 17. Juni, D-10623 Berlin, Germany, E-mail: dragan.marinkovic@tu-berlin.de

Abstract: This paper presents the methodology for solving the municipal waste collection problem in urban areas. This problem is treated as a vehicle routing problem where the demand in nodes and travel times between all pairs of nodes in a transport network are taken as stochastic quantities, known in the literature as the vehicle routing problem with stochastic demands (VRPSD). This problem is formulated as a chance-constrained programming model with normal distribution. Heuristic and metaheuristic methods, as well as their combinations, are applied to efficiently solve this model. Finally, the paper presents a comparative analysis of the obtained results with real data.

Keywords: vehicle routing problem; stochastic demands, waste collection, heuristics and metaheuristics

1 Introduction

The vehicle routing problem (*VRP*) is one of the most challenging problems in combinatorial optimization. This problem was first mentioned in 1959 by Dantzig and Ramser [1]. Since then, the *VRP* has been increasingly applied to solve various problems and it now possesses a great economic importance in the reduction of operating costs in distribution systems. The *VRP* can be defined as a problem of designing routes with the lowest transport expenses for vehicles with known capacities, which travel from a depot to a group of users, who are located in a specific geographic area, with non-negative demands [2]. Here, the basic condition that each user has to be served only once must be met. With the aim of satisfying real problems in solving the *VRP*, usually several constraints are introduced in the problem solving procedure, such as a larger number of depots, different types of vehicles (homogeneous and heterogeneous), different types of customer demands (deterministic and stochastic), infrastructural limitations (one-way streets, prohibited roads), manners in which services are performed (pickup, delivery and mixed), etc. Provided all these constraints are taken into account, it becomes much more complicated to solve the *VRP*. If the demands are deemed deterministic, then the *VRP* can be observed as: capacitated *VRP* (*CVRP*), which is, in fact, the basic *VRP* [3]; distance-constrained capacitated *VRP* (*DCCVRP*) [4]; *VRP* with backhauls (*VRPB*) [5]; *VRP* with time windows (*VRPTW*) [6]; *VRP* with pickup and delivery (*VRPPD*) [7]; *VRP* with backhauls and time windows (*VRPBTW*) [8]. However, in certain cases the demands on the given transport network might be random variables, i.e. the demands are stochastic quantities, so the standard VRP is expanded into a vehicle routing problem with stochastic demands – (*VRPSD*) [9]. Contrary to deterministic demands, examples of stochastic demands are found in various transport activities. This paper examines one of the examples of stochastic demands – municipal waste collection.

In the last several years, numerous researchers have attempted to solve the *VRPSD* by applying heuristic and metaheuristic methods. Thus, Marinakis at al. [10] dealt with solving the *VRPSD* by applying the Particle Swarm Optimization method. They examined a problem where the user demand was a variable with known distribution. Li et al. [11] considered a *VRPSD* with the service time being a stochastic variable with known distribution. They solved this problem by applying the metaheuristic Tabu search. In their paper, Bautista et al. [12] presented the application of heuristic and metaheuristic algorithms for solving the vehicle routing problem in municipal waste collection. They employed the nearest neighbour method and local search to obtain the initial solution, while the additional optimization of routes was performed using the Ant algorithm. The application of this algorithm was tested in solving a real problem for the municipality of Sant Boi de Llobregat, Barcelona. Furthermore, they tested this algorithm on the studies of certain authors and showed that the application of the Ant algorithm yielded the solutions that were 4% better than the ones offered in the analyzed studies. Vera et al. [13] considered a real problem of collecting glass, metal, PET and paper waste disposed of by users in specific locations in a specific area. This problem was presented as a periodic vehicle routing problem. They proposed a hybrid algorithm to solve the problem at hand. The hybridization related to the combination of the nearest neighbour algorithm with the local search algorithm. Applying the proposed algorithm, to certain real problems, led to the savings of around 25%. All of this points to the fact that the *VRPSD* is a pressing problem for researchers, who apply various heuristic and metaheuristic methods, as well as their combinations, with the aim of finding the best solution possible. Heuristic methods tend to find a sufficiently good (satisfactory) solution to the optimization problem in a reasonable time using the "attempts and errors" procedures and represent rules for selecting, filtering, and rejecting the solution.

Unlike heuristic methods, metaheuristic optimization methods are based on the idea that, by imitating nature, what should be looked for is the optimal complex function of several variables that represent the mathematical abstraction of a complex engineering problem [14]. Given the current importance of such problems, this paper examines a problem of optimizing a model for municipal waste collection by applying heuristic and metaheuristic methods. This problem is treated as a *VRPSD* where the demand and the travel time between the pairs of nodes are given as stochastic quantities with normal distribution.

The paper is organized as follows. Section 2 gives the mathematical formulation of the *VRPSD* for municipal waste collection. The model and the method for solving the *VRPSD* are defined in Section 3. The computational results are reported in Section 4. Section 5 concludes the paper.

2 Mathematical Formulation

In practice, municipal waste collection in urban areas can be observed as a vehicle routing problem with stochastic demands. This means that the amount of waste in nodes for the given transport network is a randomly variable quantity. The amount of waste may vary depending on the season and it can be known only after a vehicle arrives at a certain node to be served [15]. For the transport network $G = (V, A)$, where $V=\{1,..., n\}$ is the set of nodes, A is the set of the shortest distances between all pairs of nodes, node "1" represents the depot, while the other nodes are defined by $V=\{2,..., n\}$. The travel time between all pairs of nodes in the transport network and the amount of waste per node are stochastic variables with normal distribution. When determining the optimal routes of vehicles for municipal waste collection for the defined transport network, the following constraints have to be acknowledged:

- there is only one depot and each route begins and ends in that depot,
- the locations of the depot and the nodes are known,
- the amount of waste in each node is a stochastic variable with normal distribution,
- the sum of the amounts of municipal waste in a single route must not be greater than the vehicle capacity,
- the travel time for each arc is a stochastic variable with normal distribution,
- the travel time from node i to node j must not be greater than the route duration time,
- the capacity of the waste collection vehicle is known,
- the route duration time must not be greater than the given route duration time,
- each node must be visited only once.

To define the mathematical formulation of the *VRPSD* the following nomenclature was used:
m – the maximum number of used vehicles, for the *VRPSD* $m = 1$,
n – the number of nodes from which waste is collected,
n_{uk} – the number of nodes in the transport network,
V – the set of nodes, $V=\{1,2,..,n\}$,
V_0 – the depot, the place from which the vehicle departs,
Q – the maximum capacity of the vehicle,
q_i – the demand in the node i, $i \in V$; the demand in the depot is equal to zero. Let us assume that q_i is a stochastic variable with normal distribution,
d_{ij} – the shortest possible distance between node i and node j; $i, j \in V$,
c_{ij} – the transport costs of the vehicle between node i and node j; $i, j \in V$,it is assumed that $c_{ij}=d_{ij}$,
t_{ij} – the vehicle travel time between nodes i and j. Let us assume that t_{ij} is a stochastic variable with normal distribution,
q_{ij} – the capacity of the vehicle after visiting node i, and before visiting node j,
N_k – the number of waste containers per node,
v_{ij} – the vehicle movement speed between node i and node j,
T – the maximum allowed vehicle travel time in route r.
Q_{ij} – the capacity of the vehicle after visiting node i, and before visiting node j,
N_{ki} – the number of waste containers for the node i,
s_i – the time needed to serve node i; $(i \in V)$, i.e. the time needed to empty the waste container in node i,
w_i – the waiting time at the node i.

The decision-making variables:

$$x_{ij} \begin{cases} 1, \textit{ If the vehicle visits node } i \textit{ after node } j \\ 0, \textit{ otherwise} \end{cases} \quad \forall i, j \in V_0$$

$$z_i \begin{cases} 1, \textit{ If the vehicle visits node } i \\ 0, \textit{ otherwise} \end{cases} \quad i \in V_0, k \in m$$

After the introduction of the above nomenclature, the mathematical formulation of the *VRPSD* can be presented in the following manner:

$$\min F = \sum_{i=0}^{n} \sum_{j=0}^{n} d_{ij} \cdot x_{ij} \tag{1}$$

$$\sum_{i=0}^{n} x_{ij} = 1, \quad j = 1,2,\ldots,n \tag{2}$$

$$\sum_{i=0}^{n} x_{ij} - \sum_{i=0}^{n} x_{ji} = 0, \quad j = 0,1,\ldots,n \tag{3}$$

$$\sum_{j=1}^{n} x_{0j} + \sum_{j=1}^{n} x_{j0} = 2z_0 \tag{4}$$

$$P(\sum_{i \in V} q_i \sum_{j \in V} x_{ij} \leq Q\ ) \geq \alpha \tag{5}$$

$$P\left(\sum_{i=1}^{n}\sum_{j=1}^{n} t_{ij} x_{ij} \leq T\right) \geq \alpha \tag{6}$$

$$\sum_{i=0}^{n} w_i \sum_{j=0}^{n} x_{ij} \leq T \tag{7}$$

$$z_i \in \{0, 1\},\ i = 0,1,\ldots, n \tag{8}$$

$$x_{ij} \in \{0, 1\},\ i = 0,1,\ldots, n;\ j = 0,1,\ldots, n \tag{9}$$

The minimization function for the *VRPSD* is shown in equation (1). The constraint presented in equation (2) indicates that each transport network node has to be visited only once, while the constraint defined by equation (3) presents the continuation of the vehicle flow, i.e. the vehicle leaving node j after serving it. The constraint given in equation (4) implies that each vehicle has to begin and end its route in the depot. Observing the chance-constrained (Ch-C) condition assures that the amount of collected waste on the route is smaller than the vehicle capacity with probability α as given in constraint (5). Also, the Ch-C condition ensures that the total vehicle travel time on the route is not shorter than the maximum allowed time on the route, which is presented in equation (6). Constraint (7) makes sure that the waiting time at the node i is shorter than the route duration time. Constraints (8) and (9) define the intervals of variables z_i and x_{ij}. Constraints (5 and 6) can be solved by applying the Ch-C condition. It is assumed that the amount of waste per each node is a random variable with normal distribution, which can be presented as:

$$q_i \sim N(\mu_i\,,\ \sigma_i^2\ ) \tag{10}$$

where μ_i is the total expected amount of waste for the node i, σ_i^2 is the standard deviation (variance) from the amount of waste for the node i. Parameters μ_i and σ_i^2 can be written using expressions (11) and (12):

$$\mu_i = \sum_{i=0}^{n}\sum_{j=0}^{n}\ [E(q_i x_{ij})] \tag{11}$$

$$\sigma_i^2 = \sum_{i=0}^{n}\sum_{j=0}^{n}\ [Var(q_i x_{ij})] \tag{12}$$

where μ_i is the mathematical expectation of normal distribution, while σ_i^2 is the variance, i.e. the normal distribution scaling parameter.

If the expected customer demand is presented in the following way:

$$E(q_i x_{ij}) = \sum_{i=0}^{n}\sum_{j=0}^{n} [E(q_i x_{ij})] - Q \tag{13}$$

and the standard deviation as:

$$Var(q_i x_{ij}) = \sum_{i=0}^{n}\sum_{j=0}^{n} [Var(q_i x_{ij})] \tag{14}$$

using expressions (13) and (14) one can rework the Ch-C condition with constraint (5) into expression (15) [11].

$$P\left(\eta \le -\frac{\sum_{i=0}^{n}\sum_{j=0}^{n} [E(q_i x_{ij})] - Q}{\sqrt{\sum_{i=0}^{n}\sum_{j=0}^{n} [Var(q_i x_{ij})]}} \right) \ge \alpha \tag{15}$$

It is important to emphasize that expression (15) holds if and only if expression (16) holds as well:

$$\Phi^{-1}(\alpha) \le -\frac{\sum_{i=0}^{n}\sum_{j=0}^{n} [E(q_i x_{ij})] - Q}{\sqrt{\sum_{i=0}^{n}\sum_{j=0}^{n} [Var(q_i x_{ij})]}} \tag{16}$$

Expression (16) can be written as a deterministic equivalent:

$$\Phi^{-1}(\alpha)\sqrt{\sum_{i=0}^{n}\sum_{j=0}^{n} [Var(q_i x_{ij})]} + \sum_{i=0}^{n}\sum_{j=0}^{n} [E(q_i x_{ij})] \le Q \tag{17}$$

where Φ is the standard function of normal distribution, while Φ^{-1} is the inverse function of function Φ .

Similarly, it can be assumed for constraint (6) that the travel time between the transport network nodes is stochastic with normal distribution, which can be written as:

$$t_{ij} \sim N(\mu_{ij}, \sigma_{ij}^2) \tag{18}$$

Parameter μ_{ij} defines the travel time from node *i* to node *j* that can be represented as a quotient of the distance between node *i* and node *j* and the vehicle movement speed between node *i* and node *j*, i.e. $\mu_{ij} = \frac{d_{ij}}{v_{ij}}$, while parameter σ_{ij}^2 represents the standard deviation of the travel time from node i to node j. After defining parameter μ_{ij} , the expression of normal distribution can be written as:

$$\mu_{ij} \sim N\left(\frac{d_{ij}}{v_{ij}}, \sigma_{ij}^2\right) \tag{19}$$

If the vehicle travel time on the route is written as:

$$\sum_{i=0}^{n}\sum_{j=0}^{n} t_{ij}x_{ij} - T \tag{20}$$

and the standard deviation from the travel time on the route as:

$$\sum_{i=0}^{n}\sum_{j=0}^{n} \sigma_{ij}^2 x_{ij}^2 \tag{21}$$

then the expression of normal distribution can be written as:

$$N\left(\frac{d_{ij}x_{ij}}{v_{ij}} - T, \sigma_{ij}^2 x_{ij}^2\right) \tag{22}$$

Using expression (22), the Ch-C condition from constraint (6) can be transformed into expression (23) [16].

$$P\left(\eta \le -\frac{\sum_{i=0}^{n}\sum_{j=0}^{n}\frac{d_{ij}x_{ij}}{v_{ij}} - T}{\sqrt{\sum_{i=0}^{n}\sum_{j=0}^{n}\sigma_{ij}^2 x_{ij}^2}}\right) \ge \alpha \tag{23}$$

It is of crucial importance to emphasize that expression (23) holds if and only if expression (24) holds as well:

$$\Phi^{-1}(\alpha) \le -\frac{\sum_{i=0}^{n}\sum_{j=0}^{n}\frac{d_{ij}x_{ij}}{v_{ij}} - T}{\sqrt{\sum_{i=0}^{n}\sum_{j=0}^{n}\sigma_{ij}^2 x_{ij}^2}} \tag{24}$$

Expression (25) can be written as a deterministic equivalent:

$$\Phi^{-1}(\alpha)\sqrt{\sum_{i=0}^{n}\sum_{j=0}^{n}\sigma_{ij}^2 x_{ij}^2} + \sum_{i=0}^{n}\sum_{j=0}^{n}\frac{d_{ij}x_{ij}}{v_{ij}} \le T \tag{25}$$

where Φ is the standard function of normal distribution, while Φ^{-1} is the inverse function of function Φ .

The time spent in nodes (w_i) for the transport network is calculated by multiplying the number of waste containers (N_{ki}) with the waste container emptying time (s_i). It is assumed that the waste container emptying time (s_i) is 4 *min* per container. This time is taken as the average time of the duration of emptying underground containers using a vehicle that possesses a superstructure with a telescopic crane.

3 Defining the Model and Method for the VRPSD

The *VRPSD* model considered in this paper is defined by a transport network that comprises one depot and 29 nodes. The transport network represents "area" 103 according to the division of the territory of the City of Niš by the PUC "Mediana-Niš" [16]. The nodes in the transport network present the locations of the containers as defined by the coordinates, i.e. the latitude and longitude. In the transport network, the first and the final node (the depot) is marked with "1". The other nodes of the transport network are numbered from 2 to 30. To solve the VRPSD, waste containers for municipal waste collection with the capacity of 3 m^3 are installed in the transport network. This model does not consider the optimal locations and the number of containers. The number and location of containers are selected on the basis of the previous positions of waste containers determined by the PUC "Mediana-Niš". On the locations where there are two or more containers, their positions are defined by a single node, i.e. a single coordinate. To solve the problem of location of containers can be used a number of methods [17, 18, 19]. However, in this paper, emphasis is placed on optimizing routes for vehicles and not to determine the locations.

The first step in solving this *VRPSD* is to define the matrix of the travel times between all pairs of nodes in the transport network (t_{ij}). This matrix is defined by using the matrix of shortest distances. The latter matrix represents the shortest distances between all pairs of nodes (d_{ij}) for the transport network. The next step in defining matrix t_{ij} is to divide all the members of matrix d_{ij} with the average movement speed of the municipal waste collection vehicle in the transport network (v_{ij}). The value of the average vehicle movement speed for the solution of the *VRPSD* is 0.48 *km/h*. This data was acquired from the PUC "Mediana-Niš". For the optimization of the routes for the *VRPSD*, the maximum vehicle capacity is 60 m^3. The maximum allowed route duration time is 100 *min*. In addition to the constraint related to the duration of all routes, there is also the time needed for the vehicle to reach the landfill from the depot, empty its load and return to the depot. The approximate time needed by the vehicle to reach the landfill from the depot, dispose of the collected waste and return to the depot is around 50 *min* [20]. Thus, when all these times are summed up, the time of the duration of one shift, i.e. 480 *min*, must not be exceeded. The next step in solving the *VRPSD* is the formulation of the initial solution. Bearing in mind that this is a problem with a stochastic amount of municipal waste per node and a stochastic travel time between transport network nodes, and in line with the previous explanation, the problem is reduced to solving a deterministic problem by applying expressions (16, 17, 24 and 25). The initial solution is obtained by applying the C-W savings algorithm. This solution is improved by using the 2-*OPT* local search algorithm and the improved harmony search algorithm (*IHSA*).

3.1 Stochastic Simulation for Computing the Expected Value and Probability Check

The first step in the optimization of the *VRPSD* is to compute the expected value of the amount of municipal waste (μ_i) and check the probability (β). This step is necessary due to the stochastic character of the amount of municipal waste per transport network node. Based on the input data on the assessed amount of waste per node, one can compute the expected values of the amount of municipal waste (μ_i) for each node of the transport network since the distribution is known, i.e. normal distribution. After the expected value of the amount of municipal waste is computed, the variance (σ_{ij}^2) is computed as well. Procedure 1 was used to compute the mathematical expectancy and variance, and its pseudo code is shown in Algorithm 1 [21].

***Algorithm 1*: Procedure 1**

```
Start
        Define the assessed amount of waste per transport network node;
        DefineQ;
        for n = 1; n ≤ n_uk; n = n + 1;
           sum_n = 0;
          for i =1; i ≤ 10; i = i + 1;
                    sum_n = sum_n + q_ni;
                    p_i = q_ni / sum_n:
          end for
        end for
        for  n = 1; n ≤ n_uk; n = n + 1;
          compute E_n;
          compute σ_n;
          compute Φ_(α);
          if Φ_(β) ≤ (E_n − Q) / √σ_n
                    probability condition = TRUE;
          else
                    probability condition = FALSE;
          end if
        end for
end
```

When these two parameters are computed, then the probability (β) is checked. Algorithm 1 presents the procedures to check the probability. The last step in this procedure is the checking of the Ch-C condition, and if this condition is met, the procedure continues (TRUE). In the opposite case the procedure is stopped (FALSE). The nomenclature used to define the Procedure 1 pseudo code is:

sum – the sum of the amounts of waste per transport network node, i – the number of intervals of monitoring the amount of waste assessment per transport network node, q_{ni} – the assessed amount of waste in the node, P – the probability.

3.2 Initial Solution

The next step in the *VRPSD* optimization is the formation of the initial solution. Bearing in mind that this is a stochastic problem, in line with the previous explanation, the problem is reduced to the solution of the deterministic problem by applying expressions (16, 17, 24 and 25). The C-W savings algorithm was used to obtain the initial solution. In the application of the C-W savings algorithm parameter q_i was substituted with parameter μ_i . Procedure 2 presents the pseudo code for the C-W savings algorithm (Algorithm 2).

***Algorithm 2*: Procedure 2**

```
start
        Define distance matrix;
        Define time matrix;
        Define Q;
        Define T;
        Call Procedure 1;
        Compute s';
        Sort s' in a non-increasing sequence;
        Form a partial route;
        Expected demand = μi;
        Expected time at the arc = tij + wi;
           for all savings from sequence
              if (probability condition == TRUE)
                 if met operative constraints
                    if Expected demand + μi ≤ Q
                       if Expected time at the arc + (tij + wi) ≤ T
                             Expected demand = μi + Expected demand;
                             Expected time at the arc = (tij + wi) + Expected time at
                             the arc;
                             Form route
                       end if
                    end if
                 end if
              end if
           end for
```

```
        Vehicle fullness = Expected demand;
        Print routes;
        Print vehicle fullness;
end
```

3.3 2-OPT Search and Improved Harmony Search Algorithm for the VRPSD

The first improvement of the initial *VRPSD* solution was performed by applying the 2-*OPT* local search. During the improvement of the initial solution, the number of iterations was varied (1e3 and 1e6). The initial solution was improved by applying the 2-*OPT* local search algorithm. The pseudo code of the 2-*OPT* algorithm for the improvement of the initial solution is presented in Algorithm 3.

***Algorithm 3*: 2-*OPT* algorithm for the improvement of the initial solution**

```
start
      Load initial solution U0;
      U0 = initial route length;
        for (i = 1; i ≤ n - 2; i = i + 1)
          for  (j = i + 2; j ≤ n; j = j + 1)
            U' = d(i, j) + d(i+1, j+1) - d(i, i+1)- d(j, j+1);
            if (U'< U)
              U' = U;
            end if
          end for
        end for
end
```

The next algorithm used to optimize the *VRPSD* was the *IHSA*. The solution obtained by applying the *IHSA* largely depends on adjusting the parameters of the algorithm itself. However, this paper does not consider the selection of optimal parameters for the given problem but uses the recommended parameters. The parameters of the *IHSA* used to solve the *VRPSD* are [22]: harmony memory size – *HMS* = 10; harmony memory consideration rate – *HMCR* = 0.95; pitch adjustment rate – PAR_{min} = 0.1; PAR_{max} = 0.85; bandwidth – bw_{min} = 0.001; bw_{max} = 0.8; number of improvizations – *NI* = 1e3.

***Algorithm 4*: IHS algorithm for the improvement of the initial solution**

```
      Load initial solution U0;
      Define IHS algorithm parameters;
      Best solution = U;
```

```
Harmony memory initialization;
Update best solution;
Best solution = U;
    for j = 1; j < NI; j = j + 1;
        for i = 1; i < NI; i = i + 1;
            if (rand < HMCR)
              U1 = int(rand * HMS)+1;
              U2 = HM (U1, i);
              new solution(i)  = U2;
                  if (rand < PAR)
                      if  (rand < 0.5)
                         U3 = new solution(i) + rand * bw;
                             if (PVB_lower(i) ≤ U3)
                                new solution(i) = U3;
                             end if
                      else
                         U3 = new solution(i) + rand * bw;
                             if (PVB_lower(i) ≥ U3);
                                new solution(i) = U3;
                             end if
                  end if
            else
              new solution(i) = randval(PVB_lower(i), PVB_upper(i));
            end if
        end for
          Update harmony memory;
    end for
end
```

4 Computational Results

The application of the C-W savings algorithm to the solution of the *VRPSD* yielded four routes, and this solution represented the initial solution. This solution was improved by applying the 2-*OPT* local search algorithm and the *IHSA*. The initial solution was improved by applying the 2-*OPT* local search algorithm. The application of the 2-*OPT* local search algorithm led to the improvement of the initial solution in the sense of the reduction in the number of routes, which in turn resulted in the reduction in the total route duration time. The application of the 2-*OPT* local search algorithm yielded three routes with the total route duration time of 244.48 *min*. Figure 1 shows the appearance of the transport network routes.

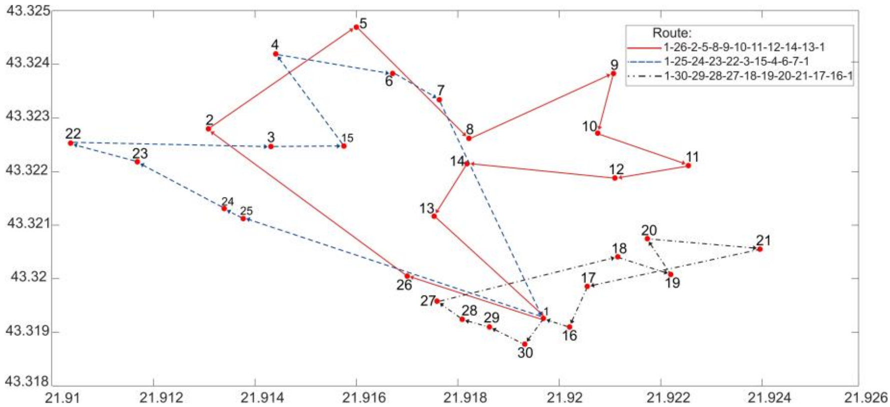

Figure 1

Graphic representation of the *VRPSD* routes obtained by the 2-*OPT* search algorithm

The application of the *IHSA* also led to an improvement in the initial solution through the use of the recommended algorithm parameters. This application yielded three routes with the total route duration time of 244.24 *min*. Figure 2 shows the appearance of the transport network routes.

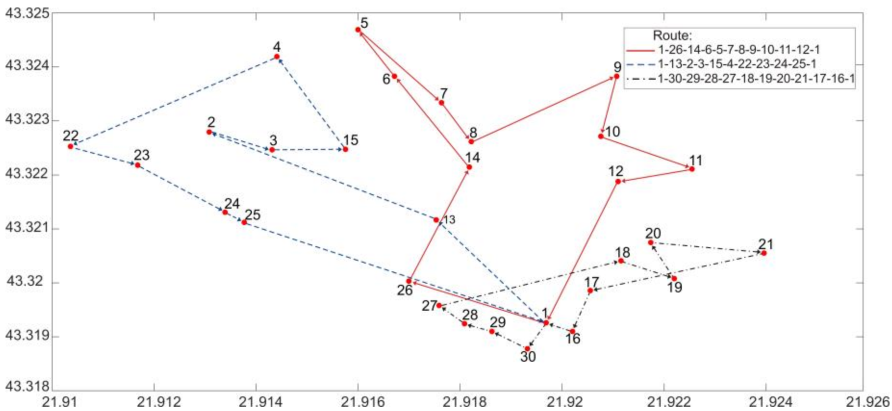

Figure 2

Graphic representation of the *VRPSD* routes obtained by the *IHS* algorithm

Conclusion

A combination of the constructive heuristic and metaheuristic algorithms was applied to optimize the movement routes of municipal waste collection vehicles for the observed transport network. The improvements introduced by thus designed routes in comparison with the existing routes used by the PUC "Mediana-Niš" vehicles relate to the reduction in the total travel distance and the reduction in the total working hours of the operator and vehicle that collect municipal waste. The average route length of the PUC “Mediana-Niš” municipal waste collection vehicles for the observed transport network is 65.33 *km/day*, while the route length for the same transport network obtained by the *VRPSD* optimization is 59.82 *km/day* [21]. These results show that the application of the proposed solution can lead to a reduction in the mechanization fuel costs of up to 10%.

Figure 3 shows the relation between the consumed time per day for the routes obtained by solving the *VRPSD* and the routes currently used by the municipal waste collection vehicles of the PUC “Mediana-Niš”. The graph shows that the *VRPSD* routes are shorter in comparison with the routes used by the PUC “Mediana-Niš” vehicles. The average route duration time obtained by solving the *VRPSD* is 6.84 *h/day*, while the average route duration time of the PUC “Mediana-Niš” vehicles is 9.05 *h/day*.

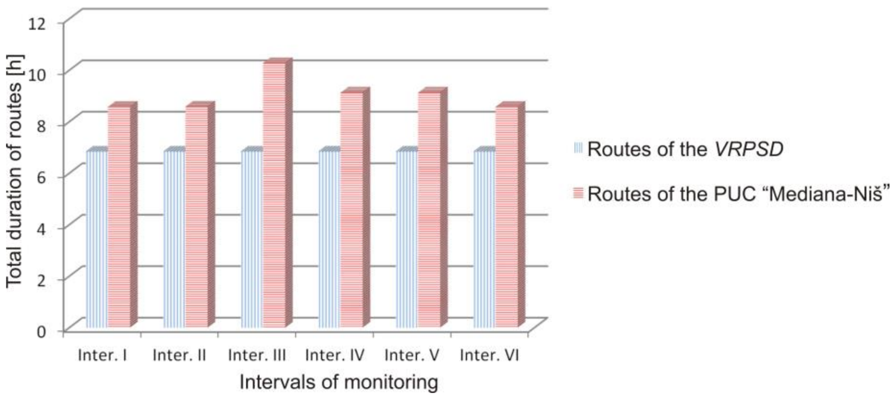

Figure 3

Graphic representation of the total duration of the *VRPSD* routes and the existing PUC “Mediana-Niš” routes

All this shows that the vehicle routes for municipal waste collection in the observed transport network are optimized. The developed *VRPSD* model represents a real model, bearing in mind that it takes into consideration all of the parameters that could influence the operation of a municipal waste collection vehicle in an urban area. Furthermore, the developed methodology possesses a universal character and it can be applied to any urban area. Results presented are compatible with current trend of inclusion of Industry 4.0 technologies in waste collection routing [23], which involves cyber-physical systems paradigm, Internet-of-things, big data, cloud computing and other technologies, which all together represents important research direction beyond our results. Also, optimization techniques used in this study are selected as most suitable and providing good resuts from a much larger set of tested algorithms, so comparative study of suitability of these techniques in considered case is also important prospect for further research.

Acknowledgement

This paper is part of the project TR-35049 implemented at the University of Niš, Faculty of Mechanical Engineering, and supported by the Ministry of Education, Science and Technological Development of the Republic of Serbia.

References

[1] Dantzig, G. B., Ramser, J. H. (1959) The truck dispatching problem, Management science, 6(1), pp. 80-91

[2] Benjamin, A. M. (2011) Metaheuristics for the waste collection vehicle routing problem with time windows, PhD thesis, Department of Mathematical Sciences, Brunel University, London, United Kingdom

[3] Letchford, A. N., Salazar-González, J. J. (2019) The capacitated vehicle routing problem: stronger bounds in pseudo-polynomial time, European Journal of Operational Research, 272(1), pp. 24-31

[4] Laporte, G., Nobert, Y., Desrochers, M., (1985) Optimal routing under capacity and distance restrictions, Operations Research, 33 pp. 1050-1073

[5] Laporte, G. (2018) Vehicle routing with backhauls, Computers and Operations Research, 91(C), pp. 79-91

[6] Csiszár, S. (2005) Route elimination heuristic for vehicle routing problem with time windows. Acta Polytechnica Hungarica, 2(2), 77-89

[7] Madankumar, S., Rajendran, C. (2018) Mathematical models for green vehicle routing problems with pickup and delivery: A case of semiconductor supply chain, Computers & Operations Research, 89, pp.183-192

[8] Mohamed, M. K., Lanzon, A. (2012) Design and control of novel tri-rotor UAV, IEEE International Conference on Control (CONTROL) UKACC, pp. 304-309

[9] Avci, M., Topaloglu, S. (2016) A hybrid metaheuristic algorithm for heterogeneous vehicle routing problem with simultaneous pickup and delivery, Expert Systems with Applications, 53, pp. 160-171

[10] Marinakis, Y., Iordanidou, G. R., Marinaki, M. (2013) Particle Swarm Optimization for the Vehicle Routing Problem with Stochastic Demands, Applied Soft Computing, 13(4), pp. 1693-1704

[11] Xiangyong, L., Peng, T., Stephen, C. H. L. (2010) Vehicle routing problem with time windows and stochastic travel and service times, International Journal Production Economics, 125, pp. 137-145

[12] Bautista, J., Fernadez, E., Pereira, J. (2008) Solving an urban waste collection problem using ants heuristics. Computers & Operations Research, 35(9), pp. 3020-3033

[13] Vera, H., Karl F, D., Richard F, R., Stefan, R. (2013) A heuristic solution method for node routing based solid waste collection problems. Journal of Heuristics, 19,(2), pp. 129-156

[14] Radiša, R., Dučić, N., Manasijević, S., Marković, N., Ćojbašić, Ž. (2017) Casting improvement based on metaheuristic optimization and numerical simulation. Facta Universitatis, Series: Mechanical Engineering, 15(3), 397-411

[15] Marković, D. (2018) Development of a logistic model for municipal waste management by applying heuristic methods, PhD Thesis, University of Niš, Serbia

[16] Tao, Z., Chaovalitwongse, W. A., Yuejie, Y. (2012) Scater search for the stohastic travel-time vehicle routing problem with simultaneous pick-ups and delivers. Computers & Operations Research, 39, pp. 2277-2290

[17] Coutinho-Rodrigues, J., Tralhão, L., Alçada-Almeida, L. (2012) A bi-objective modeling approach applied to an urban semi-desirable facility location problem. European Journal of Operational Research, 223(1), 203-213

[18] Tomić, V., Marinković, D., Marković, D. (2014) The selection of logistic centers location using multi-criteria comparison: case study of the Balkan Peninsula. Acta Polytechnica Hungarica, 11(10), 97-113

[19] Ghiani, G., Laganà, D., Manni, E., Triki, C. (2012) Capacitated location of collection sites in an urban waste management system. Waste management, 32(7), 1291-1296

[20] PUC “Mediana-Niš”, 2017, Public utilities company “Mediana-Niš”, Serbia

[21] Marković, D., Petrović, G., Ćojbašić, Ž., Stanković A. (2017) The vehicle routing problem with stochastic demands in an urban area –a case study. Facta Universitatis, Series: Mechanical Engineering, DOI:10.22190/FUME190318021M

[22] Marković, D., Madić, M., Petrović, G. (2012) Assessing the performance of improved harmony search algorithm (IHSA) for the optimization of unconstrained functions using Taguchi experimental. Scientific Research and Essays, 7(12), pp. 1312-1318

[23] Bányai, T., Tamás, P., Illés, B., Stankevičiūtė, Ž., & Bányai, Á. (2019) Optimization of Municipal Waste Collection Routing: Impact of Industry 4.0 Technologies on Environmental Awareness and Sustainability. International journal of environmental research and public health, 16(4), pp. 634

The Impact of Audit Committees on the Performance of Business Entities

Timea Melinda Fülöp

Babeș - Bolyai University of Cluj - Napoca, Faculty of Economics and Business Administration, 58 - 60 Th. Mihali Street, Cluj - Napoca 400591, Romania, melinda.fulop@econ.ubbcluj.ro

Abstract: Audit committees represent a central instrument of corporate governance. During the last decade a series of studies concerning audit committees and corporate governance have been conducted without providing a comprehensive overview of their impact on the financial aspects of the business entities. Different levels of empirical studies divided into different categories are available on this subject. Corporate governance is necessary to the financial transparency but not sufficient. This paper aims to study and develop the impact which the audit committees have on the performance of the listed business entities.

Keywords: audit committee; performance; stock exchange

1 Introduction

Nowadays, Audit Committees are in the center of interest as a key mechanism for corporate governance. Corporate governance committees and regulators around the world called for the need of creating a supervisory European committee. After the admission, that the establishment of an audit committee by itself does not guarantee its usefulness, the focus shifted towards the composition and activities of these committees. The result of this investigation suggests that there is a considerable divergence between the recommended structure and the role of the audit committees [11].

The concept of the audit committee was introduced in 1939 by the New York Stock Exchange (NYSE). In the early seventies, the Securities and Exchange Commission (SEC) of the United States suggested to the listed companies to create an audit committee composed of non-executive directors. In 1979 the NYSE imposed as a listing obligation that members of an audit committee must be independent.

Corporate governance is a topic of great interest in the present financial system being debated, in specialized scientific fields of economics under a variety of definitions [44] [9] [36] [28] [31] [45[5]. The concept of 'good corporate governance' was first mentioned in 1932 by Adolf Berle and Gardiner Means in their *agency theory* "The Modern Corporation and Private Property (1932)". Kim et al. (2005) define it as a mixture of different mechanisms that direct and control the entities [29] [26].

Many studies are focused on the correlations involving elements of corporate governance and audit function as, for instance, the relation between internal audit and corporate governance [32] [6] [42] [13] [21] [41] [39] [40] between audit committees and corporate governance [3] [11] [23] [18] [20] [49] between external audit and corporate governance [19] [1] [24] [12] and the implications of the principle of transparency in corporate governance [8] [41] [37] [15] [38] [47].

Corporate governance (CG) deals, on the one hand, with conformance, while on the other hand, with performance [48]. Conformance is related to monitoring and surveillance, thus, being associated with various stakeholders [27] Performance contributes to the improvement of the performance of mongers.

Several empirical studies use a specific governance variable or mechanism in investigating the relation between entity value and performance [46] [4] [50] [51]. Other authors [22] [14] [7], demand the usage of a corporate governance index (CGI - a multi-dimensional variable).

One of the primary European surveys regarding the relation between corporate governance and peformance of entities, was carried out by Drobetz [16]. In this study, the authors used a Corporate Governance Rating (CGR) based on multidimensional answers given to a questionnaire based on the Germany Corporate Governance Code voluntarily adopted by the entities.

Other studies have shown that corporate governance positively influences the financial performance of the entities. It has a positive influence on the performance of the listed entities on stock exchanges [10] [34] [35] [33].

This paper contributes to the literature in the field of audit in special in the field of audit committees and performance of the listed business entities. The remainder of this paper presents in the next section the impact which the audit committees have on the performance of the listed business entities. In the last part of the paper are the conclusions, limits and perspectives for future researches in this challenging and debatable area of knowledge.

2 Methodologies and Model Design

Literature defines the methods of scientific knowledge and the text of the work building that they must follow to achieve their objectives, information and survival. The processes, techniques and tools used in the scientific incursion are the methods, seen as supporting or concrete elements to exploit it [25] [17].

In order to study the impact of audit commitees on the performane of business entities a deductive approach [25] combined with an inductive method [30] relying on observations and induction was used. To achieve the objectives of this research, the scientific approach is based on a deductive approach [25] which starts from the theory, but also, an inductive method [30] relying on observation and induction.

The hypotheses had been formulated and verified by use sing the OLS (squash regression) model. The OSL model has been applied to several independent variables to achieve results as close as possible to reality.

As a measure of association between the X and the A_{it} variables, the multiple correlation coefficients noted with R are introduced. This can be defined as the maximum coefficient of a simple correlation (Pearson) between X and a linear combination of A_{it} variables. This explains the fact that the calculated value of R is always positive and tends to increase as the number of independent variables increases.

Thus, **the method of Ordinary Least Squares (OLS)** can be considered as a way to maximise the correlation between observed values and estimated values. A value of the coefficient R close to 0 indicates a minor regression. The regression is considered to be insignificant when the forecasted regression values are no better than those obtained by random guessing.

Since R tends to overestimate the association between X and A_{it}, the above-defined indicator is preferred, namely the coefficient of determination R^2 which represents the square of the multiple correlation coefficients.

The F-test of global significance, the first test used to analyze regression, is a global significance test of all coefficients. The test hypotheses are:

$$H0: \alpha 1 = \alpha 2 = \ldots = \alpha p = 0 \quad (1)$$

$$H1: (\Xi) i, \text{ so that } \alpha i \neq 0$$

For the null hypothesis it is determined that the F statistic, calculated in the ANOVA table, is distributed Fisher-Snedecor $F_{p-1;n-p}$, so that the null hypothesis can be verified. If the null hypothesis is not rejected, the observed data will not allow the identification of a valid linear model. Thus the regression is not appropriate for the initially established forecasting aim.

Multicollinearity emerges when a group of independent variables are strongly correlated. In this case, should a variable from the group in the model be included, the rest of the variables from the group will not bring any significant information.

Multicollinearity can be tested using SPSS using tolerance or Variation Inflation Factor (VIF). A low tolerance value (usually less than 0.1) reflects a R_i^2 value close to 1, thus a strong linear correlation between X and the rest of the independent variables. Therefore xi is collinear with the other independent variables. VIF represents the opposite value of tolerance. This interpretation derives from that of tolerance: a high value of *VIF* (usually over 10) denotes collinearity [2].

3 Research Design and Results

3.1 Methodology Framework

To carry out the case study on the analysis of the role of the audit committee in the context of corporate governance, a sample of 23 entities listed on the Bucharest Stock Exchange has been chosen. These entities are part of the main index of the Bucharest Stock Exchange (Premium category). The following the next steps have been carried:

First step (construction of the sample)	• Analysis of the corporate governance code implementation guide • Selecting the entities included in the study • Selecting the relevant information for each company • Defining the analysis method Appropriate analysis and interpretation of the results
Second step (analysis of several relevant issues for each company in the sample)	• The existence of the audit committee; • The independence of the audit committee chairman; • The expertise of the chairman of the audit committee; • The structure of the audit committee; • The position of the audit committee within the company; • Independence of the audit committee; • The expertise of the members of the audit committee; • The number of the annual meeting of the audit committee;
Third step (analyze the Comply or Explain Statement)	• Recommendation 27 Is there an audit committee within the company • Recommendation 28 Does the Board of Directors or the audit committee, as appropriate, regulatory review the effectiveness of financial reporting, internal control and risk management system adopted by the company?

	• Recommendation 29 the audit committee meets at least twice a year, these meetings being devoted the preparation and dissemination to the shareholders and the public of the half-yearly and annual results • Recommendation 32 the audit committee recommends to the board of directors the selection, appointment and replacement of the financial auditor and the terms and condition of his remuneration
Fourth step (selection of audit committee characteristics)	• Number of members • Number of meetings • Professional experience • Independence of audit committee members • Independence of the audit committee chairman

In 2008, the Bucharest Stock Exchange developed a new Code of Corporate Governance starting from the core principles established by OECD. The new code came into effect only in 2009, and it has been applied voluntarily by listed entities, which have been requested to submit a conformity declaration. According to the new Code of Corporate Governance, „issuers will attach to the Annual Report, starting with the Report for 2010 (optional for 2009), a statement regarding the compliance or non-compliance with the Code of Corporate Governance (The "Comply or Explain" Statement)."

To achieve the objective, the methodology involved quantitative research methods. With this method, information has been classified, statistical models has been build, and results have been explained. For the case study, a sample of 19 listed entities on the Bucharest Stock Exchange has been selected, and the companies' annual financial reports available on their website or the BVB website. Based on these reports, the financial ratios have been calculated for each company, results which were then imported into SPSS to perform an empirical analysis of the impact that the audit committee has on the entity's performance characteristics.

The reasons behind choosing only 19 entities out of the total of 23, in the Premium category is due to the fact that 4 entities did not publish the "comply or explain" statement, had no audit committee mor the data needed to calculate the financial indicators were published.

Based on these elements, five hypotheses (with alternatives) have been formulated:

H1.a The number of members of the Audit Committee does not influence the performance of the entity.	H1.b The number of members of the Audit Committee influences the performance of the entity/
H2.a The number of meetings does not affect the performance of the entity.	H2.b The number of the meeting will influence the performance of the entity.
H3.a The independence of the Audit Committee Chairman does not influence the performance of the entity.	H3.b The independence of the Audit Committee influence the performance of the entity.
H4.a The independence of the Audit Committee does not influence the performance of the entity.	H4.b The independence of the Audit Committee affects performance. Entity.
H5.a The professional experience of members of the audit committee does not influence the performance of the entity	H5.b The professional expertise of members of the audit committee affect the performance of the entity

3.2 Data and Results

This section consists of the analysis on whether there is a correlation between the characteristics of the audit committee and the performance of the selected entities in the sample, represented by:

- Market Share Value (MSV)
- Market capitalisation (MC)
- Stock Dividends (SD)

The initial form of the model is as follows:

$$MSV / MC / SD = \alpha 0 + \alpha 1 \ m\_number + \alpha 2 \ m\_mettings + \alpha 3 \ m\_experience + \alpha 4 \ m\_inDependentce + \alpha 5 \ inDependent\_CCA \quad (2)$$

a.) Market Share Value

The first analysed indicator is the market share value (MSV). Table 1 highlights the result for the ANOVA test, with the dependent variable MSV.

Tabel 1

ANOVA - Dependent Variable MSV

Model	Sum of Squares	df	Mean Square	F	Sig.
Regression	82012.430	4	16402.486		
Residual	118970.410	15	9151.570	1.792	.184[a]
Total	200982.839	19			

a. Predictors: (Constant), m_experience, m_mettings, m_inDependentce, inDependent_CCA, m_number

Analyzing the significance in the Table 1 (SIG), is can be observed that it is greater than 0.1 (Tabel 1), so the linear relation among the variables is not considered significant. Consequently, the general shape of the model is not proper, and removal of variables is necessary. By analyzing the Correlations table (see Table 2), the variables whose significance exceeds the permissible limits Sig are removed, namel: m_mettings, inDependent_CCA.

Tabel 2

Correlation: Dependent Variable MSV

		MSV	m_mettings	m_number	inDependent_CCA	m_inDependentce	m_experience
Person Correlation	MSV	1.000	.002	.333	.267	.508	.489
	m_mettings	.002	1.000	.217	.363	.036	.067
	m_number	.333	.217	1.000	.444	.569	.543
	inDependent_CCA	.267	.363	.444	1.000	.474	.502
	m_inDependentce	.508	.036	.569	.474	1.000	.318
	m_experience	.489	0.67	.543	.502	.318	1.000
Sig.(1-tailed)	MSV		.496	.082	.135	.013	.017
	m_mettings	.496		.187	.063	.442	.393
	m_number	.082	.187		.028	.006	.008
	inDependent_CCA	.135	.063	.028		.020	.014
	m_inDependentce	.013	.442	.006	.020		.092
	m_experience	.017	.393	.008	.014	.092	

By constructing a new regression with the remasive variables, later results of the ANOVA test are obtained, shown in Table 3.

Tabel 3

ANOVA - Dependent Variable MSV

Model	Sum of Squares	df	Mean Square	F	Sig.
Regression	78677.641	2	26225.880	3.216	.053[a]
Residual	122305.198	17	8253.680		
Total	200982.839	19			

a. Predictors: (Constant), m_experience, m_inDependentce, m_number

The final regression obtained:

$$MSV = \alpha 0 + \alpha 2 \text{ m\_number} + \alpha 3 \text{ m\_experience} + \alpha 4 \text{ m\_independence} \quad (3)$$

The value F = 3.216 (see Table 3), tests the global significance of the independent variables. The value of the ANOVA model sig is 0.053, which is less than the significance threshold of 0.1. Consequently, the linear link among the variables analysed is significant. Consequently, hypothesis H1.a and H3.a are rejected, and therefore their alternatives H1.b and H3.b are accepted, namely that the number of meetings and the independence of the president influence the market shares value.

Referring to the coefficients of the selected variants, it is found that the audit committee is directly proportional to the market shares value. From the model summary, the variance of the market shares value is explained by 39.1% of the independent variables, as indicated by the value of R Square.

Tabel 4
Coefficient - Dependent Variable MSV

Model	Unstandardized Coefficients		Standrdized Coefficients	t	sig	Correlations			Collinearity Statistice	
	B	Std.Error	Beta			Zero-oder	Partial	Part	Tolerance	VIF
(Constant)	-115.529	54.060		-2.137	0.49					
m_number	-20.801	35.015	-.164	-.594	.561	.333	-.152	-.120	.531	1.884
m_inDependentce	37.794	19.909	.465	1.898	.077	.508	.440	.382	.676	1.479
m_experience	35.675	19.909	.430	1.792	.093	.489	.420	.361	.706	1.417

In this case (see Tabel 4), the generally significant factor is the variable number of members, the result being the extent to which the number of members of the audit committee greatly influences the market shares value.

b.) Capitalization on the Market

The next analysed indicator is the capitalization on the market (MC). Table 5 shows the result for the ANOVA test, with the dependent variable MC.

Tabel 5
ANOVA - Dependent Variable MC

Model	Sum of Squares	df	Mean Square	F	Sig.
Regression	1.452	3	2.904		
Residual	5.324	16	4.095	.709	.627[a]
Total	6.776	19			

a. Predictors: (Constant), m_experience, m_mettings, m_inDependentce, inDependent_CCA, m_number

Analyzing the significance in the Table 5 (SIG), it is greater than 0.1 (see results in Table 5), thus the linear relation among the variants is not considered significant. Consequently, the general form of the model is not appropriate, and some variable should be removed. By analyzing the correlation Table 6, the variables whose significance exceeds the permissible limits Sig are removed: m_mettings, independent_CCA, m_experience.

Tabel 6

Correlation: Dependent Variable MC

		MC	m_mettings	m_number	inDependent_CCA	m_inDependentce	m_experience
Person Correlation	MC	1.000	-.021	.392	.218	.365	.117
	m_mettings	-.021	1.000	.217	.363	.036	.067
	m_number	.392	.217	1.000	.444	.569	.54
	inDependent_CCA	.218	.363	.444	1.000	.474	.502
	m_independentce	.365	.036	.569	.474	1.000	.318
	m_experience	.117	.067	.543	.502	.318	1.000
Sig.(1-tailed)	MC		.466	.049	.184	.061	.317
	m_mettings	.466		.187	.063	.442	.393
	m_number	.049	.187		.028	.006	.008
	inDependent_CCA	.184	.063	.028		.020	.014
	m_independentce	.062	.442	.006	.020		.092
	m_experience	.317	.393	.008	.014	.092	

In Table 6, Sig value exceeds the chosen significance threshold. Therefore, the model is not appropriate. Thus, variables that do not meet this criterion are removed, and only the correlation between the number of members and the independence of the members of the Audit Committee and Market Capitalization will be studied.

By constructing a new regression with the remaining variables, the later results and the ANOVA test are presented in Table 7.

$$MC= \alpha 0+ \alpha 2m\_number. \quad (4)$$

Tabel 7

ANOVA - Dependent Variable MC

Model	Sum of Squares	df	Mean Square	F	Sig.
Regression	1.243E20	2	6.214E19		
Residual	5.534E20	17	3.458E19	1.797	.198[a]
Total	6.776E20	19			

a. Predictors: (Constant), m_experience, m_independentce, m_number

Table 7 shows the significance is greater than 0.1, therefore the linear relation among the variables is not considered significant, thus the variable m_independence is removed.

The final regression and ANOVA results is (see Table 8).

$$MC= \alpha0+ \alpha2 \text{ m\_number}. \quad (5)$$

Tabel 8

ANOVA - Dependent Variable MC

Model	Sum of Squares	df	Mean Square	F	Sig.
Regression	1.039E20	1	1.039E20		
Residual	5.738E20	18	3.375E19	3.077	.097[a]
Total	6.776E20	19			

a. Predictors: (Constant), m_number

The value for F = 3.077 (as seen in Table 8) tests the global significance of the Dependent variables. The SIG value is 0.097, which is less than the significance threshold of 0.1. Therefore, the linear link among the variables analysed is significant. As a result of this analysis, hypotheses H1.a, H3.a, H4.a, H5.a are rejected, therefore their alternatives H1.b, H3.b, H4.b, H5.b are accepted.

The variables of this regression explain the change in the stock market capitalisation at a rate of 15.3%, as indicated by the value of R Square. Therefore, there is a low correlation between the MC and the non-dependent variables.

Tabel 9

Coefficient - Dependent Variable MC

Model	Unstandardized Coefficients		Standrdized Coefficients	t	sig	Correlations			Collinearity Statistice	
	B	Std.Error	Beta			Zero-oder	Partial	Part	Tolerance	VIF
(Constant)	1.405	2.321		.605	.553					
m_number	2.880	1.641	.392	1.754	.097	.392	.392	.392	1.000	1.000

In this case (as seen in Table 9), the most significant ratio is found in the variable m_number, resulting in the degree of independence of the audit committee members influencing the market capitalisation to the most significant extent.

From the coefficients table (Table 9). the linear regression is:

$$MC = 1.405 + 2.880 * \text{m\_number}. \quad (6)$$

c.) Stock Dividends (SD)

Table 10 highlights the result for the ANOVA test with the dependent variable stock dividends (SD).

Tabel 10

ANOVA - Dependent Variable SD

Model	Sum of Squares	df	Mean Square	F	Sig.
Regression	874.627	5	174.925	1.772	.188[a]
Residual	283.306	14	98.716		
Total	2157.933	19			

a. Predictors: (Constant), m_experience, m_mettings, m_independence, independent_CCA, m_number

Analyzing the significance in the Table 10 above (SIG), it is greater than 0.1, thus the linear link among the variables is not considered significant. Consequently, the general form of the model is not appropriate, and some variables need to be removed. Analyzing the Correlations Table 11 the variables whose significance exceeds the permissible limits Sig are removed: member_mettings, m_independence.

Tabel 11

Correlation - Dependent Variable SD

		SD	m_mettings	m_number	inDependent_CCA	m_inDependentce	m_experience
Person Correlation	SD	1000	.001	.327	.279	.510	.486
	m_mettings	.001	1.000	.217	.363	.036	.067
	m_number	.327	.217	1.000	.444	.569	.543
	inDependent_CCA	.279	.363	.444	1.000	.474	.502
	m_inDependentce	.510	.036	.569	.474	1.000	.318
	m_experience	.486	.067	.543	.502	.318	1.000
Sig.(1-tailed)	SD		.498	.086	.123	.013	.017
	m_mettings	.498		.187	.063	.442	.393
	m_number	.086	.187		.028	.006	.008
	inDependent_CCA	.123	.063	.028		.026	.014
	m_inDependentce	.013	.442	.006	.020		.092
	m_experience	.017	.393	.008	.014	.092	

After an analysis of the correlation in Table 11 a new regression with the remaining variables is constructed, with the following results (Table 12).

Tabel 12

ANOVA - Dependent Variable SD

Model	Sum of Squares	df	Mean Square	F	Sig.
Regression	848.278	3	282.759	3.239	.052[a]
Residual	1309.655	16	87.310		
Total	2157.933	19			

a. Predictors: (Constant), m_experience, m_inDependentce, m_number

The final regression is:

$$SD = \alpha 0 + \alpha 1\ m\_number + \alpha 3\ m\_experience + \alpha 4\ m\_independence. \quad (7)$$

The value F = 3.239 (see Table 12) tests the global significance of the Dependent variables. The ANOVA sigma value is 0.052, which is less than the significance threshold of 0.1. Therefore, the linear link between the variables analysed is significant. As a result hypothesis H1.a and H3.a are rejected, therefore their alternatives H1.b and H3.b are accepted.

The independent regression variable explains the variation of dividends per share at a rate of 39.3% (see Table 12), as indicated by the value of R Square. Therefore, an average correlation between the Dependent variable and the independent variable is found.

Tabel 13

Coefficient - Dependent Variable SD

Model	Unstandardized Coefficients		Standrdized Coefficients	t	sig	Correlations			Collinearity Statistice	
	B	Std.Error	Beta			Zero-oder	Partial	Part	Tolerance	VIF
(Constant)	-12.125	5.594		-2.167	.047					
m_number	-2.311	3.623	-.176	-.638	.533	.327	-.163	-.128	.531	1.884
m_inDependentce	3.982	2.060	.473	1.933	.072	.510	.447	.389	.676	1.479
m_experience	3.710	2.060	.431	1.801	.092	.486	.422	.362	.706	1.417

As seen in Table 13, the most significant ratio is found in the variable m_number, resulting in the degree of independence of the members of the audit committee influencing the dividend per share to the most significant extent.

Conclusions

After a literature review on the concept of corporate governance, a relationship between the concept of corporate governance and entity performance has been found. This relationship can be described as being unable to reach a harmony, regarding the nature of the link between the two ideas. Although the empirical evidence is inconclusive, the critical importance of performance governance is recognised globally, particularly in the interests of managers and associates.

The performed regression analysis is limited to a specific corporate governance mechanism, however, this model can be extrapolated to several corporate governance mechanisms, although this action is practically tricky, as different tools are indifferently connected. The Smith Report (2003) emphasises that an audit committee can be effective only in a broader process of corporate governance. Therefore, the results of the present study must be carefully interpreted. Secondly, the independent variable is not a continuous variable as the audit committee is effective within the limits of the variables taken into consideration. However, the current statistical analysis is probably significant, at least for reference.

Finally, the connection between the audit committee and an entity's performance has been studied:

- The Audit Committee is a corporate governance mechanism which can alleviate the problem of allocating power within the Principal-Agent Theory;
- The contribution of Audit Committees in corporate governance is to assess both the quality of financial reports and their approval. Financial reporting focuses on individual and consolidated financial statements, including the verification of external auditors;
- Creating an Audit Committee can have beneficial effects which can eventually lead to a consolidation of a company's corporate governance.

	H1.a	H1.b	H2.a	H2.b	H3.a	H3.b	H4.a	H4.b	H5.a	H5.b
Market Share Value	X	✓			X	✓				
Market capitalisation			X	✓	X	✓	X	✓	X	✓
Stock Dividends	X	✓			X	✓				

As a general conclusion, it was found that entities listed on BVB are not aware of the role of the audit committee in corporate governance. A proper evolution of the Premium category can be seen, and it is believed that in the coming years these statistics will evolve positively. Last but not least, the audit committee plays an essential role in decision-making within a company and, at the same time, helps the Board of Directors, the Management, and last but not least, the internal and external audit process.

References

[1] Barton, J. (2005), Who Cares about Auditor Reputation? *Contemporary Accounting Research* 22 (3): 549-586

[2] Belsley, D. A., Kuh, E. and Welsch, R. E. (1980) *Regression Diagnostics: Identifying influential data and sources of collinearity*, New York: John Wiley

[3] Bertschinger, Peter/Schaad, Martin (2003*):"Beitrag zur Corporate Governance in der Schweiz"* Zürich, http://www.auditcommittee.ch/library/pdf/OrdnerTeil_5_AC.pdf

[4] Bhagat, S., Black, B. (2002) The Non-Correlation between Board Independence and Long-Term Firm Performance. *Journal of Corporation Law*. 27, 231-273

[5] Braithwaite, T. (2010) 'Votes on US financial reform to be tight amid bill's late changes,' *Financial Times (Asia),*10 May, p. 4

[6] Broadley, Derek (2006) Auditing and its role in corporate governance, FSI Seminar on Corporate Governance for Banks, Bank for International Settlements

[7] Brown, L. D., Caylor, M. L. (2006) Corporate governance and entity valuation. *Journal of Accounting and Public Policy,* 25(4), 409-434

[8] Bushman R., Chen Q., Engel E.& Smith A. (2004), Financial Accounting Information, Organizational Complexity and Corporate Governance Systems, *Journal of Accounting & Economics*, 2004, *37*(2), pp. 167-201

[9] Cadbury Report: http://www.ecgi.org/ codes/all_codes.php

[10] Chen, K. C. W., Zhihong, C., Wei, K. C. J. (2009) "Legal protection of investors, corporate governance, and the equity cost of capital", Journal of Corporate Finance, 15(3): 273- 388

[11] Collier, P. & Zaman, M. (2005) 'Convergence in European corporate governance: The audit committee concept', *Corporate Governance*, Vol. 13, No. 6, pp. 753-68

[12] Coram, P., Mock T., Turner J., and Gray G. (2011) The communicative value of the auditor's report, *Australian Accounting Review* 21 (3): 235-252

[13] Coram, Paul, Colin Ferguson and Robyn Moroney (2007) The importance of internal audit in fraud detection, Working Paper, University

[14] Core, J. E., Guay, W. R., Rusticus, T. O. (2006) Does Weak Governance Cause Weak Stock Returns? An Examination of Firm Operating Performance and Investors' Expectations, *The Journal of Finance*, LXI (2)

[15] Doh, J. P. & Tashman, P., (2012) Half a World Away: The Integration and Assimilation of Corporate Social Responsibility, Sustainability, and Sustainable Development in Business School Curricula, Corporate Social Responsibility and Environmental Management, Article first published online, DOI: 10.1002/csr. 1315

[16] Drobetz, W., Schillhofer, A., Zimmermann, H. (2004) Corporate Governance and Expected Stock Returns: Evidence from Germany. *European Financial Management,* Vol. 10, 267-293

[17] Dunbar A. E. & Weber D. P. (*2014*) What Influences Accounting Research? A Citations-Based Analysis. Issues in Accounting Education: February 2014, Vol. 29, No. 1, pp. 1-60

[18] Edwards J. S. S. et al. (2008) *Corporate Governance and Pay for Performance: Evidence from Germany*, Economics of Governance 10, 2008, 1-26

[19] Francis, J. R. (2004) What do we know about audit quality? *British Accounting Review* 36 (4): 345-368

[20] Fülöp M. T. (2013) Audit opinions for listed entities for the first category on the Romanian Stock Exchange, Studia Universitatis "Vasile Goldiș" Arad, Economic Series Vol. 23, issue 4, pp.103-108

[21] Gennaro, Mauro Di (2007) The role of internal audit in corporate governance. Case: Fiat Group, *International In-house Counsel Journal*, Vol. 1, No. 2, November

[22] Gompers, P., Ishii, J., Metrick, A. (2003) Corporate Governance and Equity Prices. *Quarterly Journal of Economics*,118: 107-155

[23] Goodwin-Stewart, J. & Kent, P. (2006) 'Relation between external audit fees, audit committee characteristics and internal audit', *Accounting and Finance*, Vol. 46, No. 3, pp. 387-404

[24] Gordon F. Woodbine J. L. (2010) Leadership Styles and the Moral Choice of Internal Auditors, EJBO *Electronic Journal of Business Ethics and Organization Studies*, Vol. 15, No. 1, pp. 28-35

[25] Gray P., Williamson J. B., Karp D. A. & Dalphin J. R.(2007) The Research Imagination – an introduction to qualitative and quantitative methods, Cambridge University Press, ISBN-13 978-0-511-33417-7, Cambridge, p. 480

[26] Hassan, M. K. (2008) The corporate governance inertia: the role of management accounting and costing systems in a transitional public health organization, *Research in Accounting in Emerging Economies*, 8, 409-454

[27] Hassan, M. K., Halbouni, S. S. (2013) Corporate governance, economic turbulence and financial performance of UAE listed firms. *Studies in Economic and Finance*, 30(2), pp. 118-138

[28] Keasey K., Thompson St. & Wright M. (2005) *Corporate Governance: Accountability, Enterprise, and International Comparisons.* Wiley

[29] Kim, B., Prescott, J. E., Kim, S. M. (2005) Differentiated governance of foreign subsidiaries in transitional corporations: an agency theory perspective, *Journal of International Management*, 11, 43-66

[30] Lesage, C., Wechtler, H. (2012) "An inductive typology of auditing research",Contemporary Accounting Research, Vol. 29, No. 2, pp. 487-504

[31] Mallin Ch. A. (2006) *Handbook on International Corporate Governance Country Analyses,* Edward Elgar, ISBN-13: 978 1 84542 034 5, ISBN-10: 1 84542 034 9

[32] Moeller, R. R. (2004) Sarbanes-Oxley and the new internal auditing rules. Hoboken, N. J.:Wiley

[33] Ntim C. G. (2013) "An Integrated Corporate Governance Framework and Financial Performance in South African Listed Corporations", MPRA Paper No. 45805, Online at http://mpra.ub.uni-muenchen.de/45805/…

[34] Ntim, C. G., Opong K. K., Danbolt, J., (2011) "The Value Relevance of Shareholder versus Stakeholder Corporate Governance Disclosure Policy Reforms in South Africa", Corporate Governance: An International Review, Forthcoming

[35] Nuryaman, (2012) "The influence of corporate governance practices on the company's financial performance", Journal of Global Business and Economics, Vol. 5, No. 1

[36] OECD Principiile Guvernării corporative www.oecd.org

[37] Porter, B. A., (2009) - The audit trinity: the key to securing corporate accountability, *Managerial Auditing Journal*, Vol. 24, No. 2, pp. 156-182

[38] Saltaji I. MF., (2013) "Corporate Governance in Eastern Europe: Case of Romania and Russian Federation", Theoretical and Applied Economics Volume XXI, No. 4(593), pp. 99-112

[39] Sarens, G., De Beelde, I. and Everaert, P. (2009) Internal audit: the expert in providing comfort to the audit committee – the case of risk management and internal control, *British Accounting Review*, Vol. 41, No. 2, pp. 90-106

[40] Susmanschi, G. (2012) Internal audit and corporate governance in time of economic crisis, *Journal of Applied Economic Sciences*, Vol. 7, pp. 189-194

[41] Szántai T., Kovács E. and Egri A. (2018) Inventory Control in Sales Periods, Acta Polytechnica Hungarica Vol. 15, No. 1, pp.87-104

[42] Szívós L. and Orosz I. (2014) The Role of Data Authentication and Security in the Audit of Financial Statements, Acta Polytechnica Hungarica Vol. 11, No. 8, pp.161-176

[43] Themistokles G. L. &Evaggelos, D. (2008) The Missing Link to an Effective Corporate Governance System, Corporate *Governance: The International Journal of Business in Society, Vol. 8, No. 1, pp. 73-82*

[44] Tricker, R. I. (1984*) Corporate Governance-Practices, procedures and power in British entities and their board of directors*, Oxford

[45] Tricker, R. I. (2009) *Corporate Governance - principles, policies and practices*, Oxford University Press, Oxford

[46] Yermack, D. (1996) Higher Market Valuation for Firms with a Small Board of Directors. *Journal of Financial Economics*, XL, 185-211

[47] Dragos, S. L., Mare, C., Dragota, I. M., Dragos, C. M., & Muresan, G. M. (2017) The nexus between the demand for life insurance and institutional factors in Europe: new evidence from a panel data approach. *Economic research-Ekonomska istraživanja*, 30(1), 1477-1496

[48] Kao M. F., Hodgkinson L., and Jaafar A., (2019) Ownership structure, board of directors and firm performance: evidence from Taiwan, *Corporate Governance: The International Journal of Business in Society*, Vol. 19 Issue: 1, pp. 189-216, https://doi.org/10.1108/CG-04-2018-0144

[49] Sultana N (2015) Audit committee characteristics and accounting conservatism. *International Journal of Auditing* 19: 88-102

[50] Zhou, H., Owusu-Ansah, S. & Maggina, A. (2018) Board of directors, audit committee, and firm performance: Evidence from Greece. *Journal of International Accounting, Auditing and Taxation*,31,20-36

[51] Zraiq M. A. A., Fadzil F. H. B. (2018) The Impact of Audit Committee Characteristics on Firm Performance: Evidence from Jordan. *Sch J Appl Sci Res*. Vol: 1, Issu: 5 (39-42)

Environmental Aspects of Product Life Cycle Management and Purchasing Logistics: Current Situation in Large and Medium-Sized Czech Manufacturing Companies

Lucie Hrbáčková[1], Anđelka Stojanović[2], David Tuček[1], Denisa Hrušecká[1]

[1] Tomas Bata University in Zlín, Faculty of Management and Economics, Department of Industrial Engineering and Information Systems, Mostní 5139, 760 01 Zlín, Czech Republic

[2] University of Belgrade, Technical Faculty in Bor, Vojske Jugoslavije 12, 19210 Bor, Republic of Serbia

E-mails: lhrbackova@utb.cz; anstojanovic@tfbor.bg.ac.rs; tucek@utb.cz; hrusecka@utb.cz

Abstract: This paper is focused on current approaches to the environmental behavior of large and medium-sized Czech manufacturing Companies, in relation to the control of environmental aspects through the whole product life cycle and the management of environmental risks in individual phases of product life cycle. This work addresses environmental aspects of product life cycle including design, manufacturing and selected logistics activities, specifically solution for environmental risk management and levels of environmental system considering environmental activities in manufacturing companies. Based on the qualitative and quantitative research performed through the structured interviews combined with questionnaire survey, authors provide an analysis of the actual insight into managing environmental risks and aspects through the whole product life cycle in Czech manufacturing companies. Results are considered also from the viewpoint of individual elements of environmental system and relation of environmental activities to the country's legislative requirements and other system standards across the business environment. Based on the research activities, the authors found out that the final customer is the most important stakeholder influencing risk management in the individual phases of the product life cycle. Further research steps will be directed towards the comparative study of the environmental performance of medium and large manufacturing companies in other countries. Practical use of research results is focused especially on the new agreement of the environmental requirements with customers throughout the whole logistics chain.

Keywords: Level of environmental management system; product life cycle; environmental aspects; risk-based thinking; purchasing logistic

1 Introduction

Nowadays, businesses are influenced by the following trends – a Green Economy and Circular Economy. Global trends determine the future business behavior. This article is focused on the environmental performance of large and medium-sized manufacturing companies in order to identify the underlying motives for managing environmental aspects and risks from raw material purchase, product development, through logistics and manufacturing to recycling.

Sustainable development involves 17 goals to assure sustainability for future generations. The voluntary approach in business environmental area is presented by the Corporate Social Responsibilities in economic, social and environmental area (CSR) of small and medium companies in the Czech Republic. This guide involves three pillars, one of them is the environmental area with several recommended activities (Business Leaders Forum, 2004). This approach brings both the direct and indirect advantage and ensures long term competitiveness. (Amaeshi, Nnodim and Osuji, 2013). From a different point of view, Hitchens et al. (2005) prove that companies with average financial performance could be compared to high-performing competitors in environmental initiatives.

The main goal of Circular Economy (CE) is to maintain the value of materials, products and other resources as long as possible and return them back into the product cycle by reusing them and minimizing the generation of waste at the same time (Eurostat, 2018). Vranjanac and Spasić (2017) demonstrated positive and negative economic effects of waste management in their study focused on recycling of packaging waste and concluded that the presence of economic effects is not always instantly visible and have to be considered in all relevant relations. However, Leising et al. (2018) emphasize that the concept of the Circular Economy is not only about closing loops in terms of reusing waste but it includes also the concept of slowing material loops by introducing the long lasting reusable components and products. The products that become unusable at the end of their life cycles should be made predominantly of materials that can be recycled or incinerated in a waste incinerator or at least rapidly degraded to low molecular weight harmless substances in the dumping ground (Gregász et al., 2008).

Product life cycle in environmental concept was determined through the requirements of the norm ČSN EN ISO 14001: 2016, where the top management should determine risks and opportunities, which are related to environmental aspects of the company throughout the product life cycle. Siebert et al. (2017) highlight that life-cycle assessments assessing the impact of sustainability from a regional perspective have not been fully developed yet. It means assessing products' social implications as they are determined by the national and regional socio-economic conditions.

The risk assessment should be evaluated in all processes of a company and also in the environmental process (ČSN EN ISO 9001: 2016). According to the requirements the environmental activities of companies are focused on aspects in the area of air protection, nature and landscape, water and waste management. The main external factors influencing business in the area or environmental protection is a compliance with legislative requirements of Ministry of the Environment of Czech Republic and EU environmental legislation. There are two ways to establish environmental management system in Czech Republic. The first solution is to implement the EMAS (Eco-Management and Audit Scheme) and the second possibility is the norm ČSN EN ISO (the International Organization for Standardization) 14001: 2016 – Environmental management system. Both systems integrate environmental care to the business strategy, improve the environmental performance, achieve the environmental objectives and fulfil the compliance with obligations.

Many studies point out to the positive impacts of companies' competitiveness by using environmental activities in the companies. However, none of them explains what environmental activities are being implemented in the business area. The authors of the article focused on manufacturing companies in the Czech Republic, legislative requirements, standards and other environmental regulations to analyze the current environmental behavior of selected companies. Current studies deal with the importance of re-using waste, but none of them provides information about the current approach of manufacturing companies to this issue.

The aim of this paper is to describe the current environmental behavior of medium-sized and large manufacturing companies in Czech Republic to confront this behavior with the current legislative and system requirements and to identify potential barriers in following of new environmental trends.

Based on the results of theoretical research and qualitative study, we have defined the following hypotheses:

- H1: The level of environmental system positively affects the approach of the company to the environmental aspects through the whole product life cycle.
- H2: Companies that consider environmental risks through the whole product life cycle have implemented a complex methodology for determination and measurement of environmental risks for all stages of product life cycle.

2 Literature Review

Organizations have to implement sustainable actions, particularly in the field of environmental policy and energy. The European Union agreed to reduce greenhouse gas production by 20% by 2020. Renewable energy sources seem to be a significant part of the solution to this problem. From this perspective the potential for renewable energy and pro-active environmental and energy approach do not meet the present trends in developed countries (Ministry of the Environment, 2008-2018). In the following sections we shorty discuss current studies and legislative in the field of environment and their risk for management.

2.1 Environmental Aspects and Product Life Cycle

Innovations in the field of environment clearly represent a competitive advantage. Hojnik & Ruzzier (2017) suggested some solutions how companies can be profitable on one side and environmentally friendly on the other one. They simply stated that introducing eco-innovation would result in significant positive benefits.

Salim et al. (2018) mention world trends in imposing environmental management systems, ISO 14001 in particular. The authors highlighted increasing interest in environmental research in a research dated from 2000 to 2016. Voluntary environmental management system (EMS) plays an important role in achieving sustainable production and consumption practices.

Life cycle thinking (Loiseau et al., 2017) means an evaluation of the holistic impacts of land use planning policies on the environment. It signifies that we should take into account several aspects which relate to the territorial features and consumption patterns.

It is important to consider environmental aspect already during the phase of product design. As Kramoliš and Staňková (2017) point out, product design not only leads to innovative and modern products but it can significantly influence the financial performance of enterprises which is very closely connected with environmental aspects of production process.

According to Sarkis et al. (2010), the pressure of stakeholders to apply ecological practices lead to three types of measures: eco-design procedures, resource reduction procedures, and implementation of environmental management system procedures. The concepts of eco-design and product life cycle assessment (LCA) are well implemented theoretical concepts which bring measurable practical results.

Kolotzek et al. (2017) deal with the raw materials used in final products based on the triple bottom line approach. The authors of this study suggest a corporate-oriented raw material assessment model which considers an up to date sustainability assessments as well as the recent development in the field of critical analysis, life cycle impact assessment (LCIA) and social life cycle assessment (SLCA). Recommendations are the following: using alternative raw materials or technologies and the variation in the purchase of raw material.

An emerging research field called corporate environmental behavior, on which, more and more research is focused, gives rise to new environmental theories, such as, the theory of ecologically significant behavior (Stern 2000). Both pressures from outside and individual business characteristics encourage companies to adopt active environmental behaviors (He et al., 2016). However, government regulations have the most important impact. For this reason, research on corporate environmental behavior should inform environmental policy (Clark, 2005).

Vogtlander et al. (2017) explain a method called Eco-Efficient Value Creation to analyze the costs, market value and eco-costs of innovative product and service designs, which should be used in Business to Business (B2B) markets. The main goal of this method is to find lower eco-costs of materials depletion and pollution. However, despite the fact that situation in cost management is improving, many companies still maintain adherence to historical and conservative cost management systems (Novák & Vencálek, 2016). Therefore, the implementing of above mentioned approaches would require longer time and changing the way of thinking.

2.2 Risk Management in Environmental Area

Particularly, during an economic downturn in a country, an organization needs to determine and address its associated risks (Medic et al., 2016). As Taraba et al. say (2016) the risk-free projects and processes do not exist and therefore, it is necessary to set up measures in order to be able to identify and solve risks in any area even environmental one. Zhang et al. (2017) present a method for the application of dynamic Bayesian networks (DBNs) in conducting accident scenario analysis and dynamic quantitative risk assessment in their study. The authors used the following procedure: an accident scenario of the assessed activity is determined, the root causes, safety barriers, and potential consequences related to this activity are found, and then it is analyzed by performing a cause-consequence. Finally, uncertainties of events likely to occur are assessed. Berec at al. (2018) highlight the importance of risk assessment and risk management to achieve maximum security levels.

Khan et al. (2017) present holistic framework for environment conscious based product risk modelling and assessment. The authors assessment the product risk in following steps: establish relationship among parameters, develop relationship graph for parameters, generate risk function, evaluate the ideal value of Risk index, evaluate risk index for individual design, repeat the steps for all other alternatives, rank all the design concepts based on index and select the best alternative.

Ning et al. (2018) describe safety risk assessment models in a construction site environment. These models consist of three parts, i.e. factor identification and classification from more categories, factor analysis, and assessment function development. The factor analysis is based on quantifying the risk factors according to five ranks and evaluating the likelihood of accident occurrence.

Németh-Erdődi (2008) describes, that before starting an innovative project in value to assess the market risk and risk of product implementation and decide on the way and cost of product development taking into account the acceptable risk. Wong (2017) describes the risk-based thinking in daily operations in a practical and effective way for chemical testing. Wong recommended to use the Plan-Do-Check-Act cycle (PDCA) in a specific form: Risk assessment, planning actions, progress monitoring and reporting for review. This form of PDCA cycle shall achieve the integration of risk-based thinking into the quality management system.

3 Methodology

In the first step the authors performed a qualitative analysis in order to get a realistic general knowledge about the current state and situation in the field of environmental management system in Czech manufacturing companies. The method of structured interviews was used to gain a basic information describing the level of environmental management and related risk based-thinking and environmental aspects in the whole product life cycle. Respondents of qualitative research were precisely selected in order to cover the whole considered segment. Our sample included 3 large and 3 medium-sized companies from different industrial branches (mechanical engineering, automotive, textile, food, chemical and plastic industry). The results showed that all interviewed companies with implemented environmental system also actively attend to the management of environmental aspects through the whole product life cycle. However, the level of implemented environmental risk management system is slightly different among all interviewed companies. The same respondents were also used for testing the comprehensibility and structure of the questionnaire used for evaluating set of hypotheses.

To realize the quantitative research, authors used an electronically distributed questionnaire. Based on the questionnaire, the authors approached 5 000 large and medium-sized Czech manufacturing companies in the first half of 2018. A total of 247 large and medium-sized Czech manufacturing companies from different industrial branches answered the questionnaire and participated in our survey. The structure of our respondents includes different industrial branches - production of food products, beverages, clothes, textiles, wood processing, paper production, production of chemical substances and chemical preparations, pharmaceutical products, rubber and plastic products, repairs and installation of machinery and equipment, manufacture of machinery and equipment, production of transport and equipment, car manufacturing, engineering and electrical equipment manufacturing. The second aspect taken into account during the research was the ownership structure. The sample of respondents includes 55% of companies with domestic majority owner, 27% with foreign majority owner, 12% subsidiary companies with foreign majority owner and 6% of subsidiary company with domestic majority owner. The main goal of our study is to understand better the main barriers influencing the management of environmental risks because it becomes more and more important nowadays.

Both hypotheses were tested by appropriate statistical methods. First of all, the Pearson correlation test was applied to detect the existence of correlations between all groups of questions. It was supplemented by Cronbach Alpha test in order to prove gained results and measure the level of internal consistency of each group. After that the SPSS v.17 and AMOS v.18 software were used to test first hypothesis and parametric paired sample, Student's T-test was applied to test the second hypothesis.

A questionnaire based research was used to obtain data for evaluating the above mentioned hypotheses. Besides the initial basic identification and classification questions (industry, size of the company, owner structure etc.), the questionnaire includes 6 questions related to the level of environmental management system applied (Q1 – Q6) and the next 3 questions (Q10 – Q12) describing the risk-based thinking and environmental aspects related to the product life cycle.

Table 1
The list of questions asked via questionnaires

No.	Question	Type
Q1	The reason of implementing EMS	Closed
Q2	Interaction of TOP management in EMS	Closed
Q3	Defining the competences and responsibilities in the area of company´s environmental activities	Closed
Q4	Strategic concept for environmental policy till 2020	Closed
Q5	Training of employees in the area of EMS	Closed
Q6	Monitoring of current environmental trends	Closed
Q8	Does a company consider environmental risks through the whole product life cycle?	Closed
Q9	How does a company determine the environmental risks?	Closed
Q10	Does a company consider suppliers´ approach to environmental matters as one of their evaluation criteria?	Dichotomous
Q11	Does a company consider the environmental impact when purchasing a new machines and technologies?	Dichotomous
Q12	Does a company consider environmental aspects in a process of product design and development?	Dichotomous

Source: authors´ own

To evaluate the first hypothesis, H1: The level of environmental system positively affects the approach of the company to the environmental aspects through the whole product life cycle, we divided all related questions into two groups. The following figure (Figure 1) shows the scheme of evaluating hypothesis H1 which is more complicated and includes more questions influencing the result. According to our hypothesis, the positive answers in a group of questions related to the maturity of environmental systems cause the positive answers in a group of questions related to the management of environmental aspects through the whole product life cycle. In case of the negative results we are going to study the relations between the questions separately.

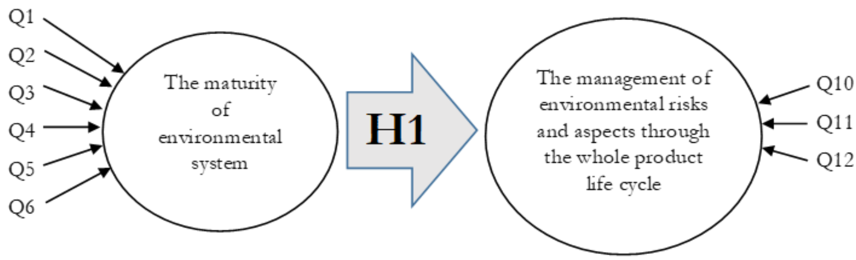

Figure 1
Scheme of evaluating the hypothesis H1 (source: authors´ own)

The second hypothesis looks at the level of environmental risk management regarding companies considering environmental risks through the whole product life cycle. The sample used for evaluation of the second hypothesis includes only respondents that answered positively to question no. 8. To confirm the hypothesis, the respondents farther had to choose both answers a) and b) in question no. 9.

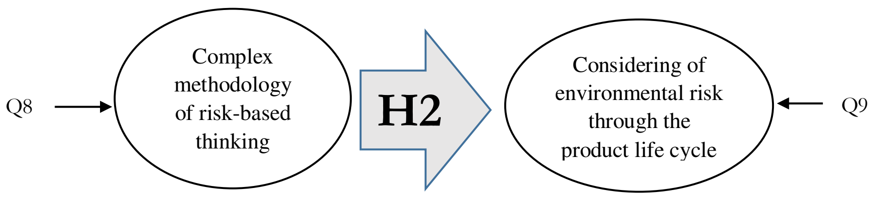

Figure 2
Scheme of evaluating the hypothesis H2 (source: authors´ own)

4 Empirical Results and Discussion

The following section provides a brief interpretation of the empirical results to both defined hypotheses. In order to get the most relevant results, we tried to keep the structure of the sample similar to the universe regarding the complexity of industrial activities included (see NACE structure in Figure 2) and owner structure.

4.1 Evaluation of the First Hypothesis

Hypothesis H1 says that the level of environmental system positively affects the approach of the company to the control of environmental aspects through the whole product life cycle. In order to prove/disprove the hypothesis, two group of questions were formulated. First group (Q1 – Q6) examines the maturity of environmental systems and the second group (Q10 – Q12) examines the level of managing environmental aspects through the whole product life cycle.

The hypothesis was tested via LISREL Structural Equation Model, where individual questions represent observed variables and group 1 (G1) and group 2 (G2) are latent variables consisting of observed ones.

In order to check whether observed variables are referred to appropriate latent variables the existence of correlations between individual questions in groups G1 and G2 were tested (Table 2). This is also important parameter which can lead to conclusion if LISREL structural equation modeling can be used to available questionnaire results. Subsequently EFA (Exploratory Factor Analysis) was performed. After reviewing the results of EFA and the correlation matrixes for both groups of questions the question Q3 is removed from further analysis due to very low correlations with other items from group. The rest of the questions from group G1 belongs to one factor with high factor loadings presented in Table 3. Reliability checked using Cronbach's α coefficient for G1 is 0.843 and it is considered as highly reliable.

Table 2

Pearson Correlation between all questions

	Q1	**Q2**	**Q3**	**Q4**	**Q5**	**Q6**	**Q10**	**Q11**	**Q12**
Q1	1								
Q2	0.498**	1							
Q3	0.215**	-0.134*	1						
Q4	0.596**	0.545**	-0.090	1					
Q5	0.532**	0.589**	-0.125*	0.847**	1				
Q6	0.414**	0.523**	-0.057	0.536**	0.536**	1			
Q10	0.366**	0.489**	-0.220**	0.399**	0.439**	0.421**	1		
Q11	-0.154*	-0.071	0.115	-0.133*	-0.088	0.020	0.069	1	
Q12	-0.087	0.055	0.154*	-0.036	0.005	0.032	0.088	0.239**	1

Correlation significance: *p<0.05, **p<0.01

Table 3

The results of Exploratory Factor Analysis

Maturity of environmental systems		**Level of managing environmental aspects through the whole product life cycle**	
Questions	Factor loading	Questions	Factor loading
Q1	0.750	Q10	-0.414
Q2	0.774	Q11	0.738
Q4	0.880	Q12	0.753
Q5	0.885		
Q6	0.736		
Eigenvalue	3.308	**Eigenvalue**	1.282
Variance explained %	55.131	**Variance explained %**	42.741

Source: authors´ own

The questions from group G2 generated one factor with factor loadings presented in Table 3. Considering all output questions (questions from G2) individually, we can observe statistically significant correlation of question Q11 with the question Q12. It is caused by the fact that many organizations have started to consider environmental aspects during the phases of designing new processes or products. Therefore, the company that consider environmental aspects in a process of product design and development takes care also about the environmental friendly technologies used for its production. It is not the same situation in case of question Q10, which is highly influenced by the negotiating power of suppliers and this situation is changing more slowly. In case of connection between Q10 to the other output questions (Q11 and Q12), a small negative correlation occurs in the most cases. Generally, the second group seems to be inconsistent. The same results were gained also by a component matrix analysis and Cronbach Alpha test which were used to test the reliability of both groups of questions before testing the hypothesis. According to the Cronbach Alpha test we detected a negative average covariance among answers in the second group (Cronbach´s Alpha reached negative value -0.068). The reasons for all observed inconsistencies can be various. Obviously the wrong structure of questionnaire or wrong formulation of questions can lead to a negative covariance among answers. However, this is not case of presented study because the authors avoided this risk by preliminary research and testing the comprehensibility of the questionnaire during the phase of qualitative research. The main reason is explained in the following paragraph.

70% of interviewed companies is certified according to ČSN EN ISO 14001:2016. These companies declare fulfilling all requirements of this norm saying that companies should determine risks and opportunities which are related to environmental aspects of the company throughout the product life cycle. Questions Q10, Q11 and Q12 were selected based on interviews in the preliminary phase as the most often occurred ones. Just suppliers´ evaluation and purchasing of new machines and technologies in the phase of new products´ design and development must be realized with regard to their environmental impacts. However, sometimes the force of external involved sides is too strong that it does not allow companies to fulfil all set goals in the environmental area. Therefore, as the main reason of above mentioned inconsistencies among the answers in the second group of questions is considered just this external involved side, obviously customers. Customers very often highly affect decision making processes of their suppliers including also environmental aspects and they have crucial influence to their planning and control of key business processes.

After defining the conceptual model, it has to be verified whether the model appropriately describes the relations among observed and latent variables by Measurement variables analysis and evaluate hypothesis with Path analysis.

The model fit indices in Table 4 show that proposed model is valid due to the obtained values of fit indices are acceptable or above recommended values (Jovanović et al., 2018; Schumacker & Lomax, 2004).

Table 4
The fit indices of proposed model

Fit indices	χ^2	df	χ^2/df	RMSEA	RMR	GFI	CFI	NFI	AGFI	IFI
Recommended values	-	-	<3	<0.08	<0.1	>0.9	>0.9	>0.9	>0.9	>0.9
Values for structural model	37.25	17	2.21	0.07	0.03	0.96	0.98	0.97	0.92	0.98

Source: authors´ own

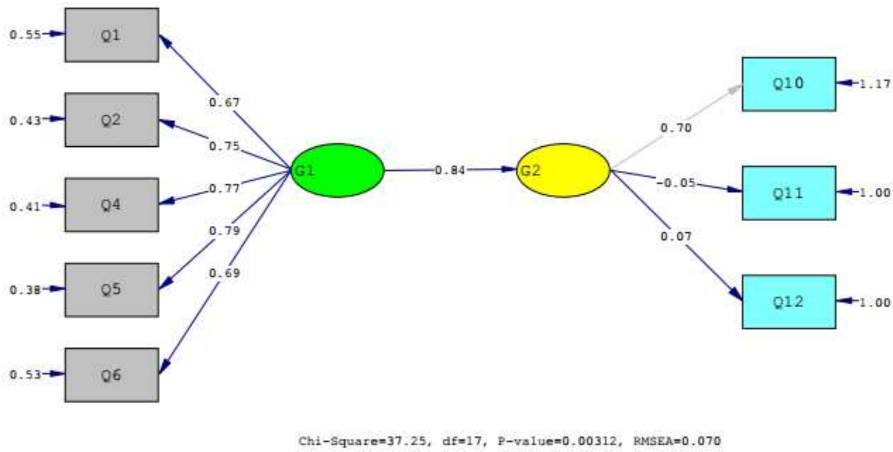

Figure 3
Final model describing correlations between two tested groups of questions based on standardized solution for the structural model (source: authors´ own)

The tested structural model presented in Figure 3 indicates that hypothesis 1 is confirmed since path analysis resulted with the β coefficient value 0.84 while t-test is 9.27 and it is statistically significant ($p<0.05$). The test is positive despite detecting a negative average covariance among answers in the second group as mentioned above. This inconsistency occurred especially in case of respondents with a low level of environmental system management and therefore it did not influenced the structural model at all.

It means that the higher level of environmental system management leads to the more serious approach of the company to the environmental aspects through the whole product life cycle.

4.2 Evaluation of the Second Hypothesis

Hypothesis H2 focuses on the management of environmental risks through the whole product life cycle. It assumes that companies considering environmental risks through the whole product life cycle have implemented a complex methodology for determining and measuring of environmental risks for all stages of product life cycle. Regarding the fact that this hypothesis examines connection between two single questions (Q8 and Q9), it was evaluated by Pearson correlation analysis and parametric paired sample Student's T-test.

The following correlation matrix (Table 3) proves that there is a statistically significant relationship between our two considered questions Q8 and Q9 (2-tailed significance < 0.01 and Pearson correlation r = 0.213).

Table 3

Pearson Correlation for hypothesis H2

	Q8	**Q9**
Q8	1	
Q9	0.213^{**}	1

Correlation significance: *p<0.05, **p<0.01
Source: authors´ own

Also the Student's T-test proved the relationship between both tested questions on the confidence level of 95%. However, regarding the fact that the average difference between both variables is 0.551 and the t-value is quite low (t = 16.567), we cannot state that there is a positive correlation between considered questions with adequate statistical significance.

While interviewed companies consider environmental risks in relation to the product life cycle, just the minority of them is establishing a complex methodology for determining and measuring of environmental risks for all stages of product life cycle. Such kind of a methodology is a voluntary activity of an organization which is not ordered by any norm or regulation. Therefore, hypothesis H2 was not unambiguously proven.

Conclusions

Business behavior is determined by global trends, which include, environmental aspects focusing on improving environmental sustainability, higher usage of renewable resources, clean production and protecting nature and all natural resources. Companies are very often forced to prove compliance to legislative requirements, usually EN ISO 14001. This norm leads to manage environmental aspects and risk through the whole product life cycle including design and development, purchasing logistics, manufacturing process, sales and reverse logistics and re-using of materials.

The main goal of presented study, was to examine what level of environmental system is currently used by large and medium-sized Czech manufacturing companies, how it affects the approach of the company to the environmental aspects through the whole product life cycle and what are the main barriers influencing the management and measuring of environmental risks in individual phases of product life cycle. Our results showed that environmental issues are highly influenced by the legislation and other regulations or system norms across the whole business environment. Nevertheless, a significant player in the strategic direction of the companies within the supply chain is the customer - an external stakeholder. When evaluating the second hypothesis, we identified customer as the most crucial barrier affecting the management of environmental risks within the whole product life cycle.

Another observed phenomenon resulting from the absence of environmental strategy is the fact that some companies just try to keep minimal required compliance with relevant norms, regulation or legislation but they do not care about management of environmental aspects and risks during all phases of product life cycle in depth. Therefore, in our future research we will focusing on development of the complex framework. for better transferring requirements of EN ISO 14001 or EMAS into the individual phases of product life cycle including all relevant environmental aspects and risks. Another potential for further research is the focus on a comparative study in other countries, which are actively involved within the corporate sector, in environmental activities according to existing statistics.

Acknowledgement

The authors are thankful for the financial support received from the project Development of complexly methodology of process planning, management and organization by implementation and utilization of INDUSTRY 4.0 concept in SMEs (VaV-IP-RO/2018/03) at the Tomas Bata University in Zlín. This work was also supported by the internal grant project IGA/FaME/2017/016 - Environmental and energy risk management in relation to the triple bottom line concept within selected industrial sector in the Czech Republic and the SHAPE ENERGY project founded by the European Union’s Horizon 2020 research and innovation programme under grant agreement No 731264.

References

[1] Amaeshi. K.; Nnodim. P.; & Osuji O. (2013) *Corporate social responsibility. entrepreneurship. and innovation*. London: Routledge. Taylor & Francis Group. Routledge studies in business ethics. ISBN 978-0-415-88079-4

[2] Berec. T.; Kovács J. (2018) Risk Assessment of the Human Factor in the Field of Building and Infrastructure Defense. *Acta Polytechnica Hungarica.* 15(8) 195-207, 10.12700/APH.15.8.2018.8.10

[3] Business Leaders Forum (2004) Společenská odpovědnost firem průvodce nejen pro malé a střední podniky. *Business Leaders Forum.* [2018-03-18] Retrieved from: http://csronline.cz/wpcontent/uploads/2012/11/BLF_Pruvodce_CSR.pdf

[4] Clark. M. (2005) Corporate environmental behavior research: informing environmental policy. *The Economics of Corporate Social Responsibility*. 16(3) 422-431, doi:10.1016/j.strueco.2004.04.006

[5] ČSN ISO 9001:2016 *Quality management system - Requirements.* 2016. Prague: Czech Normalization Institute. Classificatory sign: 99316. ČSN ISO 14001:2016 Environmental management system – Requirements with quadance for use. 2016. Prague: Czech Normalization Institute. Classificatory sign: 99312

[6] Eurostat. (2018) *Circular Economy*. (2018-02-22) Retrieved from http://ec.europa.eu/eurostat/web/circular-economy

[7] Gregász. T.; Korondi E. (2008) Influence of Maitenance Strategies on Environmental Load. Acta Polytechnica Hungarica. 5(3), 29-37

[8] Hitchens. D.; Thankappan. S.; Trainor. M.; Clausen. J. & De Marchi. B. (2005) Environmental performance. competitiveness and management of small businesses in Europe. *Tijdschrift voor economische en sociale geografie.* 96(5) 541–557. ISSN 1467-9663

[9] He. Z. X. Xu. S. CH.; Shen. W. X.; Long. R. Y. & Hong Chen. H. (2016) Factors that influence corporate environmental behavior: empirical analysis based on panel data in China. *Journal of Cleaner Production*. 133. 531-543. ISSN 0959-6526

[10] Hojnik. J. & Ruzzier. M. (2017) Does it pay to be eco? The mediating role of competitive benefits and the effect of ISO14001. *European Management Journal*. 35(5) 581-594, doi:10.1016/j.emj.2017.07.008

[11] Jöreskog. K. G., & Sörbom. D. (1996) *LISREL 8: Structural equation modelling with the SIMPLIS command language*. London: Scientific Software International

[12] Jovanović,I.; Arsić, M.; & Nikolić, Đ. (2018) Entrepreneurial personality traits and SMEs profitability in transition economy. *Serbian Journal of Management*, 13(1) 89-104

[13] Kramoliš, J.; & Staňková, P. (2017) Design and its Impact on The Financial Results of Enterprises (Based on Managers´ Opinions). *Journal of Competitiveness*, 9 (2) 62-77, Doi: 10.7441/joc.2017.02.05

[14] Leising. E.; Quist. J. & Bocken. N. (2018) Circular Economy in the building sector: Three cases and a collaboration tool. *Journal of Cleaner Production*. 176. 976-989. Doi: 10.1016/j.jclepro.2017.12.010

[15] Loiseau. E.; Aissani. L.; Le Féon. S.; Laurent. F.;Cerceau. J.; Sala. S. & Roux. P. (2017) Territorial Life Cycle Assessment (LCA): What exactly is it about? A proposal towards using a common terminology and a research agenda. *Journal of Cleaner Production.* 176 (2018) 474-485. Doi: 10.1016/j.jclepro.2017.12.169

[16] Khan. R. A.; Anand. A. & Wani. M. F. (2017) A holistic framework for environment conscious based product risk

[17] modeling and assessment using multi criteria decision making. *Journal of Cleaner Production*. 174 (2018) 954e965. doi: https://doi.org/10.1016/j.jclepro.2017.11.005

[18] Kolotzek. Ch.; Helbig. Ch.; Thorenz. A.; Reller. A. & Tuma. A. (2017) A company-oriented model for the assessment of raw material supply risks. environmental impact and social implications. *Journal of Cleaner Production.* 176 (2018) 566-580. doi: https://doi.org/10.1016/j.jclepro.2017.12.162

[19] Medić. S.; Karlović. B.; Cindrić Z.; (2016) New standard ISO 9001:2015 and its effect on organisations. *Interdisciplinary Description of Complex Systems*. 14(2). pp. 188-193, DOI: 10.7906/indecs.14.2.8

[20] Ministerstvo životního prostředí. (2008-2018) [2018-03-19] Retrieved from: https://www.mzp.cz/cz/parizska_dohoda

[21] Németh-Erdödi. K.; Risk Management and Loss Optimization at Design Process of Products. *Acta Polytechnica Hungarica*. 5(3). 105-115

[22] Ninga. X.; Qia. J. & Wub Ch. (2018) A quantitative safety risk assessment model for construction site layout Planning. Safety Science. 104 (2018) 246-259, Doi: https://doi.org/10.1016/j.ssci.2018.01.016

[23] Novák, P.; & Vencálek, O. (2016) Is It Sufficient to Assess Cost Behavior Merely by Volume of Production? Cost behavior research results from Czech Republic. *Montenegrin Journal of Economics*, 12 (3), 139-154, Doi: 10.14254/1800-5845.2016/12-3/10

[24] Sarkis. J.; Gonzalez-Torre. P. & Adenso-Dian. B. (2010) Stakeholder pressure and the adoption of environmental practices: The mediating effect of training. *Journal of Operations Management*. 28(2). 163-176, ISSN 0272-6963

[25] Salim. H. K.; Padfield. R.; Hansen. S. B.; Mohamad S. E.; Yuzir A.; Syayuti. K.; Tham. M. H & Papargyropoulou. E. (2018) Global trends in environmental management system and ISO14001 research. *Journal of Cleaner Production.* 170 (Supplement C) 645-653, doi:10.1016/j.jclepro.2017.09.017

[26] Schumacker, R. E.; & Lomax, R. G. (2004) *A Beginner's Guide to Structural Equation Modeling*. 2nd ed. New Jersey: Lawrence Erlbaum Associates, Inc

[27] Siebert. A.; Bezama. A.; O'Keeffe. A.; & Thraen. D. (2017) Social life cycle assessment indices and indicators to monitor the social implications of wood-based products. *Journal of Cleaner Production*. 172 (2018) 4074-4084, Doi: 10.1016/j.jclepro.2017.02.146

[28] Stern. P. C. (2000) New environmental theories: toward a coherent theory of environmentally significant behavior. *Journal of social issues*. 56(3) 407-424, ISSN 1540-4560

[29] Taraba, P.; Hart, M. & Pitrová, K. (2016) Risk Management of Projects in the Czech Republic. *Polish Journal of Management Studies*, 13 (1) 181-191, DOI 10.17512/pjms.2016.13.1.17

[30] Vogtlander. J. G.; & Scheepens. A. E.; Nancy M. P. Bocken. N. M. P. & David Peck. D. (2017) Combined analyses of costs. market value and eco-costs in circular business models: eco-efficient value creation in remanufacturing. *Jnl Remanufactur*. 7:1-17, DOI 10.1007/s13243-017-0031-9

[31] Vranjanac. Ž. & Spasić. D. (2017) Economic and Environmental Effects of Collection and Primary Recycling of Packaging Waste from Hygiene and Cleaning Products in Serbia. *Serbian Journal of Management*. 12 (2) 317-330, doi: http://dx.doi.org/10.5937/sjm12-11998

[32] Wong S. K.; (2017) Risk-based thinking for chemical testing. *Accred Qual Assur*. Issue 22, pp. 103-108, DOI 10.1007/s00769-017-1256-x

[33] Zhang. L.; Wu. S.; Zheng. W.; Jianchun Fan. J. (2017) A dynamic and quantitative risk assessment method with uncertainties for offshore managed pressure drilling phases. *Safety Science*. 104 (2018) 39-54, https://doi.org/10.1016/j.ssci.2017.12.033

Migration Determinants and Potential Impact of Brexit on Migration from the CEE Countries to the UK

Mihaela Simionescu

Institute for Economic Forecasting of the Romanian Academy, 13, Calea 13 Septembrie, District 5, Bucharest, Romania; mihaela.simionescu@ipe.ro

Yuriy Bilan, Stanisław Gędek

Faculty of Management, Rzeszow University of Technology, al. Powstańców Warszawy 10, 35-959 Rzeszów, Poland; y.bilan@prz.edu.pl; gedeks@prz.edu.pl

Abstract: The aim of this study is to identify the determinants of migration from the selected Central and Eastern European (CEE) countries to the UK and to measure the potential effects of Brexit on the migration from these states. The inclusion of CEE countries (Poland, Latvia, Lithuania, Bulgaria, Romania, Czech Republic, Cyprus, Slovakia, Hungary) into the EU has increased the number of the UK immigrants, on average, by almost 1300% over 2004-2015, as compared to Turkey, Russia and Ukraine. There is high uncertainty regarding the future UK policies on migration and consequently, regarding the number of immigrants from the CEE countries, but some models were built under two hypotheses: restrictions and no restrictions in the UK immigration. Mixed-effects Poisson models were built under the hypothesis that the CEE migrants will be treated as in the period before their EU entrance. The empirical findings indicate that, after Brexit, the number of the UK immigrants from the mentioned CEE countries might decrease by 2 times, until 2020. Under the hypothesis of no restrictions for the EU immigration, the number of immigrants from the EU in the sample might increase by 4 times until 2020, according to the Bayesian ridge regressions. In this context, the UK should focus on policies that promote immigration of a high-skill labor force and do not limit the number of low-skill immigrants in those fields where there is a deficit of UK-born workers. In case of a decline in the immigration, from the CEE countries, economic issues related to labor productivity, economic growth and government expenditures might appear.

Keywords: immigrants; economic integration; Brexit; CEE countries; migration policy

1 Introduction

In the UK, most of the immigrants came from non-EU countries, but in the course of the Brexit debates, its supporters frequently mentioned EU membership among the causes to leave the Union. Migrants coming from the Central and Eastern European (CEE) countries are perceived as a threat for the UK economy, and this idea has already found some reflection in media. However, the empirical studies suggest that the post-2004 workers' mobility improved economic growth, increased employment rate, and reduce labor shortages in the EU-15 countries. CEE immigrants in the UK contributed to the welfare system in the host country more than they spent using public services. In this sense, Petroff highlighted the contribution of migrants to the public budget which accelerates economic growth [28]. The EU immigrants to the UK did not harm salaries, public services or jobs. Moreover, they alleviate the issue of population ageing. The real cause of the output decrease in the UK was the global financial and economic crisis which started in 2008 and not the EU immigrants' inflow.

There is a high uncertainty regarding UK migration policies after Brexit. Knowing that the migration issue was one of the arguments for Brexit, lower immigration from the EU states, CEE especially, is expected in the coming years. The UK restrictions on the EU migration will have consequences for British economy that might experience lower economic growth and more government's expenses for public services [46] [44].

In this paper, the main objective is to measure the impact of economic integration and of Brexit on the migration process from the selected CEE countries to the UK. We will identify some economic and social determinants of migration from the CEE countries to the UK. Moreover, the increase in the number of the UK immigrants due to the EU membership will be analyzed, making also comparisons with those CEE countries that are not EU members. Only the CEE countries with a large number of immigrants in the UK were included in this analysis. The specific nature of data allows us estimating Poisson models to assess the impact of the EU membership on the UK immigration and to predict the possible effects from Brexit on the UK immigration. Moreover, the impact of the EU membership on migration was assessed by comparison with other non-EU countries like Russia, Turkey and Ukraine that have been also sending migrants to the UK quite actively. According to difference-in-difference estimations, if no policies of reducing migration will be applied, until 2020 the number of immigrants coming from the mentioned CEE countries after Brexit could decrease twofold. The current immigrants could choose to come back to their countries of origin or, most probably, they will migrate to other EU countries. In case no migration restrictions are applied, the same economic and social factors will continue attracting migrants to the UK, thus, their number will continue to increase by 4 times until 2020, as compared to 2017.

The paper is structured as follows. After this Introduction, a brief literature review is provided, highlighting the main directions in research on the issues of migration from the CEE countries to the UK. Next two sections provide a methodological framework and empirical results on the economic and social determinants of migration in the UK and the EU membership on migration. Based on these empirical results, two types of scenarios are provided concerning the number of the UK immigrants after Brexit. The last section concludes.

2 Literature Review

The literature review will focus on few directions of research related to migration from CEE countries to the UK:

- The economic and social determinants of the migration from less developed countries in the Central and Eastern Europe to the UK, highlighting the importance of the EU membership for migration in case of some CEE countries
- The issue of immigrants from EU countries as argument for Brexit
- The potential impact of Brexit on the number of immigrants in the UK, especially immigrants from CEE countries [39]

The labor resources migration to a destination country might be described by the neo-classical approach that explains the decision to migrate by the structural determinants at macroeconomic level and the individuals' decisions at microeconomic level that act in a rational way for improving the living conditions [1] [2]. The unequal geographical distribution of labor force and capital is the main cause of migration. The macroeconomic determinants of migration (differences in income and unemployment rate between origin and destination country, social welfare and life cost in the receiving country compared to origin state) are connected with microeconomic determinants (the individual decision based on the comparison between costs and benefits of migration). The migration is justified only if the benefits in the destination country are higher than in the origin country [18].

If we focus on the determinants of migration to the UK, the economic reasons are the most important cause for migrating to the UK. The macroeconomic determinants from neo-classical theory apply also for the UK together with individual decisions based on better living conditions. The economic determinants for moving in the UK refer to output per capita, unemployment and wage differentials as well as consistent economic disparities between regions as Simionescu showed [38]. Contrary to previous studies from literature [15] [28] [41] in this empirical study, the economic and social determinants of migration to the UK were determined for each EU member state in the CEE. Actually, a specific profile of macroeconomic determinants for each origin country of migrants was built.

Galgóczi et al. indicated that the decision of migration from CEE countries to the UK is related to the need of a job [15]. Initially, the decision of migrating is freewill and with the intention to stay a limited period, but, after leaving the origin country, the emigration might become permanent. Unlike the non-EU citizens, the EU migrants from Central and Eastern Europe intend to stay only few weeks or months.

According to Springford (2013), the welfare gap is one of the main reasons of migration for migrants from CEE states. Therefore, the migrants are interested in receiving a job in the UK. Springford showed that only 0.8% of the EU immigrants have unemployment benefits one year after their arrival in the UK [41]. 71% of immigrants from EU countries chose to come in the UK for jobs. 6% of the EU migrants from UK are unemployed, but they do not ask for allowance support [28].

Unlike the previous period of communist regime, when migration reasons were related to the issues of transition economy and poverty pressure, after joining the EU, migrants from CEE countries were driven by the desire for a better life.

The migration decision to the UK of migrants from A10 countries might also be explained by the dual labor market approach. Before third EU enlargement, the UK had a lot of jobs in sectors with intensive physical work and low productivity that were not wanted by natives. Therefore, the United Kingdom was one of the countries that agreed with the EU enlargement from 2004 and was one of the few countries that did not impose high restrictions to migrants from CEE countries, as Cini and Borragán explained [6]. Before enlargement, the UK had the right to control its borders and it was exempt from a few asylum regulations and common standards on immigration in relation to CEE countries migrants [42].

The migration networks also contributed to a large immigration during the last ten years. For example, the Poles had a big community in the UK even before Poland's integration in the EU and after 2004 a climate of enthusiasm encouraged the Poles movement to the UK, as Salt and Okólski showed [35]. Actually, Poland is the country with the largest community of migrants in the UK. The higher wages in the UK than those in Poland attracted many Poles, even if illegal migrants have lower salaries than the minimum level in the UK. Drinkwater et al. [9] and Pollard et al. [29] used regression models to show that Polish migrants emigrated in the UK for economic reasons like: high unemployment and low salaries in Poland and slow economic growth in the origin country. Even if some Poles are high skilled, they make unqualified work, because they receive more money than in Poland [23] [24]. According to Clark and Drinkwater and Scott, even the other high-skilled migrants from CEE countries accepted unqualified jobs [8] [36]. The empirical results based on surveys among Polish immigrants identified the following determinants of migration: few opportunities in Poland, financial issues and high aspirations for personal and professional development [7]. Moreover, English is the second more spoken language in Poland which encouraged Poles to choose the UK as destination country [35].

This large number of immigrants from Poland and other CEE countries represented a strong argument for Brexit. In this context, the migration control was proposed after Brexit. Indeed, Ebell and Warren proved that EU membership had a positive impact on the number of UK immigrants, because of free capital movement and because of free goods and services trade, including labor mobility and pass porting that transformed the UK is a favorite destination country for emigrants in the entire Europe [12]. Moreover, the recent studies from literature do not underline the large number of immigrants from A10 countries, but also the negative attitude of media regarding some communities from CEE countries [10] [13] [22] [33] [37] [40]. For example, Spigelman (2013) showed that the negative attitude regarding Poles in the period 2004-2008 was not consistent with reality. The British media and population consider that uncontrolled immigration will negatively influence the Britons' salaries, jobs and even the life quality [4]. On the other hand, the economists showed the benefits of the EU immigrants for the UK economy. The immigrants use services and goods that stimulate demand and bring more jobs opportunities. Many recent studies in literature [11] [31] [46] showed that the immigration growth did not have a significant impact on the number of jobs and on the wage levels of the UK-born workers. Wadsworth et al. observed that the regions with high increase in the number of EU immigrants did not have greater fall in the number of jobs and in wage levels for the UK-born people [46]. After 2008, the wages decreased because of the global financial crisis.

The extra resources brought by the UK immigrants could be used for growing the spending on local health and education for the UK-born people. The EU migrants brought more resources for public services than their expenditure for education and health. The reduction of EU immigration would bring greater austerity. Geay et al. did not find any significant impact of immigration on education expenditure [16] while Wadsworth showed a lower usage of medical services by the UK immigrants from EU countries, because most of the EU immigrants are younger than non-EU ones [47].

According to empirical researches, the EU immigrants brought also other benefits to the UK economy. Ortega and Peri and Ottaviano et al. identified a positive effect of high-educated migrants on the labor productivity in the UK [25] [26]. Moreover, Felbermayr et al. concluded that the increase in the immigrants' stock by 10% generates, in average, an increase in the income per capita by 2.2% [14].

In this empirical study, we assess the impact of immigration from some EU countries in the CEE on some macroeconomic indicators (real economic growth, employment rate, health and education expenditure). In this case, we use a Bayesian approach that was not employed before in literature, but that is suitable for small time series.

The evaluation of the impact of Brexit on EU migrants in various studies from literature takes into account the number of immigrants after Brexit and, consequently, the effects of changes in immigration on the UK economy. In case of restrictions on immigration from CEE countries, our empirical findings are in line with other studies from economic literature. Portes and Forte and Vargas-Silva anticipated a decrease in the number of EU immigrants in the UK, because of the possible restrictive migration policies after Brexit [31] [43]. On the other hand, the young people from 1.5 generation, living in the UK and coming from Central and Eastern Europe, do not intent to leave this country after Brexit and they feel they belong in Britain [43].

However, none of the previous research focused only on CEE countries immigrants. Actually, the real problem of Brexit supporters was the migrants from CEE states and not from all EU countries.

It is possible that more restrictions on these specific countries, will be imposed, in terms of migration policies, after Brexit. In this context, the UK policies should focus on the attraction of new immigrants. According to Woodford, government policies should concentrate on skills and not on workers' origin countries [48]. This type of policy might increase the productivity. After Brexit, fewer workers with low salaries might exist.

Other restrictions for reducing the number of migrants from CEE countries will not be in the benefit of the UK economy. In case of a significant decrease in the number of EU immigrants, the benefits of even highly-skilled sectors are doubtful [3] [4]. The high decrease in the number of migrants will have damaging effects in sectors like manufacturing, health, food processing, cleaning and tourism [4].

The Brexit supporters expect a control of EU migration, but if the UK will chose trade agreements with the EU (European Economic Area or European Free Trade Area), it should ensure free labor movement for EU citizens like Switzerland and Norway [42]. If Norway model is taken, more EU immigrants than wanted will be received in the UK. If the Switzerland model will be followed, the access to the Single Market is partial, but the EU immigration is not controlled [34]. According to Vargas-Silva, a restriction might appear when the UK asks for a more relaxed trading agreement, having more trade costs [45].

In our empirical research, we also considered a scenario after Brexit when no restrictions on migration are taken into account. A liberal policy on migration might grow the GDP until 2030 [3]. Chu showed that a lower decrease in the UK economic performance will be achieved after Brexit in case of a low decrease in the EU immigration [5]. In our opinion, the UK should receive the EU immigrants from CEE countries in order to cover the necessity of low-skilled jobs. This will stabilize the GDP and will ensure a growth in income per capita [3].

In the case of a post-Brexit points system, the UK should implement a temporary migration scheme or a preferential treatment for the EU migrants [34]. Another solution could be some bilateral agreements with certain EU countries.

Considering the possible effects of Brexit on the number of EU immigrants and on the UK economy, we consider some post-Brexit scenarios for the number of migrants from some EU countries in the central and Eastern Europe. Moreover, some policy measures are indicated in order to alleviate the negative consequences of migrant decline on the UK economy. These scenarios after Brexit were considered by taking into account macroeconomic determinants of migration to the UK (optimistic scenario with no restrictions on migration) and EU membership (pessimistic scenario with restrictions on migration).

3 EU Membership as Determinant of Migration to the UK and a Pessimistic Scenario for the Number of Immigrants after Brexit

The mixed-effects Poison regression models are used to estimate the number of CEE countries immigrants in the UK. In general, mixed-effects Poison regression model are employed for describing the expected counts number in a period when certain events are registered. The event in this study reflects the entrance of a CEE country in the EU and it takes place in a certain year (2004 or 2007). The count data for dependent variable allows the use of the Poisson models.

We considered 7 countries that entered EU in 2004 (Poland, Latvia, Lithuania, Czech Republic, Cyprus, Slovakia, Hungary), 2 states that became members of the EU in 2007 (Bulgaria, Romania) and 3 countries out of the EU (Turkey, Russia and Ukraine).

The differences-in-Differences (DD) estimation is used to make comparisons between groups of elements after a certain treatment or intervention. In our case, the entrance into the EU is the event and the groups are represented by countries that entered the EU and countries that are not in the EU. In this case, there are two groups of countries: countries in treatment (those that entered into the EU at a certain moment) and control countries for years before and after the European economic integration. Y_{ist} is the outcome for country *i* from group *s* (country *s*) by moment *t,* being represented by the number of immigrants. A dummy variable I_{st} is added for marking the effect of the intervention (entrance in the EU) of that group at a certain time.

$$Y_{ist} = A_s + B_t + cX_{ist} + \beta I_{st} + e_{ist}$$

A_s, B_t- fixed effects

X_{ist}- individual control

e_{ist}- error

The dependent variable in the approach based on difference-to-difference estimator is represented by the number of immigrants from the 10 mentioned CEE countries. The explanatory variables will refer to: the quality of EU member (it takes the value 1 in case of EU membership and 0 else), the year when the entrance in the EU took place and a variable computed as a product of the previous two variables. The impact of the intervention (the entrance in the EU) is measured by the estimate of β.

In this empirical research, only some particular CEE countries were chosen from a representative sample of 60 countries that have a large number of emigrants in the UK. For the rest of the CEE countries, the data are not available or the number of emigrants is not significant. In the mixed-effects Poisson models, several explanatory variables were considered: real wage, real GDP per capita and unemployment rate in these origin countries of the migrants, distance between London and the capital of each country. We introduced a dummy variable (denoted by EU member) to show the countries that are EU member states in a certain year. The models use panel data for the mentioned 12 countries and the period 2004-2015. Poland, Latvia, Lithuania, Czech Republic, Cyprus, Slovakia, Hungary entered the EU in 2004. Bulgaria and Romania became EU member state in 2007. The data for the number of immigrants were provided by the Office for National Statistics in the UK. The distances between London and the capital of each state were provided by http://www.distancefromto.net/, being measured in kilometers and they refer to air distances. The data for the other variables are taken from the World Bank database.

Table 1

Mixed-effects Poisson models for explaining the number of the UK immigrants from selected countries (2004-2015)

	M1			M2		
Variable	Coefficient	z-computed	P>|z|	Coefficient	z-computed	P>|z|
Wage	0.011	80.88	0.000			
GDP per capita	-0.0004	-77.55	0.000	-0.00005	-22.26	0.000
Unemployment rate	-0.09	-26.55	0.000	-	-	-
EU member	10.178	40.26	0.000	6.5253	28.75	0.000
Distance	-	-	-	0.0073	0.74	0.000

Constant	2.770	11.47	0.000	-1.6367	-6.05	0.000
Random effects parameter						
EU member: independent	Estimate					
sd(ln(distance))	0.0022	0.0012	-	0.0014	0.0007	-
sd(constant)	$3.89 \cdot 10^{-9}$	0.0415	-	$2.23 \cdot 10^{-8}$	0.0430	-

As expected, the M1 model indicated that the EU membership encouraged the emigration from selected countries to the UK. The EU countries sent by 2 times more migrants in the UK compared to the non-EU countries. The results are consistent with expectations. Most of the EU states imposed restrictions to migrants from new EU members, excepting Cyprus and Malta, because of the concerns about negative impact of migration on labor market. Only the UK with Ireland and Sweden opened the labor market immediately after 2004 [20] [58] and attracted many migrants eager to work. The only restriction imposed by the UK referred to the adoption of a scheme requiring the registration of the EU-28 workers with the Home Office.

The changes in the GDP per capita in the selected CEE countries had a very low and negative impact on the emigration process towards the UK. As expected, states with low GDP per capita send more migrants to developed countries like the UK. The fall in GDP per capita is associated with higher poverty and less jobs opportunities. All the CEE countries have lower GDP per capita than UK and some migrants from CEE countries choose the UK as destination country. This behavior of the migrants explained by economic reasons is in line with other conclusions from literature. For example, Hatton and Wiliamson showed the correlation between GDP per capita changes in host country and the migration flow in the richer destination country for more continents [17]. If the GDP per capita in West Europe grows by 10 percent, then the migration to the US decreases by 12.6 percent. In our case, if the GDP per capita in a CEE country doubles, the number of migrants to the UK decreases by only 0.04 percent. If we compare the results with the previous ones for EU membership, we can conclude that CEE migrants were stimulated more to come to the UK by the free movement of workers than by the poverty in the origin country.

Contrary to expectations, unemployment rate had a negative impact on the number of the UK immigrants belonging to the mentioned countries and the wage had a positive impact. An explanation for these results might be the fact that the CEE emigrants are not necessarily represented by people that do not have any job in the origin country. They were looking for a higher salary in the UK, the wage in the origin country being not satisfactory. The recent economic literature focused on the brain drain phenomenon in the Central and Eastern Europe [19]. The high skilled labor resources go to developed countries where the salaries are better. The public policies in the origin countries are not in the favor of qualified adults and the brain drain represents an important capital loss. On the other hand, the brain drain might have long run positive effects in terms of remittances sent to origin countries [21].

In the case of Brexit, the number of immigrants in the UK from EU countries in the sample might decrease by 99.9%, according to M1 model. Moreover, the negative impact of unemployment has to be cautiously considered, because there are a lot of low-skilled immigrants in the UK from CEE countries. Many of these migrants are not considered when the unemployment rate in the origin country is computed, because as low-skilled people they are part of the underground economy.

The results based on second mixed-effects Poisson model (M2) were similar with those based on the first model. The reasons for these findings are exactly the same as for the previous model. The M2 model showed again that the EU membership positively influenced the UK immigrants from CEE countries, because of the labor market openness after the 2004 EU enlargement. The distance did not have a significant impact on the emigration from CEE countries to the UK. This empirical finding is similar with the conclusion of Pytlikova who indicated that distance has a low influence in selecting emigrants' destination country in the last decades [32]. The fall in the GDP per capita in the origin country is not a strong argument for migration in the case of CEE emigrants that come to the UK. This result is contrary to the expectation of Hatton and Wiliamson for the migration between continents [17]. The correlation between migration and GDP per capita is negative, but not so strong. A possible explanation could be the fact that the underground economy still could ensure jobs in the origin country. In the case of Brexit, the conclusion is similar with that based on the previous model. According to M2 model, the number of UK immigrants in the UK from EU countries in the Central and Eastern Europe might decrease by 99.8%.

A second approach supposes a comparison between EU states from Central and Eastern Europe and Turkey, Russia and Ukraine. A type of counterfactual analysis (difference-to-difference estimator) measures the impact of the intervention (CEE countries integration in the EU).

Table 2

The approach based on difference-to-difference estimator for explaining the number of the UK immigrants (M3 model) from selected countries (2004-2015)

Variable	Coefficient	t-computed	P>|z|
Year	1.2664	1.72	0.089
EU member	-25934.96	-2.38	0.019
Year x EU member	12.9453	2.38	0.019
Constant	-2514.32	-1.70	0.092

Prob. > chi-square=0.000
Source: own calculations

According to the approach based on difference-in-difference estimator, the integration of some CEE countries in the EU had a positive impact on the number of UK immigrants. The coefficient corresponding to variable *year* is not significant at 5% level of significance. Therefore, we can state that even before the integration in the EU, many migrants from CEE countries chose the UK as destination country. Actually, the political context after 1990s when CEE states made the transition from communist regime to a market economy and a democratic society changed the migration behavior. Since 1990 these CEE countries sent many emigrants to developed states from the West of Europe. The 2004 EU enlargement intensified the labor mobility from seven of the CEE countries to the UK. The 2007 enlargement increased the number of immigrants from Romania and Bulgaria in the UK [27].

Being in the EU, the number of the CEE countries emigrants to the UK increased, in average, by almost 13 times during 2004-2015 compared to the group of countries represented by Turkey, Russia and Ukraine. This group of non-EU countries has some migrants in the UK, but their behavior was influenced a long time by the political context in their origin countries. Most of the Turkish people in the UK came from Northern Cyprus because of the economic issues and of difficult political context with Greek Cypriots. Many Russians came to UK from Baltic countries after their entrance in the EU. Large groups of Ukrainian people were moved to UK after the end of the Second World War. From this moment until the mid-1980s, because of the restrictions regarding emigration from the USSR, only few Ukrainians came to the UK. The number of Ukrainian people in the UK increased only after the liberalization of the political system in the second part of the 1980s.

So, it is more than likely that the Brexit will have a high impact on the number of the UK immigrants from the CEE countries that are already EU member states. Possible restrictions of the UK regarding the free access of foreign people on the labor market will bring changes in the number of CEE immigrants. Some of them could orient to the remained developed countries from the EU [38].

4 Economic and Social Determinants of Migration to the UK and an Optimistic Scenario for the Number of Immigrants after Brexit

For each country in the selected sample, we check the empirical determinants of emigration from that country to the UK. Among potential determinants several macroeconomic indicators registered for UK economy were considered: real economic growth, health expenditure (% of GDP), employment to population ratio (%), adjusted net national income per capita (constant 2010 US$), GDP per person employed (constant 2011 PPP $), expenditure on education as % of total government expenditure (%). Some Bayesian ridge regressions were estimated and the significant explanatory variables were identified. The dependent variable that is explained is represented by the number of the UK immigrants from each country. The coefficients of the ridge regressions follow a normal distribution and the errors' variance follows an inverse gamma distribution. An explanatory variable in the regression is significant if PP1SD (Posterior probability that the standardized coefficient is within 1 standard deviation of 0) is less than 0.5.

For Cyprus and Turkey, none of the proposed macroeconomic determinants did not influence the number of UK immigrants. In case of Poland, the migrants were attracted by health expenditure, income per capita and expenditure on education in the UK. All these indicators reflect a better standard of living in the UK compared to CEE countries. So, the immigrants were attracted by the high expenses on public services meaning a better quality of public services and by better living conditions. Our results are more close to the conclusions of Ciżkowicz et al. (2007) based on surveys that consider the high aspirations of Poles for personal development an important determinant for migration in the UK [7]. Health expenditure and income per capita were the main determinants for Lithuanian migrants.

In case of Romania, Czech Republic, Slovakia, Bulgaria and Latvia, the migrants were attracted by health expenditure, income per capita and GDP per person employed in the UK. This shows that the migrants from these countries are more interested in the living conditions. Beside these indicators, migrants from Ukraine are also attracted by employment opportunities, while migrants from Hungary take also into account the expenditure on education. Russian migrants are only interested in the employment opportunities in the UK. Our empirical findings confirmed previous studies from literature that show that the main cause of the migration from CEE countries to the UK is the welfare gap [41]. Moreover, our empirical results are a step forward, because the causes of migration in the UK are identified separately for each CEE country. Russians and Ukrainians are focused on employment compared to the EU countries in the sample that look only for a better standard of living.

Table 3

Macroeconomic determinants of immigration in the UK from mentioned countries (2004-2015)

Country	Coefficient of (PP1SD in brackets):						Determinants:
	Real GDP growth	Health expenditure	Employment rate	Income per capita	GDP per person employed	Expenditure on education	
Poland	-6.544 (0.66)	164.696 (0.048)	18.533 (0.638)	138.388 (0.124)	13.363 (0.643)	-48.350 (0.434)	-health expenditure -income per capita -expenditure on education
Lithuania	5.262	31.778	-2.061	36.294	-9.043	-7.958	-health expenditure

	(0.634)	(0.128)	(0.658)	(0.103)	(0.539)	(0.562)	-income per capita
Czech Republic	0.288 (0.6010	8.753 (0.022)	0.387 (0.658)	8.952 (0.027)	-2.421 (0.363)	-0.747 (0.624)	-health expenditure -income per capita -GDP per person employed
Romania	-0.803 (0.603)	52.172 (0.14)	20.253 (0.51)	65.422 (0.082)	29.765 (0.285)	-8.542 (0.617)	-health expenditure -income per capita -GDP per person employed
Cyprus	-0.296 (0.658)	0.884 (0.621)	-0.557 (0.646)	0.905 (0.619)	1.066 (0.602)	-0.679 (0.638)	-
Bulgaria	2.765 (0.625)	18.887 (0.041)	4.665 (0.543)	15.199 (0.13)	-6.718 (0.341)	-4.253 (0.501)	-health expenditure -income per capita -GDP per person employed
Slovakia	-3.031 (0.559)	7.979 (0.216)	-1.043 (0.649)	8.219 (0.23)	6.133 (0.262)	-0.573 (0.658)	-health expenditure -income per capita -GDP per person employed
Hungary	3.678 (0.635)	25.249 (0.076)	12.014 (0.375)	28.65 (0.059)	-14.626 (0.159)	-7.396 (0.446)	-health expenditure -income per capita -GDP per person employed -expenditure on education
Latvia	5.745 (0.599)	23.474 (0.121)	4.944 (0.609)	26.292 (0.104)	-10.621 (0.376)	-5.456 (0.567)	-health expenditure -income per capita -GDP per person employed
Turkey	0 (0.663)	0 (0.663)	0 (0.663)	0 (0.663)	0 (0.663)	0 (0.663)	-
Ukraine	-0.743 (0.536)	1.433 (0.313)	1.272 (0.346)	1.748 (0.246)	1.152 (0.338)	-0.018 (0.663)	-health expenditure -income per capita -GDP per person employed -employment rate
Russia	1.248 (0.592)	1.822 (0.531)	-1.973 (0.501)	3.089 (0.355)	1.157 (0.557)	-1.13 (0.607)	-employment rate
EU member states in the sample	-1.198 (0.663)	345.586 (0.058)	71.895 (0.586)	359.788 (0.065)	-73.585 (0.539)	-94.773 (0.459)	- health expenditure -income per capita -education expenditure

In case the UK will chose to eliminate any restriction for migration of the people from the mentioned EU member states (Bulgaria, Poland, Romania, Latvia, Lithuania, Hungary, Slovakia, Czech Republic and Cyprus), the number of immigrants from these countries might increase by 4 times. This is an optimistic scenario under the assumption that free movement of people from EU countries will not be restricted. If we take all the EU member states in the sample, education and health expenditure as well as income per capita are the main causes of migration. Therefore, we will consider only these three determinants as seen in the equation (2), being the most relevant from the set of six potential determinants. The Bayesian regression based on these predictors will be used to forecast the number of UK immigrants from these countries until 2020. We will keep the same public expenditures like in 2015, while the income per capita will have the value of the World Bank's prediction for 2020:

Immigrants= 292.239 x health_expenditure+ 302.549 x income_per_capita – 68.4 x education_expenditure (2)

The previous equation will be used to predict the number of immigrants from the EU member states in the sample after Brexit until 2020, under the hypothesis that the UK will not put any restrictions to migration from EU countries.

The empirical results based on a Bayesian approach (Bayesian ridge regression models) showed that the number of immigrants from the seven countries that became EU member states after the second enlargement had a significant, but low impact on employment rate and health expenditure. When the immigration from these countries increased, the employment rate decreased, because many of these migrants work in black market. When the number of immigrants increased, the health expenditure also increased, but very low. A similar result was presented by Wadsworth who measured a low positive impact of EU immigration on the health spending [46]. A possible explanation could be that EU immigrants are younger and do not need special medical care.

Table 4

The impact of immigrants on various economic variables (2004-2015) (immigrants from Poland, Hungary, Slovakia, Czech Republic, Lithuania, Latvia, Cyprus)

Dependent variable	Coefficient of immigrants	PP1SD
Real GDP rate	0	0.663
Employment rate	-0.272	0.32
Health expenditure	0.4	0.013
Education expenditure	-0.004	0.646

The immigrants from the selected countries did not have a significant impact on the UK economic growth or on the education expenditure. Our empirical results are in line with Geay et al. (2013) who showed no impact of the UK immigrants on education expenditure. Therefore, we can state that our empirical results are in line with the previous studies from literature [11] [30] [46], that do not consider the immigrant issue as a correct argument for Brexit.

Conclusions

In this paper, some macroeconomic determinants of migration from CEE countries to the UK were identified and possible impact of Brexit on the number of migrants from these countries was assessed. As expected, the EU membership of some countries had a significant and positive impact on the number of the UK immigrants. In the case of Brexit, the number of EU states from Central and Eastern Europe might decrease by 2 times until 2020, according to results based on mixed-effects Poisson models. Compared to Russia, Turkey and Ukraine, the number of CEE migrants in the UK increased, in average, by 13 times in the period 2004-2015 just because of the EU membership.

If we strictly consider the macroeconomic determinants of migration to the UK, the better living conditions attracted many CEE migrants as the results of Bayesian ridge regressions indicated. In case no restrictions on migration will be considered for A10 countries, the number of immigrants from these countries might continue to increase by 4 times until 2020. On the other hand, our empirical results confirmed the previous studies and CEE migrants did not affect the education expenditure or the jobs of natives [30] [46].

This empirical research is limited by the data availability for some indicators. For the other CEE countries, the Office for National Statistics did not provide the number of the UK immigrants. A lower number of migrants from CEE countries in the UK could be explained by the expected restrictions of the UK Government for migration from these countries. The decrease in the number of EU immigrants was also predicted by Portes and Forte [31].

Two important migration policies should be taken into account after Brexit. The UK imposed a cap of 20,700 Tier 2 visas for each year. If this measure is applied to EU nationals, the number of EU workers will dramatically decrease. Moreover, another policy stated that most non-EU nationals with Tier 2 visas could stay permanently in the UK only if they earn a minimum of £35,000 per year. With some exceptions, the migrants who earn less than this threshold could not stay more than 6 months in the UK. Most of the actual EU nationals do not earn this money and if the rule is applied, they have to leave the UK or temporary stay here (Vargas-Silva, 2016). So, the current migration policies of the UK indicated a clear decrease in the number of EU immigrants.

After Brexit, a policy that controls immigration would lower the economic growth, even if the impact on the output per capita GDP could not be so significant. The UK has many policy options after Brexit. The Switzerland or Norway models will promote free movement, but some bilateral agreements with several states will negatively affect the UK economic performance. In case the UK will not choose policies for a limited reduction in the number of EU immigrants, the labor market flexibility and labor productivity will decrease and the UK economy could have more frequent recessions. A good recommendation could refer to policies that take more into account the labor market flexibility after Brexit than measures for limiting migration in the origin countries of the immigrants.

This study could be continued by selecting other determinants of immigration in the UK. The poverty that affects the CEE countries could explain the orientation towards an economically developed country as the UK, but a long data series for poverty rate is not available for all the CEE states. In the context of restrictions on migration after Brexit, the emigrants from CEE countries should consider other destination countries from EU. The number of the existing UK immigrants could be affected by the policy measures after Brexit, but stable immigrants have low chances to leave the UK.

Our empirical results have some limitations, being affected by the uncertainty regarding the future UK policies on immigration after the exit from the UK. In the first scenario, we work under the assumptions that all the advantages of EU members in terms of migration before Brexit will be dropped. We made this hypothesis because migration issue was brought as a strong argument for Brexit. Vargas-Silva also considered that free movement of workers will be an unpopular option, because the migration issue as Brexit argument [46]. If the UK government will not impose significant restrictions, regarding labor market mobility of the CEE countries migrants, the number of immigrants from these states will not be significantly affected. In the second scenario, free movement is promoted, as in the period after the A10 integration in the EU. In this case, the number of immigrants will continue to increase.

Acknowledgement

This work was supported by a grant of Ministry of Research and Innovation, CNCS - UEFISCDI, project number PN-III-P1-1.1-PD-2016-0163, within PNCDI III.

References

[1] Alecke, B., Huber, P., & Untiedt, G. (2001) What a difference a constant makes: how predictable are international migration flows?. *Migration Policies and EU Enlargement The Case of Central and Eastern Europe: The Case of Central and Eastern Europe*, 200163

[2] Arango, J. (2000) Explaining migration: a critical view. *International social science journal*, *52*(165), 283-296

[3] Booth, S. (2015) *What would Brexit mean for immigration?*, (Open Europe, March 23, 2015)

[4] Boswell, C. (2016) *Migration: would limiting the free movement of labour be good or bad?, In: Jeffery, C. & Perman, R., Britain's Decision: Facts and Impartial Analysis for the EU referendum on 23 June 2016*, Edinburgh: The David Hume Institute

[5] Chu, B. (2016) *Post-Brexit Britain would need to keep migration high to prevent economic fallout*, (The Independent, March 22, 2016)

[6] Cini, M., & Borragán, N. P. S. (2016) *European union politics*. Oxford University Press

[7] Ciżkowicz, P., Hołda, M., & Sowa, U. (2007) The new wave of polish migration after EU enlargement-current state, determinants and outlook. MPRA Paper No. 18596. Munich

[8] Clark, K., & Drinkwater, S. (2008) The labour market performance of recent migrants. *Oxford Review of Economic Policy*, *24*(3), 495-516

[9] Drinkwater, S., Eade, J., & Garapich, M. (2009) Poles apart? EU enlargement and the labour market outcomes of immigrants in the United Kingdom. *International Migration*, *47*(1), 161-190

[10] Drzewiecka, J. A., Hoops, J. F., & Thomas, R. J. (2014) Rescaling the state and disciplining workers in discourses on EU Polish migration in UK Newspapers. *Critical Studies in Media Communication*, *31*(5), 410-425

[11] Dustmann, C., Fabbri, F. & Preston, I. (2005) 'The Impact of Immigration on the UK Labour Market', *Economic Journal,* 115, 324-341

[12] Ebell, M., & Warren, J. (2016) The long-term economic impact of leaving the EU. *National Institute Economic Review*, *236*(1), 121-138

[13] Esses, V. M., Medianu, S., & Lawson, A. S. (2013) Uncertainty, threat, and the role of the media in promoting the dehumanization of immigrants and refugees. *Journal of Social Issues*, *69*(3), 518-536

[14] Felbermayr, G. J., Hiller, S., & Sala, D. (2010) Does immigration boost per capita income?. *Economics Letters*, *107*(2), 177-179

[15] Galgóczi, B., Leschke, J., & Watt, A. (2009) Intra-EU labour migration: Flows and policy responses. *Béla Galgóczi, B., Leschke, J. & Watt, A. (eds.)*, 1-28

[16] Geay, C., McNally, S. & Telhaj, S. (2013) Non-Native Speakers in the Classroom: What are the Effects on Pupil Performance?. *Economic Journal* 123, 281-307

[17] Hatton, T. J., & Williamson, J. G. (2005) What fundamentals drive world migration?. In *Poverty, international migration and asylum* (pp. 15-38) Palgrave Macmillan UK

[18] Hille, H., & Straubhaar, T. (2001) The impact of EU-enlargement on migration movements and economic integration: Results of recent studies. *Migration Policies and EU Enlargement The Case of Central and Eastern Europe: The Case of Central and Eastern Europe*, 200179

[19] Ienciu, N. M., & Ienciu, I. A. (2015) Brain drain in Central and Eastern Europe: new insights on the role of public policy. *Southeast European and Black Sea Studies*, *15*(3), 281-299

[20] Kahanec, M., Zaiceva, A., & Zimmermann, K. F. (2009) Lessons from migration after EU enlargement. In *EU labor markets after post-enlargement migration* (pp. 3-45) Springer Berlin Heidelberg

[21] Kim, J., & Lee, N. Y. (2016) The Effect of High-Skilled Emigration, Foreign Direct Investment, and Policy on the Growth Rate of Source Countries: A Panel Analysis. *East Asian Economic Review*, *20*(2) 229-275

[22] Mikalauskiene, A., Streimikiene, D., Mazutaityte-Cepanoniene, E. (2017) Employers' Openness to Labour Immigrants. *Economics and Sociology*, 10(3) 25-45

[23] Miłaszewicz, D., Milczarek, A., Nagaj, R., Szkudlarek, P., & Zakrzewska, M. (2015) Determinants of Polish international migration in the area of the European Union after 2004. *Journal of International Studies*, *8*(3) 62-78

[24] Okólski, M. (2001) Incomplete migration: a new form of mobility in Central and Eastern Europe. The case of Polish and Ukrainian migrants. In *Patterns of migration in Central Europe* (pp. 105-128) Palgrave Macmillan UK

[25] Ortega F., & Peri, G. (2014) Migration, Trade and Income. *Journal of International Economics,* 92, 231-51

[26] Ottaviano, G., Peri, G., & Wright, G. (2016) Immigration, Trade and productivity in services. *CEP Discussion Paper*. 1353 (http://cep.lse.ac.uk/pubs/download/dp1353.pdf)

[27] Pemberton, S., & Scullion, L. (2013) The policies and politics of managed migration: Exploring mature labour migration from Central and Eastern Europe into the UK. *Journal of Ethnic and Migration Studies*, *39*(3) 443-461

[28] Petroff, A. (2016) The truth about UK immigration, (CNN, April 7, 2016)

[29] Pollard, N., Latorre, M., & Sriskandarajah, D. Floodgates or turnstiles? Post-EU enlargement migration flows to (and from) the UK. (2008) *Institute for Public Research (online at: http://www. ippr. org/publicationsandreports/publication. asp*

[30] Portes, J. (2016) Immigration, Free Movement and the UK Referendum. *NIESR Review* 236

[31] Portes, J., & Forte, G. (2016) The Economic Impact of Brexit-induced Reductions in Migration. National Institute of Economic and Social Research. 7 December 2016

[32] Pytlikova, M. (2006) Where Did Central and Eastern European Emigrants Go and Why. *Aarhus: University of Aarhus, School of Business, CIM and Department of Economics. Online: http://pure. au. dk//portal/files/482/6_phdchap4_MP. pdf (accessed: 31 December 2014)*

[33] Robinson, W. D., Bowlin, M. S., Bisson, I., Shamoun-Baranes, J., Thorup, K., Diehl, R. H., & Winkler, D. W. (2010) Integrating concepts and technologies to advance the study of bird migration. *Frontiers in Ecology and the Environment*, *8*(7) 354-361

[34] Ruparel, R. (2016) *Where next? A liberal, free-market guide to Brexit* (Open Europe, April 13, 2016)

[35] Salt, J., & Okólski, M. (2014) Polish emigration to the UK after 2004; why did so many come?. *Central and Eastern European Migration Review* (02) 11-37

[36] Scott, J. (2012) *Social network analysis*. Sage

[37] Spoonley, P., & Butcher, A. (2009) Reporting superdiversity. The mass media and immigration in New Zealand. *Journal of Intercultural Studies*, *30*(4), 355-372

[38] Simionescu, M. (2016) Macroeconomic Determinants of Permanent Emigration from Romania: a Bayesian Approach. *Journal of International Studies*, *9*(2) 170-180

[39] Simionescu, M., Bilan, Y., & Mentel, G. (2017) Economic Effects of Migration from Poland to the UK. *Amfiteatru Economic*, *19*(46) 757

[40] Simionescu, M., Bilan, Y., Smrčka, L., & Vincúrová, Z. (2017) The effects of European economic integration and the impact of brexit on the UK immigrants from the CEE countries. *E+ M Ekonomie a Management,* 1(20) 29-47

[41] Spigelman, A. (2013) The depiction of Polish migrants in the United Kingdom by the British press after Poland's accession to the European Union. *International Journal of Sociology and Social Policy*, *33*(1/2) 98-113

[42] Springford, J. (2013) *Is immigration a reason for Britain to leave the EU?* (Centre for European Reform, October 2013)

[43] Staiger, U. (2016) *Migration, the lightning rod of the EU referendum*, (openDemocracy, April 14, 2016)

[44] Tvaronavičienė, M., & Gatautis, R. (2017) Peculiarities of income distribution in selected countries. *Economics & Sociology*, *10*(4) 113-123

[45] Vargas-Silva, C. (2016) EU Migration to and from the UK After Brexit. *Intereconomics*, *51*(5) 251-255

[46] Wadsworth, J. (2015) Immigration and the UK Labour Market. CEP Election Analysis No. 1 (http://cep.lse.ac.uk/pubs/download/EA019.pdf)

[47] Wadsworth, J., Dhingra, S., Ottaviano, G., & Van Reenen, J. (2016) Brexit and the Impact of Immigration on the UK. *CEP Brexit Analysis*, No. 5

[48] Woodford. (2016) The economic impact of ‘Brexit’, (Woodford, February 17, 2016)

The Use of Advanced Manufacturing Technology to Reduce Product Cost

Fatmir Azemi[1], Goran Šimunović[1], Roberto Lujić[1], Daniel Tokody[2], Zoltan Rajnai[3]

[1]Mechanical Engineering Faculty in Slavonski Brod, JJ Strossmayer University of Osijek, Trg Ivane Brlić Mažuranić 2, 35000, Slavonski Brod, Croatia; fazemi@sfsb.hr, gsimun@sfsb.hr, rlujic@sfsb.hr

[2]Doctoral School on Safety and Security Sciences, Óbuda University, Népszínház utca 8, 1081 Budapest, Hungary; tokody.daniel@dosz.hu

[3]Bánki Donát Faculty of Mechanical and Safety Engineering, Óbuda University, Népszínház utca 8, 1081 Budapest, Hungary; rajnai.zoltan@bgk.uni-obuda.hu

Abstract: The rapid development of new technologies has led to a change in the ways of manufacturing in industrial organizations. As a result of this development, many companies and factories started to look for new forms of organizational structure and the implementation of new technologies in their manufacturing process. In this context, the CAD/CAM/CAE systems play a crucial role in the process of manufacturing and generally in the transition to digital manufacturing, as the basis of a new industrial revolution. This paper presents the application of new technologies in a product life-cycle, namely the application of an advanced CAD/CAM/CAE system to support the organizational lean manufacturing initiative of SMMEs in Kosovo as a means to achieve world-class performance. Two case studies have been completed, one on the advantages of applying the CAD/CAM system in product development and the second by applying traditional manufacturing. A further aim of this present paper is to bring initiatives to the collaborative environment and to bridge the gap between industry and educational institutions.

Keywords: CAD/CAM/CAE system; Lean Manufacturing; Smart Factory; SMMEs of Kosovo

1 Introduction

The use of ICT (Information and Communication Technology) and other technological options are still at an early stage for enterprises in Kosovo [1]. Introducing computerized systems and other ICT facilities in the process of manufacturing still pose a problem for company managers and their staff and most of them are hesitating to take initiatives in the process of replacing traditional manufacturing with advanced manufacturing technology. The lack of knowledge and training programs, the high costs of purchasing/maintaining such technology, the inadequate education of unskilled workers, the lack of creative administrative leadership and poor research in this field at the enterprises in Kosovo are the main challenges in the process of transforming enterprises using traditional manufacturing into ones using advanced manufacturing technology [2].

However, a recent survey carried out in South-East Europe found that 71% of the enterprises reported a profit of more than 5% in the last financial year. This is a good opportunity to open the door for technological investments which are essential in the transition process [3].

Adopting ICT and other technological facilities at the enterprises in Kosovo is a great challenge, especially if we take into account that the Kosovar market has a limited size, and the possibilities to distribute products in external markets are also very limited. However, most enterprises in Kosovo show a positive tendency toward the growing use of Computer and other ICT facilities in the development process of manufacturing [1].

The term of Advance Manufacturing Technology - AMT refers to the usage of computer technologies in the process of design, process of manufacturing, testing, transportation and controlling, etc. AMT ensures an organization with a possibility to successfully market place and establish for itself a competitive advantage. Academics and manufacturers believe that Advance Manufacturing Technologies can decrease operating cost, provide high levels of output by reducing inconsistent human input, improve flexibility in manufacturing and lead time to market [4].

AMT represents a wide diversity of mainly systems based on computer, that providing firms to be more adopted with the potential to improve operations in manufacturing greatly. It is extensively expected that the consequent improvement in performance of operational will increase the firm's ability to gather the underlying market, business and strategic benefits for whom the systems were adopted. Another definition of AMT may refer as a family of technologies which include engineering systems and computer-aided design (CAD), MRP systems (materials resource planning systems), computer controlled machines, automated materials handling systems, flexible manufacturing systems, electronic data interchange, robotics and computer-integrated manufacturing systems. AMT has been related as a system of programs machines or programmable machine that can produce a diversity of parts or products with almost no time lost for changes. The machines, linkages and computer control, as well as the human operator involvement, seems to be on a windy path from islands of technology towards some far wider grade of computer integration, noted to as computer integrated manufacturing (CIM) [5].

Successful AMT (Advanced Manufacturing Technology) implementations, such as the use of integrated CAD/CAM /CAE[1] systems and other new technologies are considered as the means to overcome the difficulties in manufacturing competitiveness. Among other tools which are important in the process of transforming traditional manufacturing into modern manufacturing, the CAD/CAM/CAE systems can have a special role.

Integrated CAD/CAM/CAE systems provide support for companies through reducing costs, improving product quality, saving time and fulfilling new customer requirements. Lean product development in this context [6] constitutes of several engineering methods and techniques. Therefore, the application of advanced CAD/CAM/CAE systems in product development can support organizational Lean Manufacturing initiatives in SMEs. Until now, relatively little quantitative research has been carried out on lean product development with the application of integrated CAD/CAM/CAE systems, especially at the enterprises in Kosovo.

Advanced industrial organizations have profoundly changed their manufacturing processes through the adoption of computerized technologies [7] [8]. This development is frequently viewed as the basis for a new industrial revolution—the advent of the "factory of the future"- and a new form of organizational structure [9]. Manufacturing in today’s world has developed and changed due to new technologies and worldwide competition. As a consequence, a need for faster product development has arisen. Other design and manufacturing technologies such as concurrent engineering, design for manufacture, just-in-time production, and computer aided design (CAD) have pushed the design envelope further [10].

The transformations happen through digital manufacturing and design from paper-based processes to digital processes in the manufacturing industry. The CAD/CAM/CAE system applies to all phases of activities from the product design to customer support in an integrated way (Figure 3), using different methods, means and techniques in order to increase production improvement, quality improvement, cost reduction, fulfilment of scheduled delivery dates, and total flexibility in the manufacturing system [11] [12].

[1] CAD – Computer Aided Design, CAM – Computer Aided Manufacturing, CAE – Computer Aided Engineering

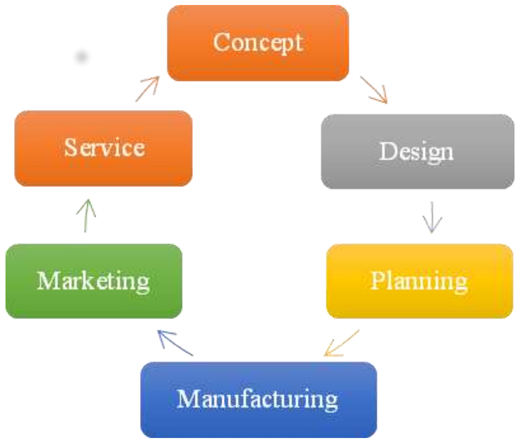

Figure 1
Product development cycle [10]

This paper presents the advantages of using ATM instead of traditional manufacturing technologies in order to encourage managers and other decision-makers to take initiatives in their start-ups to achieve advanced manufacturing through the implementation of integrated CAD/CAM/CAE systems in Small and Medium Manufacturing Enterprises (SMME). Through the examples of the following case studies, our paper also aims to bring initiatives for the collaborative environment to bridge the gap between industry and educational institutions.

2 Case Studies

The first case study has been done at the Laboratory of Faculty of Mechanical and Computer Engineering – University of Mitrovica "Isa Boletini" in Mitrovica. At the Faculty of Mechanical and Computer Engineering, currently there are five different programs: BSc Industrial Machinery, BSc Economic Engineering, BSc Engineering Informatics, MSc Engineering Informatics and MSc Production Technology. Among other equipment and machines, the laboratory provides the students of Mechanical Engineering with state-of-the-art engineering workstations and CAD/CAM/CAE software for a variety of applications in solid modelling, kinematics, dynamics, finite element modelling and analysis, numerical control machining simulation and others [13] [14].

The second case study has been done in a factory of mechanical production parts. This factory, established in 1974, was one of the biggest manufacturers of automotive parts in the region. Since the end of the war, however, this company has failed to apply any advanced technologies which could have increased efficiency and quality in production, and it is still using traditional manufacturing.

From these case studies we are tried to focus on the transformation of traditional manufacturing into digitalized manufacturing as well as on bridging the gaps between industry and education [15].

2.1 Methodology of the Case Studies

This part of the paper explains which method has been used to reach the objectives of the present study. The final objective was to present the advantages of the application of advanced manufacturing in the process of product development, which can help companies to reduce production time and costs and improve quality. To achieve this goal, two different types of inputs have been used; literature review and case studies. At the beginning our research focused on literature review, which was followed by the case studies. Two case studies were carried out to gather data from a factory and from an educational institution and finally the comparison of both data analyses were done.

2.2 Literature Review

To maintain or to be competitive and profitable, a manufacturing company or enterprise must have the ability to respond to a number of challenges, including rapid improvements in technology, workforce and in strategy in all aspects of product manufacturing due to globalization. Additionally, substantial changes in government policies have had significant impacts in many countries, as well as the increasing level of global trade. Manufacturing companies need to be clearer understanding of what their customers want and why customers purchasing their products instead of their competitors. Therefore, they need to fully understand the objectives of their business in terms of its customers, market segments, product attributes and geographical markets. The adoption of management technologies by SMEs may be the result of the pressure from the government, associated companies or customers.

In product development, wastes are inevitable, but they should be minimized as much as possible to have sound profit and sustain product development performance. Most of these wastes are time and process dependent and can be expressed in terms of costs, lead time, rework, defect rate, etc. To be successful in a competitive business environment, products and managers need a know-how of organizing as well as product development and manufacturing. Lean product development is a way to organize product development according to a set of principles [16] [17].

Lean product development in this context, constitutes of several engineering methods and techniques. The application of advanced CAD/CAM/CAE systems in product development supports organizational Lean Manufacturing initiatives in SMEs. However, relatively limited quantitative research has been carried out on lean product development with the application of integrated CAD/CAM/CAE systems, especially in Kosovo.

Recently, there have been an improvement in computer performance and manufacturing technologies, companies have integrated computer aided design [18] (CAD) into their design strategy, as well as CAD/CAM/CAE systems to increase efficiency. Lean production can be supported and facilitated by these tools.

Other deployment methods include training, supplier integration, machine configuration, the provision of greater understanding of the internal processes within the case company by illustrating ways in which ideas are generated, the approach taken and how the CAD/CAM system changed the organization’s work methods [19] [20].

Liu and Barrar suggested that a firm with a higher level of strategy-technology integration has achieved a degree of “fit” between strategy and technology, and thus would make the firm compete more effectively in the marketplace and attain a better operational as well as financial performance [21]. They also stress on the need for consistency between manufacturing strategy and business objectives. Apparently, many organizations lack this consistency [22] [23].

Studies of different AMTs suggests that they can be successfully introduced into SMEs, but that they will be implemented in ways that differ from large businesses. For example, in implementing TQM[2], small companies put more emphasis on leadership, employee involvement and quality information whereas larger firms emphasize training, feedback, quality assurance, and supplier cooperation [24].

The advantage of dealing with the issue of creating an NC code in the CAD/CAM system’s CATIA model for machining on a vertical milling machine tool system is that the creation of the NC program takes relatively short time regarding the complexity of the shape components utilized in milling. These systems are facilitated by the sufficiently rapid generation of NC codes and their easy adaptation to a suitable form for the CNC machining center. Using the systems with a CNC machining center in practice reduces the risk of errors arising during operation [25].

2.3 Case Study 1: The Use of an Integrated CAE/CAD/CAM System during the Parts Design

Computer Aided Design (CAD) systems are involved most of the activities in the design cycle, they are recording all data of the product, and they are used as a platform for collaboration between remotely placed design teams. CAD systems can shorten the design time of a product, enable the application of concurrent engineering and can have a significant effect on final product cost, functionality and quality [26].

[2] TQM – Total Quality Management is a management approach that originated in the 1950s and has steadily become more popular since the early 1980s

The objective of the two case studies presented in this paper is to elaborate the main advantages of using an integrated CAE/CAD/CAM system in product development instead of traditional methods. The first case study was carried out with the participation of nine students with an average knowledge of the CAD techniques in the process of design. The time spent for designing three parts with CAD software was measured. Results are presented in Table 1.

Computer Aided Manufacturing (CAM) creates physical models, generally refers to the use of numerical control (NC) computer software applications to generate detailed instructions (G-code) that drive computer numerical control (CNC) machine tools for the manufacturing of parts. In order to create the actual model, CAM works alongside CAD data designs, CAM uses numerical coding to run the machine that makes the product. A CAD/CAM package software allows companies to develop and save their own product designs, and program machines to make the actual component [27].

Table 1

The time for product design by students using CAD software

	Time for design product 1	**Time for design product 2**	**Time for design product 3**
	Unit [h:mm:ss]	Unit [h:mm:ss]	Unit [h:mm:ss]
Average	0:18:41	0:20:27	0:19:02

To measure the time of processing products, procedures were separated in two phases: the time for code generations with CAM software and the time for machining parts in CNC machines. Three products were produced with the involvement of nine students who produced the parts, and the time for the generation of G-Code and the time for machining was measured. Table 2 shows the measured time in the phase of product processing-manufacturing with the application of CAM software and a CNC machine.

Table 2

Average time of three products, measured during product processing with the aid of CAM software and a CNC machine

	Time for G-code generation CAPP[3] and CAM software [h:mm:ss]	**Time for machining in CNC machines [h:mm:ss]**	**Total time [h:mm:ss]**
Average	0:12:06	0:03:15	0:15:21

After the pieces had been manufactured in the CNC machines, they were measured with the help of various measuring tools and equipment. Results are presented in Figure 2.

3 CAPP – Computer Aided Process Planning

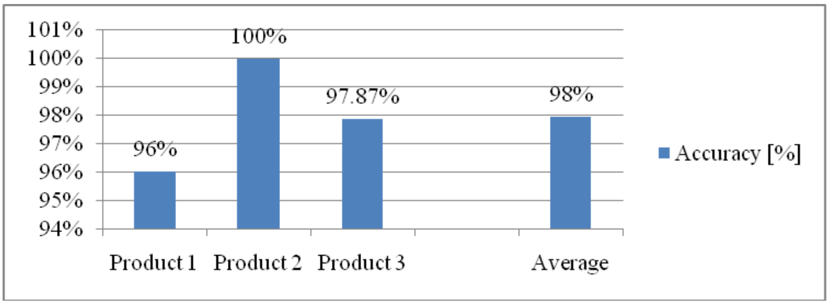

Figure 2
Accuracy of the pieces produced with advanced manufacturing

2.3.1 Cost of Product with the Application of Advanced Manufacturing

Cost of product refers to the costs used to make a product. Cost of manufacturing is the amount of the costs of all resources used in the process of making a product. The manufacturing cost is assorted into three categories: direct labor cost, direct materials cost and manufacturing overhead. To calculate the cost of the product we will focus only on the parameters which directly affect the ways of processing, and on the time which was spent on the process of design, on code generation and on product processing. The time which is required to produce one unit of Product 1 with the application of a CAD/CAM system is based on the above time results.

Participants: a design engineer, a production engineer and an operator.

Time for product manufacturing (case study 1):

$$T_m = t_d + t_m + t_s + t_{add} \quad (1)$$

Where are:

t_d[min] – design time, t_m[min] – machining time, t_s[min] – setup time, t_{add}[min] – additional time.

Where are:

Average design time (table 1)

$t_d = 18.683\ min = 0.31\ h$

Average machining time (table 2):

$t_m = 15.35\ min = 0.26\ h$

Setup time is supposed to be the same for both methods of manufacturing:

$t_s = 0.083\ h$

Additional time is:

$t_{add} = 0.030\ h$

Now, time for the manufacturing of one piece of the product is:

$\boldsymbol{T_m = 0.31+0.2558+0.083+0.030=0.703\ h}$

The price of the product in function of time, according to the time spent per workforce:

$\boldsymbol{C_w = DE \cdot t_d + PE \cdot t_m + 2 \cdot O \cdot (t_s + t_{add}) = 2.66\ €}$

Where:

***DE* = 4 €/h** – payment per hour of Design Engineer.

***PE* = 3.8 €/h** – payment per hour of Production Engineer.

***O* = 2 €/h** – payment per hour of Operator.

Price of stocks is the same for both methods, therefore it will not be calculated.

Then, the cost of product in function of consumed time per workforce is:

$\boldsymbol{C_p = C_w = 2.66\ €}$

It should be noted that in the calculation of the cost of the product some factors which do not depend on the method of manufacturing were not taken into consideration.

2.4 Case Study 2

Case study 2 served to collect data about the time spent on product design and product processing, about the accuracy and the cost of product when using conventional methods.

To obtain the results of the product design time in case of using conventional methods, the time spent on designing three products with the involvement of nine Design Engineers was measured. Results of the time spent on the process of design are presented in Table 3.

To measure the time of processing products, procedures were separated in two phases: the time for code generations by hand and the time for manufacturing parts. Three pieces have been produced with the involvement of nine students. Table 4 shows the measured time results in the phase of product processing-manufacturing with the application of conventional methods.

Table 3
The time of products design by Engineers using conventional methods

	Time for design product 1	**Time for design product 2**	**Time for design product 3**
	Unit [h:mm:ss]	Unit [h:mm:ss]	Unit [h:mm:ss]
Average	0:37:16	0:42:39	0:40:46

Table 4
Average time of three products measured during the processing of products using conventional methods

	Time for machine operation calculations - process planning [h:mm:ss]	Time for machining [h:mm:ss]	Total time [h:mm:ss]
Average	0:19:47	0:05:37	0:25:24

After the pieces had been manufactured in the machines, they were measured with the help of various measuring tools and equipment. Results are shown in Figure 3.

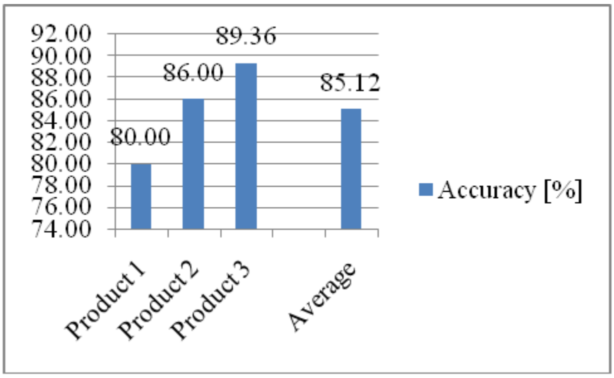

Figure 3
Accuracy of pieces produced by traditional manufacturing

2.4.1 Cost of Product Produced by Conventional Manufacturing

The required time for the production of one piece of product 1 with conventional methods based on the results from Table 3 and Table 4.

Participants: a design engineer, a production engineer and two operators.

Time for product manufacturing (case study 2):

$$T_m = t_d + t_m + t_s + t_{add} \quad \textbf{(2)}$$

Where are:

t_d[min] – design time, t_m[min] – machining time, t_s[min] – setup time, t_{add}[min] – additional time.

Average design time (Table 3):

$$t_d = 37.266 \text{ min} = 0.621 \text{ h}$$

Average machining time (table 4):

$$t_m = 25.04 \text{ min} = 0.4233 \text{ h}$$

Setup time is supposed to be the same for both methods of manufacturing:

$t_s = 0.083\ h$

Additional time is:

$t_{add} = 0.054\ h$

Now, the time for manufacturing one piece of the product with traditional manufacturing is:

$T_m = 0.6211+0.4233+0.083+0.054 = 1.044\ h$

The price of the product in function of time, according to the time spent per workforce:

$C_w = DE \cdot t_d + PE \cdot t_m + 2 \cdot O \cdot (t_s + t_{add}) = 4.54\ €$

Where are:

$DE = 4\ €/h$ – payment per hour of Design Engineer.

$PE = 3.8\ €/h$ – payment per hour of Production Engineer.

$O = 2\ €/h$ – payment per hour of Operator.

Price of stocks is the same for both methods, therefore it will not be calculated.

Then, the cost of product in function of consumed time per workforce is:

$C_p = C_w = 4.54\ €$

2.7 Comparison of Methods

This part of the thesis presents the issues of the measurement and the comparison of advanced manufacturing technology (AMT) and traditional manufacturing in the process of product development. Comparison is made between the product development using an integrated CAD/CAM/CAE system at the Laboratory of Faculty of Mechanical and Computer Engineering – University of Mitrovica "Isa Boletini" in Mitrovica and in a factory producing mechanical parts through traditional manufacturing.

Figure 4 presents the comparison of the average time of designing three products by nine students with the application of CAD software, and by nine engineers using traditional methods.

As it can be seen from Figure 4, the average time of designing products with Advanced Manufacturing Technology is less than the average time of designing products through Traditional Manufacturing. Figure 5 presents the comparison of the average time of processing products with advanced manufacturing technology and by using traditional manufacturing.

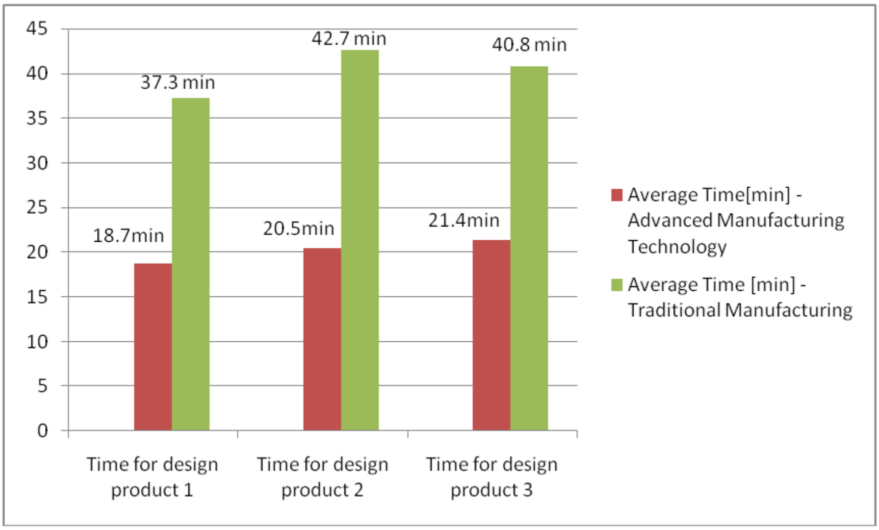

Figure 4
Comparison of average time of product design by AMT and TM

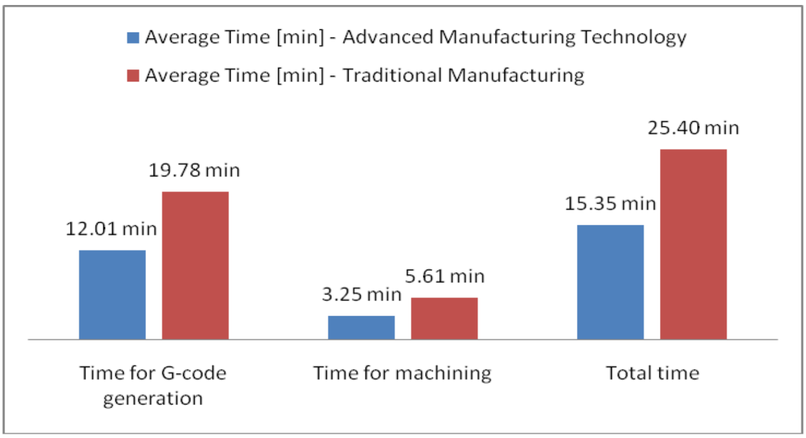

Figure 5
Comparison of the average time of processing

Figure 6 shows that the time of processing products with advanced manufacturing technology is also less than the time of processing products through traditional manufacturing.

Figure 6 shows the comparison of the accuracy of the production of three parts using AMT and TM. The accuracy rate is 98% with the application of advanced manufacturing technology, whereas it is 83% in the case of traditional manufacturing.

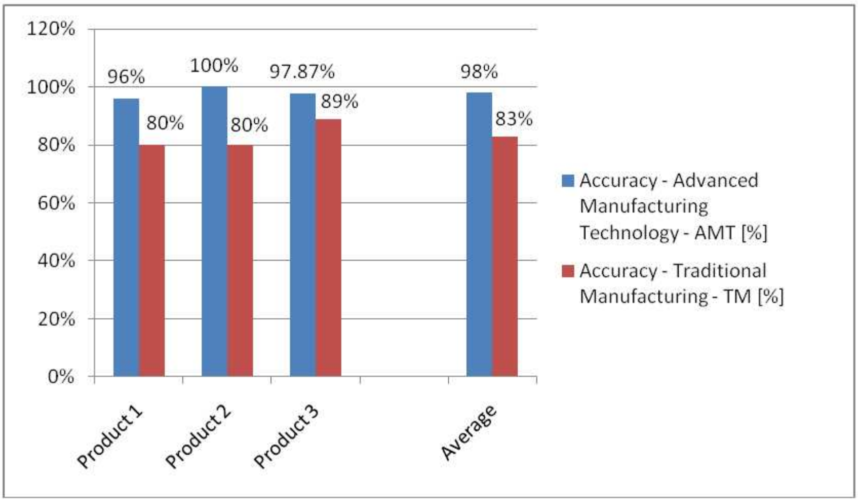

Figure 6
Comparison of the accuracy of the pieces produced with AMT and TM

Except for the above mentioned features, AMT has also been shown to reduce the amount of rework and wastes, which assign into improved quality and confidence to the customer. This reduction has been connected to the elimination of the manipulator (ATM has been automated the process of production), as well as the elimination of operator upset and fatigue.

Use of CAD/CAE also helps to create the better innovations in the product. By integrating analysis and process of design in development of product at the earlier stages the productivity can be enhanced and could be obtained superior designs (Authors Study) [28] [29].

3 Conclusions and Recommendations

The implications for educational institutions, for manufacturing firms and for the Kosovo government are substantial. Some businesses have already started to implement some of the new advanced technology in their production (questionnaire, interview), but many of them are not positioned to succeed in the implementation of any new advanced manufacturing technology. Enterprises in Kosovo need to radically change their approach to providing a constant and consistent framework within which all firms aspire to prosper.

The findings of this research conclude some phenomena based on case study analyses and literature review, as below:

- Traditional manufacturing processes face more difficulties than advanced manufacturing technology (Integrated CAD/CAM/CAE system).
- Advanced manufacturing technology processes save more time in production than traditional manufacturing. With AMT the time of production is 32.66 % less than in case of traditional manufacturing (case studies).
- CAD/CAM system processes can produce more accurate products in terms of the dimensions of parts than traditional manufacturing.
- The application of AMT can save material of stocks, increase productivity and improve communication.
- The cost of product with the application of advanced manufacturing technology is about 40% less than in case of traditional manufacturing (case studies).

The implementation of integrated CAD/CAM/CAE systems at the enterprises in Kosovo is essential to achieve Lean Manufacturing, to reduce overproduction, over-processing, defects, costs and workforce, and to improve quality.

4 Future Prospects and Challenges

At present, the main direction of development, within European industry, is defined by digitalization. Similar to the way the Industrial Revolution changed manufacturing, digitalization is having a profound impact on the transformation of today's industrial processes. Among other things, it provides basis for the creation of smart manufacturing systems and smart factories. Furthermore, this new technology enables manufacturing companies to move from mass production to customized production at a rapid pace. The future, therefore, is digital and digitalization is affecting all industries and all aspects of life.

This transformation, however, also presents some challenges. Computer Integrated Manufacturing (Industrial Automation Systems), for example, can be rather rigid in view of the frequent changes of demand. This means that existing systems may prove to be difficult to transform or expand, and performance can significantly decrease in anomalous circumstances. Strongly hierarchical and centralized systems are usually characterized by rigid interconnection, which results in non-flexible communication systems, where the flow of information implies the realization of a top-down autocratic hierarchy.

Manufacturing companies have been considered to be rather slow to take the opportunities presented by digital technologies, such as the use of intelligent robots, sensor technology, drones, artificial intelligence, nanotechnology and 3D printing. The digital transformation of manufacturing is also affected by such trends as IoT, Industry 4.0, data and analytics, artificial intelligence and machine learning. IoT can have an especially important role in the manufacturing industry, as it can significantly streamline and simplify various manufacturing processes by providing real-time feedback and alerting companies in case of errors or defective products.

Currently, these algorithms change the methods of data collection, performing skilled work or predicting costumer behavior. Smart factories using integrated IT systems can provide sufficient data for both sides of the supply chain in a much more convenient way, which can significantly increase production capacity. Big data analyses, however, can be a rather complex and time-consuming process, therefore digitalized factories may struggle with the management, update and analysis of product and customer information. Despite all these difficulties, the above changes seem to be inevitable. It is certain that Smart Factories, Smart Manufacturing and Smart Products will soon become integral parts of our lives.

Acknowledgement

We would like to thank the staff of the Faculty of Mechanical and Computer Engineering – University of Mitrovica “Isa Boletini” in Mitrovica that they have given us the opportunity to do research work at the Laboratory, as well as the staff of the factory (who wished to remain anonymous) for their support in the experimental research in the department of manufacturing.

References

[1] Azemi, F., Lujic, R., Simunovic, G., Maloku, B.: Utilization and impact of ICT on SMEs: The case study of the Kosovo private sector at furniture and metalworking industry. 17^{th} International Multidisciplinary Scientific GeoConference SGEM 2017, 29 June – 5 July 2017, Albena – Bulgaria, 751-758

[2] Azemi, F., Hajrizi, E., Maloku, B.: Maturity Level of Kosovo Manufacturing Industry with regard to Industry 4.0. 6^{th} International Conference on Business, Technology and Innovation 2017, October 27-29, 2017, Durrës, Albania

[3] K. D. Gunawardana, “Introduction of Advanced Manufacturing Technology: a literature review,” *Sabaragamuwa Univ. J.*, 2010

[4] P. Milgrom and J. Roberts, “The Economics of Modern Manufacturing: Technology, Strategy, and Organization,” *Am. Econ. Rev.*, 2008

[5] OECD; How South East European Countries' Statistics Measure Foreign Direct Investment. Paris: Organisation for Economic Co-operation and Development. 2007

[6] Bencsik, A. L., Lendvay, M., Trimmel A. K., Némethy, K., "Integration of new equipment by advanced process optimization," 2016 IEEE 11^{th} International Symposium on Applied Computational Intelligence and Informatics (SACI 2016) Timisoara, 2016, pp. 305-310, doi: 10.1109/SACI.2016.7507391

[7] Horvath, L., Rudas, I. J., Generic modeling of manufacturing processes using Petri net representations (1997) IEEE International Conference on Intelligent Engineering Systems, Proceedings (INES 1997) pp. 539-544

[8] Lojka, T., Bundzel, M., Zolotová, I., Service oriented Architecture and Cloud Manufacturing, Acta Polytechnica Hungarica Vol. 13, No. 6, 2016, pp. 25-44

[9] Belassi, W., Fadlalla, A., "An integrative framework for FMS diffusion". Omega. 26: pp. 699-713, 1998

[10] Roy U., Bharadwaj B., Kodkani SS., Cargian M. (1997) Product development in a collaborative design environment. Concurr Eng Res Appl 5:347-365

[11] Rudas, I. J., Horvath, L., Modeling man-machine processes in CAD/CAM and flexible manufacturing system (1996) IECON Proceedings (Industrial Electronics Conference) 3, pp. 1484-1489

[12] Radhakrishnan, P., Subramanyan, S., Raju, V., CAD/CAM/CIM, New Delhi 2008

[13] Pokorádi, L., Uncertainties of vehicle system modelling and simulation (2010) Proceedings of the Mini Conference on Vehicle System Dynamics, Identification and Anomalies, pp. 511-519

[14] Horvath, L., Rudas, I. J., Tenreiro Machado, J. A., Hancke, G. P. Application of part manufacturing process model in virtual manufacturing (1999) IEEE International Symposium on Industrial Electronics, 3, pp. 1367-1372

[15] Tokody D., Digitising the European Industry - holonic systems approach, 11th International Conference Interdisciplinarity in Engineering, INTER-ENG 2017, manuscript

[16] Szakál, A., "Application of Product Model for Engineering Process Definition," 2011 Fourth International Conference on Emerging Trends in Engineering & Technology, Port Louis, 2011, pp. 66-71, doi: 10.1109/ICETET.2011.36

[17] Morgan, J. M. & Liker, J. K. (2006) The Toyota product development system: Integrating people, processes, and technology. NY: Productivity Press

[18] Horváth, L., Rudas, I. J. Integrating expert knowledge in behavioral feature based product models (2002) IECON Proceedings (Industrial Electronics Conference) 3, pp. 2479-2484

[19] Horvath, L., Rudas, I. J., Bencze, J., Petri net modeling of manufacturing processes for CAD/CAM and FMS applications (1997) IECON Proceedings (Industrial Electronics Conference) 3, pp. 1216-1221

[20] Esan A. O., Khan M. K., Qi H. S., Naylor C., (2013) Integrated manufacturing strategy for deployment of CAD/CAM methodology in a SMME. Journal of Manufacturing Technology Management, 24 (2): 257-273

[21] Liu H., Barrar P., "Performance implications of strategy-technology connections: an empirical examination", Journal of Manufacturing Technology Management, Vol. 20, No. 1, pp. 52-73, 2009

[22] Dangayach, G. S., Deshmukh, S. G., "Advanced manufacturing technology implementation: evidence from Indian small and medium enterprises (SMEs)", Journal of Manufacturing Technology Management, Vol. 16, No. 5, pp. 483-96, 2005

[23] Sonntag, V., "The role of manufacturing strategy in adapting to technological change", Integrated Manufacturing Systems, Vol. 14, No. 4, pp. 312-323, 2003

[24] Sun, H., Cheng, T.-K., "Comparing reasons, practices and effects of ISO9000 certification and TQM implementation in Norwegian SMEs and large firms" International Small Business Journal 20(4): 421-442

[25] Jambor, J., Quality of production process with CAD/CAM system support, in: DAAAM International Scientific Book 2012, Vol. 11, Austria, pp. 277-286

[26] Bilalis, N., Computer Aided Design CAD; Report produced for the EC funded project, Technical University of Crete, January 2000

[27] Leondes, C.; Systems Techniques And Computational Methods, London, 2001

[28] F. Azemi, X. Mehmeti, and B. Maloku, "The Importance of CAD/CAE systems in development of Product Design and Process of Optimization," 2019

[29] F. Azemi, G. Šimunović, R. Lujić, and D. Tokody, "Intelligent Computer-Aided resource planning and scheduling of machining operation," Procedia Manuf., Vol. 32, pp. 331-338, 2019

Commissioning Integrated Process at Industrial Plants

Gloria Maria Alves Ney, Marcio Zamboti Fortes*

MPMI, Engineering School, Fluminense Federal University, Passo da Patria St., 156, E-431 Room, 24210-240, Niteroi, RJ, Brazil

E-mail: gloria.alves@aluno.cefet-rj.br; mzf@vm.uff.br

Abstract: This paper is a case study about the gasification system commissioning. After collecting data and information about this system analysis were made, related to TEXACO, SHELL, LURGI and E-GAS, then a flowchart was created. Simulations were made in the ARENA software for verification of commissioning performance. The results showed the importance of commissioning management in a standard commissioning process and other integrated proposed were compared.

Keywords: Commissioning; Gasification Process; Flowchart; ARENA Software

1 Introduction

Commissioning is a challenge for companies, because less time and warranty that all technical issues attended is the target, which will transform the enterprise in a competitive one. The results of enterprise's competitiveness is cost reduction, increase profits and improve the process. An industrial plant commissioning is very important to verify equipment's functionality which is part of systems inside the plant. If the commissioning were planned correctly, it is possible mitigate problems with main benefit cost and works reduction.

It is required to verify the activities of all involved disciplines. Sometimes it can be very hard to define which are those activities without rework, excessive duration, exceeding cost and a good relationship between disciplines. Bendiksen and Young [1] says that during commissioning phase erection problems show up and will be necessary increase the cost and time to repair those problems. So, changes and upgrades will be done in commissioning activities at the same time that they occur.

The gasification process is getting more attention in the last decades because of the high demand in clean fuels and the reduction in fossil fuels use [2] and the high demand of renewable fuels because of petroleum crises [3]. Gasification is a flexible, a safe process and a commercial technology that contributes to reducing the use of petroleum and natural gas, being a clean alternative to energy generation, fertilizers industry, and fuel and chemical industry. This process can convert any material that has high levels of carbon in syngas [4].

In order to understand the process will be presented a flowchart, which will allow customizing system, as project needs. Shafiee [5] says that configuration systems can support the decision process and show the product alternatives.

This paper aims to present and evaluate a gasification process flowchart that will reduce the time of the commissioning phase.

2 Background

Brito et al. [6] says that commissioning is a process that certify units. Equipments are tested, installed, designed and operated as client's installation operational requirements. Commissioning can be applied to new or existent plant.

Enterprises have general or particular procedures to attend each discipline process. At PG-25-SEQUIETCM/CEND from PETROBRAS [7] is shown remembrances to personal qualification, which will work in the commissioning phase. This document presents commissioning as a group that contains knowledge, practices, procedures and skills to become a unit operational according to desired performance requirements. This transfer needs to be done fast, ordered and safe, being certified in terms of performance, reliability and tracking information.

There is a possibility to deduce that commissioning practices have the main target to ensure the system operation and the Project requirements were attended in order to enable project's start up. This is the concept that is used in this paper. PMKB [8] divide commissioning in five phases, which are:

- Planning and Engineering: analyses of contract's requirements, engineering design and suppliers documents are done;
- Pre-commissioning: in this moment is verified equipment, systems and subsystems conformity, through inspections and unload tests;
- Commissioning: tests are executed as equipment/system operation;
- Start up: systems start up, maintenance, initial operations and performance tests are realized;
- Assisted Operation: operation team is trained, pendencies are solved and the unit is delivered to client.

These information are important to understand the process and to plan correctly. A flowchart is composite with many stages that has a free time between them.

A process is composed by activities sorted with start and finish well defined. So, a process is a mix of resources that brings value or results to the company.

To identify the flowchart is positive in order to establish priorities and to help decision-making in priority processes, those processes cause more impact and are complex [9]. Process management is required to ensure that processes reach their targets and be efficient. It is important to get view of the whole project and to have performance indicators to evaluate the flowchart according to enterprise objectives. Mapping processes gives support in identifies wastes and decisions making are done in visible flows, according Gomes and Souza [10].

This paper will present a flowchart of gasification process. Breault et al. [11] says that gasification is a technology that transforms any material with high level of carbon in syngas. ThyssenKrupp Uhde [12] presents gasification as partial oxidation process in high temperature to convert materials with high level of carbon in syngas, which contains carbon monoxides and hydrogen.

Chiu et al. [13] says that should be considered the life cycle of a product and how this production will affect the environmental. This sustainable product can be categorized in: reduction of product quantity, expansion service, reduction of energy consumption, improvement of resource sustainability and reduction of the environmental damage risk. According to U.S. Department of Energy [14] the benefit of gasification to environment are the low emissions of oxides and particulates from burning coal, because of the treatment after burning fuel. It is also possible the use of garbage the energy generation with two processes, incineration and gasification. Transform the uses of non-recycle materials in electricity reduce the amount of waste in landfill in order to prevent is and water contamination [15].

After all these information's about gasification, it will be presented the processes that were studied in order to create a flowchart.

In TEXACO gasification process petroleum and steam are mixed inside the boiler. This blend goes into the gasifier together with oxygen. The syngas with impurities goes through two scrubbers until leaves the process as a clean syngas [16]. The Figure 1 shows a simplified diagram of this process.

The second process is from SHELL. The Shell Gasification Process (SGP) has the advantage to convert different materials in syngas, including heavy and viscous oil and with high level of sulfur [17]. In Figure 2 is presented SPG Diagram.

Higman and Burgt [16] say that the gasifier from SHELL is vertical and contains many intermediate burners. This process reuses the heat which would be lost, first is used in syngas cooling and later in boiler feed water. The gas partly rusty when it leaves the gasifier a small amount of free carbon. This carbon is removed with ashes in two stages of washing with water. After this process, the syngas leaves with a temperature of 40ºC.

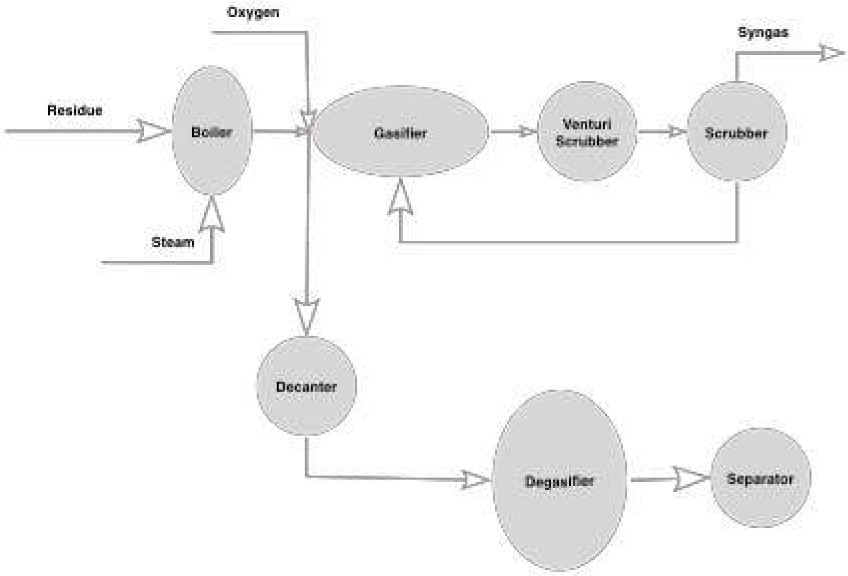

Figure 1
TEXACO's Simplified Diagram

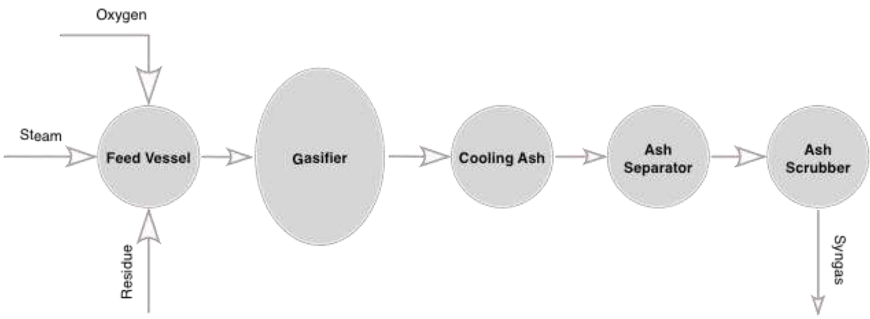

Figure 2
SGP Diagram

The third process is from LURGI. In this process is possible to be done with natural gas or recycle gases, which are preheated before entering the reactor. Oxygen is also preheated using a small amount of high-pressure steam that comes from the heat recovery boiler. A purification water tower removes traces of soot, hydrocyanic acid and ammonia. In this process, the soot formation in process is extremely low, not requiring extra filtration [18].

In Figures 3 and 4 are presented possible diagram to this process, because LURGI's gasification can be done in two different options according the cooling system chosen.

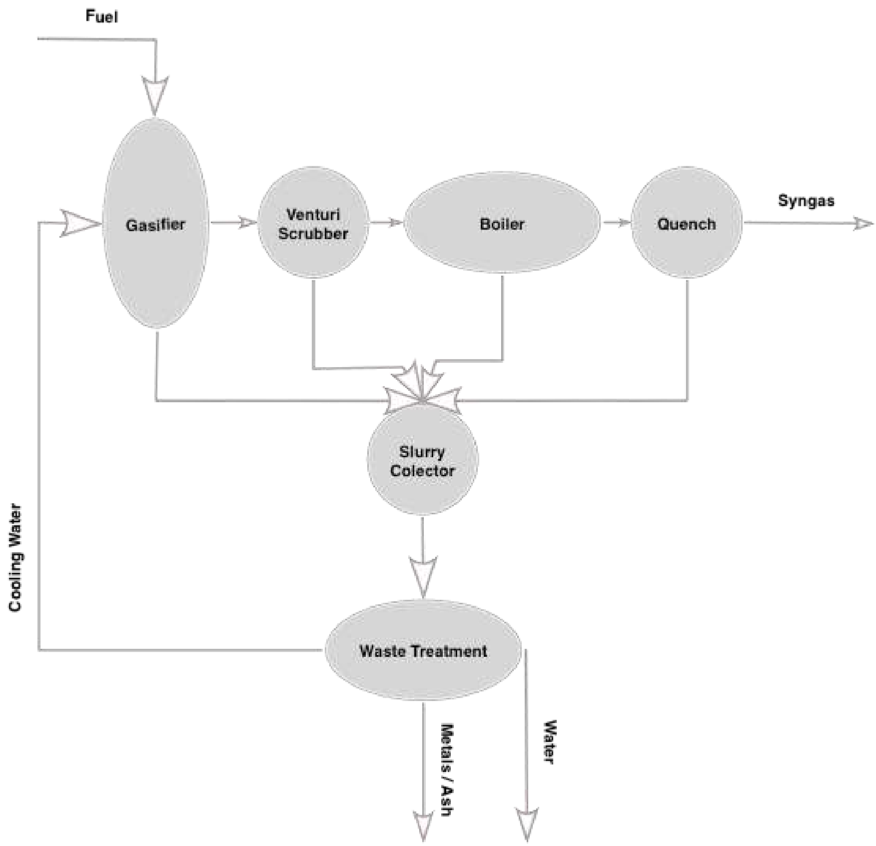

Figure 3
LURGI Process with Water Cooling System

The last process that will be presented in this paper is from E-GAS. The first stage is the treatment of the fuel before gets inside the gasifier. The fuel can be petroleum coke or coal, which are smashed and mixed with water and transform this in slurry. The E-GAS gasifier is multiple stages; this will increase the efficiency of the process and reduce oxygen consumption. When syngas leaves the gasifier, it is quenched and the heat is recovered and high pressure steam is produced. The gas is filtrated in order to remove all the ashes. These ashes are recycle and returned to the gasifier. In the end of the process, the hydrogen with high level of syngas is burned inside a turbine to energy generation [8]. E-GAS diagram is shown in Figure 5.

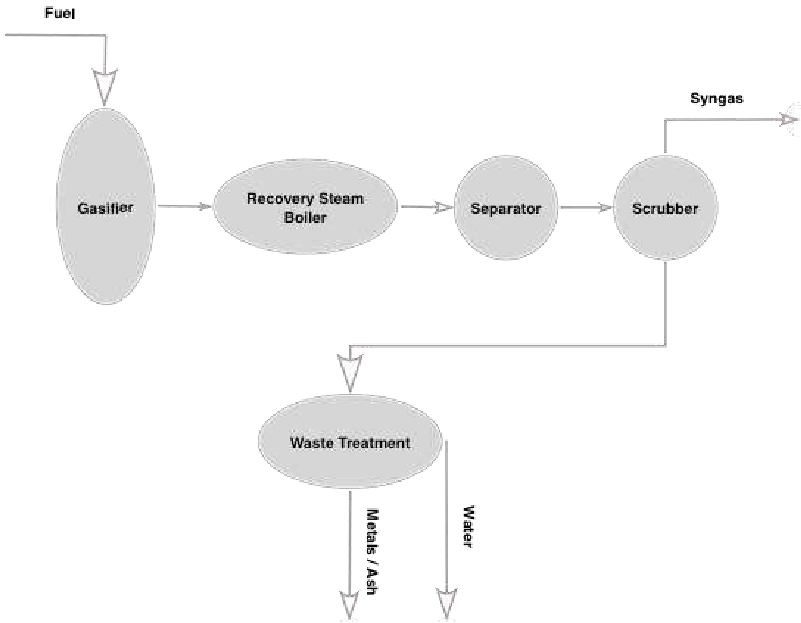

Figure 4
LURGI Process with with Syngas Cooling System

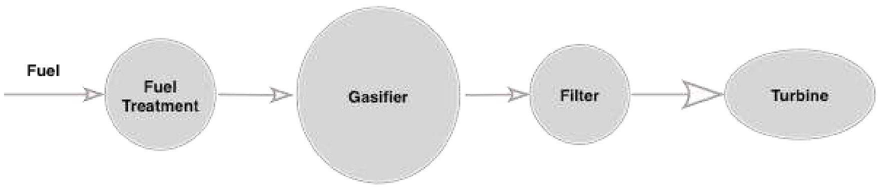

Figure 5
E-GAS Gasification Process

TEXACO process is pioneer in the use of oil derivate as fuel to the gasifier and this moment existed a boiler to burn the feed. In chronological order, SHELL presented a few years later, a multiple stages gasifier that increase the efficiency at the system and allow the use of different materials.

LURGI gasifier uses inside the reactor only natural gas and doesn't use wastes from the process and does wastes treatment. This avoids the reuse of water in the cooling system.

Another technology is presented at E-GAS enterprise, which petroleum coke feeds the gasifier to generate syngas that will be used in a turbine to energy generation.

The study of different gasification systems, which use petroleum derivate as fuel, allowed understanding and seeing resemblances between them and which are the main equipments. Those informations were necessary to elaborate a flowchart.

3 Flowchart

To map the gasification process is relevant, because it is possible to understand and to allow a global view of the project [9]. Mapping activities is to search for operational excellence and to create an improvement continuous cycle, according to Carmo [9]. Aleu and Aken [20] say that continuous improvement is a planned, organized and systematic approach that increases the organization performance. To model is to do a deep analysis to reach a target. This paper aims to optimize the gasification process commissioning. When the process mapping is done, it is possible to know the positive and the negative points of the process. Knowing these points allows to reduce costs, failures, to get simple and optimized process.

The application of product configuration system is possible to obtain these benefits, according to Hvam [21]:

- Lead time is the time between the beginning of specification process until it be finished;
- On-time delivery is the percentage of how many specifications were completed in the agreed time;
- Resource consumption for making specifications is the analysis made with the aim to reveal the resources consumption;
- Quality of specifications can be the evaluation of the client that is difficult of measure or this can be the quantity of errors in the specification;
- Optimization of products and services in specification processes occurs when configuration system is used to optimize products according to customer requirements.

After the processes analysis, it is possible to perceive a resemblance between processes. With those information's, an abridgment of the biggest flows is made with concept of flowchart and minimizes stages. In Figure 6 is presented a diagram with main equipment's.

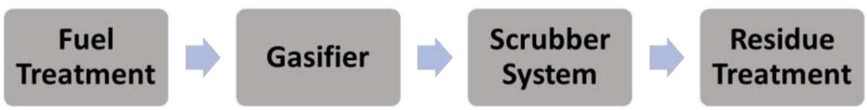

Figure 6

Gasification Process Diagram

This flowchart allows to adapt the gasification process and to customize it according project needs. Bonev et al. [22] explains that this customization aims to use configuration systems, adjustable products, flexible process and adaptive organizations. Another point presented by Bonev et al. [22] is that common platforms provide an alternative to standardization strategy of traditional construction.

4 Results

The simulation resorts a flowchart to model's methodology base, the system identification becames easier to identify. An analysis was done with entrance data, which cross the system using available resources [23].

Two simulations were made; the first one is to compare two-studied process (SHELL and TEXACO) in order to get in touch with the behavior in time and resources use of complexes processes. These two were chosen because they have necessary data to accomplish the simulation and better activities descriptions. The second simulation was made comparing SHELL process with the flowchart presented in Section 4, the objective is to measure the behavior of the flowchart created and compare it with a real process.

The simulations were made considering 8 hours of labor per day and total duration of 120 hours, this time was important to bring forth enough data to a statistic analysis.

At Figure 7 is presented the model based at SHELL process. This model counts with three entrance data (oxygen, residue and steam) and these are mixed inside the gasifier. To simulate was necessary the volume data that enter in the gasifier. The volume required to each process were presented at Higman & Burgt [16]. The fuel leaves the gasifier and passes by cooling process and ashes treatment to delivered syngas.

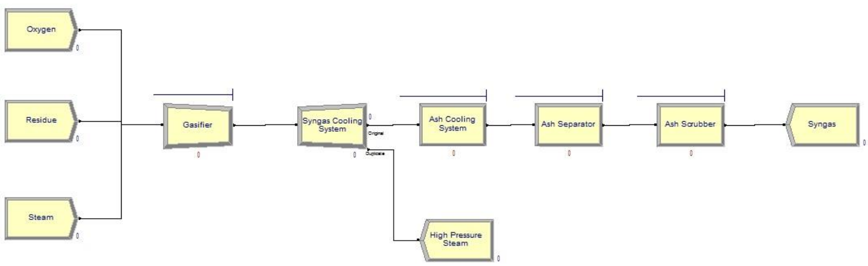

Figure 7
SHELL Gasification Process Model

The Figure 8 shows the TEXACO gasification process model. This process uses, also, the same three entrance data and the volume is shown at Table 1. In this process steam and residue enter in the boiler and this mixture gets into the gasifier with oxygen, then it goes to a scrubber process and leaves as syngas.

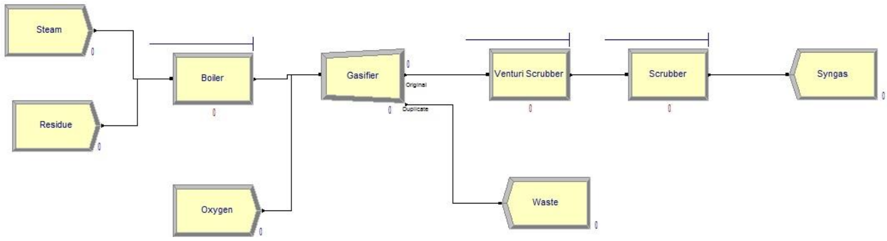

Figure 8
SHELL TEXACO Gasification Process Model

At Tables 1 and 2, it is presented the time required to fuels cross the system, since the beginning of the process until it leaves as syngas.

Comparing both models, it is possible to realize an increase of 37% in the oxygen that remains inside the process, 0.2% in the residue that remains and 1% in the steam that remains. These results show that there is not a meaningful difference of time between processes, it happens a balance in process duration and in the time that oxygen crosses the process.

Table 1
SHELL Model Results (units in hours)

SHELL			
Fuel	Average	Minimum Value	Maximum Value
Oxygen	5.527	3.529	7.380
Residue	5.924	4.046	8.111
Steam	5.812	3.957	8.072

Table 2
SHELL TEXACO Model Results (units in hours)

TEXACO			
Fuel	Average	Minimum Value	Maximum Value
Oxygen	4.011	2.278	6.304
Residue	5.913	3.441	8.757
Steam	5.875	3.632	7.841

It was also done a simulation to evaluate the using of resources. It was considered engineers and technicians of four disciplines – mechanical, electrical, process and instrumentation & control. As it is a general evaluation, it was considered that the four disciplines work a the same amount of time in each equipment, if it were a real Project it would be a rare situation, but in this studied it is a limit for do not need to quantify and rating differences between disciplines. The quantities of amount hours occupied and requested were generated by ARENA, based on each equipment's interaction.

In the Tables 3 and 4 are presented the results about the using of resources, in other words, the amount requested.

Table 3
Amount Requested - SHELL Model

Resources	Amount Resource Requested
Mechanical Engineer	1,658
Electrical Engineer	1,658
Process Engineer	1,658
Instrumentation & Control Engineer	1,658
Mechanical Technician	1,658
Electrical Technician	1,658
Process Technician	1,658
Instrumentation & Control Technician	1,658

Table 4
Amount Requested - TEXACO Model

Resources	Amount Resource Requested
Mechanical Engineer	1,926
Electrical Engineer	1,926
Process Engineer	1,926
Instrumentation & Control Engineer	1,926
Mechanical Technician	1,926
Electrical Technician	1,926
Process Technician	1,926
Instrumentation & Control Technician	1,926

The TEXACO model requests more resources, perhaps in this process exists one extra equipment (boiler), which is absent at SHELL process. This equipment requires more resources to verify and to calibrate. Beside these informations, the SHELL process was chosen to do the comparison with the integrated flowchart.

In Figure 9 is presented the integrated model, which is composed by the minimum stages of gasification process. There is only one entrance data, which will be called slurry, because it was considered that the fuel was treated before the entrance into the gasifier. This step can be modified according to project/system needs.

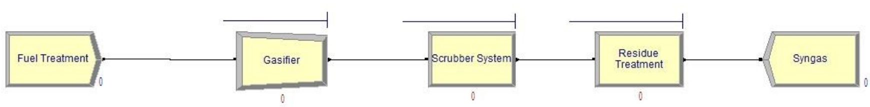

Figure 9
Integrated Gasification Process Model

The time that fuel takes to the beginning of the process until it leaves as syngas is described in Table 5. The results present the average, the minimum and maximum duration.

Table 5
Gasification Integrated Process Model Results (units in hours)

Gasification Integrated Model			
Fuel	Average	Minimum Value	Maximum Value
Slurry	4.512	3.064	6.189

Analyzing the SHELL model (Table 1) and the integrated one (Table 5), the difference of duration was 1.412 hours, in other words the integrated model corresponds to 76.2% of the duration of SHELL model. This duration is smaller, because there are less input data, steps and interactions.

In Table 6 are shown the differences between input and output data that shows fuel losses during the processes.

Table 6
Process Losses

SHELL Model			
Fuel	Entrance	Output	Losses
Oxygen	2,010	1,929	-81
Residue	207	202	-5
Steam	605	585	-20
Integrated Model			
Fuel	Entrance	Output	Losses
Slurry	490	478	-12

Total fuel losses in SHELL model were 106 units and in integrated model were 12 units lost, it is a reduction of 88.7%. In this simulation, ARENA foreseen a reduction in the amount of fuel consumed, which indicates a possible cost reduction with raw materials.

It was also made a simulation with possible needed resources. Engineers and technicians of four disciplines were considered. To compute the value of each engineer worked/hour, it was considered that the commissioning professional has experience of five years and his salary is the double of the one determined by CREA-RJ [24] and the technician salary was considered the one determined by CREA-RJ [24]. At Table 7 is presented the value of each work/hour.

Table 7
Engineer and Technician Cost per Hour

	Salary	Cost per Hour
Commissioning Engineer (R$)	14,960	85
Technician (R$)	6,600	37.50

The simulation was made for SHELL and integrated model. In the Table 8 shows worked hours to each resource in SHELL model.

Table 8
Worked Hours – SHELL Model

Worked Hours			
Resource	Average	Minimum Value	Maximum Value
Mechanical Engineer	25,073	0	32
Electrical Engineer	25,073	0	32
Process Engineer	25,073	0	32
Instrumentation & Control Engineer	25,073	0	32
Mechanical Technician	25,073	0	32
Electrical Technician	25,073	0	32
Process Technician	25,073	0	32
Instrumentation & Control Technician	25,073	0	32

Tables 9 and 10 present the quantity of hours worked and the amount of resource requested for the integrated model.

Table 9
Worked Hours – Worked Hours – Integrated Model

Worked Hours			
Resource	Resource	Resource	Resource
Mechanical Engineer	4,552	0	12
Electrical Engineer	4,552	0	12
Process Engineer	4,552	0	12
Instrumentation & Control Engineer	4,552	0	12
Mechanical Technician	4,552	0	12
Electrical Technician	4,552	0	12
Process Technician	4,552	0	12
Instrumentation & Control Technician	4,552	0	12

Table 10
Amount Requested – Integrated Model

Resource	Amount Resource Requested
Mechanical Engineer	487
Electrical Engineer	487
Process Engineer	487
Instrumentation & Control Engineer	487
Mechanical Technician	487
Electrical Technician	487
Process Technician	487
Instrumentation & Control Technician	487

The results show that more input data and more activities result in a bigger number of interactions and a greater need of resources. The founded values allowed evaluating the cost of labor work in both models. In the Tables 11 and 12 are presented the cost to SHELL model and integrated model.

Table 11
Each Engineer and Technician Cost – SHELL Model

	Hour Cost	Amount Used	Total Cost
Each Engineer Cost	R$ 85	41.570,21	R$ 3,533,467.43
Each Technician Cost	R$ 37.50	41.570,21	R$ 1,558,882.69

Table 12
Each Engineer and Technician Cost – Integrated Model

	Hour Cost	Amount Used	Total Cost
Each Engineer Cost	R$ 85	2216,824	R$ 188,430.04
Each Technician Cost	R$ 37.50	2216,824	R$ 83,130.90

Therefore the cost of the four disciplines in SHELL model would be R$20,369,400.45 and in the integrated model it would be R$1,086,243.76. This is a difference of R$19,283,156.69 and the cost of the integrated model would correspond a 5.3% of SHELL model.

This difference shows that excessive amount of activities represents a cost increase, in other words, when the project has more activities, more input data that will be required it spends more money to attend the resources needed. Thus have the knowledge of gasification system and to do an integrated commissioning permits reducing the cost at the end of the project. It is important to remember that according to gasification process chosen this cost difference cannot be so meaningful, because the integrated process has the minimum stages quantity and depending of process complexity can exits more stages, which will increase the cost.

In this section were presented the results founded at ARENA simulation, the object of this was evaluate the commissioning duration comparing processes. The differences founded represent the bigger number of items and by consequence this increases in commissioning hours and final cost.

Conclusion

An integrated commissioning is an excellent option to reduce cost and time. It is very common to introduce a commissioning team only at the final project's steps before plant startup. This practice leaves commissioning oversized, because many hours are used to understand and evaluation of the process by commissioning team.

This study comes up with a minimum team that works in the project since the beginning, this team can support basic and detail engineering and when commissioning officially starts, this group already has information to do the integrated commissioning, which processes are grouped and the commissioning activities are focused only in power up and start up the plant.

Gasification is a flexible process, which can be used in different kinds of industry, like energy generation, chemical industry, products fabrication, etc.

Through flowchart could be noticed the importance of prepare and choose feed fuel of the gasifier. It needs to be analyzed each case to understand each project's peculiarities. Doing a fuel treatment adequate, there is a reduction in entrance data that results time, the using of resources and volume of fuel required. These reductions were noticed at software ARENA simulation. It is also very important turn the attention in waste generated in the gasifier.

At ARENA simulation, it could be noticed that the use of the flowchart brought a reduction of commissioning time, which shows how important is to analyze an industrial process and commission the main equipment. It allows also perceiving the difference in time and cost when there is a model with excessive amount of activities and multiple input data. It shows that depending on gasification system can have an overkill of activities that requires more time and professionals, for consequence the commissioning will spend more resources and time.

References

[1] Bendiksen T, Young G (2015) Commissioning of Offshore Oil and Gas Projects: The Manager's Handbook. AuthorHouse. 177 p.

[2] Materazzi M, Lettieri P, Taylor R, Chapman C (2016) Performance analysis of RDF gasification in a two stage fluidized bed–plasma process, Waste Management 47-V: 256-266.doi: 10.1016/j.wasman.2015.06.016.

[3] Lazarinos JGC (2007) Tratamento de Revestimentos Gastos de Cuba Eletrolítica da Indústria de Alumínio. Master Dissertation,Pontifícia Universidade Católica do Rio de Janeiro, Brazil. Available from: https://www.maxwell.vrac.puc-rio.br/10023/10023_1.PDF [accessed 2018.1.12]

[4] Available from: http://www.gasification-syngas.org/technology/the-gasification-process/ [accessed 2016.11.11]

[5] Shafiee S, Hvam, L.; Bonev, M. (2014) How to Scope a Product Configuration Project in an Engineering Company. In: 6th International Conference on Mass Customization and Personalization in Central Europe. Available from: http://orbit.dtu.dk/files/100481481/How_to_scope_a_product.pdf, [accessed 2017.8.17]

[6] Brito AS, Ribeiro H, Matos LM (2010) Comissionamento em Sistemas de Tubulações de Utilidades: Aplicação do Comissionamento a um Sistema de Resfriamento. Final Engineering Course Project, Instituto SENAI de Educação Superior, Brazil, 195 p.

[7] Petrobras (2010) Manual de Gestão da Engenharia: Volume 2: Implementação de Empreendimentos. Available from: http://docslide.com.br/documents/01-magescapitulo15-comissionamentoh.html, [accessed 2017.5.14]

[8] Project Management Knowledge Base (2015) Requisitos básicos de Comissionamento. Available from: http://pmkb.com.br/download/requisitos-basicos-de-comissionamento/, [accessed 2017.6.13]

[9] Carmo JP (2016) Modelagem de Processos. Final Engineering Course Project, Instituto Federal do Espírito Santo, Brazil, 42 p.

[10] Gomes DR, Souza SDC (2010) Mapeamento do Processo de Produção Em Uma Fábrica Do Pólo de Cerâmica Vermelha Do Norte Fluminense. In: XXX Encontro Nacional De Engenharia De Produção, Associação Brasileira de Engenharia de Produção. ABEPRO

[11] Breault RW (2010) Gasification Processes Old and New: A Basic Review of the Major Technologies. Energies 3(2):216-240. doi: 10.3390/en3020216

[12] Thyssenkrupp UHDE (2012) Gasification Technologies. Available from: http://www.thyssenkrupp-industrial-solutions.com/fileadmin/documents/brochures/gasification_technologies.pdf, [accesed 2018.5.13]

[13] Chiu MC, Chang CH, Yu-Ting C,Jr-Yi C, Yi-Jie C (2015) Redesign for Sustainability and Assemblability Using Particle Swarm Optimization Method. Journal of Industrial and Production Engineering 33(2):103-113. doi: 10.1080/21681015.2015.1111264

[14] U. S. Department Of Energy (2016) Gasification. Available from: http://energy.gov/fe/science-innovation/clean-coal-research/gasification, [accessed 2018.4.24]

[15] Klein A (2002) Gasification: An Alternative Process for Energy Recovery and Disposal of Municipal Solid Wastes. Columbia University, 50 p.

[16] Higman C, Burgt MVD (2011) Gasification. Gulf Professional Publishing, 456 p.

[17] Shell Global Solutions (2014) Residue Gasification: Converting the Bottom of the Barrel into Valuable Products. Available from: http://www.shell.com/business-customers/global-solutions/gasification-licensing/residue-gasification/_jcr_content/par/textimage_330759342.stream/1444052720177/a5e92982dafaa7c1aca6dea89fc596d705c8c08a32cae05a531e3a7ab368021e/residue-gasification-factsheet-v2-screen.pdf, [accessed 2018.1.18]

[18] Liebner W, Ulber D (2000) MPG – Lurgi Multi Purpose Gasification: Application in "Gas-Gasification". In: 2000 Gasification Technologies Conference, Gasification & Syngas Technologies Council, 1-10. Available from: https://www.globalsyngas.org/uploads/eventLibrary/Gtc00340.pdf, [accessed 2018.1.12]

[19] Available from: http://www.cbi.com/technologies/e-gas-process-overview [accessed 2016.12.12]

[20] Aleu FG, Aken EMV (2016) Systematic Literature Review of Critical Success Factors for Continuous Improvement Projects. International Journal of Lean Six Sigma 7(3):214-232. doi: 10.1108/IJLSS-06-2015-0025

[21] Hvam L, Haug A, Mortensen NH, Thuesen C (2013) Observed Benefits from Product Configuration Systems. The International Journal of Industrial Engineering: Theory, Applications and Practice 20(5-6):329-338

[22] Bonev M, Wörösch M, Hvam L (2014) Utilizing Platforms in Industrialized Construction: A Case Study of a Precast Manufacturer. Construction Innovation 15(1) 84-106. doi: 10.1108/CI-04-2014-0023

[23] Brahmadeep ST (2014) A Simulation Based Comparison: Manual and Automatic Distribution Setup in a Textile Yarn Rewinding Unit of a Yarn Dyeing Factory. Simulation Modeling Practice and Theory 45:80-90. doi: 10.1016/j.simpat.2014.04.002

[24] Available from: https://www.crea-rj.org.br/documentos-e-formularios/salario-minimo-profissional/

Model-based Power Generation Estimation of Solar Panels using Weather Forecast for Microgrid Application

Roland Bálint, Attila Fodor and Attila Magyar

University of Pannonia, Faculty of Information Technology,
Egyetem u. 10, H-8200 Veszprém, Hungary

E-mails: balint.roland@virt.uni-pannon.hu, foa@almos.uni-pannon.hu, magyar.attila@virt.uni-pannon.hu

Abstract: An electrical power production estimation model has been proposed in this paper for PV panels. The model uses weather forecast data of a time interval (e.q. one day ahead) as input and gives an estimation to electricity generation for the same time interval. The proposed method takes into account the thermal effects taking place in a solar panel as well as the temperature dependent nature of the solar panel efficiency. The results of this paper could be utilized by transmission system operator, distribution system operator, virtual power plant and microgrid operators. The precise mathematical model of the renewable energy resources, which the function of the weather forecast is necessary for the very large scale integration to the electrical transmission system.

Keywords: PV power plant; Power estimation; modeling; thermal dependence; distributed energy resources

1 Introduction

Solar radiation models have been used for the prediction of the amount of energy available by solar irradiance. The primary application area of such models were ecological studies. The irradiance model proposed in [1] determines the amount of solar irradiance for given areas in a monthly and daily manner for climatic studies.

Nowadays, the primary field of application of irradiance models is photovoltaic generation using solar power plants. As the number of such appliances constantly grows the importance of any solution that improves the stability, power quality, optimality of the distribution network using photovoltaic units is increasing as well.

Unfortunately, solar generation (and wind generation as well) lacks the advantageous properties of predictability and controllability, which is available for fossil and nuclear power plants. The electrical power generated by PV panels can only be optimized by geometric parameters of the installation and the design of an appropriate solar tracking system [2]. The electrical power generated by renewable generators highly depends on actual weather, i.e. the amount of power generated is constantly fluctuating. As the proportion of renewables in the total electrical energy increases this unpredictably fluctuating generation causes several power network safety related issues [3].

In some countries to counterweight the uncertainty represented by the renewable generation, the operators of non home size photovoltaic power plant are obligated to present a power generation plan. The distribution system operator specifies the rules for amount of curtailment and possible compensation (penalty), that case there is difference between the planned and the actual generation. From the PV power plant (PVPP) operator point of view the minimization of this penalty is vital, and any solution for the prediction of the generation is welcome.

The power production timing is one of the most important tasks of the transmission system operator (TSO), distribution system operator (DSO), virtual power plant (VPP) and microgrid operators. The opertator has to estimate the customer loads and the power generation from renewable energy sources (RES). There are different operation and management strategies for the operators of the distribution network, the transmission network, the power generators or the microgrid [4], [5]. It is crucial for the microgrid operation algorithm to have an approximate information about the electrical power generated from the renewable sources (solar or wind) so that the changes can be compensated (e.q. by charging/discharging a battery, enable/disable loads, turning diesel generator on/off, etc.) [6].

On the other hand, power network security regards are just as important as the previously mentioned financial viewpoints. There are several network stability and energy quality related indicators, among them energy balance is crucial for the operation safety point of view. In order to ensure the energy balance of the power network, the classical power plants are controlled in order that the total generation meets the demand despite of the uncertainty of the renewable generators present on the network. The successful energy balancing depends on two main factors, the available energy generation reserve that can be prescribed to the power plants, and an appropriate demand and renewable generation forecast. Moreover, for the operation and control of energy-positive systems the estimation and/or prediction of power is a key issue [7], [8].

The solar energy comes to the Earth in the form of radiation from the Sun. Therefore, every solar power prediction model, is based on some solar geometry model. These models differ mainly in the level of detailedness, e.g. [9] presents a geometry model taking the different wavelength into account. On the other hand, e.g. [10], [11] gives a more simple model. The first class of photovoltaic models deal with the PV panel characteristics [12], [13], in the work [14] the PV model parameters are estimated from long-term outdoor measurements. Others involve cooling effect (either air cooling of hybrid panel), e.g. the paper [15] examines the effect of cooling medium and the cooling system on the panel parameters. Hybrid panels are investigated in [16], where the efficiency of the panel is increased by a model based technique [17]. In the modeling of hybrid PV panels the temperature of the water is a key variable, which is estimated in [18].

The temperature dependent modeling of PV panels is important because the efficiency decreases with the temperature rising [19]. Work [20] proposed a thermal model of a PV panel that takes the infrared domain into account, others, e.g. [21] propose a simplified thermal model. Different geometrical parameters (e.g. inclination and orientation) might have effect on the thermal behavior [22].

Data-driven methods are very popular in every field of engineering [23], [24], the same holds for predictive solar generation models [25], [26], [27], [28]. In Ref. [29] an adaptive predictive model is proposed that adapts the model parameters to the actual measurements; however, it uses only clear sky data, i.e. does not take the clouds into account. Artificial intelligence based prediction is a popular subclass, e.g. [3] proposes a short-term (1-2 hours) prediction where an AI based forecast method learns from the measurements and the actual cloud level. The authors of Ref. [30] propose a short-term irradiance forecast model that uses the results of several models.

The proposed predictive photovoltaic power generation model uses standard weather forecast data as input and predicts the generated power by taking the thermal efficiency decreasion of the panel into account. The model is based on a previously developed solar geometry model [31].

2 Modeling and Estimation of Solar Power Generation

The power generation estimation of PV power plants involves three functional modules:

- estimation of the global solar irradiation of the PV panel slope,
- estimation of the PV panel temperature for actual modul efficiency,
- weather forecast data for PV plant localization.

The following sections describe the above modules of the proposed estimation method.

2.1 Estimation Model of Power Generation

In the previous work [31] a simple model has been described for calculating the global horizontal solar irradiance using astronomical relationships (equations (1)-(3)). From this data the global solar irradiance has been calculated on a surface for a given orientation (azimuth and tilt angle) (4). The solar irradiance on the PV panels can be calculated from the irradiance on the horizontal surface using the geometrical parameters of the installation of the PV panels [31].

$$G_{hor} = I_n \cdot \sin(\alpha) \cdot A_d \cdot e^{-B_d \cdot T_m \cdot z} \cdot \left(1 - a_d \cdot N^{b_d}\right) \tag{1}$$

$$S_{hor} = I_n \cdot \sin(\alpha) \cdot A_d \cdot q^{T_m \cdot z} \cdot \left(1 - N^{b_d}\right) \tag{2}$$

$$D_{hor} = G_{hor} - S_{hor} \tag{3}$$

$$G_{pv} = S_{hor} \cdot \frac{\sin(\alpha_{pv})}{\sin(\alpha)} + D_{hor} \cdot \frac{1+\cos(\beta_{pv})}{2}) \tag{4}$$

The α_{pv} is the solar beam altitude angle on the PV surface. The power production of a PV power plant is given as the parametric model defined by equation (5).

$$P_{pv} = G_{pv}(N, \beta_{pv}, \gamma_{pv}) \cdot A_{pv} \cdot \eta_{pv}(T_{pv}), \tag{5}$$

where G_{pv} is the global solar irradiance on the modul surface as a function of cloudiness (N) and orientation (γ_{pv} azimuth and β_{pv} tilt angle), the total surface A_{pv} of the PV power plant and the PV moduls actual efficiency is η_{pv} which depends on the module temperature T_{pv}.

As opposed to the previous model [31] this model takes the clouds and the panel efficiency into account. The PV panels nominal efficiency (irradiance of 1000 W/m^2 and 25 °C cell temperature) and the temperature coefficients are obtained from the PV panel datasheet. The actual model efficiency is determined from the module temperature, which is also a variable of the proposed model. The level of cloudiness is represented by a value between 0 and 1 defined by formula (6).

$$N = \begin{cases} f_C(cloud), & if\ cloud < threshold \\ 1, & if\ cloud \geq threshold \end{cases} \tag{6}$$

If the cloud value (type of cloudiness) reaches a threshold value, then the *N* is constant 1. Below the threshold the *N* is a function of the type of cloudiness. In case of cloudless sky the *N* value is zero.

$$f_C := -0.5 \cdot \cos\left(\frac{cloud \cdot \pi}{theshold}\right) + 0.5 \tag{7}$$

2.2 PV Modul Temperature Estimation Model

As it was stated before in Section 2.1 PV panel efficiency depends on the panel temperature T_{pv}, i.e. the proposed model has to have a thermal module that estimates panel temperature. Panel temperature is influenced by solar irradiance on the PV panel (G_{pv}), the temperature of the environment (T_{air}) and of the panel (T_{pv}), the heat transfer coefficient (α_{air}) between panel and air (depends on the wind) and the efficiency (η_{pv}) according to formula (8) below.

$$\Delta T_{pv} = f_T(G_{pv}, T_{air}, \eta_{pv}, \alpha_{air}, T_{pv}) \tag{8}$$

This thermodynamic effect can be described by the ordinary differential equation (ODE) (9), where C_{pv} is the heat capacity and m_{pv} is the mass of the PV modul. A multiplier of 2 is appearing next to the surface A_{pv} since both the top and bottom sides of the panel are taken into account in the heat conduction.

$$\dot{T}_{pv} = (T_{air} - T_{pv}) \cdot \alpha_{air} \cdot \frac{2 \cdot A_{pv}}{c_{pv} \cdot m_{pv}} + \frac{1-\eta_{pv}}{c_{pv} \cdot m_{pv}} \cdot G_{pv} \tag{9}$$

The overall value of the expression $c_{pv} \cdot m_{pv}$ in (9) can be expressed in more details based on the elementary building materials of the PV panel (formula (10)).

$$c_{pv} \cdot m_{pv} = c_{glass} \cdot m_{glass} + c_{Al} \cdot m_{Al} + c_{Si} \cdot m_{Si} + c_{plastic} \cdot m_{plastic} \tag{10}$$

The inhomogeneous ordinary differential equation (9) can be expressed in state space representation using the state and input vector defined in formula (11).

$$\mathbf{x} = \left[T_{pv}\right], \qquad \mathbf{u} = \begin{bmatrix} T_{air} \\ G_{pv} \end{bmatrix} \tag{11}$$

Afterwards, the state space model of the thermal module is given by formula (12) below.

$$\dot{T}_{pv} = \left[-\alpha_{air} \cdot \frac{2 \cdot A_{pv}}{c_{pv} \cdot m_{pv}}\right] \cdot \left[T_{pv}\right] + \left[\alpha_{air} \cdot \frac{2 \cdot A_{pv}}{c_{pv} \cdot m_{pv}} \quad \frac{1-\eta_{pv}}{c_{pv} \cdot m_{pv}}\right] \cdot \begin{bmatrix} T_{air} \\ G_{pv} \end{bmatrix} \tag{12}$$

It is important to note, that although a linear time invariant (LTI) state space model is used here, the model is nonlinear, since η_{pv} is a linear function of the panel temperature (with the slope of $-0.4\,\%/°C$).

Since the estimator is implented in a discrete time manner, the thermal model (12) has to be discretized. In order to do that the parametric values of the state (**A**) and input matrix (**B**) are needed (13).

$$\mathbf{A} = \begin{bmatrix} -\alpha_{air} \cdot \frac{2 \cdot A_{pv}}{c_{pv} \cdot m_{pv}} \end{bmatrix}, \quad \mathbf{B} = \begin{bmatrix} \alpha_{air} \cdot \frac{2 \cdot A_{pv}}{c_{pv} \cdot m_{pv}} & \frac{1-\eta_{pv}}{c_{pv} \cdot m_{pv}} \end{bmatrix} \tag{13}$$

The equistant sampling ($T_S = 15\,\text{min}$) of the state equation (12) gives a discrete time state equation which is a different equation of the form (14)

$$x((k+1) \cdot T_s) = \mathbf{\Phi} \cdot x(k \cdot T_s) + \mathbf{\Gamma} \cdot u(k \cdot T_s), \tag{14}$$

where the discrete time state ($\mathbf{\Phi}$) and input ($\mathbf{\Gamma}$) matrices are obtained using the formula (15).

$$\mathbf{\Phi} = e^{\mathbf{A} \cdot T_s}, \quad \mathbf{\Gamma} = \mathbf{A}^{-1} \cdot \left(e^{\mathbf{A} \cdot T_s} - \mathbf{I} \right) \cdot \mathbf{B} \tag{15}$$

The parametric state matrix is given below in equation (16), where T_S is the sample time in seconds.

$$\mathbf{\Phi} = e^{\mathbf{A} \cdot T_s} = \begin{bmatrix} e^{-\alpha_{air} \cdot \frac{2 \cdot A_{pv}}{c_{pv} \cdot m_{pv}} \cdot T_s} \end{bmatrix} \tag{16}$$

The discterized input matrix can be calculated using (16). The input matrix of the disctere time model is given parametrically in equation (17) below.

$$\mathbf{\Gamma} = \mathbf{A}^{-1} \cdot \left(e^{\mathbf{A} \cdot T_s} - \mathbf{I} \right) \cdot \mathbf{B} = \\ = \begin{bmatrix} 1 - e^{-\alpha_{air} \cdot \frac{2 \cdot A_{pv}}{c_{pv} \cdot m_{pv}} \cdot T_s} & \frac{1-\eta_{pv}}{\alpha_{air} \cdot 2 \cdot A_{pv}} \cdot \left(1 - e^{-\alpha_{air} \cdot \frac{2 \cdot A_{pv}}{c_{pv} \cdot m_{pv}} \cdot T_s} \right) \end{bmatrix} \tag{17}$$

Note, that $\mathbf{\Gamma}$ and $\mathbf{\Phi}$ depend on the wind through α_{air} and the panel temperature through η_{pv}. However, this functional relationship has a constrained derivative, and it is regarded to change slowly with time (through panel temperature). This is why the above matrix $\mathbf{\Phi}$ and $\mathbf{\Gamma}$ have to be calculated in each sampling interval.

2.3 Weather Forecast Data

The reliable weather forecast is important for the correct operation of the proposed model. Unfortunately, different weather forecast providers use different time resolution, level of detail, data included, moreover, they are using different models to calculate the forecast. The power prediction model uses the weather forecast variables (T_{air}, N, wind) for the next 24 hours (15 minutes step), but the weather forecasts usually give data of 1 or 3 hours time step.

For validation purposes, several different meteorological models and weather forecast providers are used for the same geographical location (where the PV panels are located). In the present work, the following six different weather forecast are used obtained from [32]:

- Global Forecast System model (GFS) [33]: 3 days forecast, 3 hours resolution
- Icosahedral Nonhydrostatic model (ICON) [34]: 3 days forecast, 1 hour resolution
- Action de Recherche Petite Echelle Grande Echelle model (ARPEGE) [35]: 3 days forecast, 1 hour resolution
- Global Environmental Multiscale model (GEM) [36] [37]: 3 days forecast, 3 hours resolution
- High Resolution Limited Area Model (HIRLAM) Finland (FMI) [38] [39]: 2 days forecast, 1 hour resolution
- High Resolution Limited Area Model (HIRLAM) Netherlands (KNMI) [38] [39]: 2 days forecast, 1 hour resolution

The data structure of the weather forecast contains the following weather variables:

- date [yyyy-mm-dd HH:MM]
- temperature [°C]
- wind speed [m/s]
- cloud ϵ {0, 1, 2, 3, 4, 5, 6}
    - 0: cloudless
    - 1: few clouds
    - 2: moderate clouds
    - 3: cloudy
    - 4: full cloudy with little rain
    - 5: full cloudy with rain
    - 6: full cloudy with thunderstorm

As the power production model uses a 15 minute sample time, the above forecasts need to be interpolated with third order splines.

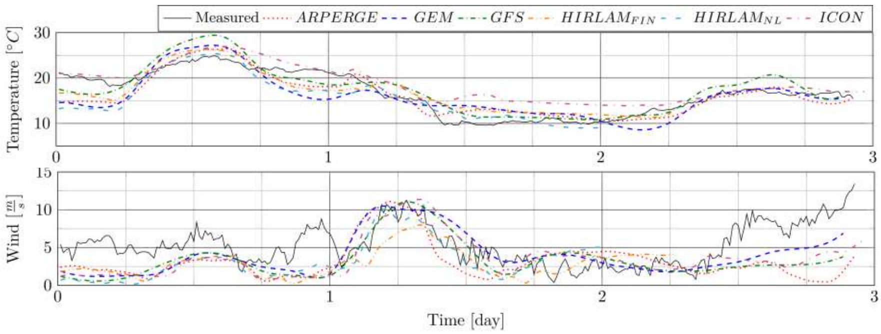

Figure 1

Weather forecast temperature (T_{air}) and wind of the different models together with the real (measured) weather data in a three day interval

Figure 1 shows a three day sample of the different weather forecast together with the measured weather data (T_{air} and wind) It is apparent on the top of Figure 1, that the temperature forecasts are reliable since the main dynamics changes in the measured data which appears in all the forecasts.

The wind forecast (bottom of Figure 1) have a higher level of error since the wind gusts, the quick changes are not predictable and the terrain objects also affect wind speed. $5 m/s$ difference between the forecast and the real wind speed causes only 2 or 3 °C error in PV modul temperature. This error only results in a 1-2% deviation in the estimation of power production.

Figure 2 summarizes the different cloud forecasts of the weather models. The plots show the values of the functional relationship (6) based on the different cloud forecasts. As the lower level of clouds would result in faulty irradiance data due to the locally appearing clouds, these forecasts are not verified using measurements.

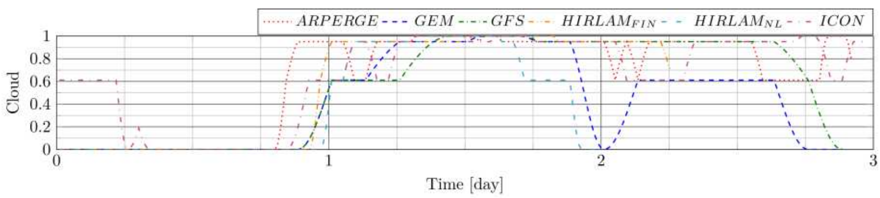

Figure 2

Cloud forecast for a 3 day horizon

It is important to note, that the cloud has the main effect on the PV power generation. Therefore, it is worthwhile to look at the performance of the models in terms of cloud forecast.

3 Verification and Validation of the Model

As a first step, the model proposed in Section 2 needs to be verified against engineering expectations. In order to do that, measured weather data has been used instead of forecast, and the model output has been examined against the actually measured power generation data. The proposed thermal model and the power generation estimation model are investigated in Sections 3.1 and 3.2, respectively. Section 3.3 proposes the validation results of the model using weather forecast data.

For both verification and validation the measured data and the parameters of installation (angles, surface size, efficiency) of a real system has been used. As the aim is to keep the model as simple as it is possible the territorial specialties (shadows of panels, trees, buildings) have been neglected.

3.1 Verification of the PV Panel Temperature Estimation Submodel

The PV panel temperature estimation submodel has been tested using measured input variables (global irradiance, wind, environment temperature) and the results (estimated PV module temperature) has been compared with to the actually measured module temperature. The results of the experiments are depicted in Figure 3 and Figure 4.

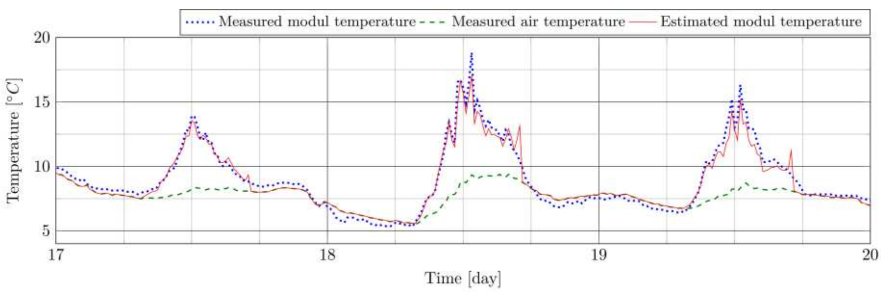

Figure 3

PV panel temperature estimation results on cloudy days

It is apparent in both figures that there is a difference between measured air and panel temperatures during the night hours although, due to expectations the panel temperature should converge to air temperature. This difference comes from the calibration error of the module temperature measurement system and the fact, that panel temperature and air temperature measurements were performed at different points of the facility.

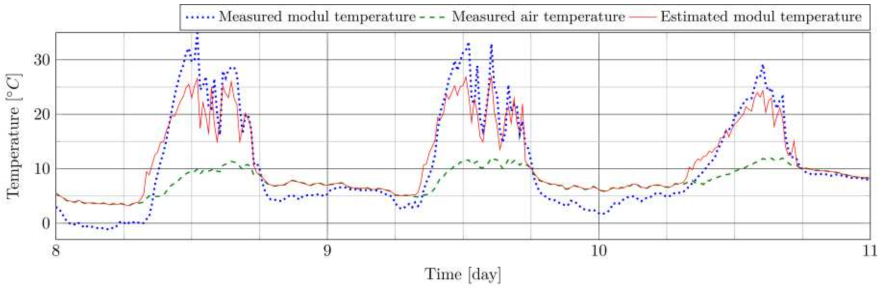

Figure 4

PV panel temperature estimation results on partially cloudy days

The error between the estimated and measured module temperature is more noticeable in Figure 4, however, the key dynamics are reproduced by the thermal submodel of the proposed estimator.

As a result of the verification it can be stated that the PV module temperature estimation model is acceptable for our purposes and it can serve as one of the components of the proposed PV production estimator model. Note that the role of temperature is important in panel efficiency (η_{pv}).

3.2 Verification the Photovoltaic Power Generation Estimator Submodel

In what follows, the whole solar power generation model is verified in the similar way as the thermal module was tested in Section 3.1. Note, that this time the estimated panel temperature is used for estimating the thermal efficiency η_{pv}. All the input variables of the model (environment temperature, wind speed and global solar irradiance) are obtained from historical measurements. The calculated power generation estimate is compared to the measured power generation for the same time interval.

A sample plot is presented in Figure 5 where the power generation of three consecutive days with different levels of cloudiness can be seen (sunny, fully cloudy, partially cloudy, respectively).

The power production model of PV plant with measured data input performs well and using appropriate weather forecasting the power production can be estimated for the next days.

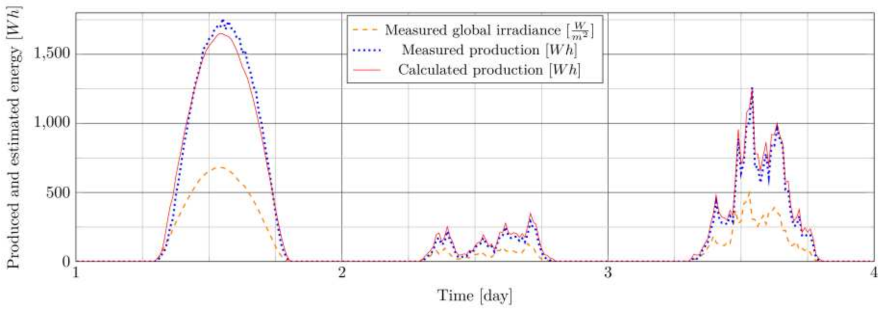

Figure 5

Powered energy estimation of the PV model with using measured temperature, wind and global irradiance data

3.3 Validation of the Estimation Model using Weather Forecast Data

As a next step in the analysis of the proposed estimator, it has been validated using different weather forecasts as inputs and the model output (electrical energy generation) has been compared to the actual measured power generation for a five day interval with several different weather conditions.

Energy suppliers and network operators use a 15 minute time step for data acquisition and control/scheduling. Therefore, selection of 15 minute as a sampling time for the model is natural. On the other hand, weather forecasts generally use a larger sampling time (1-3 hours) this complication is resolved by interpolating (linear or spline) the weather forecast data at the intermediate time instances.

The results of the validation experiments and measurements are collected in Figure 6, where the predicted power generation together with the measured data are ploted for two days with different weather conditions.

The left plot of Figure 6 shows the results for a sunny day, where the solid line corresponds to the measured solar power generation while the dotted and dashed lines denote the predicted power production based on two of the weather forecast models (ARPEGE and HIRLAM_FIN, respectively). The dashdotted and the dashdotdotted lines show the cloudiness predicted by the corresponding weather models.

The right plot of Figure 6 is more interesting since it belongs to a cloudy day. The fluctuation in the measured power generation (oscillations on the solid line) caused by the shadowing clouds passing by over the solar panel. Each such event starts with a drop in the generation because of the decreased irradiation.

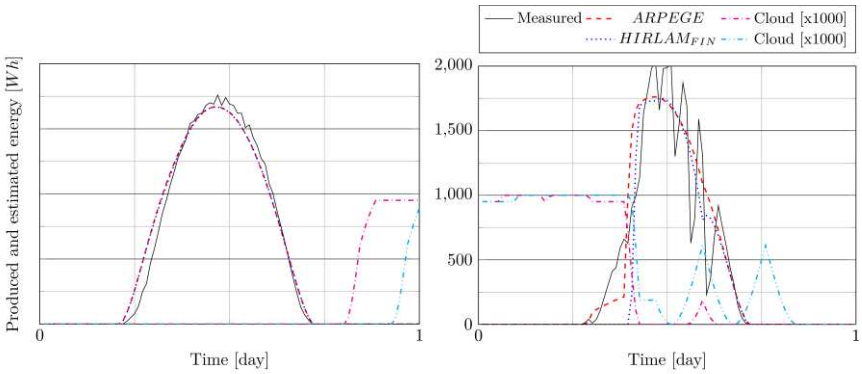

Figure 6

Measured and estimated energy production and cloud of two models on a sunny (left) and a cloudy (right) day

As the lack of sunshine cools down the panels, their efficiency η_{pv} increases which results in a jump in the power generation when the shadows leave the panel. These transients do not appear in the power prediction curves as weather forecasts are not able to give such a precicse information about clouds.

Table 1 summarizes the results of the 5 day experiment using the input data of six different weather forecasts. Note, that each days power generation was predicted from a one day ahead either forecast. The data appearing in the cells are the prediction errors (both in *Wh* and relative error) of the proposed model using the corresponding weather forecast model as input. It is important to note, that the precision of the power generation prediction correlates with the precision of the weather forecast, i.e. the goodness of the proposed power production is determined by the goodness of the used weather forecast model.

The first two days of the examined 5 day interval were cloudless days with sunshine while the last three days were fully and partially cloudy days. In the first and second columns of Table 1 it can be seen that most of the models predicted the weather (and consequently, the power generation) well except ARPEGE and ICON (a few clouds were promised by these two forecast providers for this day). The most interesting is the last three columns of the cloudy days, where the weather forecast models separate well.

The average and the average absolute deviations of each forecast model are given in the last two columns of Table 1.

It can be seen that by the end of the examined interval, the solar power generation model based on the ARPEGE weather forecast performed the best, followed by the HIRLAM_FIN based predictor.

Table 1

The difference values between the measured and estimated power generation based on the 6 different weather forecast models (first column) and 5 continuous day forecasted data series in *Wh* and % (100% is the measured production). The last two columns are the average of the 5 days difference and the average of the absolute values.

	Day 1 sunny	Day 2 sunny	Day 3 fully cludy	Day 4 part cloudy	Day 5 part cloudy	AVG	AVG (abs)
ARPEGE [35]	-5737,4 Wh	1027,3 Wh	-963,8 Wh	2935,9 Wh	1220,6 Wh	-303,5 Wh	2377,0 Wh
	-12,27%	2,15%	-16,94%	14,17%	3,31%	-1,92%	9,77%
GEM [36] [37]	656,8 Wh	878,2 Wh	4114,4 Wh	14930,0 Wh	-8938,7 Wh	2328,1 Wh	5903,6 Wh
	1,40%	1,83%	72,31%	72,05%	-24,26%	24,67%	34,37%
GFS [33]	1931,9 Wh	711,9 Wh	-3501,0 Wh	-13813,0 Wh	-22365,0 Wh	-7407,0 Wh	8464,6 Wh
	4,13%	1,49%	-61,53%	-66,60%	-60,69%	-36,64%	38,89%
HIRLAM_FIN [38] [39]	1606,2 Wh	880,9 Wh	-1031,4 Wh	-10432,0 Wh	-4165,5 Wh	-2628,4 Wh	3623,2 Wh
	3,43%	1,84%	-18,13%	-50,35%	-11,30%	-14,90%	17,01%
HIRLAM_NL [38] [39]	-2248,6 Wh	1082,0 Wh	-4117,4 Wh	11222,0 Wh	-2117,6 Wh	764,1 Wh	4157,5 Wh
	-4,81%	2,26%	-72,36%	54,16%	-5,75%	-5,30%	27,87%
ICON [34]	-28650,0 Wh	579,3 Wh	1195,5 Wh	-13910,0 Wh	-6746,9 Wh	-9506,4 Wh	10216,3 Wh
	-61,27%	1,21%	21,01%	-67,13%	-18,31%	-24,90%	33,79%

3.4 Discussion of the Results

To summarize the simulation and experimental results of the verification and validation analysis Sections 3.1-3.3 it can be stated that the model proposed in Section 2 is viable.

The verification experiments (Figure 3, Figure 4 and Figure 5) confirmed that the solar power generation model together with the thermal submodel performs well and using actual measured weather data instead of forecasts, the proposed model reliably produced the results almost identical with the measured values (panel temperature, and produced energy).

The weather forecast based validation experiment showed that the key question is in the selection of the weather forecast. As for the experiments performed, ARPEGE [32] model supplemented out model the best however, the goodness of the weather forecast depends on several factors.

Although this five day experiment is far from being enough in the statistical sense, but it is enough to see that the proposed model based solar power generation prediction framework is a viable approach.

Conclusions

A model based approach has been presented in this paper that is able to estimate the energy production of solar panels based on an appropriate weather forecast. It is important to note that the preciseness of the proposed method is determined by the preciseness of the applied weather forecast model. The selection of the best weather forecast model for a certain geographical location or classifying the forecast models based on the weather events is not out of the scope of this paper.

The model can also be used with a short-term (few hours ahead) and more precise weather forecast in order to improve the short-term energy balance and to avoid possible system failures (e.q. energy loss because of a cloud drift).

The furher research directions include the improve the weather forecast precision by contacting the local meteorological service to provide a geologically more focused foracast. Another improvement that will be made is to not only take into account the extension but also the type of clouds (i.e. density, height). The model can also be used for sizing energy storage capacities fo fill the gaps between energy peaks and valleys caused by clouds.

Acknowledgement

This research is partially supported by the National Research, Development and Innovation Office - NKFIH through grant No. 120422. We acknowledge the financial support of Széchenyi 2020 under the GINOP-2.2.1-15-2017-00038.

References

[1] Brock, T. D.: Calculating solar radiation for ecological studies, Ecological Modelling 14 (1981) pp. 1-19

[2] Tudorache, T., Kreindler L.: Design of a Solar Tracker System for PV Power Plants, Acta Polytechnica Hungarica Vol. 7, No. 1 (2010) pp. 23-39

[3] Inman, R. H., Pedro, H. T. C., Coimbra C. F. M.: Solar forecasting methods for renewable energy integration, Progress in Energy and Combustion Science 39 (2013) pp. 535-576

[4] Kanchev, H., Lu, D., Colas, F., Lazarov, V., Francois, B.:Energy management and operational planning of a microgrid with a PV-based active generator for smart grid applications, IEEE transactions on industrial electronics 58.10 (2011) pp. 4583-4592

[5] Pudjianto, D., Ramsay, C., Strbac, G.: Virtual power plant and system integration of distributed energy resources, IET Renewable Power Generation 1.1 (2007) pp. 10-16

[6] Rigo-Mariani, R., Sareni, B., Roboam, X.: A fast optimization strategy for power dispatching in a microgrid with storage, Industrial Electronics Society, IECON 2013-39th Annual Conference of the IEEE. IEEE, 2013

[7] Csáji, B. Cs., Kovács, A., Váncza, J.: Prediction and Robust Control of Energy Flow in Renewable Energy Systems, IFAC Proceedings Volumes Vol. 47, Issue 3 (2014) pp. 3663-3669

[8] Kovács, A., Bátai, R., Csáji, B. Cs., Dudás, P., Háy, B., Pedone, G., Révész, T., Váncza, J.: Intelligent control for energy-positive street lighting, Energy Vol. 114 (2016) pp. 40-51

[9] Iqbal, M.: An introduction to solar radiation, Academic Press, London (1983)

[10] Szokolay, S. V.: Solar geometry, Passive and Low Energy Architecture International (1996)

[11] Braun J. E. , Mitchell, J. C.: Solar geometry for fixed and tracking surfaces, Solar Energy Vol. 31, No. 5 (1983) pp. 439-444

[12] Tsai, H. L., Tu, C. S., Su, Y. J.: Development of Generalized Photovoltaic Model Using MATLAB/SIMULINK, Proceedings of the World Congress on Engineering and Computer Science 2008, San Francisco, USA

[13] Salmi, T., Bouzguenda, M., Gastli, A., Masmoudi, A : MATLAB/Simulink Based Modelling of Solar Photovoltaic Cell, International Journal of Renewable Energy Research Vol. 2, No. 2 (2012) pp. 213-218

[14] Kichou, S., Silvestre, S., Nofuentes, G., Torres-Ramírez, M., Chouder, A., Guasch, D.: Characterization of degradation and evaluation of model parameters of amorphous silicon photovoltaic modules under outdoor long term exposure, Energy 96 (2016) pp. 231-241

[15] Tonui, J. K., Tripanagnostopoulos, Y.: Air-cooled PV/T solar collectors with low cost performance improvements, Solar Energy 81 (2007) pp. 498-511

[16] Tiwari, A., Sodha, M. S.: Performance evaluation of solar PV/T system: An experimental validation, Solar Energy 80 (2006) pp. 751-759

[17] Zerhouni, F. Z., Zerhouni, M. H., Zegrar, M., Benmessaoud, M. T., Stambouli, A. B., Midoun A.: Proposed Methods to Increase the Output Efficiency of a Photovoltaic (PV) System, Acta Polytechnica Hungarica Vol. 7, No. 2 (2010) pp. 55-70

[18] Zondag, H. A., De Vries, D. W., Van Helden, W. G. J., Van Zolingen, R. J. C, Van Steenhoven, A. A.: The thermal and electrical yield of a PV-thermal collector, Solar Energy Vol. 72, No. 2 (2002), pp. 113-128

[19] Chow, T. T.: Performance analysis of photovoltaic-thermal collector by explicit dynamic model, Solar Energy 75 (2003) pp. 143-152

[20] Jones, A. D., Underwood, C. P.: A thermal model for photovoltaic systems, Solar Energy Vol. 70, No. 4 (2001) pp. 349-359

[21] Mattei, M., Notton G., Cristofari, C., Muselli, M., Poggi, P.: Calculation of the polycrystalline PV module temperature using a simple method of energy balance, Renewable Energy 31 (2006) pp. 553-567

[22] Alonso García, M. C., Balenzategui, J. L.: Estimation of photovoltaic module yearly temperature and performance based on Nominal Operation Cell Temperature calculations, Renewable Energy 29 (2004) pp. 1997-2010

[23] Li, D. H. W., Chau, N. T. C., Wan, K. K. W.: Predicting daylight illuminance and solar irradiance on verticalsurfaces based on classified standard skies, Energy 53 (2013) pp. 252-258

[24] Liu, B. Y. H., Jordan, R. C.: The Interrelationship and of Direct, Diffuse and Characteristic Distribution Total Solar Radiation, Solar Energy Vol. 4, Issue 3 (1960) pp. 1-19

[25] Ekström, J., Koivisto, M., Millar, J., Mellin, I., Lehtonen, M.: A statistical approach for hourly photovoltaic power generationmodeling with generation locations without measured data, Solar Energy 132 (2016) pp. 173-187

[26] Li, D. H. W., Chau, T. C., Wan, K. K. W.: A review of the CIE general sky classification approaches, Renewable and Sustainable Energy Reviews 31 (2014) pp. 563-574

[27] Li, D. H. W., Lou, S., Lam, J. C., Wu, R. H. T.: Determining solar irradiance on inclined planes from classified CIE (International Commission on Illumination) standard skies, Energy 101 (2016) pp. 462-470

[28] Ruiz-Arias, J. A., Gueymard, C. A.: Worldwide inter-comparison of clear-sky solar radiation models: Consensus-based review of direct and global irradiance components simulated at the earth surface, Solar Energy 168 (2018) pp. 10-29

[29] Reno, M. J., Hansen, C. W., Stein, J. S.: Global Horizontal Irradiance Clear Sky Models: Implementation and Analysis, Sandia National Laboratories (2012)

[30] Akarslan, E., Hocaoglu, F. O., Edizkan, R.: Novel short term solar irradiance forecasting models, Renewable Energy 123 (2018) pp. 58-66

[31] Bálint, R., Fodor, A., Szalkai, I. , Szalkai, Zs., Magyar, A.: Modeling and calculation of the sun global irradiance on slopes, Hungarian Journal of Industry and Chemistry Vol. 47(1) (2019) pp.57-63

[32] Wetterzentrale, Bad Herrenalb: http://www.wetterzentrale.de

[33] Kanamitsu, M.: Description of the NMC Global Data Assimilation and Forecast System, Weather and Forecasting Vol. 4 (1989) pp. 335-342

[34] Zängl, G., Reinert, D., Rípodas, P., Baldauf, M.: The ICON (ICOsahedral Non-hydrostatic) modelling framework of DWD and MPI-M: Description of the non-hydrostatic dynamical core, Quarterly Journal of the Royal Meteorological Society 141 (2015) pp. 563-579

[35] Déqué, M., Dreveton, C., Braun, A., Cariolle, D.: The ARPEGE/IFS atmosphere model: a contribution to the French community climate modelling, Climate Dynamics (1994) pp. 249-266

[36] Côté, J., Gravel, S., Méthot, A., Patoine, A., Roch M., Staniforth A. : The Operational CMC–MRB Global Environmental Multiscale (GEM) Model. Part I: Design Considerations and Formulation, Monthly Weather Reaview Vol. 126 (1998) pp. 1373-1395

[37] Côté, J., Desmarais, J. G. , Gravel, S., Méthot, A., Patoine, A., Roch M., Staniforth A.: The Operational CMC–MRB Global Environmental Multiscale (GEM) Model. Part II: Results, Monthly Weather Reaview Vol. 126 (1998) pp. 1397-1418

[38] Undén, P., Rontu, L., Järvinen, H., Lynch, P., Calvo, J., Cats, G., Cuxart, J., Eerola, K., Fortelius, C., Garcia-Moya, J. A., Jones, C., Lenderlink, G., McDonald, A., McGrath, R., Navascues, B., Nielsen, N. W., Odegaard, V. , Rodriguez, E., Rummukainen, M., Rööm, R., Sattler, K., Sass, B. H., Savijärvi, H., Schreur B. W., Sigg, R., The, H., Tijm, A.: HIRLAM-5 Scientific Documentation (2002)

[39] Lynch, P., Huang, X. Y.: Initialization of the HIRLAM Model Usiong Digital Filter, Monthly Weather Reaview Vol. 120 (1992) pp. 1019-1034

A Survey on Relationship between Leadership Styles and Leadership Outcomes in the Banking Sector in Serbia

Nemanja Berber[1], Agneš Slavić[2], Slavomir Miletić[3], Zoran Simonović[4], Marko Aleksić[5]

[1]University of Novi Sad, Faculty of Economics in Subotica, Segedinski put 9-11, 24000 Subotica, Republic of Serbia, berber@ef.uns.ac.rs

[2] University of Novi Sad, Faculty of Economics in Subotica, Segedinski put 9-11, 24000 Subotica, Republic of Serbia, slavica@ef.uns.ac.rs (Corresponding author)

[3]University of Priština/Kosovska Mitrovica, Faculty of Economics, Kolašinska 156, 38220 Kosovska Mitrovica, Republic of Serbia, slavomir.miletic@pr.ac.rs

[4]Institute of Agricultural Economics, Volgina 15, 11000 Belgrade, Republic of Serbia, zoran_s@iep.bg.ac.rs

[5]The Disability and Pension Fund of the Republic of Serbia, Branch in Subotica, Serbia, marko.aleksic@pio.rs

Abstract: The purpose of this paper is to explore leadership styles and relationships between the dominant leadership style and the outcomes that are related to leadership. The research methodology incorporates an analytical investigation of the available literature in the area of leadership, as well as a statistical analysis of the data collected during the empirical research. The empirical research is focusing on the leadership styles in the banking sector of Serbia, on a sample of 140 managers, using the Multifactor Leadership Questionnaire (MLQ). The hierarchical regression model was used to explore the relations between leadership styles and outcomes. The results of the research pointed-out that there are positive statistically significant relations between the transformational and transactional leadership styles and the analyzed outcomes (satisfaction with the leader, extra efforts, and efficiency). In most of Serbian banks the dominant leadership style is transformational style.

Keywords: transformational leadership; transactional leadership; passive leadership; Serbia; banking sector; MLQ questionnaire

1 Introduction

The characteristics of the unstable external environment of the modern organizations have a significant influence on finding new ways of doing business with the aim to add values to the customers achieve and sustain competitiveness and sustainable development [49]. The last economic crisis, followed by political, cultural, social and moral pressures, lead to new conditions for organizations, and many of them could not survive [10]. Organizations and their management have to pay special attention to the intellectual capital they possess [10, 33] where human capital is one of the most important part [34]. Contemporary research related to business success focus on the following themes: organizational culture, organizational learning, teamwork, leadership and motivation [12, 31, 32].

One of the very important concepts that are in the focus of scientific research and business practice is leadership. It is seen as the ability of a person to influence other people in the processes of work, creativity, and achievement of the goals of the organization. Leadership is a critical factor for the success of organizations, and a resource for building a competitive advantage and corporate performances [35, 40]. There is no one right leadership approach; it depends on the actual state of the company, its level of development and contemporary issues. Changes on the market and inside the organizations require new styles and approaches of leadership [8, 30, 36] that will make a greater contribution to the business goals.

The banking sector is described as “a work environment where employees are often busy, work under pressure and are constantly in an emotionally laborious state. This is related to the demand of work, prudence in financial management, and extended time of interaction between bank employees and customers, directly on a daily basis” [17, p. 42]. “Banking employees, like others, must remain committed to their employers, to live the brand, particularly during periods of economic uncertainty and customer frustration. Effective leadership fosters employee commitment and brand supporting behaviors” [45, p. 165]. Therefore, leadership can be one of the ways for fulfilling the strategic demands and challenges in the banking sector.

The main aim of the paper is to explore the leadership styles and relationships between the dominant leadership style and the outcomes that are related to leadership. The methodology of the research encompasses an analytical investigation of the available literature in the area of leadership, as well as a statistical analysis of the data gathered during the empirical research. The empirical research focuses on the leadership styles in the banking sector of Serbia, on a sample of 140 managers, using the Multifactor Leadership Questionnaire (MLQ).

The paper is made up of three parts. In the first part, the authors introduce the key assumptions on leadership, its advantages, and importance for contemporary business, research results from the past period related to the leadership styles, and its relations with the managerial outcomes and performances. In the second part of the paper the research methodology is presented. The authors introduced the MLQ questionnaire and its methodology. The dependent and independent variables of the applied regression model are presented. The third final part of the paper is dedicated to the summary of the theoretical and empirical analysis and to the discussion of main research implications. This paper adds new value to the leadership concept in banking, especially since it is rarely analyzed in that field of the service sector.

2 Theoretical Background

Leadership is a multi-dimensional process, formed under the influence of a large number of factors and is significantly determined by the characteristics of the leader, situation, and followers [37, 38]. The different definitions of leadership are based on different assumptions and theories. According to Bennis, it is possible to understand leadership based on experience, culture and history that influence behavior and thinking, and allows leadership skills to emerge [9]. Leadership is the process of individuals' influence on a group of people in order to achieve common goals [44] and it has very important role in determining the success or failure of an organization [29]. Leaders should stimulate, motivate, encourage, and recognize their followers in order to get high performance results [14, 21]. Leadership assumes an unequal distribution of power in the group because, in order to activate and direct effort and behavior of followers, the leader must possess a higher level of power [44].

Considering the behavioral factors in economics, Thaler emphasizes the importance of incorporating psychological factors such as "framing, self-control, and fairness into economics analyses" [42, p. 1597]. Based on the idea of an influence of people behavior on economics decisions, there is a need of reviewing behavioral theories of leadership. The behavioral leadership theories claimed that the way that the leader is behaving is the key factor that distinguishes them from their followers. Behavioral theories focus on the actions of the leaders, not on their mental characteristics, and state that the great leaders are made, not born. According to these theories, people can learn how to become leaders, mainly through learning and observation. Behavioral leadership theories analyze if a leader is oriented to tasks, or to people, or both. So, the two main forms of the leadership behavior are task-oriented and relationship-oriented leadership [41].

On the contrary, the contingency approach is based on the assumption that the relationship between the leadership style and organizational results is influenced by several situational factors related to the environment. This is why the results cannot be predicted solely on the basis of the leadership style, but it is important to be familiar with the situational variables, too [15]. Besides, the leadership style depends on the staff's personal characteristics and abilities, on the elements of social surroundings and business environment, as well as other cultural, ethnical and historical aspects, too [39].

Based on the above-mentioned leadership theories several leadership styles have been developed. One of the most prominent ways for classifying and studying leadership includes three leadership styles – passive (lack of leadership), transactional, and transformational [18, 19, 26].

A transactional leader appears when one person takes the initiative in establishing contact with others for purposes of exchange [13]. Bass described the transactional leadership on the assumption that the followers were motivated by rewards and punishments and those they followed the instructions of their leaders [4]. Transaction leaders promise rewards for the effort and good performance, and their subordinates work well when they got clear orders [20]. Leaders who apply this style promote the strengthening of individual interests of both themselves and their followers; they tend to monitor, inspect results and establish goals [7, 40]. Transactional leadership is composed of contingent reward (CRW) and active management by exception (MBEA) [2, 7].

Transformational leadership emphasizes ideals, inspiration, innovation, and individual problems. Conger and Kanungo [16] described the five characteristics of charismatic leaders' behavior including a more transformational, and less transactional or passive perspective: vision and articulation, sensitivity to the environment, sensitivity to members' needs, personal risk-taking and unconventional behavior. Burns' definition treats transformational leadership as a method that uses charisma to attract followers to the values of leaders [13]. Transformational leadership occurs when one or more people engage with others in such a way that leaders and followers are mutually raised to more levels of motivation and morality. They support initiatives related to the change in business practices, business processes or organizational structures [40, 45]; changing the everyday scope of work through identifying new business activities and implementation of new business concepts based on a more flexible business process [40]. Transformational leadership is found to have a positive relation to employee employability and wellbeing [47] and motivate subordinates to go beyond their self-interest for the purpose of achieving organizational goals [24]. Transformational leadership is composed of idealized influence (attributed) (IA), idealized influence (behavior) (IB), inspirational motivation (IM), intellectual stimulation (IS), individualized consideration (IC), [4, 25, 31].

Passive leadership includes behaviors such as avoiding decisions, neglecting workplace problems, and failing to model or reinforce appropriate behavior. Passive leaders generally do not take proactive steps to model and reward appropriate conduct [22]. A passive leadership is comprised of passive management by exception (MBEP) and avoiding the involvement (LF) [5, 6, 7]. Passive leadership is generally considered as a less effective style of leadership behavior [6] and frequently called the absence of leadership. Overall responsibility for decision making is delegated to followers, leading to poor results if the followers do not possess sufficient experience and knowledge necessary for decision making. For this leadership style the absence of support and assistance to followers is typical in the process of meeting needs, as well as the lack of feedback on the quality of their work [44].

Transformational and transactional leadership are related to the group's success, which is measured by the MLQ questionnaire. In some cases, a leader can show both transformational and transactional style. This is in the case "when a situation requires managerial activities like acquisition of resources to accomplish vision" [11, p. 1623], and both transformational and transactional elements of leadership are present. The part of the questionnaire connected with the leadership outcomes points out whether followers believe that their leader knows how to motivate them, how much his/her leadership style is effective, and whether the followers are satisfied with the leadership. The three outcomes of the MLQ are: followers' extra effort (EF) – meaning that the leader is investing extra effort to encourage the followers to do more than what they expect they can, effectiveness of leader's behavior (EF) – meaning that the leaders are effective in satisfying the followers' needs, in meeting the requirements of the group and of the organization, too, and followers' satisfaction (ST) – meaning that the leader uses adequate management techniques and methods resulting in the followers' satisfaction [40].

Many studies from public and private organizations, such as banks, manufacturing facilities, educational institutions, insurance companies, information technology companies, hospitals, health clinics, military units, and government agencies have examined the effects of transactional and transformational leadership and have shown that transformational leadership promotes more efficient results than transactional leadership. It was noticed that the transformational leadership is more efficient in activating higher levels of creativity and performance in organizations [23] and that subordinates working for transformation leaders are more satisfied with their current work than those who work for transactions [4]. Also, subordinates recognize transformation leaders as more efficient than transactional leaders [3]. Burns was the first to clearly define the style of leadership as either a transactional or a transformation, and that transactional leadership is based on bureaucratic authority and legitimacy [28].

Based on the aforementioned, the authors proposed two research hypotheses:

H1: Transformational leadership behavior is positively related to leadership outcomes.

H2: Transactional leadership behavior is positively related to leadership outcomes.

Regarding passive leadership, the difference between active and passive management lies in the time of intervention by the leader. Before creating any serious problems, active leaders control the behavior of their subordinates, anticipate problems and make corrective adjustments. Passive leaders, however, are waiting for any action until certain behavior creates problems, after which they react. So, these leaders are making their own adjustments after problems arise and their ultimate goal is simply to maintain the current performance levels. Based on the aforementioned, the authors proposed the third research hypothesis:

H3: Passive leadership behavior is negatively related to leadership outcomes.

3 Methodology and Sample

The research described in this paper was made by using the MLQ (Multifactor Leadership Questionnaire) questionnaire. The MLQ was developed by Bruce J. Avolio and Bernard M. Bass in order to evaluate a wide range of leadership styles, from passive leaders, leaders who give contingent rewards to their employees, to leaders who transform, empower, and give them a chance to be leaders [5]. This questionnaire is widely used in banking sector to analyze leadership styles [1, 17, 24]. Avolio and Bass [7] state that the MLQ's purpose is not to mark the leader as a transformational or transactional, but to evaluate the leader as more transformative than the norm or less transacting than the norm. This survey consists of 36 items related to leadership styles and 9 items that are related to leadership outcomes. The composition of MLQ is reflected in 9 scales that measure three leadership styles: transformational leadership (5 scales), transactional leadership (2 scales) and passive/avoiding behavior (2 scales), as well as 3 scales that measure the outcome of leadership [7]. To assess the frequency of the observed managerial behavior, five-point Likert´s evaluation scale was used (adjusted: 1=strongly disagree, 2=partially disagree; 3=not sure, 4=partly agree, 5=agree). The nine components of leadership are measured over the entire range of managerial styles and three outcomes of management [12].

The completion of the MLQ lasts an average of 15 minutes and can be given to an individual or group, and can be used to differentiate effective from ineffective leaders, at all organizational levels, and has been confirmed in many cultures and types of organizations [2]. Also, MLQ questionnaire is recognized as one of the best validated measures of mentioned leadership styles. It is conceived as a multi-grade, which means that the assessment of leadership takes into account the self-assessment of the leader together with the estimates of his subordinates and superiors. Self and Rater form can be filled in and evaluated separately, but the validity is much weaker when only the leader (self) form is used in the assessment of leadership [7]. This is one of the limitations of the present study.

The survey was conducted on a sample of 140 managers in the banking sector of the Republic of Serbia in the period from November 2018 until February 2019. The authors sent out 500 questionnaires to the banking sector (private banks), in order to examine the leadership styles of the managers in the middle and senior level. There were 154 questionnaires filled out and returned and after a checking process, 140 of them were used in the analysis. The response rate was 28%. The authors used the SPSS program in order to investigate the proposed relations.

The reliability analysis of the items in the questionnaire (Cronbach's Alpha for 45 items is 0.937) showed that the items have relatively high internal consistency. In case of the investigation of the internal consistency of the 9 scales that measure 3 styles of leadership and 3 scales that measure leadership outcomes, Cronbach's Alpha is 0.878, which is also an acceptable result.

Table 1
Reliability statistics of observed items

Cronbach's Alpha	Cronbach's Alpha Based on Standardized Items	N of Items
0,934	0,937	45
0,830	0,878	12

Source: Authors' analysis

According to the data presented in table 2, 60% of the respondents were men and 40% were women. The majority of the respondents are of 26-35 or 36-45 years old and most of them hold Bachelor, Master or Business school diploma.

Table 2
Sample characteristics (N=140)

Age	%	Valid %	**Education**	%	Valid %
18-25	13,6	13,6	Business school	30,7	30,7
26-35	39,3	39,3	Bachelor	27,1	27,1
36-45	32,1	32,1	Diploma	18,6	18,6
46-55	12,9	12,9	Master or PhD	23,6	23,6
56-65	2,1	2,1			
Total	**100,0**	**100,0**	**Total**	**100,0**	**100,0**

Source: Authors' analysis

4 Results of the Research

Data from Table 3 show the results of Spearman's correlation that was used to identify if there are any statistically significant relations between the perceived styles of leadership in banks and the leadership outcomes. According to the results of the correlation test for the sample of banking managers in Serbia - presented in Table 3 - it is obvious that there are strong positive correlations between Transformational leadership and Extra efforts (rho=0,82, p=0,000), Effectiveness (rho=0,91, p=0,000), and Satisfaction (rho=0,88, p=0,000), and General outcome (rho=0,93, p=0,000). Also, there are strong positive correlations between Transactional leadership and Extra efforts (rho=0,77, p=0,000), Effectiveness (rho=0,83, p=0,000), and Satisfaction (rho=0,79, p=0,000), and General outcome (rho=0,85, p=0,000). In case of Passive leadership style, moderate negative correlations are found with Extra efforts (rho=-0,52, p=0,000), a strong negative correlations with Effectiveness (rho=-0,71, p=0,000), and Satisfaction (rho=-0,62, p=0,000), and General outcome (rho=-0,67, p=0,000). It is concluded that transformational and transactional style is positively related to outcomes, while passive leadership is negatively related to all dimensions of leadership outcomes.

Table 3

Means, standard deviations, and correlations between the observed variables

	M	SD	TF	TS	PS	EE	EF	ST	OUTC
TF	3,25	1,09	1,0						
TS	3,28	0,91	0,88**	1,0					
PS	2,86	0,97	-0,70**	-0,59**	1,0				
EE	3,16	1,09	0,82**	0,77**	-0,52**	1,0			
EF	3,35	1,20	0,91**	0,83**	-0,71**	0,82**	1,0		
ST	3,34	1,23	0,88**	0,79**	-0,62**	0,79**	0,85**	1,0	
OUTC	3,28	1,11	0,93**	0,85**	-0,67**	0,91**	0,95**	0,94**	1,0
**. Correlation is significant at the 0.01 level (2-tailed).									
*. Correlation is significant at the 0.05 level (2-tailed).									

Source: Authors' analysis

Besides, from table 3 it is obvious that managers in observed banks pointed to transactional (M=3,28) and transformational (M=3,25) styles as dominant, while passive leadership (M=2,86) is seen as less present in their leadership behavior. These results are in line with the previous research conducted on the leadership in Serbia. Bobera, Strugar Jelača and Bjekić [12] and Kuehneisen [27] found that the dominant leadership style in Serbia was a combination of transactional and transformational leadership, rather than the passive style of leadership.

To explore the relations between the gender, age, level of education of leaders, and styles of leadership to leadership outcomes, a hierarchical regression model was used. Multicollinearity, which often occurs in the analyses due to variables' high inter-correlations, was analyzed, too. In this model SPSS program achieved no multicollinearity (tolerance<.10 and VIF>10.0). Besides, there was no autocorrelation detected since the Durbin-Watson coefficient was between 1.5 and 2.5 in all four models.

According to the data in Table 4, the value of R for the first model (where the dependent variable was the general outcome) of 0.931 indicates a good level of prediction. R square value represents the proportion of variance in the dependent variable that can be explained by the independent variables, the proportion of variation accounted for by the regression model.

Table 4
Models summary

Model	R	R Square	Change Statistics					Durbin-Watson
			R Square Change	F Change	df1	df2	Sig. F Change	
1	0,695[a]	0,483	0,483	42,358	3	136	0,000	
2	0,931[b]	0,867	0,384	128,062	3	133	0,000	2,004
c. Dependent Variable: OUTC								
Model	R	R Square	R Square Change	F Change	df1	df2	Sig. F Change	Durbin-Watson
1	0,602[a]	0,362	0,362	25,726	3	136	0,000	
2	0,839[b]	0,705	0,343	51,400	3	133	0,000	2,115
c. Dependent Variable: EE								
Model	R	R Square	R Square Change	F Change	df1	df2	Sig. F Change	Durbin-Watson
1	0,721[a]	0,520	0,520	49,062	3	136	0,000	
2	0,931[b]	0,866	0,346	114,682	3	133	0,000	2,025
c. Dependent Variable: EF								
Model	R	R Square	R Square Change	F Change	df1	df2	Sig. F Change	Durbin-Watson
1	0,642[a]	0,412	0,412	31,822	3	136	0,000	
2	0,874[b]	0,765	0,352	66,342	3	133	0,000	1,859
c. Dependent Variable: ST								

Source: Authors' analysis

The coefficient of the determination, R square, is 0,867 which means that the model explains 83,7% of the variability of the dependent variable. Based on the results of the F test, this change in R square, from the basic model to full, was significant (F(3,136)=128,062, p<0,05). The introduction of the independents altered the coefficient of determination of the model to a significant degree. The value of R for the second model (where the dependent variable was Extra effort) of 0.839 indicates a good level of prediction. The coefficient of the determination, R square, is 0,705 which means that the model explains 70,5% of the variability of the dependent variable. Based on the results of the F test, this change in R square, from the basic model to full, was significant (F(3,136)=51,400, p<0,05). The introduction of the independents altered the coefficient of determination of the model to a significant degree. Regarding the third model, where the dependent variable was Effectiveness, the value of R of 0.931 indicates a good level of prediction. The coefficient of the determination, R square, is 0,866 which means that the model explains 86,6% of the variability of the dependent variable. Based on the results of the F test, this change in R square, from the basic model to full, was significant (F(3,136)=114,682, p<0,05). The introduction of the independents altered the coefficient of determination of the model to a significant degree. In the case of the fourth model, where the dependent variable was Satisfaction, the value of R of 0.874 indicates a good level of prediction. The coefficient of the determination, R square, is 0,765 which means that the model explains 76,5% of the variability of the dependent variable. Based on the results of the F test, this change in R square, from the basic model to full, was significant (F(3,136) = 66,342, p<0,05). The introduction of the independents altered the coefficient of determination of the model to a significant degree.

Table 5

ANOVA test of observed models

Model a		Sum of Squares	df	Mean Square	F	Sig.
1	Regression	82,156	3	27,385	42,358	0,000
	Residual	87,925	136	0,647		
	Total	170,081	139			
2	Regression	147,470	6	24,578	144,572	0,000
	Residual	22,611	133	0,170		
	Total	170,081	139			
a. Dependent Variable: OUTCOME						
Model b		Sum of Squares	df	Mean Square	F	Sig.
1	Regression	60,215	3	20,072	25,726	0,000
	Residual	106,111	136	0,780		
	Total	166,326	139			
2	Regression	117,187	6	19,531	52,864	0,000
	Residual	49,139	133	0,369		
	Total	166,326	139			
b. Dependent Variable: EE						
Model c		Sum of Squares	df	Mean Square	F	Sig.
1	Regression	104,327	3	34,776	49,062	0,000
	Residual	96,398	136	0,709		
	Total	200,725	139			
2	Regression	173,849	6	28,975	143,389	0,000
	Residual	26,876	133	0,202		
	Total	200,725	139			
c. Dependent Variable: EF						
Model d		Sum of Squares	df	Mean Square	F	Sig.
1	Regression	87,287	3	29,096	31,822	0,000
	Residual	124,347	136	0,914		
	Total	211,634	139			

2	Regression	161,824	6	26,971	72,016	0,000
	Residual	49,810	133	0,375		
	Total	211,634	139			
d. Dependent Variable: ST						

Source: Authors' analysis

According to the data presented in Table 5, all four models are statistically significant. The F-ratio in the ANOVA table showed that the overall regression model is a good fit for the data. The independent variables in the final model statistically predict the dependent variable in case of general outcome F(6, 133) = 144,572, p<0,001; in case of Extra efforts F(6, 133) = 52,864, p<0,001; in case of Effectiveness F(6, 133) = 143,389, p<0,001, and in case of Satisfaction F(6, 133) = 72,016, p<0,001.

The authors implemented a hierarchical regression analysis. The analyses were conducted in 2 steps. In Step 1, the control variables were entered into the model. In Step 2, we added variables related to the types of leadership.

Table 6

Coefficients of the hierarchical regression models

		a		b		c		d	
Model		B	t	B	t	B	t	B	t
1	(C)	1,76**	4,78	1,84**	4,56	1,65**	4,30	1,76**	4,06
	Sex	0,094	0,672	0,236	1,530	0,039	0,262	0,008	0,050
	Age	-0,214**	-2,95	-0,234**	-2,939	-0,220**	-2,90	-0,187**	-2,168
	Educ	0,585**	10,40	0,478**	7,737	,665**	11,30	0,612**	9,158
2	(C)	0,305	0,975	-0,197	-0,427	,850**	2,49	0,261	0,563
	Sex	,043	0,598	0,194	1,830	-0,013	-0,164	-0,052	-0,489
	Age	-,077**	-2,03	-0,122**	-2,183	-0,074	-1,78	-0,035	-0,629
	Educ	0,074	1,86	0,031	0,523	0,141**	3,25	0,051	0,860
	TF	0,674**	7,77	0,562**	4,398	0,559**	5,91	0,902**	7,004
	TS	0,235**	2,84	,363**	2,986	0,290**	3,221	0,051	0,413
	PS	-0,034	-0,679	0,093	1,254	-0,186**	-3,385	-0,010	-0,131
a. Dependent Variable: OUTC, b. Dependent Variable: EE, c. Dependent Variable: EF, d. Dependent Variable: ST									
**. Correlation is significant at the 0.01 level (2-tailed).									

Source: Authors' analysis

Table 6 presents the coefficients of the regression models. In the first step, the regression model showed that most of the controls had significant relations to the leadership outcomes, except the sex of the respondents. According to the beta coefficient, younger leaders are related to the higher level of leadership outcomes, when the other variables in the model are controlled (held fixed). In the case of education, results pointed to the conclusion that there is a positive relationship between more educated leaders and outcomes in all four models. There were no significant relationships between sex and leadership outcomes.

In the second step of the regression analysis, the authors added leadership styles as independents. Based on the results of the full regression model, in case of control variables (sex, age, and education level), only the education level of the leaders and age are statistically significantly related to the leadership styles in few cases. The higher level of education that leaders have is positively related to leadership outcomes in terms of effectiveness as an outcome. Older leaders in banks showed negative statistically significant relations to the general outcome and extra effort. Regarding perceived leadership styles, results of the regression models showed that transformational and transactional styles have statistically significant positive relations to general outcome of leadership, extra efforts, and effectiveness, while transformational style even to satisfaction. In the case of passive leadership style, which that is also present in the sample, statistically significant negative relations are found towards effectiveness, as a leadership outcome. In the case of the other three outcomes, there no statistically significant relations were detected.

Based on the results of the analysis, the authors proved all three hypotheses since transformational and transactional leadership styles have statistically significant positive relations to outcomes (H1 and H2), while the passive style has a negative relation to outcomes in terms of effectiveness (H3).

The results of the regression models are in line with the previous research on this theme. Transformational leadership had a significant relationship with outcomes in terms of effectiveness, extra effort, and job satisfaction. The relationship between the laissez-faire (passive) leadership style and effectiveness and job satisfaction was found to be negative [1, 43]. In the case of transactional leadership [1] statistically significant relation with the outcomes was not found. Asrar-ul-Haq and Kuchinke analyzed the dimensions of transactional style, i.e. the contingent reward and active management by exceptions, and found that contingent rewards have positive relations to effectiveness as leadership outcome. The findings of Bushra, Ahmad and Naveed [14] pointed that transformational leadership positively affects job satisfaction and organizational commitment, while Zareen, Razzaq, and Mujtaba [48] found positive impact of transformational, passive and transactional leadership on employee motivation.

Conclusions

Leadership is seen as a process of making an influence on the followers, based on different characteristics, in order to achieve organizational goals. There are many different approaches and theories on leadership, but the MLQ approach is definitively one of the well-known. It has been used in many theoretical and empirical research, in different cultures, industries, and sectors. For the purpose of this research, the authors used the MLQ approach to explore the relations between leadership styles and leadership outcomes in the banking sector of Serbia. The research included the investigation of available literature on leadership styles, based on the distinction between transformational, transactional, and passive leadership, and the relations with the leadership outcomes, focusing on the banking sector.

The research results pointed-out that there are positive statistically significant relations between transformational and transactional leadership and the leadership outcomes. Most of the Serbian banks have leaders with dominant transactional and transformational style. There are strong positive correlations between transactional and transformational leadership and extra efforts, effectiveness, satisfaction, and the general outcome. In the case of passive leadership style, moderate negative correlations are found with the extra efforts and strong negative correlations with the effectiveness, satisfaction, and general outcome. It is concluded that transformational and transactional style is positively related to outcomes, while passive leadership is negatively related to the analyzed dimensions of leadership outcomes.

A hierarchical regression model was used to explore the relations between leadership styles and outcomes. Based on the results of the full regression model, in case of control variables (sex, age, and education level), only the leaders' education level and age are statistically significantly related to the leadership styles in few cases. The higher level of education of leaders is positively related to leadership outcomes in terms of effectiveness as an outcome. Older leaders in banks showed negative statistically significant relations to the general outcome and extra effort. Regarding the perceived leadership styles, transformational and transactional styles have statistically significant positive relations to the general outcome of leadership, extra efforts, and effectiveness, while transformational style even to satisfaction. In the case of passive leadership style, statistically significant negative relations are found with the effectiveness, as a leadership outcome.

The obtained research results presented in this paper are in line with previous research in the area, in Serbia and in the banking sector in other countries. The banking sector is characterized as quite turbulent, with many changes and uncertainty, so a specific style of leadership is the need and not the choice. Since leadership is influenced by the situation (contingency approach), it is expected that managers in banks perform such a style(s) of leadership that will help them to motivate and lead their followers towards goals in a contemporary risky and unpredictable business environment. There is no one right leadership approach; it depends on the actual state of a company, its level of development and contemporary issues

The paper adds new insight to the topic of leadership, specifically in Serbia and in the baking sector, since these researches are rare, and there are not so many comparable data. The authors confirmed all three hypotheses, and once more proved the importance of transformational and transactional leadership.

Although the authors performed quite a complex investigation, the research has some limitations. The first limitation and the most important one is the usage of the self-rater MLQ questionnaire, where leaders estimated styles and outcomes of leadership. It is argued in the literature that MLQ gives more appropriate results when the outcomes are rated by followers (employees). The second limitation is the use of the data only from one period of time, so the authors could not perform more complex analysis. Besides, only the leaders from private banks in Serbia are analyzed; while the state-owned banks were omitted from the research. That is why the authors could not make general conclusions. The above-mentioned limitations can be avoided in future researches, so these could be seen as directions for further research in this area of management.

References

[1] Asrar-ul-Haq, M., & Kuchinke, K. P. (2016) Impact of leadership styles on employees’ attitude towards their leader and performance: Empirical evidence from Pakistani banks. Future Business Journal, 2(1), 54-64

[2] Atwater, L., Lau, A., Bass, B. M., Avolio, B. J., Camobreco, J., & Whitemore, N. (1994) (ARI Research Note 95-01). Alexandria, VA: U.S. Army Research Institute for the Behavioral and Social Sciences

[3] Bass, B. M. (1990) Bass & Stogdill’s handbook of leadership (3rd ed.). New York: The Free Press

[4] Bass, B. M. (1994) Transformational leadership and team and organizational decision making. In B. M. Bass & B. J. Avolio (Eds.), Improving organizational effectiveness through transformational leadership (pp. 107-117) Thousand Oaks, CA: Sage

[5] Bass, B. M., & Avolio, B. J. (1990) Transformational leadership development: Manual for the multifactor leadership questionnaire. Palo Alto, CA: Consulting Psychologists Press

[6] Bass, B. M., & Avolio, B. J. (1996) The Team Multifactor Leadership Questionnaire (TMLQ). Palo Alto: Mind Garden, Inc

[7] Bass, B.; Avolio, B. (2004) Multifactor Leadership Questionnaire Manual (Third Edition). Menlo Park, CA: Mind Garden, Inc

[8] Bencsik, A., Machová, R., Csókás, L., Juhász, T., & Lazányi, K. (2018) Survey of Ethical Managerial Behavior – a Three Country Comparative Study. Acta Polytechnica Hungarica, 15(6), 179-198

[9] Bennis, W. (1984) The four competencies of leadership. Training and Development Journal, 38(8), 14-19

[10] Berber, N., & Slavić, A. (2016) Human resource (HR) outsourcing in European compensation management in the light of CRANET research. Acta Polytechnica Hungarica, 13(3), 207-225

[11] Birasnav, M. (2014) Knowledge management and organizational performance in the service industry: The role of transformational leadership beyond the effects of transactional leadership. Journal of Business Research, 67(8), 1622-1629

[12] Bobera, D., Strugar-Jelača, M., & Bjekić, R. (2017) Analysis of leadership styles in medium and large companies on the territory of the Republic of Serbia. Annals of the Faculty of Economics in Subotica, (37), 117-127

[13] Burns, J. M. (1982) The power of leadership. In Leadership (pp. 1-28) New York: Harper & Row

[14] Bushra, F., Ahmad, U., & Naveed, A. (2011) Effect of transformational leadership on employees' job satisfaction and organizational commitment in banking sector of Lahore (Pakistan) International Journal of Business and Social Science, 2(18), 261-267

[15] Cheng, C., & Chan, M. T. (2002) Implementation of School-Based Management: A Multi-Cheung Wong & Evers C. W. London: Routledge Falmer

[16] Conger, J. A., & Kanungo, R. N. (1998) Charismatic leadership in organizations. Thousand Oaks, CA: Sage

[17] Dartey-Baah, K., & Mekpor, B. (2017) Emotional Intelligence: Does Leadership Style Matter? Employees Perception in Ghana's Banking Sector. International Journal of Business, 22(1), 41-54

[18] Deichmann, D., & Stam, D. (2015) Leveraging transformational and transactional leadership to cultivate the generation of organization-focused ideas. The Leadership Quarterly, 26(2), 204-219

[19] Delegach, M., Kark, R., Katz-Navon, T., & Van Dijk, D. (2017) A focus on commitment: the roles of transformational and transactional leadership and self-regulatory focus in fostering organizational and safety commitment. European Journal of Work and Organizational Psychology, 26(5), 724-740

[20] Fein, E. C., Tziner, A., & Vasiliu, C. (2010) Age cohort effects, gender, and Romanian leadership preferences. Journal of Management Development, 29(4), 364-376

[21] Gill, A. S., Flaschner, A. B., & Shacha, M. (2006) Mitigating stress and burnout by implementing transformational-leadership. International Journal of Contemporary Hospitality Management, 18(6), 469-481

[22] Harold, C. M., & Holtz, B. C. (2015) The effects of passive leadership on workplace incivility. Journal of Organizational Behavior, 36(1), 16-38

[23] Hay, I. (2006) Leadership of stability and leadership of volatility: Transactional and transformational leaderships compared. Academic Leadership: The Online Journal, 4(4), 1-13

[24] Iqbal, S., Farid, T., Ma, J., Khattak, A., & Nurunnabi, M. (2018) The Impact of Authentic Leadership on Organizational Citizenship Behaviours and the Mediating Role of Corporate Social Responsibility in the Banking Sector of Pakistan. Sustainability, 10(7), 2170

[25] Jiang, L., & Probst, T. M. (2016) Transformational and passive leadership as cross-level moderators of the relationships between safety knowledge, safety motivation, and safety participation. Journal of Safety Research, 57, 27-32

[26] Judge, T. A., & Piccolo, R. F. (2004) Transformational and transactional leadership: a meta-analytic test of their relative validity. Journal of Applied Psychology, 89(5), 755

[27] Kuehneisen, I. D. (2013) A cross national comparison on how transformational leadership, insurance sales performance, job satisfaction and cultural dimensions interplay in Serbia, Montenegro and Ukraine (Doctoral dissertation). University of Zurich

[28] Lee, Y. (2011) Comparison of Leadership Behaviors in the Financial Industry in the United States and Taiwan, Taiwan: Department of International Business, National Taichung University of Education

[29] Lok, P., & Crawford, J. (2004) The effect of organizational culture and leadership style on job satisfaction and organizational commitment: A cross-national comparison. Journal of Management Development, 23(4), 321-338

[30] Mura, L., Ključnikov, A., Tvaronavičienė, M., and Androniceanu, A. (2017) Development Trends in Human Resource Management in Small and Medium Enterprises in the Visegrad Group. Acta Polytechnica Hungarica, 2017, 14 (7)

[31] Muterera, J., Hemsworth, D., Baregheh, A., & Garcia-Rivera, B. R. (2018) The leader–follower dyad: The link between leader and follower perceptions of transformational leadership and its impact on job satisfaction and organizational performance. International Public Management Journal, 21(1), 131-162

[32] O'Neill, T. A., & Salas, E. (2018) Creating high performance teamwork in organizations. Human Resource Management Review, 28(4), 325-331

[33] Para-González, L., Jiménez-Jiménez, D., & Martínez-Lorente, A. R. (2018) Exploring the mediating effects between transformational leadership and organizational performance. Employee Relations, 40(2), 412-432

[34] Ployhart, R. E., & Moliterno, T. P. (2011) Emergence of the human capital resource: A multilevel model. Academy of Management Review, 36(1), 127-150

[35] Poór, J., Slavic, A., & Berber, N. (2015) The competences of HR managers and their impact on the organizational success of MNCs' subsidiaries in the CEE region. Central European Business Review, 4(1), 5

[36] Radivojević, N., Ćurčić, N., & Dević, Ž. (2016) Implementation of the model of' Transformational managerial competences' in the process of restructuring of' Zastava machines AD, Kragujevac. Ekonomika: Journal for Economic Theory and Practice and Social Issues, 62(1), 23-42

[37] Stojanović-Aleksić, V. (2016) Followers in the organizational leadership process: From attribution to shared leadership. Economic Horizons, 18(2), 139-151

[38] Stojanović-Aleksić, V. (2017) Correction: Factors and sources of leadership capabilities: Experience from Serbia. Annals of the Faculty of Economics in Subotica, (38), 317-333

[39] Stojanović-Aleksić, V., Stamenković, M., & Milanović, M. (2016) The analysis of leadership styles in Serbian organizations: Gender influence. Teme, 40(4), 1383-1397

[40] Strugar Jelača, M., Bjekić, R., & Leković, B. (2016) A proposal for research framework based on the theoretical analysis and practical application of MLQ questionnaire. Economic Themes, 54(4), 549-562

[41] Tabernero, C., Chambel, M. J., Curral, L., & Arana, J. M. (2009) The role of task-oriented versus relationship-oriented leadership on normative contract and group performance. Social Behavior and Personality: An International Journal, 37(10), 1391-1404

[42] Thaler, R. H. (2016) Behavioral economics: Past, present, and future. American Economic Review, 106(7), 1577-1600

[43] Tsigu, G. T., & Rao, D. P. (2015) Leadership styles: their impact on job outcomes in Ethiopian banking industry. Zenith - International Journal of Business Economics & Management Research, 5(2), 41-52

[44] Vasilić, N., & Brković, P. (2017) National culture as a determinant of attitudes about leadership styles. School of Business, (2), 38-55

[45] Vaccaro, I. G., Jansen, J. J., Van Den Bosch, F. A., & Volberda, H. W. (2012) Management innovation and leadership: The moderating role of organizational size. Journal of Management Studies, 49(1), 28-51

[46] Wallace, E., de Chernatony, L., & Buil, I. (2013) Building bank brands: How leadership behavior influences employee commitment. Journal of Business Research, 66(2), 165-171

[47] Yizhong, X., Baranchenko, Y., Lin, Z., Lau, C. K., & Ma, J. (2019) The influences of transformational leadership on employee employability: Evidence from China. Employee Relations, 41(1), 101-118

[48] Zareen, M., Razzaq, K., & Mujtaba, B. G. (2015) Impact of transactional, transformational and laissez-faire leadership styles on motivation: A quantitative study of banking employees in Pakistan. Public Organization Review, 15(4), 531-549

[49] Ze, Y., Abbas, H., Hussain, T., & Jiao, H. (2018) Analyzing the differentiation strategies of big companies competing with each other. Strategic Management, 23(3), 25-37

Analytical Description of the Steady-State Creep of Metals in the Presence of Direct Current

Andrew Rusinko, Peter Varga

Óbuda University, Népszínház u. 8, H-1081 Budapest, Hungary
ruszinko.endre@bgk.uni-obuda.hu, varga.peter@bgk.uni-obuda.hu

Abstract: This paper is aimed to develop a model for the analytical description of the effect of direct current (DC) upon the steady-state creep of metals. For the mathematical apparatus, the synthetic theory of irrecoverable deformation is taken. As a result, relationships between creep rate, stress, temperature, and current intensity have been derived. For this purpose, a term, taking into account the passing of DC, is entered into the constitutive equation of the theory. The model results fit well experimental data. The analysis of loading surface in steady-state creep for the ordinary loading and that coupled with DC is provided.

Keywords: steady-state creep rate; direct current; synthetic theory

1 Introduction

The electrical-mechanical behavior of materials has been extensively studied analytically and numerically for the potential applications in micro electromechanical systems and field-assisted sintering process.

A number of investigators have clearly established that mechanical properties such as flow stress, creep, and stress relaxation undergo significant changes under the influence of electrical field. Whatever the detailed mechanism for the effect of electric current on deformation behavior, the effect is most likely associated with the interaction of the electric field with the structural defects, notably dislocations. When current is imposed on the deformation, it will cause not only heating and thus expansion of material, but also will weaken the binding forces between dislocations and obstacles impeding dislocation motion that otherwise cannot be overcome by thermal activation alone. As a result, the nucleation and multiplication of dislocations will be alleviated that in turn will increase the density of mobile dislocations. Therefore, electron wind frees more and more dislocation from the pinning defects and enhances the mobility of dislocations that will be reflected as an increased rate of deformation.

Researches [1-7] report an increase steady-state creep rate due to the passage of DC, see Fig. 2, which is suggested to be caused by the following:

(i) DC-induced Joule heating causing a change in local temperature and resulting in time-dependent plastic deformation [8-10].

(ii) Themomentumexchangebetweenmovingelectronsandlatticeatomsreducesthee nergybarrierandincreasesthemigration velocity of atoms [11-13].

(iii) The intensification of the current field assisted sliding rate and diffusional creep [14-16]

Such metals and their alloys as copper, nickel, aluminum, tin, etc. [1-3, 6] show the increase in their steady-state creep due to the passage of direct current (DC). It must be noted that, so far, experimental results dominates over analytical studies about the influence DC on the steady-state creep of metals. Here can be mentioned work [2] proposing a linear relation between the creep rate and squared current intensity.

This paper continues the investigations presented in [17], where, in terms of the synthetic theory of irrecoverable deformation, formulae $\dot{\varepsilon} = \dot{\varepsilon}(\sigma, J)$ at a given temperature have been proposed (J is current intensity). At the same time, a deeper analysis of the results obtained shows unsatisfactory results for variable temperature. Consequently, the goal of this paper is to model the effect of DC upon the steady-state creep of metals encompassing all the three parameters affecting the creep, i.e. $\dot{\varepsilon} = \dot{\varepsilon}(\sigma, T, J)$.

2 Synthetic Theory

The synthetic theory incorporates the Batdorf-Budiansky slip concept [18] and the Sanders flow theory [19]. The theory models small irrecoverable (plastic/creep) deformations of hardening materials. While works [20-22] provide comprehensive information on the basic notions and relationships of the synthetic theory, here we utilize only its key formulae.

The modeling of irrecoverable deformation takes place in the three-dimensional subspace of the Ilyushin five-dimensional space of stress deviators [23]. The loading process is expressed by a stress vector, $\mathbf{S}$, whose components are converted from the stress deviator tensor components – S_{ij} ($i, j = x, y, z$) – as follows [20, 21]:

$$\mathbf{S}\left[\sqrt{3/2}S_{xx}, S_{xx}/\sqrt{2} + \sqrt{2}S_{yy}, \sqrt{2}S_{xz}\right]. \tag{1}$$

Since the synthetic theory is of two-level nature, the macrodeformation (strain vector **e**) is calculated a sum of slips occurring at the microlevel of material (strain intensity φ_N)

$$\mathbf{e} = \int_\alpha \int_\beta \int_\lambda \varphi_N \mathbf{N} dV , \quad dV = \cos\beta d\alpha d\beta d\lambda \tag{2}$$

where angles α, β and λ give the orientation of slip system and the slip direction.

The strain vector components are related to the strain-deviator tensor components, e_{ij} ($i, j = x, y, z$), in the following way

$$e_1 = \sqrt{3/2} e_{xx} , \quad e_2 = e_{xx} / \sqrt{2} + \sqrt{2} e_{yy} , \quad e_3 = \sqrt{2} e_{xz} . \tag{3}$$

For the case of steady-state creep ($\mathbf{S}(t) = const$), the strain intensity takes the form as [20, 21]

$$\dot{\varphi}_N = \frac{K}{r} \left[\left(\mathbf{S} \cdot \mathbf{N} \right)^2 - 2/3 \sigma_P^2 \right] , \tag{4}$$

$$K = K_1(T) K_2(\sigma_{eff}) , \; K_1(T) = \exp\left(-\frac{Q}{RT} \right), \; K_2(\sigma_{eff}) = \frac{9\sqrt{3} cr}{2\sqrt{2}\pi} \sigma_{eff}^{k-2} \tag{5}$$

where r, c and k are model constants; σ_P the creep limit of material in uniaxial tension, Q creep activation energy. According to Schimd's law, the driving force of plastic slip within a slip system is resolved shear stress, which is determined by the product $\mathbf{S} \cdot \mathbf{N}$, where unit vector $\mathbf{N}$ gives the orientation of slip system.

In Eq. (5), We define the function K_2 via the Bailey-Norton law (power law creep). In terms of the synthetic theory, the effect of power index is expressed by constant k.

In uniaxial tension ($S_1 = \sqrt{2/3}\sigma$, $N_1 = \cos\alpha \cos\beta \cos\lambda$ [19, 20]), Eq. (2) gets

$$\dot{e}_1 = \frac{2K}{3r} \int_{-\alpha_1}^{\alpha_1} \int_{-\beta_1}^{\beta_1} \int_{0}^{\lambda_1} \left[\left(\sigma \cos\alpha \cos\beta \cos\lambda \right)^2 - \sigma_P^2 \right] \cos\alpha \cos^2\beta \cos\lambda d\alpha d\beta d\lambda . \tag{6}$$

The boundaries of integration are [20, 21]

$$\cos\lambda_1 = \frac{\sigma_P}{\sigma \cos\alpha \cos\beta}, \quad \cos\alpha_1 = \frac{\sigma_P}{\sigma \cos\beta}, \quad \cos\beta_1 = \frac{\sigma_P}{\sigma} . \tag{7}$$

By integrating in (6), we obtain

$$\dot{e}_1 = AF(b),\ A = \frac{\sqrt{3}c\sigma_P^2}{2\sqrt{2}}\sigma^{k-2}K_1(\Theta), \tag{8}$$

$$F(b) = \frac{1}{b^2}\left(2\sqrt{1-b^2} - 5b^2\sqrt{1-b^2} + 3b^4\ln\frac{1+\sqrt{1-b^2}}{b}\right),\ b = \cos\beta_1\,. \tag{9}$$

In [20-22] it is shown that $F(b)$ increases with the decrease in b. On the other hand, the last formula in Eq. (7) shows that b decreases as the stress σ grows. Therefore, the final result is that the function F is an increasing function of the acting stress. For the sake of further simplification, we approximate function F from (9) as

$$F \approx \left(\frac{1}{b} - 1\right)^2,\ \ F(1) = F'(1) = 0\,. \tag{10}$$

3 Relationships of the Synthetic Theory in the Case of Creep Accompanied by Current

To model the action of DC which it exerts on the processes occurring in a slip system during steady-state creep, we enter into Eq. (4) terms containing current intensity, J (kA/cm^2).

1) To take into account the current passage induced temperature increase (Joule heating), we write down the function $K_1(T)$ from (5) as

$$K_1(T) = \exp\left(-\frac{Q}{R\left(T + 5.23J^2\right)}\right), \tag{11}$$

where the factor 5.23 is taken from [2].

2) A new term, C, is inserted into formula (4) for φ_N,

$$\varphi_N = \frac{K}{r}\left[(\mathbf{S}\cdot\mathbf{N})^2\left(1 + C^2\right) - 2/3\sigma_P^2\right]. \tag{12}$$

The presence of C in (12) symbolizes the increase in deformation within a slip system caused by electric field. We propose to define the function C as a product of two functions,

$$C = U(J)\cdot W(T), \tag{13}$$

both related to their arguments as power functions

$$U = u_1 J^{u_2} \,, \tag{14}$$

$$W = \left(w_1 T - w_2\right)^{w_3} + w_4 \,, \tag{15}$$

where u_i and w_j model constants to be determined to best fit experiments.

The choice to adopt the term standing for the electric field in the form of C^2 in (12) is motivated by the proposition that the creep rate can be taken as a linear function of J^2, $\dot{\varepsilon} = \dot{\varepsilon}_0 + aJ^2$ [2]. Therefore, we follow this phenomenological fashion, at least, at the microlevel of material. The further complication of the function C, which can be obtained from the observation on the microlevel of material to understand what effect the current has on the dynamics of slides, is strongly needed.

By defining the function C as the product $U(J)\cdot W(T)$, we try to follow the tendency from formula (5) when defining the K. i.e. the effect from DC is decomposed on two components: (a) the force interaction between the electron wind and the material lattice $U(J)$ and (b) temperature-dependent effect. The temperature increase (11) alone is not enough to reach a good agreement between experimental and model results.

To be in line with experimental results [2], stating that DC does not strongly affect the slope of $\log\dot{\varepsilon}\sim\log\sigma$ lines, we enter function C into formula (12) as a factor multiplying σ. This means a parallel alignment of the $\log\dot{\varepsilon}\sim\log\sigma$ plots for different current intensities at a given stress. At the same time, the change in the slope must be inspected due to formula (11).

Long-term study of the behavior of $\dot{\varepsilon} = \dot{\varepsilon}(J,\sigma)\big|_T$ and $\dot{\varepsilon} = \dot{\varepsilon}(J,T)\big|_\sigma$ dependencies has been shown that these are the relationships (14) and (15) that leads to the results fitting experimental data.

To calculate the value of the first stress inducing creep deformation in the presence of DC (σ^C), we let $\varphi_N = 0$ and $\alpha, \beta, \lambda = 0$ in Eq. (12):

$$\sigma^C = \sigma_P \Big/ \sqrt{1 + C^2} \,. \tag{16}$$

As one can see, Eq. (16) expresses the fact that the passage of current decreases the stress needed to initiate the development of creep deformation ($\sigma^C < \sigma_P$).

Now, taking into account (12)-(15), Eq. (2) takes the following form:

$$\dot{e}_1 = \frac{2K}{3r}\times$$
$$\int\limits_{-\alpha_{1C}}^{\alpha_{1C}} \int\limits_{-\beta_{1C}}^{\beta_{1C}} \int\limits_{0}^{\lambda_{1C}} \left[\left(\sigma\cos\alpha\cos\beta\cos\lambda\right)^2 \left(1+C^2\right) - \sigma_P^2 \right] \cos\alpha\cos^2\beta\cos\lambda d\alpha d\beta d\lambda \tag{17}$$

where

$$\cos\lambda_{1C} = \frac{\sigma_P}{\sigma\sqrt{1+C^2}\cos\alpha\cos\beta}, \cos\alpha_{1C} = \frac{\sigma_P}{\sigma\sqrt{1+C^2}\cos\beta},$$
$$\cos\beta_{1C} = \frac{\sigma_P}{\sigma\sqrt{1+C^2}} < \cos\beta_1 \Rightarrow \beta_1 < \beta_{1C}. \tag{18}$$

The secondary creep rate in uniaxial tension under the action of DC, $\dot{e}_1^C$, is calculated from Eqs. (17) and (18) as

$$\dot{e}_1^C = AF\left(b_C\right),\ b_C = \cos\beta_{1C}. \tag{19}$$

The following conclusions can be drawn from Eqs. (17) and (18):

1) formula (17) shows that the action of DC intensify the slips, (factor $1+C^2$),

2) formula (18) means the enlarging of integration domain, comparing to the case of ordinary creep; in other words, the number of slip systems contributing to creep strain increases under the action of DC.

Consider results obtained in terms of the synthetic theory for the steady-state creep rate of tin in uniaxial tension (melting point 505.08 K). The following four diagrams are plotted to inspect their fits with the following experiments [2]:

(i) Fig. 1a. Steady-state creep of tin $\dot{\varepsilon}$ as a function of tensile stress σ without current ($J=0$); experiments were conducted at different temperatures (323,348,373,398,423 K).

(ii) Fig. 1b. Steady-state creep of tin $\dot{\varepsilon}$ as a function of temperature T without current ($J=0$); experiments were conducted under tensile stress $\sigma = 3.09$ MPa .

(iii) Fig. 2a. Steady-state creep of tin $\dot{\varepsilon}$ as a function of tensile stress σ under the action of current of different intensities – $J = 0,\ 1.26,\ 1.89,\ 2.52,\ 2.835,\ 3.15\ \mathrm{kA/cm^2}$; experiments were conducted at $T = 323$ K .

(iv) Fig. 2b. Steady-state creep of tin $\dot{\varepsilon}$ as a function of current intensity squared J^2; experiments were conducted under tensile stress $\sigma = 3.09$ MPa at different temperatures (see (i)).

To complete the tasks announced, first, the model constants c and k must be chosen for constructing $\dot{\varepsilon}\sim\sigma$ and $\dot{\varepsilon}\sim T$ graphs at $J=0$. Plots in Fig. 1 are obtained by Eqs. (8)-(10) at $k=6$ and $c=26$ (activation energy here and further throughout is $Q=7.0\cdot10^4$ J/mole [2]). The experimental data for Fig. 1b are read from Fig. 2b at $J=0$.

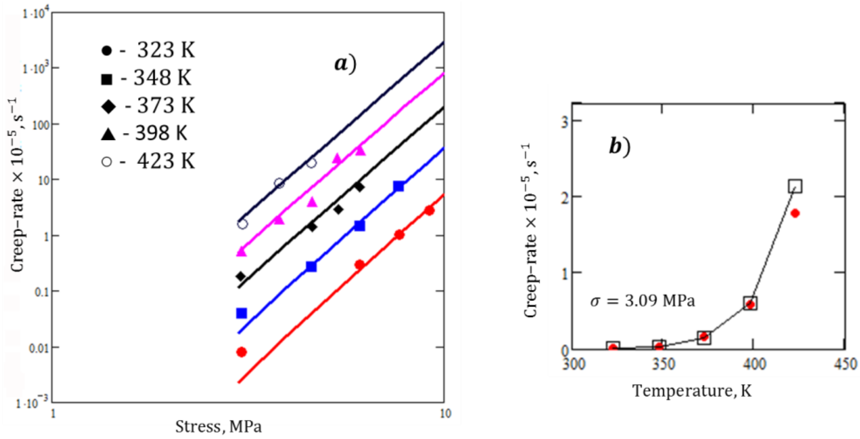

Figure 1

log$\dot{\varepsilon}$~logσ (a) and $\dot{\varepsilon}\sim T$ (b) diagrams of tin ($J=0$) (points – experiment [2], lines– model)

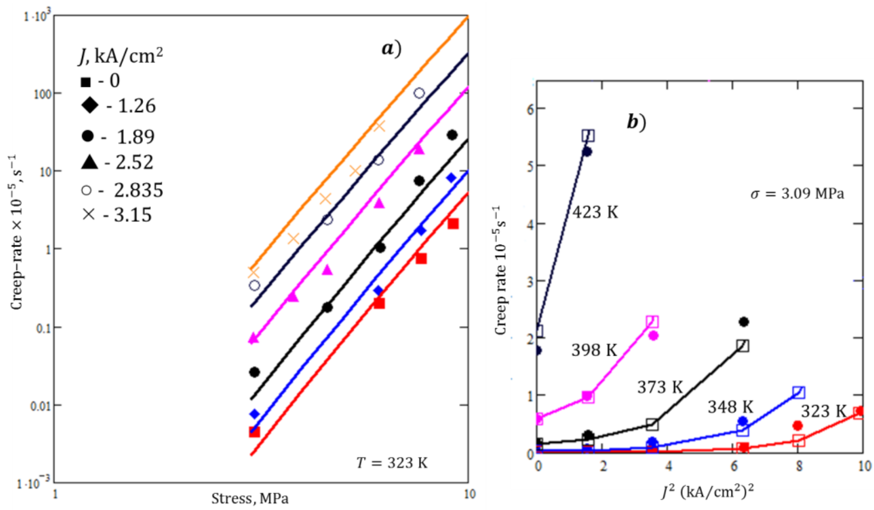

Figure 2

log$\dot{\varepsilon}$~logσ (a) and $\dot{\varepsilon}\sim J^2$ (b) diagrams of tin ($J=0$) (points– experiment [2], lines– model)

The next step is $\dot{\varepsilon}=\dot{\varepsilon}\left(J,\sigma\right)\big|_T$ and $\dot{\varepsilon}=\dot{\varepsilon}\left(J,T\right)\big|_\sigma$ diagrams of tin subjected to DC. Results obtained by Eqs. (18) and (19), together with (13-15), calculated at

$u_1 = 0.5\ \left(\mathrm{cm}^2/\mathrm{kA}\right)^{u_2}$, $u_2 = 3.0$, $w_1 = 0.0121/K$, $w_2 = 4.102$, $w_3 = 6$, $w_4 = 0.12$, are shown in Fig. 2 (the values of c and k, naturally, are the same as above). Fig. 2bdemonstrates that the synthetic theory follows Zhao's proposition [2] to express $\dot{\varepsilon}\sim J$ dependency as $\dot{\varepsilon} = \dot{\varepsilon}_0 + aJ^2$ (the model $\dot{\varepsilon}\sim J^2$ curve has a great radius of curvature.

The change in the slope of $\dot{\varepsilon}\sim\sigma$ lines in Fig. 2a, caused by formula (11), is only of 3.57%, which is in accordance with experiments.

As one can see, all the four analytical results give good agreement with the experimental data. It must be stressed once more that the analytical curves in Figs. 1 and 2 are obtained via formulae of the synthetic theories using one and the same set of constants: k, c, u_i, w_j.

4 The Analysis of Loading Surface in Steady-State Creep Coupled with DC

The essential characteristics of the plastic/creep constitutive models are:

(i) The yield criterion that defines the material state at the transition from elastic to elastic-plastic behavior. Yield function actually describes the surface in the stress space that demarks the boundary between the elastic and plastic/creep behavior of materials.

(ii) The flow rule that determines the increment in plastic strain from the increment in load.

(iii) The hardening rule that gives the evolution in the yield criterion during plastic deformation. In other words, the hardening rule describes how the yield surface changes (size, center, shape) as the result of permanent deformation. Development of yielding criteria is hence pivotal in predicting whether or not a material will begin to yield under a given stress state.

The synthetic theory utilizes the Von-Mises yield criterion, which results in the sphere in three-dimensional stress-deviator space [21, 24]:

$$S_1^2 + S_2^2 + S_3^2 = S_P^2, \tag{20}$$

where $S_P = \sqrt{2/3}\sigma_P$, and σ_P is the creep limit of material.

The flow rule is defined by Eq. (2) for one slip system at the micro-level of material, and the macro deformation is calculated via Eq. (2) (for the case of uniaxial tension we obtain formula (6)).

The evolution in yield criterion (i.e. the behavior of subsequent yield surface, or loading surface) obeys the principle proposed by Sanders [19]. The yield surface (20) is treated as the inner envelope of the planes tangential to the sphere, i.e. we have the continuous set of equidistant planes. During loading, stress vector ($\mathbf{S}$) translates at its endpoint some set of planes to which it reaches. The displacement of plane at the endpoint of the $\mathbf{S}$ symbolizes the development of permanent defamation within appropriate slip system.

In the case of steady-state creep the equations for the plane distances under the action of stress vector $\mathbf{S}$ (H_N, index N stands for the normal vector $\mathbf{N}$ that gives the orientation of the plane) are

$$H_N = \begin{cases} \mathbf{S}\cdot\mathbf{N} & \text{The stress vector displaces the plane} \\ \sqrt{2/3}\sigma_P & \text{Stationary planes} \end{cases} \tag{21}$$

The loading surface for uniaxial tension, which is the inner envelope of the planes whose distances are determined by the formulae above, is shown in Fig. 3, surface Ω. It consists of two portions:

(i) the sphere formed by stationary planes, i.e. those which are not reached by the stress vector,

(ii) the cone whose generator is made up of boundary planes reached by the stress vector (their orientation is given by angle β_1).

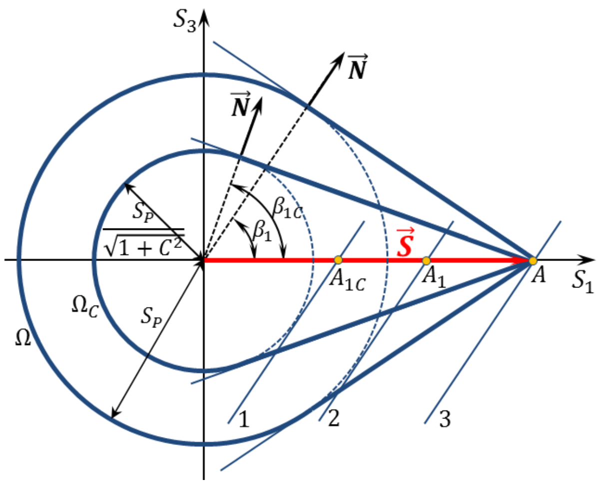

Figure 3

Loading surfaces in S_1-S_3 coordinate plane for uniaxial tension under the condition of stready-state creep; Ω – ordinary load, Ω_C – creep with DC

As one can see, the synthetic theory gives rise to a singular point on the loading surface, loading point A.

When considering the creep accompanied by direct current, formulae (16)-(18) lead to the following transformations in the loading surface.

Formula (16) results in the decreasing of the initial radius of yield surface (the virgin state of material), namely $S_P/\sqrt{1+C^2}$ instead of S_P (Fig. 3, surface Ω_C). This fact implies that the stress needed to induce plastic shift within a slip system is less for the case of simultaneous action of loading and the passage of current. Really, while, in the case of ordinary loading, the stress vector reaches plane 2 from Fig. 3 at point A_1, the plane with the same orientation (plane 1) is achieved by the stress vector at point A_{1C} (creep with DC).

Another result is that, for a given stress vector, the distance covered by a plane increases due to the action of DC. Indeed, both planes from Fig. 3, plane 1 and 2, are translated by the stress vector into position 3, but it is clear that the plane 1 travels the greater distance than the plane 2 does. This result is in accordance with the conclusion obtained from formula (17), namely, the passage of current intensifies the slip within every slip system.

In addition, Fig. 3 demonstrates the final result, the passage of current increases the number of slip systems where plastic shifts occur ($\beta_1 < \beta_{1C}$), obtained by Eq. (18).

Conclusions

The model describing the steady-state creep of metals under the action of direct current has been developed in terms of the synthetic theory of irrecoverable deformation. To catch the effect the current exerts upon the creep rate, we extend the constitutive relationships of the synthetic theory, which govern the hardening of material, by a term containing the current intensity. As a result, we have derived relationships for the steady-state creep rate coupled with DC. Results obtained in terms of our model show good agreement with experimental data. Understanding the evolution of loading surface, i.e. the onset and development of irrecoverable deformation (plastic or creep), is critical in modeling any type of deformation. For this reason the analytical results obtained are accompanied by the analysis of loading surface for the case of ordinary steady-state creep and that in electrical field.

References

[1] Braunovic, M., Myshkin, N., Konchits, V. (2006) *Electrical Contacts: Fundamentals, Applications and Technology*, CRC Press. Taylor& Francis Group

[2] Zhao, G. and Yang, F. (2014) Effect of DC current on tensile creep of pure tin, Materials Science & Engineering A, **591**: 97-104

[3] Kinney, C., Morris, J. W., Lee, T. K., Liu, K. C., Xue, J., Towne, D. (2009) The influence of an imposed current on the creep of Sn-Ag-Cu solder. *Journal of Electronic Materials*, **38**: 221-226

[4] Zhao, G. F., Liu, M. and Yang, F. Q. (2012) The effect of an electric current on the nanoindentation behavior of tin, *ActaMaterialia*, **60**: 3773-3782

[5] Yang, F. Q. and Zhao, G. F. (2010) Effect of Electric Current on Nanoindentation of Copper, *Nanoscience and Nanotechnology Letters*, **2**: 322-326

[6] Sanmartin, K. Kleinstück, N. H. Quyen and P. Paufler (1983) Influence of a direct current and a temperature gradient on the creep rate in V3Si, *Physica Status Solidi A*, **80**: K171-K174

[7] Li, Wang-Yun; Zhou, Min-Bo; Zhang, Xin-Ping (2015) Creep behavior of Cu/Sn-3.0Ag-0.5Cu/Cu solder joints under tensile stress coupled with DC current stressing, *16th International Conference on Electronic Packaging Technology (ICEPT), 11-14 Aug. 2015, Changsha, China,* pp. 187-192

[8] Chen, R. and Yang, F (2008) Impression creep of a Sn60Pb40 alloy: the effect of electric current. *Journal of Physics D-Applied Physics*, **41**: 065404

[9] Chiao, M. and Lin, L. W. (2000) Self-buckling of micromachined beams under resistive heating, *Journal of Microelectromechanical Systems*, **9**: 146-151

[10] Yang, F. (2009) Current-induced thermal stresses in a metal cylinder, *Journal of Applied Physics,* **106**: 113536

[11] Chen, R. and Yang, F. Q. (2008) Impression creep of a Sn60Pb40 alloy: the effect of electric current, *Journal of Physics D-Applied Physics*, **41**: 155406

[12] Chen, R. and Yang, F. (2010) Effect of DC Current on the Creep Deformation of Tin, *Journal of Electronic Materials*, **39**: 2611-2617

[13] Chen, R. and Yang, F. (2011) Effect of electric current on the creep deformation of lead. *Materials Science and Engineering a-Structural Materials Properties Microstructure and Processing*, **528**: 2319-2325

[14] Kumar, P. and Dutta, I. (2011) Influence of electric current on diffusionally accommodated sliding at hetero-interfaces, *ActaMaterialia*, **59**: 2096- 2108

[15] Shao, S. S., Yang, F. Q. and Xuan, F. Z. (2012) Effect of electromigration on diffusional creep in polycrystalline materials, *International Journal of Applied Electromagnetics and Mechanics*, **40**: 165-171

[16] Hamada, N., Hamada, M., Uesugi, T., Takigawa, Y. and Higashi, K., "Effect of Small Addition of Zinc on Creep Behavior of Tin, *Materials Transactions*, **51**: 1747-1752

[17] Rusinko, A. (2016) Modeling the Effect of DC on the Creep of Metals in Terms of the Synthetic Theory of Irrecoverable Deformation. *Mechanics of Materials* **93**: 163-167

[18] Batdorf, S. and Budiansky, B. (1949) Mathematical Theory of Plasticity Based on the Concept of Slip. NACA Technical Note, 871

[19] Sanders Jr., J. L. (1954) Plastic Stress-Strain Relations Based on Linear Loading Functions. *Proceedings of the Second USA National Congress of Applied Mechanics*, Ann Arbor, 14-18 June 1954, 455-460

[20] Rusinko, A. and Rusinko, K. (2009) Synthetic theory of irreversible deformation in the context of fundamental bases of plasticity, *Mechanics of Materials*, **41**: 106-120

[21] Rusinko, A. and Rusinko, K. (2011) *Plasticity and Creep of Metals*, Springer Berlin Heidelberg

[22] Rusinko, A. (2015) Irrecoverable deformation of tin in terms of the synthetic theory, *Materials Science and Engineering: A*, **631**: 97-103

[23] Ilyushin, A.A. (1963) *Plasticity*. IzdatelstvoAkademiiNauk SSSR, Moscow. (In Russian)

[24] Von Mises, R. (1913) Mechanik der festenKörperimplastischdeformablenZustand, *Göttin. Nachr. Math. Phys.*, **1**: 582-592

Formal Verification of Python Software Transactional Memory Based on Timed Automata

Branislav Kordic, Miroslav Popovic, Silvia Ghilezan

University of Novi Sad, Faculty of Technical Sciences
Trg Dositeja Obradovica 6, 21000 Novi Sad, Serbia

branislav.kordic@rt-rk.uns.ac.rs, miroslav.popovic@rt-rk.uns.ac.rs, gsilvia@uns.ac.rs

Abstract: Nowadays Software Transactional Memories (STMs) are used in safety-critical software, such as computational-chemistry simulation programs. To the best of our knowledge, the existing STMs were not developed using rigorous model-driven development process, on the contrary, the majority of proposed STMs are directly implemented in a target programming language and formally verified STMs are proven against more general models. This may result in some key aspects of implementation being omitted or interpreted incorrectly. In this paper, we demonstrate an approach to the formal verification of one particular STM, for the Python language, named Python Software Transactional Memory (PSTM), which is based on a STM design and implementation details. Based on these details, faithful models of a PSTM based system, are developed and verified. The PSTM system components are modeled as timed automata utilizing UPPAAL tool. Finally, it is verified that PSTM satisfies deadlock-freeness, safety, liveness, and reachability properties.

Keywords: formal verification; transactional memory; model checking; correctness, timed automata

1 Introduction

Transactional Memory (TM) is a programing paradigm [1, 2] which offers an alternative to traditional lock mechanisms based on mutual exclusion by replacing them with lock-free mechanism in order to harvest more performances on multicore architectures. It is considered to be a paradigm that simplifies writing and maintaining parallel programs as well. Due to the lack of hardware support Software Transactional Memory (STM) was born [3]. For a long time, STMs have been a playground for research in this area. Even today, it seems that hardware support is still not a standard feature in commercial architectures.

The correctness of a transactional memory plays a key role in a transactional based system. The common properties and correctness criteria with small variations of basic ideas [4, 5, 6, 7, 8] such as serializability, atomicity, deadlock etc., can be defined. Serializability and opacity are assumed as prevailing correctness criteria for the safety property, whereas different levels of progressiveness are commonly used for the liveness property. Predominantly, (S)TM verifications are applied on an abstract model which is drawn from specification and/or captured from transactional semantics rather than being developed directly from an implementation itself – a design and a source code details may be omitted despite the fact that a verification model is desired to be a faithful counterpart of the verified system. On the other hand, most of the formal verification models and approaches targeting STMs are general. They were created with the intention to be used as general frameworks, and not to target real implementations. In this paper we tried to overcome these shortcomings by using an approach that could be applied in an agile software development and which uses existing STM's program code as its input. In our previous work [9] we tackle this problem and presented preliminary verification results.

A motivating example which initially inspired us to search for a Python STM solution and to verify its correctness is the performance optimization of a Python application in the area of chemical and pharmacy calculation [10, 11]. The authors of these papers describe a computational-chemistry simulation program for the Protein Structure Prediction model. The aim of PSTM is to replace the existing barrier-based process synchronization in order to gain more performances. Although Python is one of the most widely used programming languages, it still lacks an applicable and reliable STM implementation. Some announcements for PyPy have been made [12], but until today, no final solution has been published.

In this paper, a formal verification of Python Software Transactional Memory (PSTM) [13] using UPPAAL tool [14] is presented. The main aims are (1) to apply a formal verification process to a real STM solution in order to derive a faithful STM model based on a particular PSTM design and implementation rather than making a general model, and (2) to use the developed PSTM model for automated machine-checked formal verification of core system properties which ensures PSTM correctness, namely deadlock-freeness, safety, liveness, and reachability properties. In the contrast to general models, fine grained parameterized automata models are developed. As a type of transactions, aligned and drifted (time shifted) read-write transactions which share a common variable are considered. For the verification purpose, a formula for calculating commit time for a given arbitrary number of transactions was derived.

This paper contributes to the related aspects of STM formal verification, in the following areas: (i) to the best of our knowledge, this is the first formal verification of an STM solution for Python language, (ii) it introduces an approach to modeling a real STM implementation by a tool based on a timed finite state machine model rather than modeling a high-level STM abstraction model, (iii) the templates of fine grained automata models can be used as a starting point for verification of any PSTM based system, (iv) it develops a framework for calculating transactions execution times as a means for verifying system temporal behavior, and lastly, (v) it formally verifies that the STM solution for Python language, namely PSTM, conforms deadlock-freeness, safety, liveness, and reachability properties, and hence it is eligible to be a part of a real-world application.

The paper is organized as follows. In Section 2 PSTM architecture is introduced. Formalization of PSTM using UPPAAL tool is presented in Section 3. In Section 4 a framework for temporal behavior analysis is introduced. Verification properties and results are provided in Section 5 and Section 6, respectively.

2 Python Software Transactional Memory

In general, a transactional memory system accommodates transactions and a component responsible to handle transactions requests, i.e. a (S)TM. In this paper, that component is PSTM [13]. A transaction may be considered as a sequence of instructions that are executed atomically over a given set of transactional variables (*t-vars*). The common behavior steps for a transaction are the following: (i) get a local set of t-vars from PSTM, also called a *snapshot*, (ii) perform a processing based on t-vars, and (iii) commit new values, if any.

PSTM architecture is shown in Fig. 1. It consists of the two main components, a *set of transactions* and *PSTM*. Transactions are executed in the context of a transactional application while the PSTM is comprised of an API provided to the transactions, and a server which implements the API functionality.

PSTM public API captures all requirements defined by the common transactions behavior. The API functions are accessible via Remote Procedure Call (RPC) interface. The RPC interface is a key part of PSTM which provides concurrent access to PSTM – it ensures transactional requests serialization. The RPC interface is implemented using Python Queue class. Transactions use a singleton queue to send requests towards PSTM. PSTM API is the following:

- `AddVars(`*q*`, `*keys*`)`
- `GetVars(`*q*`, `*keys*`)`
- `CommitVars(`*q*`, `*rw_sets*`)`
- `PutVars(`*q*`, `*vars*`)`
- `CmpVars(`*q*`, `*vars*`)`

Let us first introduce a *dictionary* and a *t-var*. A transactional variable, or t-var, denotes a variable stored in PSTM which can be accessed only through the API functions. A t-var is uniquely determined by three attributes, namely a *key*, a *version*, and a *value*. A t-var's *key* is an accessing identifier of a t-var, a *version* holds the t-var's version, which is the most recent one at the read time, and a *value* represents data. The t-vars are kept in a dictionary. Only the PSTM server is allowed to *read* and *write* directly to the dictionary. The dictionary and t-vars are implemented as Python dictionary and tuple data structures, respectively.

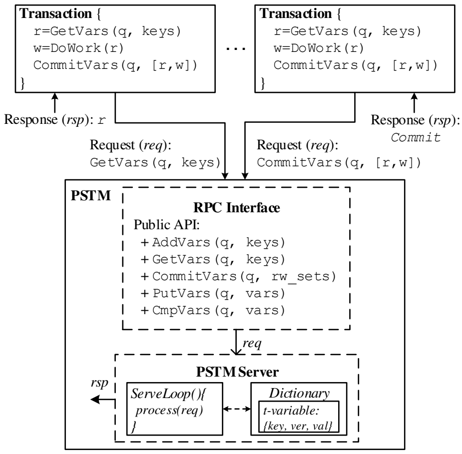

Figure 1
Overview of PSTM architecture

PSTM API functions share a mutual argument queue `q`. The queue is used as a communication channel between transactions and PSTM. The function `AddVars` introduces new t-vars to PSTM. The function `GetVars` returns the most recent version of t-vars which are currently stored in the dictionary. For both `AddVars` and `GetVars` functions a set of t-vars' keys are expected as `keys` argument. The function `CmpVars` is a helper function used to compare (or validate) a set of t-vars' versions against the current versions of corresponding t-vars in the dictionary. The argument `vars` denotes a set of t-vars with all attributes included. The function `CommitVars` tries to commit a transaction to PSTM, i.e. tries to write (update) new value to a t-var. The function `CommitVars` takes the two sets of t-vars, a *read set* and a *write set*, as the argument `rw_sets`. The read set comprises of t-vars that were previously read, i.e. a local snapshot of transactions, while the write set carries changes (a set of t-vars values) which have to be applied to the t-vars in the dictionary. The function commits only if all t-vars' versions in the local snapshot are equal to the t-vars' versions in the dictionary, which means that the particular transaction has the most recent versions of t-vars. When a transaction successfully commits, a t-var version is changed. The function `PutVars` gives another way to commit. Its attempt will be successful only if all the t-vars are up to date. Usually, it is used for t-vars initialization. For the context of this paper `GetVars` and `CommitVars` functions are the most important.

A PSTM server is used to process transactions requests. It provides functionalities behind PSTM API. The PSTM server takes a request from the queue, executes it, and sends a response message to a client (i.e. a transaction). The backbone of PSTM architecture is based on the conventional client-server architecture and it relies on multipoint-to-point and point-to-point communication. Transactional requests are sent in multipoint-to-point fashion, while a request response is sent from the PSTM server directly to a transaction.

In a PSTM execution model, a transaction starts with a *read operation*, then follows a *processing operation*, and finally, the transaction ends with a *write operation*. The mapping between PSTM API functions and transactional operations is illustrated in Fig. 2. The functions `GetVars` and `CommitVars` correspond to the operations read and write, respectively. The function `DoWork` is the processing operation and it is not a member of PSTM API.

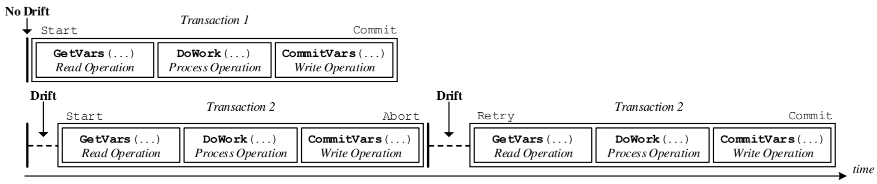

Figure 2

An example execution of aligned (*Transaction 1*) and drifted (*Transaction 2*) transactions

Let's suppose that in the example (Fig. 2) both transactions share a common t-var. The start time of the second transaction is drifted (time shifted) to the start time of the first transaction. Because of the conflict only one of them commits. Specifically, the first transaction commits while the second aborts and retires. An execution set can be comprised of *aligned* (not shifted) and *drifted* transactions. Within a set of aligned transactions, all the transactions start at the same time and they retry immediately after an abort, while within a set of drifted transactions, all the transactions may start and retry in a non-deterministic fashion.

3 PSTM Formalization

In this section we describe PSTM modeling approach, sketch up building entities of a UPPAAL PSTM system model, and introduce its timed automata models.

3.1 Modeling Approach

Due to its expressiveness and convenience, finite state machine based formalisms such as Petri nets and Timed Automata (TA), are often used in the praxis for modeling and machine verification of complex problems like scheduling [15] or synchronization problems [16]. PSTM is formalized and verified using UPPAAL tool. The UPPAAL tool [17, 18, 14] is based on TA and it is widely used by the researchers and in the industry too. In addition to the expressiveness inherited from TA, it provides powerful and user-friendly model checker tool.

A model of a PSTM verification system is made in a compositional way from a set of nondeterministic finite state automata which are coupled through communication channels and shared variables. Three major automata are:

- *Transaction*
- *Remote Procedure Call Queue*
- *Transactional Memory*

A UPPAAL PSTM system design is shown in Fig. 3. The automata are depicted as functional blocks interconnected with channels. The automata are implemented as a template with local variables and functions. The channels and template attributes are defined relying on UPPAAL native data types and C-like features.

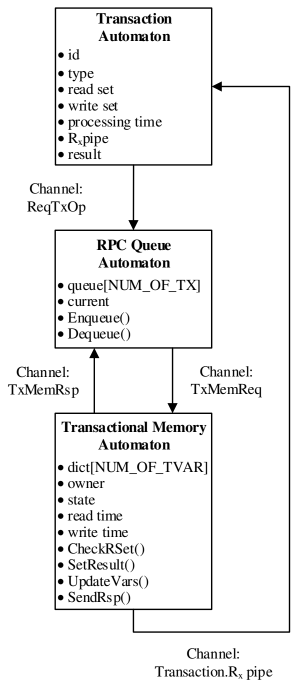

Figure 3

UPPAAL PSTM system design

3.2 UPPAAL PSTM Model

The automata *Transaction*, *RPC Queue*, and *Transactional Memory* are modeled as the templates `Transaction`, `RPCQueue`, and `TxMemory`, respectively.

3.2.1 The Automaton Transaction

An instance of the automaton `Transaction` (Fig. 4) starts with a transition from the state `go` to the state `start_tx`. Immediately after the start, the transaction instance requests a set of shared t-vars from the transactional memory.

The read request is sent during the transition from the state `start_tx` to the state `wait_rsp_TX_R` issuing a send operation to the channel *ReqTxOp*. As a part of the channel operation, transaction data (or context data) are updated: First an operation type is set (TX_R), secondly the shared t-var *SharedTvar* is defined, and finally, the data are passed to the `RPCQueue` through a global variable *RPCQueueMsg*. The *tx_id* is defined as an input argument of each `Transaction` instance. When the request in sent, the instance moves to the state `wait_rsp_TX_R` and waits until the read operation is processed.

The corresponding response is received during the transition from the state `wait_rsp_TX_R` to the state `update_tvar`. It is received by issuing a receive operation on the channel *TxPipe*[*tx_id*]. As in the case of a sending request, the response data are sent through a global variable *TxMemRspMsg*.

In the state `update_tvar` the transaction's read set *Tx*[*tx_id*].*read* contains the most recent version of the shared t-var. The transaction processing time is modeled using a time invariant. The time invariant associated to the state `update_tvar` defines the transaction processing duration. It ensures that the automaton holds in the state `update_tvar` exactly *Tx_proc* time units. For that purpose, a clock variable *c* is introduced. The clock variable *c* measures the time progress and it is local for each transaction instance. Using the time invariant and the clock variable *c* the channel *ReqTxOp* is invoked only when *c* is equal to *Tx_proc*. The variable *Tr_proc*'s value is defined as a template's input argument.

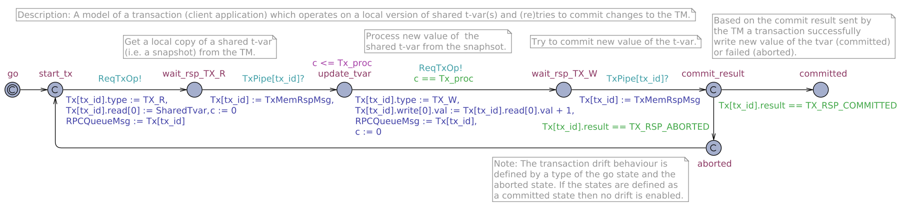

Figure 4

UPPAAL model of a transaction, i.e. the automaton `Transaction`

Each transaction process the shared t-var in the same way – it increments the t-var's current data value. Once the shared t-var is processed, it is ready for a commit. The commit operation is performed in the same two-steps as the read operation, except that the write operation is applied. When the corresponding request is ready, the transaction gets the response, and moves to the state `commit_result`. In that state, a result of the commit operation is known, so the transaction finally ends in `committed` or `aborted` state.

For the verification purposes, the two variations of the automaton `Transaction` are defined. The automaton depicted in Fig. 4 is also named *cyclic* transaction. After the abort, the cyclic transaction models the *retry* operation. A transaction model which does not retry is named a *linear* transaction. The difference between the two transaction models is in a single transition connecting the state `aborted` and the state `start_tx`, which is removed in the linear transaction.

Both the cyclic and the linear transactions may be aligned or drifted. A transaction's drift behavior is modeled with different type of the two states, namely the state `go` and the state `aborted`. The aligned transactions are modeled with a pair of committed states (time delay is not allowed), thus, the transactions start execution immediately. The drifted transactions are modeled with a pair of normal states (time can progress), which enables transactions to drift.

Based on the former descriptions, in a PSTM system verification, the four types of transactions may be used: (i) cyclic drifted transaction, (ii) cyclic aligned transaction, (iii) linear drifted transaction, and (iv) linear aligned transaction.

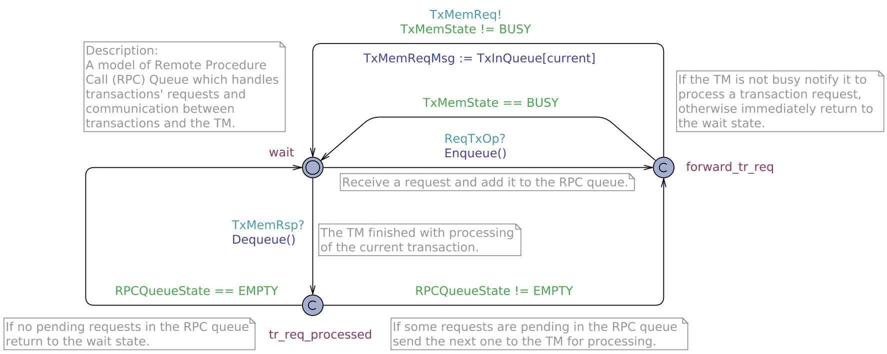

Figure 5

UPPAAL model of RPC Queue, i.e. the automaton `RPCQueue`

3.2.2 The Automaton RPC Queue

An instance of the automaton `RPCQueue` (Fig. 5) starts from the state `wait`. It waits to be notified by some of the transactions or by the transactional memory. At the beginning, the `RPCQueue` is empty, and no pending request exists. The new incoming request is received during the transition from the state `wait` to the state `forward_tr_req`. The request is stored in a local array of pending requests using the function *Enqueue*(). There are the two possibilities and both of them depends on the current state of the automaton `TxMemory`. If the `TxMemory` is not busy then the `RPCQueue` forwards to it the *current* pending request, which has to be processed. After that, the `RPCQueue` advances to the state `wait` where it waits for new incoming requests or to be notified by the `TxMemory`. If the `TxMemory` is busy than the `RPCQueue` immediately advances to the state `wait`. The received requests wait until the `TxMemory` is available.

By moving from the state `wait` to the state `tr_req_processed` the `TxMemory` notifies the `RPCQueue` that the current request is served. In that state the two possibilities exist too, but in this case, both of them depend on the number of pending requests. If the `RPCQueue` is empty, i.e. no pending requests exist, it moves to state `wait`. If the `RPCQueue` holds any pending request, it forwards the *current* request to the `TxMemory` by moving to the state `forward_tr_req`.

3.2.3 The Automaton Transactional Memory

An instance of the automaton `TxMemory` (Fig. 6) may be either available or busy. The `TxMemory` instance starts from the state `wait`. As long as it resides in the state `wait` it is available, otherwise it is busy and it serves a particular request.

In the state `wait`, it may be notified by the `RPCQueue`. Right after being notified, it moves from the state `wait` to the state `processing`. The variable *TxMemState* denotes whether the `TxMemory` is available or busy.

When the state `processing` is reached, the type of requested operation needs to be checked. Based on the operation type, the `TxMemory` switches either to a path that models the read or to a path for the write functionality.

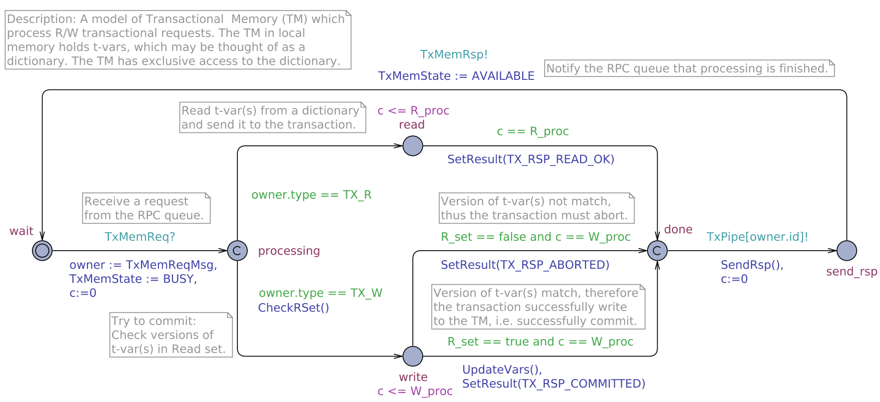

Figure 6

UPPAAL model of transactional memory, i.e. the automaton `TxMemory`

The read operation is served by moving from the state `process` to the state `read`. An additional time invariant is stitched to the state `read` defining the operation duration. Applying the same modeling approach as in the case of transaction processing duration, a clock variable *c* is introduced. The clock variable *c* ensures that a transition is taken immediately as it becomes enabled. Particularly, read and write operations are enabled after *R_proc* and *W_proc* time units, respectively. The variables *R_proc* and *W_proc* denote transactional memory operation duration and they are defined as a template argument, as well.

The transaction response is generated on the transition from the state `read` to the state `done`. The function *SetResult*() updates the transaction's read set with the specified t-vars from the dictionary. Also, it updates the result of the requested operation. The result of the read operation is always successful – the internal value *TX_RSP_READ_OK* sets an execution result value to *TX_RSP_COMMITTED*.

Once the response data are prepared, the transaction and the `RPCQueue` have to be notified. The particular transaction and the transactional memory are synchronized on the transition from the state `done` to the state `send_rsp`. Along the transition, *SendRsp*() function is executed. The function *SendRsp*() sends the response to the transaction by moving the response data to the variable *TxMemRspMbx*. Finally, on the transition from the state `send_rsp` to the state `wait`, the `RPCQueue` is notified that the transactional memory is now available.

The write operation is served in two steps. The first step is to check the t-vars in the read set. For this purpose, the function *CheckRSet*() is used. It loops through the t-vars in the read set and checks if each t-var from the set matches the most recent version of the corresponding t-var in the dictionary. Like the state `read`, the state `write` models the write operation. An additional time invariant ensures that the automaton stays in the state `write` exactly *W_proc* time units simulating the processing duration.

The second step of the write operation is to try to commit the transaction. A commit decision is made, based on the return value of the function *CheckRSet*(). Intuitively, if the result is *true,* the transaction commits, otherwise it aborts. Both paths are modeled on the transitions from the state `write` to the state `done`. The actual t-var(s) update is done by the function *UpdateVars*(). In the case of an abort, the t-vars in the dictionary are unchanged.

4. Transactions Execution Time Analysis

Driven by the desire to make a more faithful transaction model, the drift behavior is modeled as a normal (non-deterministic) state without a time invariant. The fact that a system can behave non-deterministically prevents transactions execution to be handled in a unified way. This significantly impacts the temporal behavior analysis of a PSTM system and brings us closer to the area of transaction scheduling, which, however, is not the focus of this work.

In order to verify the temporal behavior of the PSTM system for the worst case execution scenario, i.e. the scenario in which all the transactions are started simultaneously, we refine the assumptions regarding the transaction processing duration and the durations of read and write operations. The aim of this theoretical analysis is to make a framework for PSTM temporal behavior verification in the worst case scenario.

Particularly, three assumptions are made. The first assumption is that the processing operation duration t_{p_i} takes the same amount of time, $t_{p_1} = t_{p_2} = \cdots = t_{p_N} = t_p$ for all transactions. An index i denotes i –th transaction in the set of N transactions. This assumption is based on the fact that all transactions in a set, typically execute rather short functions that take similar amounts of time – for instance we can consider a banking system, some kind of an online system such as airline ticketing system, etc. For example, ATM (Automated Teller Machine) functions, such as cash withdrawals, deposits, transfer funds, or obtaining account information, all take similar amounts of time, i.e. approximately the same time t_p. The second assumption is that the transactions processing operations take the same time as the transactional read and write operations, $t_p = t_r = t_w$. In hardware transactional memories, t_r and t_w may differ, but since in PSTM t-var read and write operations perform on Python dictionary data structure it is realistic to assume that $t_r = t_w$. Further on, we assumed $t_p = t_r = t_w$ because processing operations usually are a lightweight task (money transfer, ticket reservation, etc.) rather than being compute intensive. The third assumption is that an aborted transaction immediately retries to commit, until it succeeds (aligned cyclic transaction behavior). This way a run-time execution overhead needed to restart a transaction in a real system is neglected. For the comparable overhead values, the results of the analysis would remain unchanged, otherwise the analysis would be unnecessary complicated and unrealistic for a genuine system. Hence, these assumptions enable us to handle the transactions execution times in a unified way without loss of generality of the results of the analysis.

For $N > 2$ a transactions set execution may evolve through three characteristic phases. These execution phases are used to derive a formula for the transaction commit times. Before the analysis of the execution phases, let us first introduce preliminaries.

Lemma 1. An execution time of the single transaction set takes exactly $t = t_r + t_p + t_w$.

Proof. The single transaction is executed sequentially, thus its execution time is equal to the duration of all executed operations. □

Lemma 2. In each execution attempt the maximum queue delay $d_{q_{MAX}}$ is equal to the number of pending transactions p.

Proof. The proof is rather intuitive. If all pending transactions p request a transactional memory operation at the same time, then the lastly enqueued request, is actually the p^{th} transactional request. Further, if a transactional memory operation takes some time t_p, then p^{th} transactional request in the queue will be processed after exactly the p times of the time t_p. □

Claim 1. The first transaction which requests the read operation commits at time $t_c = p \cdot t_r + t_w$.

Proof. Obviously, the transaction which requested the read operation first is ahead of all the others, thus it will also be the first to request the write operation. The write request will be executed just after the last read request in the queue, i.e. after reaching the maximum queue delay $d_{q_{MAX}}$. Since the queue delay $d_{q_{MAX}}$ depends on the number of pending transactions p, the commit time t_c is equal to p read operation times t_r and one write operation time t_w.

Claim 2. A transactions commit attempt terminates at time $t_{ter} = p \cdot (t_r + t_w)$.

Proof. All read operation requests are served at time $p \cdot t_r$. The number of pending transaction in the current attempt is unchanged, therefore $p \cdot t_w$ time is needed for all write operation requests to be served. A commit attempt is terminated at the time when the last write operation is served, $t_{ter} = p \cdot t_r + p \cdot t_w$.

Claim 3. In a commit attempt *at*, where $at \geq 2$, a transaction commits at time

$$t_c = \sum_{i=1}^{at-1} t_{ter_i} + p \cdot t_r + t_w$$

Proof. A new commit attempt starts when a read operation request from the first transaction in a set of aborted transactions is received by the transactional memory. The aborted transactions immediately retry, i.e. they send a new read operation request, but it can be served only after the termination of the previous commit attempt(s) – all p write operation requests from the previous attempt are served first. A set comprised of aborted transactions is the new pending transactions set, therefore the first transaction from the set commits at time $t_c = t_{ter_{at-1}} + p \cdot t_r + t_w$

Claim 4. The last transaction commits at time $t_c = \sum_{i=1}^{at-1} t_{ter_i} + t_r + t_p + t_w$

Proof. In the last commit attempt ($at = N$), only one transaction is running, thus it is executed sequentially (*Lemma 1*). Like to the former case, the last commit attempt starts execution after the previous commit attempt is terminated.

Based on the conducted analysis, the following formula for calculating commit times for a set of N transactions in the worst case scenario is derived:

$$t_c(c) = \begin{cases} N \cdot t_r + t_w, & | \; c = 1 \\ \sum_{i=1}^{at-1} t_{ter_i} + p \cdot t_r + t_w, & | \; c \neq 1 \; and \; c \neq N \\ \sum_{i=1}^{at-1} t_{ter_i} + t_r + t_p + t_w. & | \; c = N \end{cases} \tag{1}$$

The formula gives the commit time t_c as the function of the number of occurred commits. The number of transactions in a set is denoted as *N*. The number of committed and pending transactions are denoted as c and p, respectively. For $c = 0$ no committed transaction exists. A linear function $N = c + p$ models the relation between the total, committed, and pending number of transactions in the system. The termination time of i^{th} commit attempt t_{ter_i} is given by *Claim 1*. The formula (1) defines a framework for transactions temporal analysis.

5 PSTM Verification

As mandatory properties of almost any system, the correctness criteria include *safety*, *liveness*, *deadlock freeness*, and *reachability* properties. PSTM system is not the exception, therefore, all the former properties are checked.

An execution scenario used to verify a property may vary for each property. Namely, some properties may be verified using all types of transactions while for the others an execution scenario restricted to only one type of transactions may be more suitable. However, the property statements are formulated in such manner that they could be applied to any PSTM-based system with arbitrary number of transactions, t-vars, and read, write, and processing duration values. The given properties are generalized and formulated as statements accompanied with the equivalent CTL formulas expressed in UPPAAL query language [17].

5.1 Deadlock Freeness

The property deadlock freeness can be verified with the following query:

```
A[] not deadlock
```

Let us name the former query as *Deadlock Freenees*. It verifies that a system is deadlock free. A remark about this property is related to terminal states and how UPPAAL tool defines a deadlock state. In UPPAAL tool, a state is a deadlock state if there are no outgoing action transitions either from the state itself or any of its delay successors [17]. This is important for both linear and cyclic transactions. Namely, the linear transactions finally end up either in the state `aborted` or the state `committed` whereas the cyclic transactions end up in the state `committed`. Due to the lack of terminal states this may be considered as a deadlock. In order adapt the transaction automation to the deadlock definition, a self-loop transition is added to the final state(s) of an automaton – `aborted` and `committed` states in the case of linear transactions, and only `committed` state in the case of cyclic transactions.

5.2 Safety

Commonly, in a transactional memory environment, safety property is reduced to atomicity property. In order to get a clear picture of the problem, we need to consider a set of transactions in the PSTM system and analyze a relevant verification scenario. The safety property is verified from the two complementary angles, the perspective of transactional memory operations execution and the perspective of transactions execution in the case of the highest concurrency.

The first safety property, named *Safety I*, claims that in any execution scenario a transactional memory operation is executed atomically, i.e. the transactional memory always serves only *one* transaction's request at the time, and, more precisely, the currently *front* request in the RPC queue. The property can be verified with the following CTL query:

```
A[] TxMemory.processing imply queue[current].id ==
owner.id
```

It brings to the focus the components which are fundamental for safety. It verifies that always when the automaton `TxMemory` is in the state `processing`, the `current` request in the `queue` is actually the same request which is the `owner` of the transactional memory.

The second, stronger safety property, named *Safety II*, claims that in the case of the highest concurrency, in which all the transactions are in the conflict, only one transaction may commit at the time. It is stated as follows: from a set of *N* conflicted transactions, only *one* transaction may commit – a transaction whose commit request is received *first* – while remaining $N-1$ transactions aborts: $Tr_{commit} = Tr_{id=first}$; $Tr_{abort} \in \{Tr_{id \neq first}\} = \{Tr_{id=0}, Tr_{id=1}, \cdots, Tr_{id=N-1}\} - \{Tr_{id=first}\}$. The execution scenario for this property is composed of aligned linear transactions only. The property can be verified with the following CTL query:

```
A[] forall (i:IDs) ((i == first imply S1) and (i != first imply S2))
S1 := Tx[i].result != TX_RSP_ABORTED
S2 := Tx[i].result != TX_RSP_COMMITTED
```

The auxiliary statements `S1` and `S2` do not affect the logic behind the query, they are used to relax a query expression. The statement `S1` limits a transaction result to the two possible values, `TX_RSP_NONE` and `TX_RSP_COMMITTED`. The statement `S2` limits a transaction result to `TX_RSP_NONE` and `TX_RSP_ABORTED`. The value `TX_RSP_NONE` is used for initialization purposes, which means that the transaction did not request any operation yet.

5.3 Liveness

Liveness property is used as a warrant of a system progress. It guaranties that all transactions will finish eventually. The three liveness properties are introduced: *Liveness I*, *Liveness II*, and *Liveness III*. Each definition of the liveness property aims to verify a system progress. The difference between them is the number of details which they comprehend. These properties are defined in the increasing order of their respective power (from the weakest to the strongest). The strongest property *Liveness III*, introduces the timings of the system evolution. The properties are defined in a context of *N* cyclic transactions.

The liveness property *Liveness I* is used as a basic (sanity) functional correctness test. It checks if it is possible for a system to reach a state in which all the transactions are committed. The liveness property *Liveness I* ensures the following: for a set of *N* cyclic transactions, there is a path to a state in which all the transactions will commit eventually, in any transactions schedule. The property can be verified with the following CTL query:

```
E<> forall (i:N) TxW(i).committed
```

The liveness property *Liveness II* is stronger than the former in the sense that it includes pending transactions. It verifies that a specific relation between the committed, pending, and total number of transactions holds in any state. This relation defines the total number of transactions in a system as the sum of already committed and still running (pending) transactions. The property can be verified with the following CTL query:

```
A[] forall (i:N) ((i == pending) imply (L >= (NUM_OF_TX - i))
```

L := Tx(0).committed + ⋯ + Tx(N-1).committed

An auxiliary statement *L* defines the total number of transactions instances Tx(i), which are in the state committed. Clearly, if a transaction is not in the state committed, then it is still running (trying to commit).

Liveness property named *Liveness III*, as a warrant of a system progress enforces the strict timing of the system. It utilizes the formula (1) to define an upper bound of a time window along which the system advances. For the kind of property such like liveness, the timings of the system progress are critical. The example of a negative and undesired timing is a system *livelock*. In order to verify that a system progress is positive, a number of committed transactions must be analyzed, too.

A system progresses in a positive way as long as some of the transactions commits. This can be interpreted as the definition of the property *Liveness I*. Indeed, the property *Liveness III* may be viewed as a timed version of the property *Liveness I*. It is defined in the similar way, but with an additional criterion which defines an upper bound of time up to which a particular number of transactions must commit. Each time window with higher lower and upper bounds, increases the number of committed transactions – it increases the number of commits. With this approach, the property *Liveness III* can be considered as a proof that the PSTM system is livelock free as well. The property can be verified with the following CTL query:

E<> now == $t_{committ}$ and (*L* == *num_of_committed*)

L := Tx(0).committed + ⋯ + Tx(N-1).committed

num_of_committed ∈ *{1,⋯,N}*

t_{commit} = commit_time(*num_of_committed, N*)

An auxiliary statement *L* defines a number of transaction instances Tx(i) that are in the state committed while the value of *num_of_committed* is the expected number of committed transactions. In order to verify the commits of a set of *N* transactions, the same number *N* of verification queries has to be defined. The value of *num_of_committed* is the parameter which denotes a particular number of transaction commits which is the subject of verification. The value $t_{committ}$ is calculated by function commit_time() which actually is an implementation of the formula (1).

5.4 Reachability

The reachability property is included as additional proof of the liveness property. It is exploited to verify the system termination, i.e. the system state after all the transactions have been finished. We use the reachability to verify that the system terminates correctly in any execution scenario. The property *Reachability* can be verified with the following CTL query:

```
R --> ((TxMemory.wait and TxMemState == AVAILABLE) and
(RPCQueue.wait and RPCQueueState == EMPTY))
R := (Tx(0).committed or Tx(0).aborted) and … and
(Tx(N-1).committed or Tx(N-1).aborted
```

An auxiliary statement R claims that N `Transaction` instances are either in the state `committed` or in the state `aborted`, i.e. that all transactions are finished.

6 Verification Results

The property verification queries can be applied to a system with an arbitrary number of transactions and arbitrary duration of read, write and processing time. Despite of model's generic nature, it was not feasible to conduct verificaion for all arbitrary sets of parameters, so for all verification properties the operations read, write and processing take one time unit, $t_p = t_r = t_w = 1$. These particular values make the verification process viable, without losing anything from the generality of the applied method.

Increasing the number of transactions influences the verification time required by a model checker to explore a state space and make a verdict about the property. Considering PSTM architecture design, the correctness properties can be verified using only two transactions, which are required for minimal level of contingency that may provoke undesired system behavior. A system can be verified against an arbitrary number of transactions *N*, if it is necessary. In the conducted verification, the number of transaction instances is increased as long as the verification execution time was reasonable. Actually, at some point, due to the expanded state space, the model checker may consume all of the operating memory of the host machine. In such a case, the tool is capable of utilizing more memory by using swapping mechanism, although this causes very long verification time. However, this bottleneck is related to the host's hardware capabilities.

The summary results are given in Table 1. The results confirmed that PSTM satisfies all the previously defined properties. Although the correctness property results are the main objective of the conducted verification they are accompanied with additional data, namely the number of transactions, the verification execution time, and the number of explored states, which may be beneficial for other researchers who want to get insight into verification process statistics.

The system complexity is elevated by increasing the number of transaction instances. In addition to the number of transaction instances, transactions type is relevant as well. For example, property verification for a set of cyclic transactions is more demanding than the verification of the same property against a set of linear transactions. Further, verifying a property against drifted cyclic transactions is certainly more demanding than verifying the same property against aligned cyclic transactions. The same can be concluded for linear transactions. The reason is rooted in the automata structure – firstly, the model of linear transaction is lighter than the model of cyclic transaction, and secondly, for the model checker it is easier to deal with a committed state (aligned transaction) than with a non-deterministic state (drifted transactions).

Unquestionably, the number of time invariants, i.e. clock variables, significantly impacts a state space which has to be explored. UPPAAL tool is very sensitive to clock variables which causes state space to expand faster. Generally, relaxing the number of clock variables would reduce the state space size.

Table 1
Summary of verification results and performance statistics

Property	Number of Transactions	Type of Transactions	Time	States Explored
Deadlock Freeness	6	Linear Drift	1m 2s 110ms	9 045 757
	5	Cyclic Drift	1m 2s 440ms	10 140 401
	8	Linear Aligned	1m 2s 90ms	8 014 336
	7	Cyclic Aligned	24s 930ms	3 597 232
Safety I	6	Linear Drift	32s 180ms	9 045 757
	5	Cyclic Drift	34s 670ms	10 140 401
	8	Linear Aligned	34s 790ms	8 014 336
	7	Cyclic Aligned	12s 950ms	3 597 232
Safety II	8	Linear Aligned	38s 740ms	8 014 336
Liveness I	5	Cyclic Drift	1m 0s 20ms	17 489 881
	7	Cyclic Aligned	13s 450ms	3 597 232
Liveness II	5	Cyclic Drift	5s 510ms	1 690 633
	7	Cyclic Aligned	12s 420ms	3 577 073
Liveness III	7	Cyclic Aligned	13s 680ms	3 577 073
Reachability	6	Linear Drift	32s 500ms	9 186 157
	5	Cyclic Drift	52s 620ms	14 008 901
	8	Linear Aligned	34s 650ms	8 094 976
	7	Cyclic Aligned	13s 500ms	3 662 752

The experiments are conducted using Ubuntu 14.04 64bit OS, which is running on Intel i7-3770 CPU with 16 GB of RAM, and UPPAAL 64-4.1.19 (rev. 5648).

Conclusions

In this paper we tried to overcome the shortcomings of existing STM formal verification approaches by introducing an approach based on timed automata formalism which uses existing STM's program code as its input. Our verification approach respects a STM solution implementation details aiming to make verification models as faithful counterparts of the implementation rather than developing a generalized verification framework to cover more transaction execution models and semantics. Particularly, we demonstrated our approach to formal verification of one STM, written in the Python language, named Python Software Transactional Memory (PSTM) [13], utilizing UPPAAL tool [17, 14]. Based on the PSTM architecture and implementation details, we derived a model of a PSTM system which is formally verified by the UPPAAL model checker.

The verification of the system correctness includes checking deadlock-freeness, safety, liveness, and reachability properties. We analyzed the system execution against the types of aligned and drifted read-write transactions which share a common transactional variable. The system temporal behavior is analyzed, too. For the purpose of the system temporal behavior verification a framework for calculating transactions execution times in the worst case scenario is developed. By applying generalized property queries to a verification system based on a different number and type of transactions, we successfully verified that our PSTM system model satisfies all the formerly mentioned properties. The results presented in the paper may be useful for the academia and the industry researches as well.

The direction of future work is oriented towards development and formal verification of a distributed (P)STM for the Internet of Things.

Acknowledgement

This work was supported by the Ministry of Education, Science, and Technology Development of Republic of Serbia under grants III-44009, ON174026, III044006.

References

[1] M. Herlihy, J. E. B. Moss: Transactional memory: Architectural support for lock-free data structures, *Proceedings of the 20th Annual International Symposium on Computer Architecture (ISCA'93)*, pp. 289-300, 1993

[2] T. Harris, J. R. Larus, R. Rajwar: Transactional Memory, 2nd edition, Morgan and Claypool Publishers, 2010

[3] N. Shavit, D. Touitou: Software transactional memory, *Proceedings of the 14th Annual ACM Symposium on Principles of Distributed Computing (PODC'95)*, pp. 204-213, 1995

[4] A. Cohen, J. W. O'Leary, A. Pnueli, M. R. Tuttle, L. D. Zuck: Verifying correctness of transactional memories, *Proceedings of the 7th International Conference on Formal Methods in Computer - Aided Design (FMCAD 2007)*, pp. 37-44, 2007

[5] M. Emmi, R. Majumdar, R. Manevich: Parameterized verification of transactional memories, *Proceedings of the 31st Conference on Programming Language Design and Implementation (PLDI'10)*, pp. 134-145, 2010

[6] R. Guerraoui, M. Kapałka: On the correctness of transactional memory, *Proceedings of the 13th Symposium on Principles and Practice of Parallel Programming (PPoPP'08)*, pp. 175-184, 2008

[7] R. Guerraoui, T. A. Henzinger, V. Singh: Model checking transactional memories, *Distributed computing*, Vol. 22 (3), pp. 129-145, 2010

[8] S. Doherty, L. Groves, V. Luchangco, M. Moir: Towards formally specifying and verifying transactional memory, *Formal Aspects of Computing (FAOC)*, Vol. 25 (5), pp. 769-799, 2013

[9] B. Kordic, M. Popovic, S. Ghilezan, I. Basicevic: An approach to formal verification of python software transactional memory, *Proceedings of the Fifth European Conference on the Engineering of Computer-Based Systems (ECBS'17)*, pp. 1-10, 2017

[10] M. Amitay, M. Goldstein: Evaluating the peptide structure prediction capabilities of a purely ab-initio method, *Protein Engineering, Design and Selection*, Vol. 30 (10), pp. 723-727, 2017

[11] M. Goldstein, E. Fredj, R. B. Gerber: A new hybrid algorithm for finding the lowest minima of potential surfaces: approach and application to peptides, *Journal of Computational Chemistry*, Vol. 32, pp. 1785-1800, 2011

[12] PyPy Software Transactional Memory: http://doc.pypy.org/en/latest/introduction.html (accessed 15 October 2018)

[13] M. Popovic, B. Kordic: PSTM: Python software transactional memory, *22nd Telecommunications Forum Telfor (TELFOR 2014)*, pp. 1106-1109, 2014

[14] UPPAAL tool home page: http://www.uppaal.org (accessed 15 October 2018)

[15] C. Belwal, A. M. K. Cheng: Schedulability analysis of transactions in software transactional memory using timed automata. *IEEE 10th International Conference on Trust, Security and Privacy in Computing and Communications (TrustCom)*, pp. 1091-1098, 2011

[16] J. Perhac, D. Mihalyi, V. Novitzka: Modeling synchronization problems: from composed Petri nets to provable linear sequents. *Acta Polytechnica Hungarica*, Vol. 14 (8), pp. 165-182, 2017

[17] G. Behrmann, A. David, K. G. Larsen: A tutorial on Uppaal, *Lecture Notes in Computer Science*, Vol. 3185, pp. 200-236, 2004

[18] R. Alur, D. L. Dill: A theory of timed automata, *Theoretical Computer Science*, Vol. 126 (2), pp. 183-235, 1994

Surveying Archaeological Sites and Architectural Monuments with Aerial Drone Photos

András Molnár

Department of Applied Informatics, John von Neumann Faculty of Informatics, Óbuda University, Bécsi út 96/b, 1034 Budapest, Hungary molnar@uni-obuda.hu

Abstract: Exploring castles, ruins or the tracks of settlements with aerial photographs has long been a well-known process. Drones can make significant progress in this area. The operating cost of a robotic aircraft is at least one order of magnitude lower than that of the cheapest small manned aircraft. It is possible to take high resolution images with them when flying extremely low compared to manned airplanes. The overflight of the area surveyed is far more efficient than with small manned aircraft, as thanks to the extremely small turning radius of drones, 90-95% of flight time is utilized, while this value in the case of small aircraft is 50-60, or possibly 70%. Of course, these benefits will primarily apply when exploring small areas (about 10-20 km^2). In the case of surveying large areas, other benefits of manned aircraft (such as load bearing capacity, flight time) come to the forefront against the limited capabilities of drones.

Keywords: **:** *drone; 3D surface model; photogrammetry; orthophoto*

1 Introduction

Due to the fact that those area sizes that can be effectively applied with drones generally dominate in archaeological explorations, their use allows for cost-effective aerial survey [1]. The small and lightweight robotic aircraft can not only be made at low cost, but their operation is also cheap. Another significant advantage is the small weight (up to 2-4 kg take-off mass) in case of possible accidents. The lightweight flying structure will not cause significant harm to either humans or to the object being surveyed. Due to the low costs, the replacement of the device is not burdensome either.

Based on experience in surveying, photographing a specific area (1-2 km^2) can be accomplished with about 15-20 minutes of flight. The heights of the flights are determined by the resolution of the camera used, the frequency of image capture, the angle of view and cruising speed of the used robotic aircraft. For instance, using a Canon s100 compact camera and a robotic aircraft with 60-70 km/h cruising speed, an orthophoto of 3-3.5 cm/pixel resolution can be made from a flight altitude of 150 m [2].

In many cases, traces of buildings that are now completely destroyed can still be detected on aerial photographs. In the case of areas under cultivation, during the shooting of the fresh plowing, the traces of the former walls of buildings appear in high contrast. The discoloration of the ground and its outlines are a good reference to the layout of the former building. As geo-referenced orthophotos are made during the surveying, the outlines are measurable and can be adapted to maps. The actual location of the onetime building can be specified when fitting to the map and the interpretation of the former descriptions can also be checked.

The method of processing the images (photogrammetry) also ensures the definition of the spatial location of individual pixels. Consequently, not only flat photographs, but also 3D models can be produced without the use of additional sensors. The resolution of the 3D models in the plane is the same as the resolution of the orthophotos and the depth is 3-4 cm/pixel. Spatial information can be used to perform a number of further refinements in relation to the found monuments. Examples include surface models that have been cross-checked with written records, which can be used to infer the erosion effects of the past period. On the basis of the erosion-modified surface, it is possible to determine the exploration areas more precisely. Based on the model, the amount of soil to be removed from the given exploration area can also be defined, which makes it possible to plan the costs of earthwork preparing the exploration.

More accurate and more detailed survey of the remaining buildings or ruins can be done using multi-rotor robotic aircrafts. 3D mapping and archiving of building remnants protruding from the surface can also be done by the method of taking and processing aerial photographs. Since in this case, often very close photographs are needed (2-3 m distance from the object), a helicopter-type carrier is required. The advantage of multi-rotor robotic aircraft against helicopters is their much simpler mechanical construction. Since spinning rotors have a fixed angle of incidence, the complex rotor mechanization essential for helicopter control is lagging behind. The stability and reliability of multi-rotor robotic aircraft equipped with modern control units is satisfactory enough to fly around and photograph the given objects from a sufficient proximity.

Although the flight performance of multi-rotor robotic aircraft is limited (useful weight is heavily limited and flight time is short compared to fixed-wing robotic aircraft), in the case of photographing buildings, the floating capability and the requirement for 1-2 m^2 free landing area means an ideal carrier. The most important output when processing a plethora of overlapping photographs of a building or a ruin is a textured 3D model. This model is also suitable for accurate measurements after calibration. Further use of the textured 3D model is to archive the exact state [3] of the surveyed architectural monument.

Overall it can be stated and practical experience also shows that small robotic aircraft can provide useful additional data in a significant proportion of archaeological explorations [4]. It can also be considered that not only are they cost-effective in the assessment and archiving buildings or remnants of buildings, but they also provide new opportunities in terms of quality. Due to the rapid advances in technology and in particular robotic aircrafts, tools are expected to appear in the near future that are smaller, less susceptible to damage, require less specified knowledge and cheaper. This development will make robotic aircraft one of the basic tools for work in many areas of life, including archaeological excavations.

2 Photogrammetric Basics

Photogrammetry is almost as old as photography. Albrecht Meydenbauer [5, 6] young architect was its first documented user and the creator of its name. Simplified, with the help of the method in two or more images taken of the same object (area) but from a different perspective, different mappings of the same pixels (parallax) can, if certain conditions are met, determine the spatial position of the original object in a predefined coordinate system. The collinearity equations (1,2) and the rotation matrix (3) provide the relationship between a pixel in the image and its real spatial coordinate [7, 8]

$$X' = -C\frac{r_{11}(X-X_0)+r_{21}(Y-Y_0)+r_{31}(Z-Z_0)}{r_{13}(X-X_0)+r_{23}(Y-Y_0)+r_{33}(Z-Z_0)} \quad (1)$$

$$Y' = -C\frac{r_{12}(X-X_0)+r_{22}(Y-Y_0)+r_{32}(Z-Z_0)}{r_{13}(X-X_0)+r_{23}(Y-Y_0)+r_{33}(Z-Z_0)} \quad (2)$$

where:

(X, Y, Z)	field coordinates for the fixed spatial coordinate system,
(X_0, Y_0, Z_0)	„0” coordinates of the projection point in the same fixed spatial coordinate system,
(r_{ij})	corresponding elements of the indexes of the rotation matrix (3),
(X’, Y’)	the coordinates of the point mapped to the image, interpreted in the coordinate system of the picture plane of the point,
(C)	the camera constant.

$$R_{(\omega\varphi\tau)} = \begin{bmatrix} r_{11} & r_{12} & r_{13} \\ r_{21} & r_{22} & r_{23} \\ r_{31} & r_{32} & r_{33} \end{bmatrix} =$$

$$\begin{bmatrix} \cos(\omega)\cos(\tau) & \cos(\omega)\sin(\tau) + \sin(\omega)\sin(\varphi)\cos(\tau) & \sin(\omega)\sin(\tau) - \cos(\omega)\sin(\varphi)\cos(\tau) \\ -\cos(\varphi)\cos(\tau) & \cos(\omega)\cos(\tau) - \sin(\omega)\sin(\varphi)\sin(\tau) & \sin(\omega)\cos(\tau) + \cos(\omega)\sin(\varphi)\sin(\tau) \\ \sin(\varphi) & -\sin(\omega)\cos(\varphi) & \cos(\omega)\cos(\varphi) \end{bmatrix} \quad (3)$$

With the help of the above equation, if we make an evaluation on only one image, the determination of the „*Z*” coordinates of the field points is possible only with additional data. One is for example the digital terrain model. Figure 1 helps to interpret the meaning of symbols in the connections of the collinearity equations (1,2) and the rotation matrix (3).

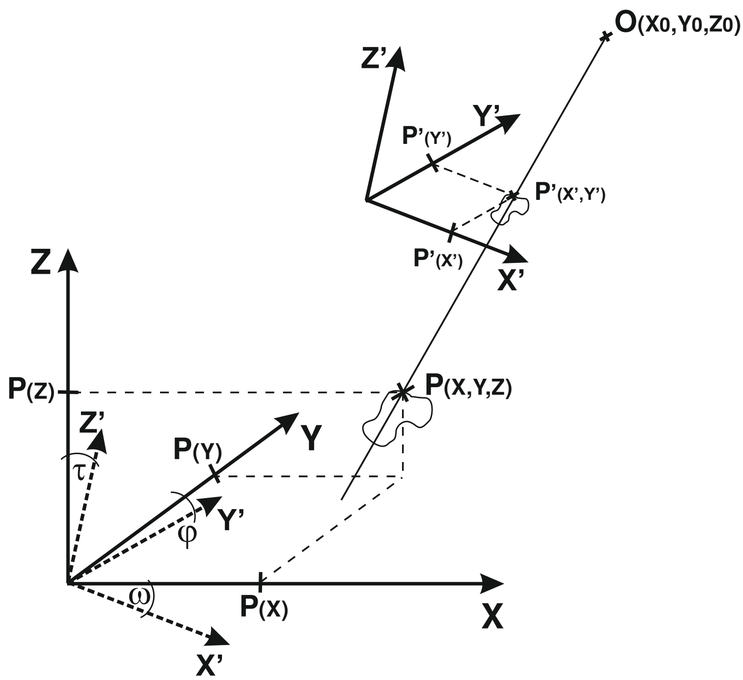

Figure 1

An illustration of the central projection

During the analysis of multiple overlapping images, the intersected projection rays of the same field points edited with different images provide the elevation coordinates of each field point.

Although the projection rays passing through the pixels of overlapping images of the same field points necessarily need to intersect at one point, in practice, due to miscalculations, this is not the case. In order to determine the intersection point close to the real intersection point, further procedure is required. The aim of the beam compensation is to „tune" the equations of those projection rays that are known to be intersected at one point with different methods. Tuning means a slight change in the parameters of the equations so that the intersections are as close as possible to each other. Mathematically, this means the method of least squares in which each parameter is estimated by minimizing the calculation error. For example, in the case of two points (points found on two images, mapping the same field point) we are looking for the solution of the following equation system (4). The process is relatively time-consuming due to the high number of point pairs, however, it can be well paralleled!

$$\left\{\begin{aligned} X^{a'} &= -C\frac{r_{11}^{a}(X-X_0^a)+r_{21}^{a}(Y-Y_0^a)+r_{31}^{a}(Z-Z_0^a)}{r_{13}^{a}(X-X_0^a)+r_{23}^{a}(Y-Y_0^a)+r_{33}^{a}(Z-Z_0^a)} \\ X^{b'} &= -C\frac{r_{11}^{b}(X-X_0^b)+r_{21}^{b}(Y-Y_0^b)+r_{31}^{b}(Z-Z_0^b)}{r_{13}^{b}(X-X_0^b)+r_{23}^{b}(Y-Y_0^b)+r_{33}^{b}(Z-Z_0^b)} \\ Y^{a'} &= -C\frac{r_{12}^{a}(X-X_0^a)+r_{22}^{a}(Y-Y_0^a)+r_{32}^{a}(Z-Z_0^a)}{r_{13}^{a}(X-X_0^a)+r_{23}^{a}(Y-Y_0^a)+r_{33}^{a}(Z-Z_0^a)} \\ Y^{b'} &= -C\frac{r_{12}^{b}(X-X_0^b)+r_{22}^{b}(Y-Y_0^b)+r_{32}^{b}(Z-Z_0^b)}{r_{13}^{b}(X-X_0^b)+r_{23}^{b}(Y-Y_0^b)+r_{33}^{b}(Z-Z_0^b)} \end{aligned}\right\} \tag{4}$$

Where:

top indexes „a" and „b" mean the values interpreted in the local coordinate system of the two images (images „a" and „b").

3 Automatic Search of Matching Point Pairs

The multi-image photogrammetric method assumes that we have the mapping points of the same field point in case of two or more images, that is, the image coordinates defined in the local coordinates of the coherent points.

Many methods are known for identifying coherent pixels on images of the same objects. Such methods include SIFT (Scaleinvariant Feature Transform) [9] and SURF (Speeded Up Robust Features) [10]. There are still many false results between the point pairs determined this way. These should be removed using additional filters. Such a frequently used filter is RANSAC (Random Sample Consensus) [11].

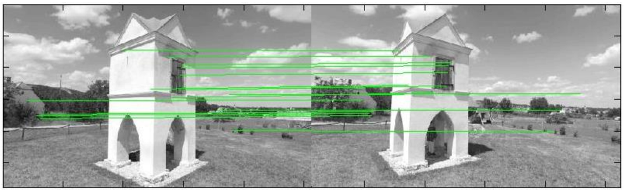

Figure 2
The result of the Matlab program searching for identical point pairs on two images of the Csákvár Powder Tower [12]

The point pairs shown in Figure 2 (the two ends of colored sections mark the point pairs on the image) were calculated by the downloadable Matlab program published by David Lowe [13]. The program uses the SIFT method. Modifying various parameters can be used to illustrate the effectiveness of the method and the appearance of faulty point pairs during the increase of the point pairs.

Finding the correct point pairs and effectively removing faulty point pairs is crucial for creating both the orthophoto and the 3D model.

4 The Schematic Process of Creating the Orthophoto and 3D Model

From the aerial images to the appearance of measurable data, image processing goes through many of the subprocesses discussed previously. The analysis of the data is back-to-back and the result of each partial analysis influences the reliability of the end result. The processing is the following:

- taking overlapping aerial photographs
- searching for characteristic points on the images, defining point pairs, eliminating faulty point pairs
- creating point clouds with multi-image photogrammetry
- refinement of the point cloud (beam compensation)
- surface model creation based on the point cloud
- texturing the surface model
- transformation according to the projection system, georeferencing
- generation of output files (orthophoto, 3D model)

Georeferencing does not necessarily follow the process described above. If the recording device connects metadata to the images and contains the coordinate of the image, then the processing software can use this data. In this case, the coordinate system of the real world is created during processing, based on the coordinates read from the images, so that the point cloud can be inserted into the map created according to the projection system of the coordinates. This method does not provide sufficient accuracy for the orthophotos and 3D models used as the basis for cartographic and other measurements, thus, actual georeferencing (projection transformation based on reference points with accurately defined coordinates) cannot be omitted.

5 Practical Surveys of Ruined Architectural Monuments

5.1 Church Ruins from the Árpád-Era in the Area of Tök

In Hungary, near the village of Tök, there is a church ruin from the Árpád-era. This ruin now has barely any parts above the surface. There are references to the church in historical documents, but unfortunately, only markings of the former shrine can be found on maps (Figure 3). These references and map markings are not suitable for the exact reconstruction of the former church.

Figure 3

Church ruin on a chamber map from the end of the 18th Century [14]

Today, the freely available satellite images provide a much more accurate picture of the position and condition of the ruin, however, these images are not detailed enough (Figure 4). Although the satellite image already shows the floor plan and the display program also provides measurement options, due to inadequate resolution and in many cases significant distortions, measurements can only be made with a very high error rate.

Figure 4
The satellite image of the ruin in Tök from the Google Earth program from different publishing periods

The ruin in Tök was photographed with a DJI multi-rotor device (Inspire 1). The shooting took 15 minutes of flight time, during which 116 12-megapixel photos were taken. These images were processed using „Agisoft PhotoScan Professional" program. The file created by the program is the orthophoto of the area on the one hand and the 3D model of the photographed area on the other (Figure 5).

Figure 5
The orthophoto of the ruin in Tök (left) and the 3D model of the ruin

The basis for the measurements is the created orthophoto. After proper calibration, the orthophoto can either be printed or displayed by electronic devices to determine the dimensions of the formations on it. In this case, the floor plan of the church is clearly visible and measurable on the finished orthophoto (Figure 6). Thanks to the resolution of the image, the thickness of the walls of the building can clearly be seen and measured.

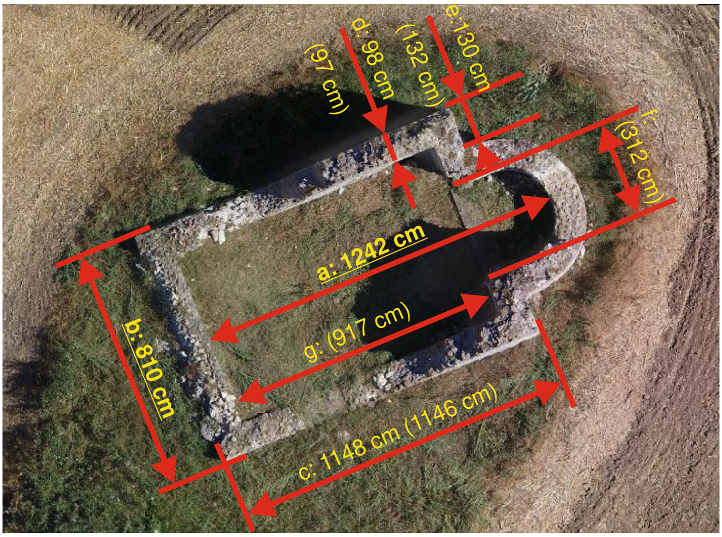

Figure 6

The orthophoto of the ruin in Tök with measured and calculated dimensions

The calibration bases of the orthophoto of the ruin are shown in Figure 6 as bold, underlined values. The base of the sections that can be measured along the length of the church is the section „a", the base of the sections parallel to its perpendicular width is section „b". These values were determined by on-site, manual measurements and were used to calculate the values in brackets. In some places there are two values (one in brackets and one unmarked). Values without brackets are the results of manual measurements on-site that are used to check the calibration.

Table 1

Table of calibration and control measurements of the ruin in Tök

section marking	section length on the photo [unit]	measured length of the section [cm]	calculated length of the section [cm]	error [%]
a	**103,00**	**1242**	**-**	**0**
b	**68,46**	**810**	**-**	**0**
c	95,05	1148	1146	0,16
d	8,20	98	97	1,03
e	11,14	130	132	1,54
f	26,34	-	312	-
g	76,07	-	917	-

Table 1 shows that the error in the direction of the width of the church is one order of magnitude greater than along its length. This is due to the uncertainty of manual measurements. The walls of the church were built of hand-carved natural stones.

The walls are not plastered, so the stones of varying sizes produce significant projections and recesses in the plane of the walls. In case of shorter sections, these unevennesses have a greater impact on the accuracy of the measurements in terms of proportions. The same unevennesses result in smaller error in case of long sections. This problem is well illustrated by the measurements of the thickness of the walls, during which we got 93 cm; 95 cm; 97 cm; 98 cm values. Based on the plethora of measurements, 98 cm proved to be the value closest to reality. Considering that the longest section along the width of the church was 810 cm, we chose this as the base. At the same time, the section parallel to the width base were significantly shorter, so the above mentioned measurement uncertainty influenced these values by a higher percentage.

5.2 Roman Fortress in the Area of Iža

The remains of the former Roman fortress are located on the left bank of the Danube in the present-day Slovakia. Kelemantia is part of the Limes Romanus fortification system. Throughout history, it was rebuilt and expanded several times, and was eventually abandoned after the fall of the Roman Empire. The exploration works of the fortress are still ongoing today.

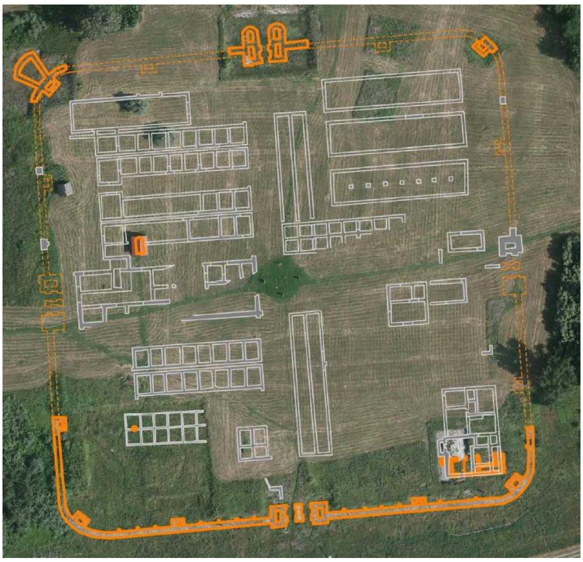

Figure 7

Remains of the „Kelemantia" Roman fortress on orthophoto and the floor plans determined based on the results of the excavations [15]

The remains of the excavated and exposed perimeter walls of the former fortress, the bastions and gates and the remnants of some inner buildings are visible on the aerial photos.

The area size and surrounding vegetation makes surveying with drone possible. One of the advantages of this is that there is no going-over on foot during the aerial photography, which could potentially damage the explored areas. Another great advantage is the cost-effectiveness of drone shooting compared to the traditional manned aircraft surveying. The surveying was done with the Inspire 1 multicopter, which was equipped with the original X3 camera of DJI. A total of 526 images were taken during the flights from a height of 15 meters. 497 of these images were processed. The images were converted to orthophotos using the „Agisoft PhotoScan Professional" software. The orthophoto field resolution is 1,08 cm/pixel.

Thanks to the high field resolution, the walls of the buildings are clearly visible. Their thickness can also be measured. Similarly to real field work, distance measurements can be performed along the inner and outer edges of the wall.

The exposed remains on the orthophoto can be extended by lines and the wall sections associated with one object can be linked. Using the written documents, the probable floor plan of the fortress can be drawn which helps plan the exploration. In the case of the Iža fortress, for example, its structure is known from descriptions, so the positions of the gates and the towers protecting the gates can be determined with great accuracy along the wall of the fortress. The floor plan of the fortress and the outlines of the assumed buildings in the fortress were drawn on the orthophoto of the Iža fortress, as shown on Figure 7. The thick orange drawings depict the remains on the surface, while the thin orange lines represent the wall sections covered by soil. The white contours depict the floor plans of the assumed buildings.

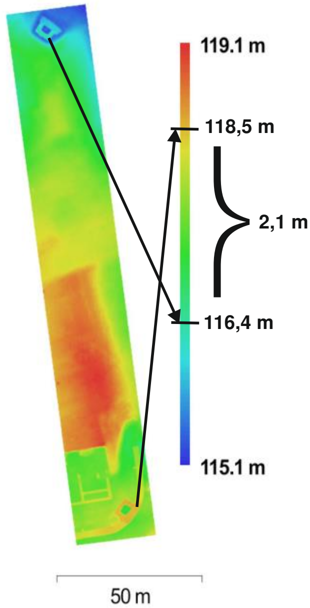

Figure 8
Coloring according to height on the orthophoto of the remains of „Kelemantia" Roman fortress (west side of the fortress)

Contours drawn on the calibrated orthophoto can help in the planning of the exploration works. The exact location of the planned exploration can be accurately measured and determined with GPS coordinates on the calibrated and georeferenced orthophoto. Using the GPS coordinates determined this way, the location of the works can be measured accurately on the field so that excavation can be made more effectively. The orthophoto with drawings also illustrates the progress of the excavation as shown in Figure 7.

During the photogrammetric procedure, not only flat images, but also the full three-dimensional terrain model is produced. As part of the terrain model, buildings or their ruins of the surveyed area are available, height measurements can also be made on the model of the area. Figure 8 illustrates the area of the western wall section of Kelemantia with gradients. Based on the range of colors shown in the picture, the height above sea level of each pixel in the area can be determined. It should be noted that during the processing, the resolution of the orthophoto (plane resolution) is better than the height resolution. The basic data of the survey and the accuracy data of the reconstructed image during the surveying of the Kelemantia fortress are shown in Table 2.

In case of the terrain model with calibrated height data, the volume of the soil moved in the excavated area can be calculated well. Based on these, the area required for deposing the moved soil can be accurately estimated and its location can be planned. Likewise, the transportation of the moved soil and its cost can also be planned. Knowing the height of the already excavated parts, the knowledge of the terrain model can help to estimate the amount of soil above the unexplored areas, so the time needed for the planned excavation can be estimated better.

Table 2
Main data of the Kelemantia survey

Height from recording start point:	29 m
Number of images:	497 pcs
Size of images:	4000 x 2250 pixels
Surveyed area:	4000 m^2
Orthophoto field resolution:	1,08 cm/pixel
Height resolution of the 3D model:	4,31 cm/pixel

The 3D model of the exploration area is useful for both documenting the progress of the exploration work and documenting the original location and position of the monuments found. Comparing the terrain models made periodically allows to track the changes in the area, determine the location and extent of possible malicious damage and detect erosion changes caused by environmental effects.

Figure 9 illustrates the detailedness of the orthophoto created during surveying. The magnified well highlighted by the red circle on the right side of the figure is located at the place indicated by the arrow starting from the circle. The enlarged detail was made directly with the magnification of the orthophoto. Any part of the orthophoto can also be enlarged in a similar way. This magnification capability demonstrates the detailedness of the orthophoto of the area.

Similarly to the magnification capability, the 3D view of a portion of the surveyed area, in a circle similar to the previous red circle, but bigger, can be seen in the middle of Figure 9. As a 3D terrain model was made of the entire surveyed area, any of the details or the entire area can be observed on the 3D model. With the help of a suitable program, the excavated wall sections, remnants of buildings or other landmarks can be virtually explored and viewed from any angle.

In the area marked with a red oval contour at the top of Figure 9, soil was removed during excavation work. The determination of the quantity of this soil is also feasible on the processed data.

Figure 9
High resolution orthophoto and 3D model created from the processed data of „Kelemantia" Roman fortress

By marking the boundaries of the exploration area, the recess can be covered with a hypothetical flat surface. After the cover, a closed area is formed, the volume of which can be easily determined. Figure 10 illustrates the covered area surveyed. The surface model contained the height data based on grid points of 10 cm x 10 cm. The amount of soil removed from the recess is 1200 m^3 .± 3%. Of course, the volume calculation was made with the assumption that the original surface of the examined area was nearly flat. Precise measurements require a pre-earthwork survey that provides a reference surface for subsequent measurements.

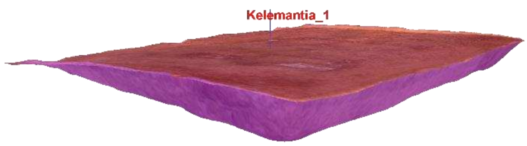

Figure 10
Analysis of the amount of removed soil during the exploration of the northern entrance of „Kelemantia" Roman fortress

Conclusion

Based on the measurements made and the experience of the evaluation results, information from aerial photography made with robotic aircraft can be utilized well. The great advantage of this method is that the area under exploration does not have to be affected at all during the survey, so neither the area, nor the archaeological finds discovered are damaged accidentally. The surveying costs are low; thus, it can be repeated at any time. Repeated measurement data is suitable for periodic documentation of the exploration and archiving field changes caused by the exploration work. Of course, the method does not replace the traditional finding archiving procedures, but effectively complements them.

Acknowledgement

This work was supported by the National Fund for Research, Development and Innovation (ED_18-1-2018-0014).

References

[1] Bakó Gábor, UAV és RPAS technológia a légi távérzékelésben (UAS és RPAS technológia légi fotogrammetriai alkalmazása. Felhasznál ási lehetőségek, elérhető típusok és szoftverek, előnyök és kockázatok, jogi környezet.), Készült a Magyar Földtani és Geofizikai Intézet megbízásából ISBN 978-963-671-300-3 (2015)

[2] Molnár A., Stojcsics D., Lovas I., Csemez L., „Damage assessment, damage control and monitoring by UAV in agriculture", In: Proceedings of the 11th International Conference on Fluid Mechanics (FLUIDS '15), ISBN:978-1-61804-358-0

[3] Szenthe Gergely – Mozgai Viktória – Horváth Eszter – Bajnóczi Bernadett, Hun kori áldozati leletegyüttes Telki határából, MAGYAR RÉGÉSZET ONLINE MAGAZIN, 2019 Tavasz

[4] V. Yordanov, A. Mostafavi, M. Scaioni, DISTANCE-TRAINING FOR IMAGE-BASED 3D MODELLING OF ARCHEOLOGICAL SITES IN REMOTE REGIONS in: The International Archives of the Photogrammetry, Remote Sensing and Spatial Information Sciences, Volume XLII-2/W11, 2019, DOI: 10.5194/isprs-archives-XLII-2-W11-1165-2019

[5] Jörg Albertz: Albrecht Meydenbauer – Pioneer of Photogrammetric Documentation of the Cultural Heritage. Proceedings 18th International Symposium CIPA 2001, pp. 19-25

[6] Grimm, A. (1980): Der Ursprung des Wortes Photogrammetrie. In: Ackermann, F. et al. (1980): Internationales Archiv für Photogrammetrie. Vol. XXIII, Teil B10, Komm. V, VI, VII Nachtrag, Hamburg 1980, pp. 323-330

[7] Somogyi József Árpád, Lézerszkennelt pontfelhők illesztésének optimalizálása, mérnöki feladatok megoldásainak hatékony támogatása pontfelhő alapú eljárásokkal, PhD értekezés 2017

[8] K. Kraus és P. Waldhäusl, Fotogrammetria. Budapest: Tertia, 1998, o.379

[9] D. G. Lowe, „Object recognition from local scale-invariant features", Proceedings of the Seventh IEEE International Conference on Computer Vision, köt. 2, sz. 8, o. 1150-1157, 1999

[10] H. Bay, A. Ess, T. Tuytelaars, és L. Van Gool, „Speeded-Up Robust Features (SURF)”, Computer Vision and Image Understanding, köt. 110, sz. 3, o. 346–359, 2008

[11] M. A. Fischler és R. C. Bolles, „Random sample consensus: a paradigm for model fitting with applications to image analysis and automated cartography”, Communications of the ACM, köt. 24, sz. 6, o. 381-395, 1981

[12] David G. Lowe, "Distinctive image features from scale-invariant keypoints," *International Journal of Computer Vision,* 60, 2 (2004), pp. 91-110

[13] https://www.cs.ubc.ca/~lowe/keypoints/ (2018)

[14] Kneidinger, Andreas, Original map of the Hungarian National Archives: S 11 No 0040/a:1

[15] Hubica Pinčíková, Magdaléna Janovská, Anna Tuhárska, FRONTIERS OF THE ROMAN EMPIRE THE DANUBE LIMES IN SLOVAKIA, Pamiatkový úrad Slovenskej republiky Bratislava 2018 ISBN 978-80-89175-81-9

LPV design for the control of heterogeneous traffic flow with autonomous vehicles

Balázs Németh and Péter Gáspár

Systems and Control Laboratory, Institute for Computer Science and Control, Hungarian Academy of Sciences, Kende u. 13-17, H-1111 Budapest, Hungary
E-mail: [balazs.nemeth;peter.gaspar]@sztaki.mta.hu

Abstract: The paper proposes a strategy to control heterogeneous traffic flow which contains both autonomous and human-driven vehicles. The purpose of the control strategy is to consider differences in the longitudinal driving characteristics of autonomous and human-driven vehicles. In the paper the modeling of the heterogeneous traffic flow based on the results of the VISSIM traffic simulator is presented. The traffic model yielded is in a Linear Parameter-Varying (LPV) form. The control design is based on the Takagi-Sugeno methodology, in which the performances, the constraints of the ramp-controlled interventions and the uncertainties are incorporated. The design task leads to an optimization with Linear Matrix Inequality (LMI) constraints. The result of the method is the optimal intervention of the freeway ramps with which traffic inflow can be controlled.

Keywords: Takagi-Sugeno LPV design, traffic control, autonomous vehicles

1 Introduction and motivation

The growing importance of autonomous functionality in vehicle control systems poses novel challenges in the research of intelligent transportation systems. One of these problems is the modeling and control of heterogeneous traffic flow, which is based on the difference between the speed profiles of conventional human-driven vehicles and autonomous vehicles. The autonomous vehicles can have more information about the forthcoming environments, e.g. road slopes and traffic signs [1], with which their current speed profile is modified. Thus, in heterogeneous traffic the participant vehicles have different motions, which makes traffic modeling and the control problem more complex.

Most of the novel traffic control design methods are based on the state-space representation of traffic flow dynamics. It is incorporated in several relationships [2], e.g. the conservation of vehicles, the equilibrium speed equation, the fundamental equation and the momentum equation. Although it can provide an enhanced description of traffic dynamics, due to the uncertainties, the estimation of model parameters may be difficult. For example, [3] proposed an identification method for traffic model parameters, especially the fundamental diagram, which has an important role in traffic control design. In a mixed traffic scenario the identification problem can be more difficult because the deviation of the measured data is more significant due to the varying speed profiles of the vehicles. The most important modeling approach for mixed traffic was summarized in the survey of [4]. The analysis of the traffic flow in which semi-autonomous and autonomous vehicles were traveling together with conventional vehicles was proposed by [5, 6]. A control law which considers the different speed profiles of the semi-autonomous vehicles was proposed by [7, 8].

In this paper a robust control design based on the Linear Parameter-Varying (LPV) method is presented [9, 10], with which the inflow ramps of the freeway in a heterogeneous traffic flow can be controlled. The proposed method can be used for the control of heterogeneous traffic flow which contains vehicles with the autonomous driving levels from 2 to 5. It means that the acceleration/deceleration functionalities of the controlled vehicles are automated. The control design is based on a control-oriented LPV system, which contains disturbances. The model is based on the simulation results of the high-fidelity VISSIM traffic simulator [11, 12]. In the method the maximization of the traffic flow is formed as an optimal control problem with Linear Matrix Inequality (LMI) constraints [13, 14], by which disturbance rejection and stability are guaranteed. The advantage of the control design based on the proposed Takagi-Sugeno LPV method is that it is able to consider several properties of the control problem, e.g. uncertainties, parameter-variation and constraints. The method is able to guarantee robustness against the uncertainty of the traffic flow model and the constraints on the physical properties on the controlled ramp can be incorporated in the control task.

The paper is organized as follows. Section 2 proposes a novel control-oriented model of the heterogeneous freeway traffic flow in an LPV form. The control design in presented in Section 3, in which the input constraints, the performances, the parameter-varying property and the disturbances are considered. Finally, the method is presented through a simulation example in Section 4 and the paper is concluded, see Section 5.

2 Modeling of heterogeneous traffic flow dynamics

Traffic dynamics represents the traffic network, which is gridded into N number of segments. The traffic flow of each segment is represented by a dynamical equation, which is based on the law of conservation. The relationship contains the sum of inflows and outflows for a given segment i. Thus, traffic density ρ_i $[veh/km]$ is expressed in the form

$$\rho_i(k+1) = \rho_i(k) + \frac{T}{L_i}\left[q_{i-1}(k) - q_i(k) + r_i(k) - s_i(k)\right], \quad (1)$$

where k denotes the index of the discrete time step, T is the discrete sample time, L_i is the length of the segment, q_i $[veh/h]$ and q_{i-1} $[veh/h]$ denote the inflow of the traffic in segments i and $i-1$, r_i $[veh/h]$ is the sum of the controlled ramp inflow, while s_i $[veh/h]$ is the sum of the ramp outflow. The model of the traffic system is illustrated in Figure 1.

Another important relation of the traffic dynamics is the fundamental relationship, which creates a connection between the outflow $q_i(k)$, the traffic density $\rho_i(k)$ and the average traffic speed $v_i(k)$, see e.g., [15]. The fundamental relationship is formed as

$$q_i(k) = \rho_i(k) v_i(k). \quad (2)$$

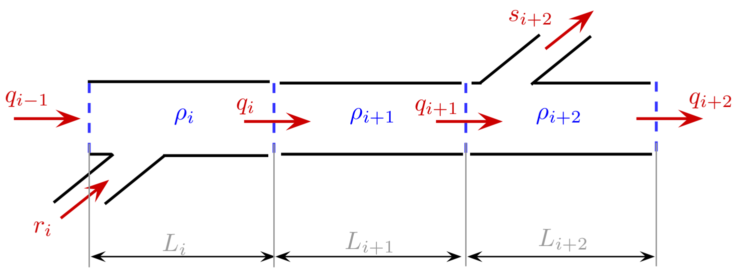

Figure 1: Illustration of the traffic system model

The average traffic speed $v_i(k)$ can be formed in the traffic flow modeling studies as a nonlinear function of traffic density [16], which results in the relationship

$$q_i(k) = \mathcal{F}(\rho_i(k)), \tag{3}$$

where $\mathcal{F}$ is a nonlinear function. Its reason for that is the increase in traffic density leads to the reduction of the distance between the vehicles on the road section. Due to the reduced distance the speed of the vehicles must also be reduced to avoid the risk of collision. Thus, the average traffic speed is also reduced due to the reduced speeds of the individual vehicles. The characteristics of $v_i(k)$ depending on $\rho_i(k)$ are decreasing and nonlinear, causing $\mathcal{F}(\rho_i(k))$ to have nonlinear characteristics as well.

Conventionally, the fundamental relationship is derived from historic measurements, and it also depends on several factors, see [2, 17]. Therefore, the analysis on the mixed traffic flow requires several experiments with various rates of autonomous vehicles κ. Figure 2 shows an example of the result of the analysis, which is performed through the VISSIM traffic simulator. It can be seen that the increase in $\kappa(k)$ has the following effects on the linear section ($\rho_i(k) \in [0; \rho_{i,crit}]$) of the fundamental characteristics, where $\rho_{i,crit}$ is the density value at the maximum of $q_i(k)$.

- Through the increase in $\kappa(k)$ the mean value of the traffic flow characteristics decreases. The decrease has a progressive tendency.
- Similarly, the increase in $\kappa(k)$ leads to the increase in the density in the set of traffic flow values. The increase in density is also nonlinear.

The experiments of the simulations on the linear section of the fundamental diagram are formulated in the following relationship

$$\begin{aligned} q_i(k) &= \big(\alpha_0 - f_\beta(\kappa(k))\big)\rho_i(k) + f_\gamma(\kappa(k))\rho_i\Delta_i \\ &= (\alpha_0 - (\beta_2\kappa^2(k) + \beta_1\kappa(k)))\rho_i(k) + \\ &+ (\gamma_3\kappa^3(k) + \gamma_2\kappa^2(k) + \gamma_1\kappa(k) + \gamma_0)\rho_i\Delta_i, \end{aligned} \tag{4}$$

where f_β, f_γ are $\kappa(k)$-dependent polynomial functions of the model with the parameters $\alpha_0, \beta_2, \beta_1$ and $\gamma_3, \gamma_2, \gamma_1, \gamma_0$. $\Delta_i \in [-1; 1]$ represents the uncertainty in the system, which results in the density in the flow characteristics.

The traffic flow model of a freeway section i is formed through the law of conservation

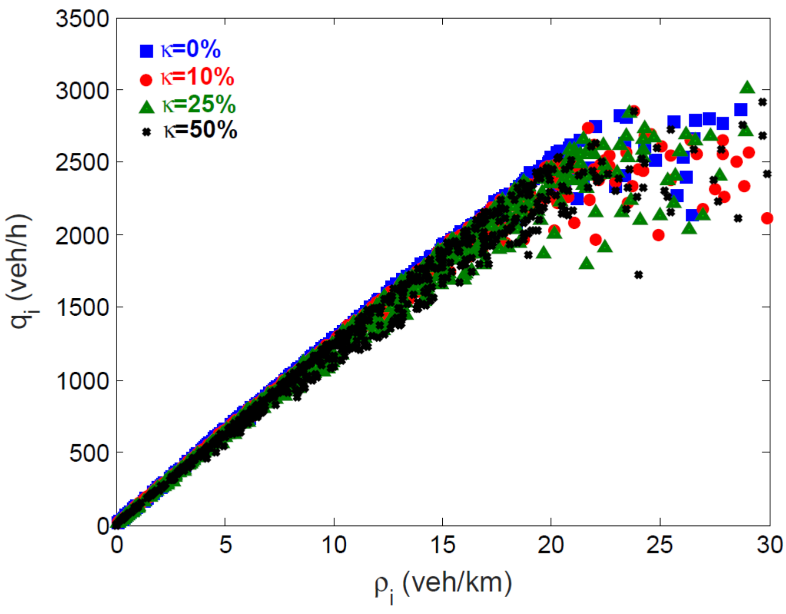

Figure 2: Charactersitics of the fundamental diagram

(1) and the proposed form of the fundamental relationship (4)

$$\rho_i(k+1) = \rho_i(k) + \frac{T}{L_i}\Big[q_{i-1}(k) + r_i(k) - s_i(k) - \\ - \big((\alpha_0 - f_\beta(\kappa(k)))\rho_i(k) + f_\gamma(\kappa(k))\rho_i\Delta_i\big)\Big] \tag{5}$$

The equation can be transformed into a state-space representation as

$$x(k+1) = A(\kappa)x(k) + B_1 w(k) + B_2 u(k), \tag{6}$$

where $x(k) = \rho_i(k)$ is the state of the system, $u(k) = r_i(k)$ is the control input and $w(k) = \begin{bmatrix} q_{i-1}(k) & s_i(k) & \Delta_i(k)\end{bmatrix}^T$ is the disturbance vector. The matrix of the system is represented by A, and simultaneously B_1 is the matrix of the disturbances and B_2 is the matrix of the control input, such as

$$A(\kappa) = \left(1 - \frac{T}{L_i}\left[\alpha_0 - f_\beta(\kappa(k))\right]\right), \tag{7a}$$

$$B_1 = \begin{bmatrix} \frac{T}{L_i} & -\frac{T}{L_i} & -\frac{T}{L_i} f_\gamma(\kappa(k))\rho_i \end{bmatrix}, \tag{7b}$$

$$B_2 = \begin{bmatrix} \frac{T}{L_i} \end{bmatrix}. \tag{7c}$$

3 Design of LPV control for the traffic flow

The purpose of this section is to find a control method by which the controlled inflow of the freeway ramp $r_i(k)$ is set, while the control input is limited and the impact of disturbances must be eliminated. Moreover, a challenge in the control design is that the dynamics of the traffic is modeled in an LPV form, see (6).

The aim of the control is to guarantee the maximum outflow $q_i(k)$ of the traffic network. However, the outflow can be improved by increasing $\rho_i(k)$ until reaching the critical density $\rho_{i,crit}$. Since $q_i(k)$ has a maximum at $\rho_{i,crit}$ [18], it must be guaranteed through the coordination of the system inputs:

$$z_1 = \rho_{i,crit} - \rho_i(k), \qquad |z_1| \to min, \tag{8}$$

Although at a low number of inflow vehicles $\rho_{i,crit}$ cannot be achieved, but increasing $\rho_i(k)$ through z_1 results in the maximization of $q_i(k)$. The value of critical density is selected through the previous analysis of the traffic network.

The design of the control requires several steps to find an appropriate controller on the existing complex problem. Thus, the following steps must be performed in the method.

1. The constraint on the control input is considered in the design method.
2. The traffic model through the consideration of (8) is reformulated.
3. The LPV system is described in a Takagi-Sugeno form, which leads to a linear control design problem.
4. The control synthesis is formed as an optimization problem, in which the impact of the disturbances on the performance is reduced.

3.1 Consideration of the input constraints

In the traffic system the value of control input $r_i(k)$ must be non-negative. Moreover, the inflow on the ramps can have a maximum capacity due to the physical limits of the road. Thus, it is necessary to design a control strategy, by which the following constraint is handled

$$0 \leq r_i(k) \leq r_{i,max}, \tag{9}$$

where $r_{i,max}$ represents the maximum capacity of the inflow ramps. The criterion is considered as a soft constraint during the control actuation in the following way.

It is necessary to consider that the control intervention has importance at high ρ_i values, which are close to $\rho_{i,crit}$. If ρ_i is significantly smaller than $\rho_{i,crit}$, $r_i = r_{i,max}$ is selected. This intervention is operated in the range of $0 \leq \rho_i(k) \leq \rho_{i,des}$, where $\rho_{i,des} < \rho_{i,crit}$ is a design parameter.

However, if $\rho_i > \rho_{i,des}$, the value of r_i must be reduced to avoid the saturation of the traffic network. In this case the dynamic control must be actuated, whose design is based on the control-oriented traffic model. The model (6) in the range of $\rho_i > \rho_{i,des}$ must be reformulated to eliminate the static density value of $\rho_{i,des}$ in the control design. The model (6) at $x(k+1) = x(k) = \rho_{i,des}$ is formed as

$$\rho_{i,des} = A(\kappa)\rho_{i,des} + B_1 w_{st} + B_2 u_{st}, \tag{10}$$

where w_{st} is considered to be an average disturbance at $\rho_{i,des}$ and u_{st} is the related control input, which is computed as

$$u_{st} = B_2^{-1}\big[(1 - A(\kappa))\rho_{i,des} - B_1 w_{st}\big]. \tag{11}$$

Moreover, the avoidance of the saturation requires a dynamic actuation $u_{dyn}(k)$, which guarantees the performance (8) and reduces the impact of $w_{dyn}(k)$ on the performance. $w_{dyn}(k) > 0$ is considered to be the difference between $w(k)$ and w_{st}. Thus, the control-oriented traffic model (6) for the control design on the range of $\rho_{i,des} \leq \rho_i(k) \leq \rho_{i,crit}$ is reformulated as

$$x_{dyn}(k+1) = A(\kappa)x_{dyn}(k) + B_1 w_{dyn}(k) + B_2 u_{dyn}(k), \tag{12}$$

where $x_{dyn}(k) = x(k) - \rho_{des,i}$. Simultaneously, the overall control actuation is

$$r_i(k) = u(k) = u_{st} + u_{dyn}(k), \tag{13}$$

from which the constraints of $u_{dyn}(k)$ is

$$-u_{st} \leq u_{dyn}(k) \leq r_{i,max} - u_{st}. \tag{14}$$

The main result of the reformulation is that the dynamic control input u_{dyn} can have both positive and negative values, see (14), with which the complexity of the control design can be significantly reduced. However, the overall control input on the traffic system $u(k)$ is always non-negative.

3.2 Performance-driven reformulation of the traffic model

The goal of the control design is to guarantee the defined performance (8). Thus, it is necessary to minimize the difference between the current traffic density and the critical density value. Due to the partition of the system into static and dynamic parts, performance z_1 is modified to

$$e(k) = \rho_{ref} - x_{dyn}(k), \qquad |e(k)| \to min, \tag{15}$$

where $\rho_{ref} = \rho_{i,crit} - \rho_{i,des}$ is a constant value.

The error for $k+1$ is derived as $e(k+1) = \rho_{ref} - x_{dyn}(k+1)$. Using the relationship (12), the dynamics of the error is

$$\begin{aligned} e(k+1) &= \rho_{ref} - A(\kappa)x_{dyn}(k) - B_1 w_{dyn}(k) - B_2 u_{dyn}(k) = \\ &= \rho_{ref} - A(\kappa)(\rho_{ref} - e(k)) - B_1 w_{dyn}(k) - B_2 u_{dyn}(k) = \\ &= A(\kappa)e(k) + (1 - A(\kappa))\rho_{ref} - B_1 w_{dyn}(k) - B_2 u_{dyn}(k). \end{aligned} \tag{16}$$

The controller of the traffic system is considered to be full-state feedback, whose input is $e(k)$. Thus, the control law is $u_{dyn} = Ke(k)$, where K represents the controller. Using the relationship between u_{dyn} and $e(k)$, the error dynamics is formed as

$$e(k+1) = \big(A(\kappa) - B_2 K\big)e(k) + W(k) = A_{cl}(\kappa, K)e(k) + Wd(k), \tag{17}$$

where $Wd(k)$ is an upper-bound approximation of the overall disturbance $(1-A(\kappa))\rho_{ref} - B_1 w_{dyn}(k)$, in which $||d(k)|| \leq 1$ is a noise and W represents its scaling. The formulated system on the tracking error (17) is an LPV system, in which K must be selected to stabilize the system, guarantee the performances and reduce the impact of $d(k)$ on $e(k)$.

3.3 Takagi-Sugeno description of the system

In the following the LPV system (17) is reformulated to the sum of Linear Time Invariant (LTI) systems using the Takagi-Sugeno description, see [10]. The advantage of the method is that the control design becomes simpler due to the linear formulation.

The scheduling variable κ has lower $\overline{\kappa}$ and upper $\underline{\kappa}$ limits. Similarly, the limits determine the lower and upper limits of $A_{cl}(\kappa, K)$, such as $\underline{A_{cl}} = A_{cl}(\underline{\kappa}, K)$ and $\overline{A_{cl}} = A_{cl}(\overline{\kappa}, K)$. Thus, $A_{cl}(\kappa, K)$ can be reformulated as

$$A_{cl}(\kappa, K) = \frac{A_{cl} - \underline{A_{cl}}}{\overline{A_{cl}} - \underline{A_{cl}}}\overline{A_{cl}} + \frac{\overline{A_{cl}} - A_{cl}}{\overline{A_{cl}} - \underline{A_{cl}}}\underline{A_{cl}} = \mu_1 \overline{A_{cl}} + \mu_2 \underline{A_{cl}}, \tag{18}$$

where $0 \leq \mu_1, \mu_2 \leq 1$ are the multipliers of the matrices $\underline{A_{cl}}, \overline{A_{cl}}$. Similarly, the system (17) can be reformulated using (18) as

$$e(k+1) = \mu_1(\overline{A_{cl}}e(k) + Wd(k)) + \mu_2(\underline{A_{cl}}e(k) + Wd(k)), \tag{19}$$

which means that the original LPV system can be reformulated as a sum of two linear systems, which represent the convex hull of the κ-dependent LPV system.

3.4 Synthesis of the optimal control

During the control synthesis it is necessary to guarantee the stability of the system and the improvement of the performances. In addition, the impact of the disturbances on the tracking must be reduced. These criteria are formed in the following way.

- **Stability**: For the stability of the set of LTI systems (19) it is necessary to guarantee that all trajectories of the systems converge to zero as $t \to \infty$ [14]. Thus, it is necessary to guarantee the stability criterion

  $$\Delta V(e(k)) < 0, \tag{20}$$

  where $V(e(k)) > 0$ is the Lyapunov function. $\Delta V(e(k))$ is selected in a quadratic form, such as $V(e(k)) = e(k)^T Pe(k)$, $P > 0$ and P is a symmetric matrix. The stability criterion for the system $\overline{A}_{cl}e(k) + Wd(k)$ is derived as

  $$\begin{aligned} &\Delta V(e(k)) = V(e(k+1)) - V(e(k)) = \\ &= (\overline{A}_{cl}e(k) + Wd(k))^T P(\overline{A}_{cl}e(k) + Wd(k)) - e(k)^T Pe(k) = \\ &= e^T(k)(\overline{A}_{cl}^T P\overline{A}_{cl} - P)e(k) + e^T(k)\overline{A}_{cl}^T PWd(k) + W^T d^T(k)P\overline{A}_{cl}e(k) + \\ &+ W^T d^T(k)PWd(k) = \begin{bmatrix} e(k) \\ d(k) \end{bmatrix}^T \begin{bmatrix} \overline{A}_{cl}^T P\overline{A}_{cl} - P & \overline{A}_{cl}^T PW \\ W^T P^T \overline{A}_{cl} & W^T PW \end{bmatrix} \begin{bmatrix} e(k) \\ d(k) \end{bmatrix} < 0. \end{aligned} \tag{21}$$

  The result of the derivation can be formed as a Linear Matrix Inequality (LMI) condition on system $\overline{A}_{cl}e(k) + Wd(k)$, such as

  $$\begin{bmatrix} \overline{A}_{cl}^T P\overline{A}_{cl} - P & \overline{A}_{cl}^T PW \\ W^T P^T \overline{A}_{cl} & W^T PW \end{bmatrix} \prec 0. \tag{22}$$

Similarly, the LMI condition for system $\underline{A_{cl}}e(k) + Wd(k)$ is

$$\begin{bmatrix} \underline{A}_{cl}^T P \underline{A}_{cl} - P & \underline{A}_{cl}^T PW \\ W^T P^T \underline{A}_{cl} & W^T PW \end{bmatrix} \prec 0. \tag{23}$$

Since $\underline{A}_{cl}, \overline{A}_{cl}$ depend on the controller K, it is necessary to select K and $P > 0$, by which the previous conditions are guaranteed.

- **Performance**: The tracking capability of the system (8) can be improved through the selection of K. Since the control input is defined as $u_{dyn}(k) = Ke(k)$, the tracking can be improved by increasing the gain K.
- **Disturbance**: The reduction of the impact of $d(k)$ on $e(k)$ requires that the $\mathcal{H}_\infty$ norm of the transfer function $T_{d,e}$ from $d(k)$ to $e(k)$ be reduced. In the system $\overline{A}_{cl}e(k) + Wd(k)$ the transfer function is computed as

$$T_{d,e} = \left(zI - \overline{A}_{cl}\right)^{-1} W, \tag{24}$$

where I is an identity matrix. Thus, the condition is

$$||T_{d,e}||_\infty = \left|\left|\left(zI - \overline{A}_{cl}\right)^{-1} W\right|\right|_\infty < \gamma, \tag{25}$$

where $\gamma > 0$ is a predefined upper bound of the norm. If $\gamma < 1$ is selected then the robustness of the system can be guaranteed, see [19]. Similarly, the criterion on the system $\underline{A_{cl}}e(k) + Wd(k)$ is

$$\left|\left|\left(zI - \underline{A}_{cl}\right)^{-1} W\right|\right|_\infty < \gamma. \tag{26}$$

The conditions of (25) and (26) can be composed with the criteria (22) and (23) through the dissipativity of the system, the construction of the supply function and the Schur lemma, see [14]. Thus, the LMI conditions which incorporate the stability and the distrubance rejection criteria are

$$\begin{bmatrix} P & 0 & \underline{A}_{cl}^T P & I \\ 0 & \gamma^2 I & W^T P & 0 \\ P\underline{A}_{cl} & PW & P & 0 \\ I & 0 & 0 & I \end{bmatrix} \succeq 0, \tag{27a}$$

$$\begin{bmatrix} P & 0 & \overline{A}_{cl}^T P & I \\ 0 & \gamma^2 I & W^T P & 0 \\ P\overline{A}_{cl} & PW & P & 0 \\ I & 0 & 0 & I \end{bmatrix} \succeq 0. \tag{27b}$$

During the control synthesis it is necessary to minimize γ, while K is maximized. Therefore, during the optimization $\frac{1}{\gamma}$ in a cost function

$$J = K + \alpha\gamma \tag{28}$$

is maximized, where α is a scaling parameter. Thus, the resulting optimal control problem is

$$\max_{K,\gamma} K + \alpha\gamma \tag{29a}$$

$$\text{subject to} \quad P \succ 0, \tag{29b}$$

where

$$\begin{bmatrix} P & 0 & \underline{A}_{cl}^T P & I \\ 0 & \gamma^2 I & W^T P & 0 \\ P\underline{A}_{cl} & PW & P & 0 \\ I & 0 & 0 & I \end{bmatrix} \succeq 0, \tag{30a}$$

$$\begin{bmatrix} P & 0 & \overline{A}_{cl}^T P & I \\ 0 & \gamma^2 I & W^T P & 0 \\ P\overline{A}_{cl} & PW & P & 0 \\ I & 0 & 0 & I \end{bmatrix} \succeq 0. \tag{30b}$$

The resulting optimal controller K is used to compute u_{dyn}, which is applied as a control input to the system together with the u_{st}.

4 Simulation example

In the following a simulation example on the robust LPV control is presented. In the simulation a 1.5-km-long section of the Hungarian M1 freeway between Tatabánya and Budapest with two lanes is examined. Previously, several simulations have been performed in the VISSIM traffic simulator to generate the fundamental characteristics of the freeway. During these simulations several traffic scenarios with various κ and q_0 values were performed. Some preliminary results can be found in [20]. During the simulations it was observed that ρ_{crit} was around $25\ veh/km$, which resulted in the setting of $\rho_{des} = 22\ veh/km$.

In the simulation the freeway section has two inflows. First, q_0 is the uncontrolled inflow from the previous highway section. Second, the traffic system has one controlled ramp with inflow u. The controlled gate is located at the beginning of the freeway section. Moreover, the vehicles can leave the freeway section on an outflow ramp s_1 and they can also transfer to the next freeway section with the flow q_1. During the simulation the ratio of the autonomous vehicles κ continuously varies. In the traffic model the freeway section is handled as one segment, thus $i \equiv 1$.

Figure 3 illustrates the disturbances of the system, which are q_0 and s_1. These signals cannot be influenced through the designed control, but the role of the control strategy is to guarantee the maximum outflow and reduce the impact of disturbances on it. It can be seen that the current q_0 oscillates around $1800\ veh/h$, which can result in a high value for ρ_1 together with r_1, see e.g. at $t = 1000\ s$ $q_0 = 2100\ veh/km$, which yields $\rho_1 = 28\ veh/km$. Thus, it is necessary to limit the inflow of the vehicles on the inflow ramp. Moreover, s_1 has a small value, which means that most of the vehicles along the freeway section are driven.

The ratio of the autonomous vehicles in the heterogeneous traffic is shown in Figure 4(a). During the simulation it varies between $10\% \ldots 40\%$, which is a significant variation. Moreover, the resulting density ρ_1 can be seen in Figure 4(b). The results show that the required $\rho_{crit} = 25\ veh/km$ is tracked by the controlled system with low error, which provides maximum outflow.

Finally, the control input and its components are illustrated in Figure 5. The control input u_{st} has a higher value, with which the constraint on r_1 is guaranteed. Moreover, u_{dyn} guarantees low error in the tracking. The efficiency of the control can be illustrated at time $t = 1000\ s$. In this case the freeway section has a high load on q_0, which can lead to a congestion. Thus, the control input u is significantly reduced with components u_{st} and u_{dyn}, see Figure 5. Throughout simulation the overall control input $u = u_{st} + u_{dyn}$ has

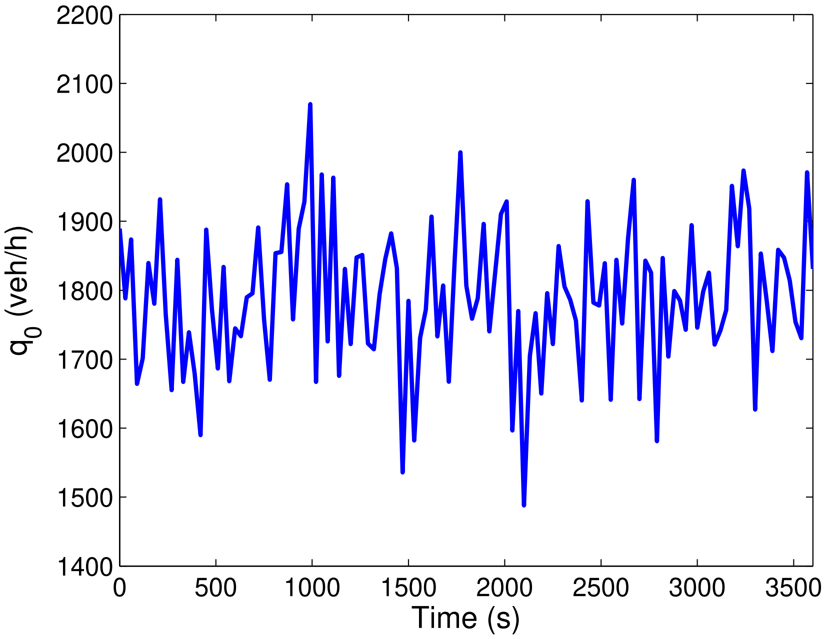

(a) Uncontrolled inflow on the freeway

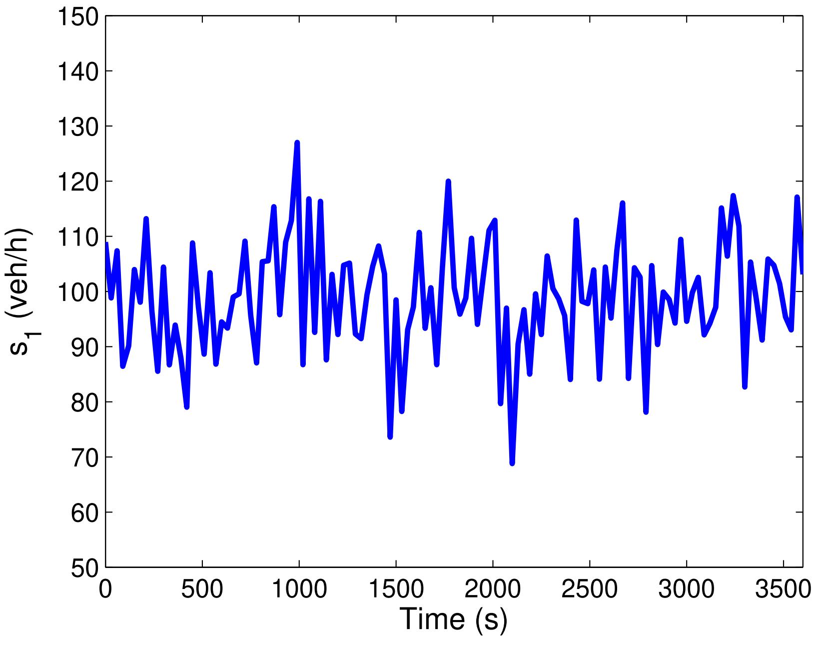

(b) Outflow on the ramps

Figure 3: Disturbances in the simulation

a value between $0 \ldots 2450\ veh/h$, whose mean is $1100\ veh/h$. As a result the mean of the entire inflow of the section $q_0 + r_1$ is $2900\ veh/h$. In spite of the high inflow and the varying κ performance is guaranteed, which proves that the LPV-based control strategy is suitable for the solution of the traffic control problem.

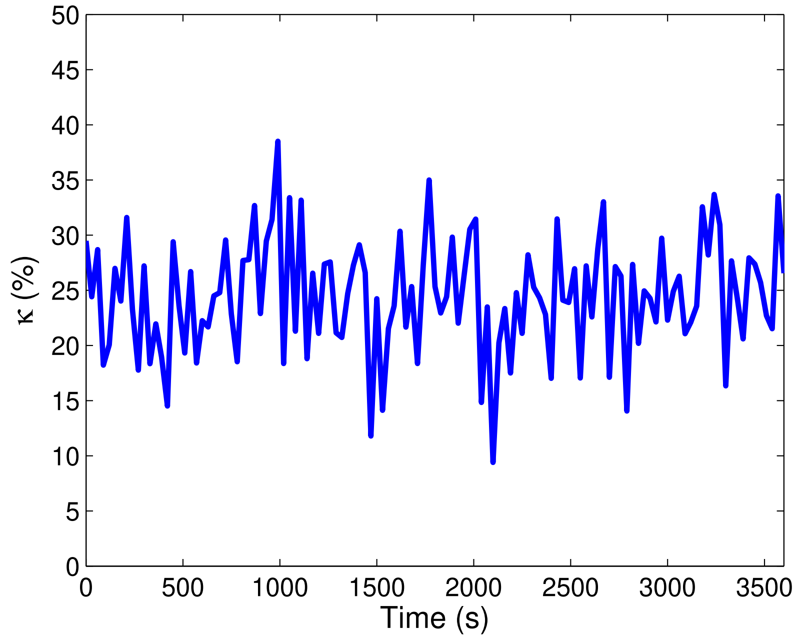

(a) Ratio of the autonomous vehicles

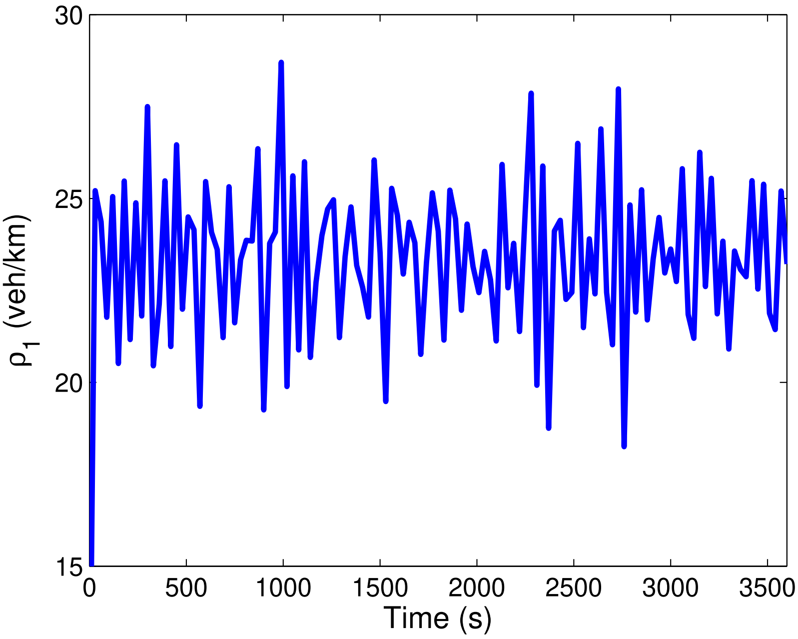

(b) Traffic density on the section

Figure 4: Simulation results

5 Conclusions

The paper has presented a control strategy for the optimization of heterogeneous traffic flow, which contains conventional human-driven and autonomous vehicles. It has been derived

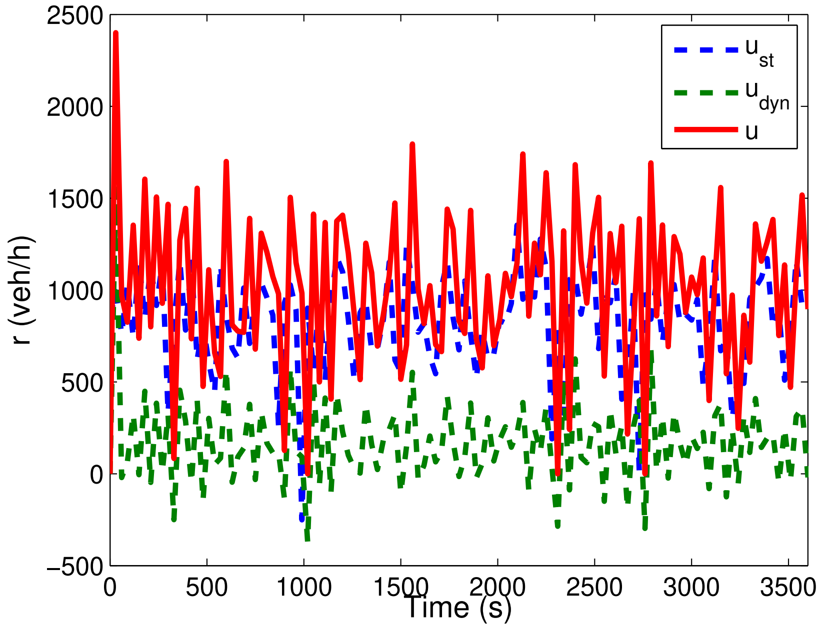

Figure 5: Control input in the simulation

from a LPV model for the heterogeneous traffic flow, in which the ratio of the autonomous vehicles is incorporated in a scheduling variable. The robust control design is based on a maximization criterion, which incorporates LMI conditions. Moreover, the control strategy handles the constraints on the control input. The simulation example has illustrated that the proposed robust LPV control is able to guarantee the performance specification of the system, which results in the required traffic density.

Acknowledgement

This work has been supported by the GINOP-2.3.2-15-2016-00002 grant of the Ministry of National Economy of Hungary and the European Commission through the H2020 project EPIC under grant No. 739592.
The work of Balázs Németh was partially supported by the János Bolyai Research Scholarship of the Hungarian Academy of Sciences and the ÚNKP-19-4 New National Excellence Program of the Ministry for Innovation and Technology.

References

[1] B. Németh and P. Gáspár, "The relationship between the traffic flow and the look-ahead cruise control," *IEEE Transactions on Intelligent Transportation Systems*, vol. 18, no. 5, pp. 1154–1164, May 2017.

[2] A. Messmer and M. Papageorgiou, "Metanet - a macroscopic simulation program for motorway networks," *Traffic Engineering and Control*, vol. 31, pp. 466–470, 1990.

[3] J. R. D. Frejo, E. F. Camacho, and R. Horowitz, "A parameter identification algorithm for the Metanet model with a limited number of loop detectors," in *51st IEEE Conference on Decision and Control*, 2012, pp. 6983–6988.

[4] F. Wageningen-Kessels, H. Lint, K. Vuik, and S. Hoogendoorn, "Genealogy of the traffic flow models," *European Journal on Transportation and Logistics*, vol. 4, pp. 445–473, 2015.

[5] W. Schakel, B. Van Arem, and B. Netten, "Effects of cooperative adaptive cruise control on traffic flow stability," in *13th Int. Conference on Intelligent Transportation Systems*, 2010, pp. 759–764.

[6] B. Arem, C. Driel, and R. Visser, "The impact of cooperative adaptive cruise control on traffic-flow characteristics," *IEEE Transactions On Intelligent Transportation Systems*, vol. 7, no. 4, pp. 429–436, 2006.

[7] A. Bose and P. Ioannou, "Analysis of traffic flow with mixed manual and semi-automated vehicles," *IEEE Transactions on Intelligent Transportation Systems*, vol. 4, no. 4, pp. 173–188, 2003.

[8] C. Zhang and A. Vahidi, "Predictive cruise control with probabilistic constraints for eco driving," in *ASME Dynamic Systems and Control Conference*, vol. 2, 2011, pp. 233–238.

[9] F. Wu, "A generalized LPV system analysis and control synthesis framework," *International Journal of Control*, vol. 74, pp. 745–759, 2001.

[10] P. Gáspár, Z. Szabó, J. Bokor, and B. Németh, *Robust Control Design for Active Driver Assistance Systems. A Linear-Parameter-Varying Approach.* Springer Verlag, 2017.

[11] R. Wiedemann, "Simulation des Strassenverkehrsflusses," *Schriftenreihe des Instituts für Verkehrswesen der Universität Karlsruhe*, vol. 8, 1974.

[12] M. Fellendorf and P. Vortisch, *Fundamentals of Traffic Simulation*, ser. International Series in Operations Research & Management Science. New York, NY: Springer, 2010, vol. 145, ch. Microscopic Traffic Flow Simulator VISSIM.

[13] S. Boyd, L. E. Ghaoui, E. Feron, and V. Balakrishnan, *Linear Matrix Inequalities in System and Control Theory*. Philadelphia: Society for Industrial and Applied Mathematics, 1997.

[14] C. Scherer and S. Weiland, *Lecture Notes DISC Course on Linear Matrix Inequalities in Control*. Delft, Netherlands: Delft University of Technology, 2000.

[15] W. Ashton, *The Theory of Traffic Flow*. London: Spottiswoode, Ballantyne and Co. Ltd., 1966.

[16] N. Gartner and P. Wagner, "Analysis of traffic flow characteristics on signalized arterials," *Transportation Research Record*, vol. 1883, pp. 94–100, 2004.

[17] M. Treiber and A. Kesting, *Traffic Flow Dynamics: Data, Models and Simulation*. Berlin,Heidelberg: Springer-Verlag, 2013.

[18] C. Daganzo, *Fundamentals of transportation and traffic operations*. Oxford: Pergamon., 1997.

[19] K. Zhou, J. Doyle, and K. Glover, *Robust and Optimal Control*. Prentice Hall, 1996.

[20] P. Gáspár and B. Németh, *Predictive Cruise Control for Road Vehicles Using Road and Traffic Information*. Springer International Publishing, 2019.